

Bioactivation of Drugs by Cytochromes P450
New Tools and Concepts for the Characterization
of Reactive Metabolites of Drugs

Micaela Christina Damsten

Bioactivation of Drugs by Cytochromes P450
New Tools and Concepts for the Characterization of Reactive Metabolites of Drugs

Micaela Christina Damsten

Printed by PrintPartners Ipskamp B.V.

Cover Picture: The Sibelius Monument by Christoffer Damsten

© Micaela Christina Damsten, Brussels 2009. All rights reserved. No parts of this thesis may be reproduced in any form or by any means without permission from the author.

ISBN 978-90-8659372-9

VRIJE UNIVERSITEIT

**Bioactivation of Drugs by Cytochromes P450
New Tools and Concepts for the Characterization
of Reactive Metabolites of Drugs**

ACADEMISCH PROEFSCHRIFT

ter verkrijging van de graad Doctor aan
de Vrije Universiteit Amsterdam,
op gezag van de rector magnificus
prof.dr. L. M. Bouter,
in het openbaar te verdedigen
ten overstaan van de promotiecommissie
van de faculteit der Exacte Wetenschappen
op vrijdag 23 oktober 2009 om 10.45 uur
in de aula van de universiteit,
De Boelelaan 1105

door

Micaela Christina Damsten

geboren te Neuilly-sur-Seine, France

promotor : prof.dr. N. P. E. Vermeulen
copromotor : dr. J. N. M. Commandeur

Reading Committee :

prof.dr. K. Park
dr. M. Monshouwer
dr. D. Noort
prof.dr. M. Smit
prof.dr. R. Orru

The investigations described in this thesis were carried out in the Leiden Amsterdam Center for Drug Research (LACDR), Division of Molecular Toxicology, Department of Chemistry and Pharmaceutical Sciences, Faculty of Sciences, Vrije Universiteit, De Boelelaan 1083, 1081HV Amsterdam, The Netherlands.

CONTENTS

PART I	INTRODUCTION	9
Chapter 1	General Introduction	11
PART II	NOVEL <i>IN VITRO</i> TOOLS FOR THE GENERATION, IDENTIFICATION AND CHARACTERIZATION OF REACTIVE METABOLITES	65
Chapter 2	Application of drug metabolising mutants of cytochrome P450 BM3 (CYP102A1) as biocatalysts for the generation of reactive metabolites	67
Chapter 3	The role of glutathione S-transferases in the trapping of reactive intermediates of drugs	87
Chapter 4	Trimethoprim: novel reactive intermediates and bioactivation pathways by cytochromes P450	107
PART III	NOVEL TOOLS FOR THE BIOMONITORING OF REACTIVE METABOLITES <i>IN VIVO</i> IN HUMANS	125
Chapter 5	Liquid chromatography/tandem mass spectrometry detection of covalent binding of acetaminophen to human serum albumin	127
Chapter 6	Automated detection of covalent adducts to human serum albumin by immunoaffinity chromatography, on-line solution phase digestion and liquid chromatography-mass spectrometry	153
PART IV	CONCLUSIONS	175
Chapter 7	Summary, Conclusions and Perspectives	177
APPENDICES		191
List of Abbreviations		193
Nederlandse Samenvatting		195
Curriculum Vitae		199
List of Publications		201
Acknowledgements		203

PART I

INTRODUCTION

Chapter 1

General Introduction

Abstract

The main topic of the research described in this thesis concerns adverse drug reactions (ADRs) and idiosyncratic drug reactions (IDRs). The first part of this thesis therefore consists of a general introduction which describes the present knowledge on ADRs and IDRs, the role of metabolism and reactive metabolite formation in this type of toxicity and the strategies currently applied by pharmaceutical industries to minimize risks related to this issue during drug development programs.

Contents

Adverse Drug Reactions	14
Significance	14
Types of ADRs	16
Clinical characteristics of IDRs	18
Mechanistic hypotheses	20
<i>Hapten Hypothesis</i>	20
<i>Danger Hypothesis</i>	21
<i>Pharmacological Interaction Hypothesis</i>	22
<i>Nonimmune Hypotheses</i>	23
Drug Metabolism and ADRs	24
Drug Metabolism	24
<i>Metabolism of drugs</i>	24
<i>Bioactivation of drugs</i>	24
<i>Defense mechanisms</i>	27
Examples of bioactivation pathways	30
<i>Acetaminophen</i>	30
<i>3-Hydroxyacetanilide</i>	32
<i>Diclofenac</i>	33
<i>Clozapine</i>	35
<i>Carbamazepine</i>	36
Screening methods for reactive intermediates	38
“Early phase/discovery” <i>in vitro</i> screening tools	38
<i>Trapping experiments</i>	38
<i>(Bio)synthesis of (reactive) metabolites</i>	42
<i>Covalent Binding Studies</i>	43
“ <i>Avoiding structural alerts</i> ”	44
“Late phase/development” <i>in vivo</i> biomonitoring tools	45
<i>Protein adduct analysis</i>	46
<i>In vivo biomonitoring methods</i>	51
Aims and outline of the thesis	53
State of research when starting in 2003	53
Aims and scope of the thesis	54
Outline of the thesis	55
References	56

Adverse Drug Reactions

Significance

Adverse drug reactions (ADRs) defined by the World Health Organization are noxious, unintended and undesirable effects of a drug, which occurs at doses used in humans for prophylaxis, diagnosis, or therapy [1]. Although much effort has been spent on the development of safer drugs, ADRs still remain a major complication in drug development programs and during drug therapy. Overall, it is estimated that 7% of the general population may be affected by ADRs [1-3]. Demoly *et al.* described that ADRs occur in 10-20% of hospitalized patients, with up to one-third being of allergic or pseudo-allergic nature [4]. Drug hypersensitivity syndromes, anaphylactic reactions, Stevens Johnson syndrome and toxic epidermal necrolysis are all potentially life-threatening conditions that are associated with significant mortality in patients. Lazarou *et al.* showed in the United States that 0.32% of hospitalized patients died from ADRs, causing more than 100.000 deaths per year in the US in 1994 [2]. This implied that fatal ADRs were ranked between the fourth and the sixth leading cause of death in the United States in 1994. More recently, a study performed in the United Kingdom showed that 6% of hospital admissions were due to ADRs, with a mortality rate of approximately 2% [5]. These statistics are in agreement with those observed by Einarson [6]. Apart from serious health risks for patients, ADRs also have a high socio-economic impact due to hospitalization prolongations, increased treatment costs, etc... [1, 2].

Toxicity and prevention of ADRs therefore constitute a major challenge for the pharmaceutical industry. Lasser *et al.* recently highlighted that from 548 new chemical entities approved by the FDA in 1975-1999, 45 drugs (8.2%) acquired one or more black box warnings and sixteen (2.9%) were withdrawn from the market [7]. The economical impact for pharmaceutical companies concerned is huge. Another consequence is reluctance of physicians to prescribe drugs that were shown to be safe and efficacious in more than 99 % of the population.

The main difficulty resides in the fact that ADRs can not always be predicted from (pre-)clinical studies. Because of their unpredictability and potential severity, ADRs constitute a major concern in clinical practice and in drug development processes.

Table 1. Examples of drugs withdrawn from the market for safety reasons.

Drug	Therapeutic class	Warning/Toxicity	Year of withdrawal
Azaribine	Dermatologic (psoriasis)	Thromboembolism	1976
Ticrynafen	Antihypertensive	Hepatotoxicity	1980
Benoxaprofen	Analgesic	Hepatotoxicity	1982
Zomepirac	Analgesic	Anaphylaxis	1983
Nomifensine	Antidepressant	Hemolytic anemia	1986
Suprofen	Analgesic	Flank pain syndrome	1987
Terfenadine	Antihistamine	Fatal arrhythmia	1998
Encainide	Antiarrhythmic	Fatal arrhythmia	1991
Temafloxacin	Antibiotic	Hemolytic anemia Kidney failure	1992
Flosequinan	Congestive heart failure	Increased mortality	1993
Mibefradil	Antihypertensive calcium-channel blocker	Drug interactions Fatal arrhythmia	1998
Bromfenac	Analgesic	Hepatotoxicity	1998
Astemizole	Antihistamine	Fatal arrhythmia	1999
Grepafloxacin	Antibiotic	Fatal arrhythmia	1999
Cisapride	Heartburn	Fatal arrhythmia	2000
Troglitazone	Antidiabetic	Hepatotoxicity	2000
Levomethadyl	Opiate dependence	Fatal arrhythmia	2003
Rofecoxib	Analgesic	Heart attack, stroke	2004
Valdecoxib	Analgesic	Skin disease	2005

Table adapted from [7-9].

Types of ADRs

Typically, ADRs can be classified in four main types [9, 10] (Table 2).

Type A: Pharmacological. Type A reactions are the most frequent, usually dose-dependent and can be predicted from the known pharmacology of the drug. Toxicity generally arises from an exaggeration of the pharmacological effect and can usually be eliminated by discontinuation of therapy.

Type B: Idiosyncratic. These reactions are generally not predictable from the known pharmacology of the drug and do not necessarily show classic dose-response relationships. Reactions usually have a high degree of individual susceptibility, a delayed time of onset, are likely to have an immunological basis and to involve reactions between macromolecules and drugs and/or reactive metabolites. No animal model is currently available and idiosyncratic drug reactions (IDRs) therefore remain poorly understood.

Type C: Chemical. These ADRs also involve the reaction of a drug and/or reactive metabolite with macromolecules but there is a rapid response. In this case, covalent binding to macromolecules can be predicted or rationalized by the chemical structure of the drug and/or of its metabolites. Covalent binding to proteins may lead to alteration of protein function, redox cycling, oxidative stress and ultimately cell death and/or necrosis.

Type D: Delayed. These ADRs occur from long-term treatment with a drug and show a delayed response. Examples of this type of reactions include carcinogenicity and teratogenicity. These types of toxicities can usually be detected in pre-clinical screening assays and may therefore be prevented.

Table 2. Clinical characteristics of the different types of ADRs.

Type	Characteristic	Dose-dependence	Predictable	Toxicity	Incidence	Delay	Examples
A	Pharmacological	Yes	Yes	Primary or secondary pharmacology	Most common	No	Allosetron Mibefradil
B	Idiosyncratic	No	No	Direct organ toxicity	Rare	Yes	Terafloxacin Zomepirac
		Although higher frequency of IDRs with higher drug doses		Can affect all organs but usually involves hepatic, skin and hematopoietic systems	Probably individual susceptibility factor		
C	Chemical	Yes	Yes	Direct organ toxicity	Probably individual susceptibility factor	No	Acetaminophen
			Can be predicted/rationalized from chemical structure				
D	Delayed	Yes	Yes	Carcinogenicity Teratogenicity	Should be preventable	Yes	Diethylstilbestrol Thalidomide
		Long-term treatment	Available bioassays			years	

Adapted from [9, 10].

Clinical characteristics of IDRs

The work described in this thesis mainly focused on compounds causing idiosyncratic drug reactions (IDRs). Characteristic points of IDRs are:

Low incidence. The frequency of occurrence of IDRs is usually less than one in 5000 individuals [11]. Others report incidences of drug-related hepatotoxicity ranging from 1 in 10.000 to 1 in 100.000 patients [12] (Table 3). The low incidences explain why IDRs usually go undetected during clinical trials and only appear once the drug is launched on the market and that a large population is exposed to the compound.

Organs and Systems affected. Four major forms of idiosyncratic drug toxicities are typically observed (Table 3). These include anaphylactic reactions, blood dyscrasias (e.g. hemolytic anemia, agranulocytosis, idiosyncratic aplastic anemia...), hepatotoxicity (varying from asymptomatic increase in serum transaminases to fulminant hepatic necrosis) and severe cutaneous reactions (e.g. Stevens-Johnson syndrome and toxic epidermal necrolysis) [13].

Table 3. Clinical characteristics of IDRs: systems affected, toxicities and incidence rates.

Target system	Drug	Toxicity	Incidence (%)	References
Anaphylaxis	Penicillin	Allergic reaction	8	[14]
		Anaphylaxis	0.001	
		Anaphylactic fatality	0.0001	
Hematopoietic system	Carbamazepine	Blood dyscrasias	0.2	[3, 15, 16]
	Clozapine	Agranulocytosis	0.8	[17]
	Ticlopidine	Agranulocytosis	1-2	[18]
	Vesnairone	Agranulocytosis	1-2	[19]
	Amodiaquine	Agranulocytosis	0.005	[20, 21]
Liver	Amodiaquine	Hepatotoxicity	0.005	[20]
	Carbamazepine	Hepatotoxicity	0.2	[15, 16]
	Diclofenac	Hepatotoxicity	0.004-0.02	[22]
	Tienilic acid	Hepatotoxicity	0.1-0.7	[23]
Cutaneous system	Carbamazepine	Rash	1	[3, 15, 16]
	Cimetidine	Cutaneous ADR	1.3	[24]
	Co-trimoxazole (trimethoprim-sulfamethoxazole)	Cutaneous ADR	3.4	[24]
	Diazepam	Cutaneous ADR	0.1	[24]
	Phenytoin	Rash	3.3	[25]

Time to onset. One characteristic of IDRs is the delay between exposure to the drug and the onset of the adverse reaction. This delay can differ from drug to drug; varying from a few days, to weeks or even months (Table 4).

Dose-dependence. IDRs are usually considered as not dose-dependent. However, it has been observed that IDRs are rare for drugs given at a dose of 10 mg per day or less [11, 26] (Table 4). Li *et al.* have indeed observed that many drugs involved in idiosyncratic hepatotoxicity are “high-dose” drugs (given at more than 100 mg per day) [11]. One important factor to consider, however, is that the critical exposure factor is not the administered dose but the concentration of drug (and/or metabolite) present at the target organ that could elicit the adverse event.

Table 4. Clinical characteristics of IDRs: toxicity, dosage and time of onset.

Drug	Toxicity	Dose (mg/day)	Onset (months)	References
Felbamate	Aplastic anemia	800-5400	0.8-25	[27]
Felbamate	Hepatotoxicity	1200-3600	0.8-18	[27]
Bromfenac	Hepatotoxicity	100-200	2-3	[28]
Troglitazone	Hepatotoxicity	400	0.5-9	[29]
Talcapone	Hepatotoxicity	300-600	2-4	[30]
Clozapine	Agranulocytosis	300	1-75	[31]
Carbamazepine	Stevens-Johnson syndrome Toxic epidermal necrosis	500-1500	0.3-1	[32]
Phenytoin	Stevens-Johnson syndrome Toxic epidermal necrosis	500-1500	0.5-1	[32]
Phenobarbital	Stevens-Johnson syndrome Toxic epidermal necrosis	150	0.2-1.2	[32]

Adapted from [33].

Risk factors. Genetic predisposition might explain the susceptibility of a few patients to a drug that is safe in the majority of individuals. Several studies have tried to find an association between a specific genotype and a higher risk of developing IDRs. However, only few weak associations were found until now. For example, the slow acetylor phenotype has been associated with a higher risk to develop IDRs to isoniazid and sulfonamides [34, 35]. Different human leukocyte antigen (HLA) genotypes have been associated with hypersensitivity reactions to abacavir [36, 37] and allopurinol-induced Stevens-Johnson/toxic epidermal necrolysis syndromes [38]. A weak association between cytokine genotypes and diclofenac-induced hepatotoxicity was also found [39]. Next to genetic predisposing factors, other parameters may represent a risk for developing specific IDRs. For example, women have higher risks in developing halothane-induced hepatitis [40] and clozapine-

induced agranulocytosis [17]; while age, weight and pre-existing diseases and/or infections may predispose to other types of IDRs [26, 41].

Mechanistic hypotheses

Little is known about the exact mechanisms of IDRs. However, most of the mechanistic hypotheses proposed so far have an immune basis. Additionally, they suggest that reactive drugs and/or reactive drug metabolites might play an important role in the onset of IDRs [26].

Hapten Hypothesis

The hapten hypothesis is based on the classic concept that the immune system is able to differentiate “self” from “non-self”. This theory is also based on the observation that chemicals are usually too small to be recognized by the immune system. A reactive drug (hapten) and/or reactive metabolite of a chemically inert drug (pro-hapten), however, can covalently bind to a protein. The drug-protein adduct may be perceived as foreign by the immune system and elicit specific B and T cell immunologic responses [23, 26]. The protein adduct must be taken up by antigen presenting cells (APCs), processed into peptides, and presented via the major histocompatibility complex (MHC) to T cells in order to generate an immune response. Recognition of processed antigens by the T cell receptor (also referred to as “Signal 1”) leads to an immune response. A scheme of the hapten hypothesis is depicted in Figure 1.

Examples of drugs associated with IDRs having a mechanism consistent with the hapten hypothesis include penicillin allergies, as well as halothane- and tienilic acid-induced hepatitis. It should however be emphasized that not all reactive metabolites generate IDRs and that covalent binding to proteins as such does not necessarily mean toxicity.

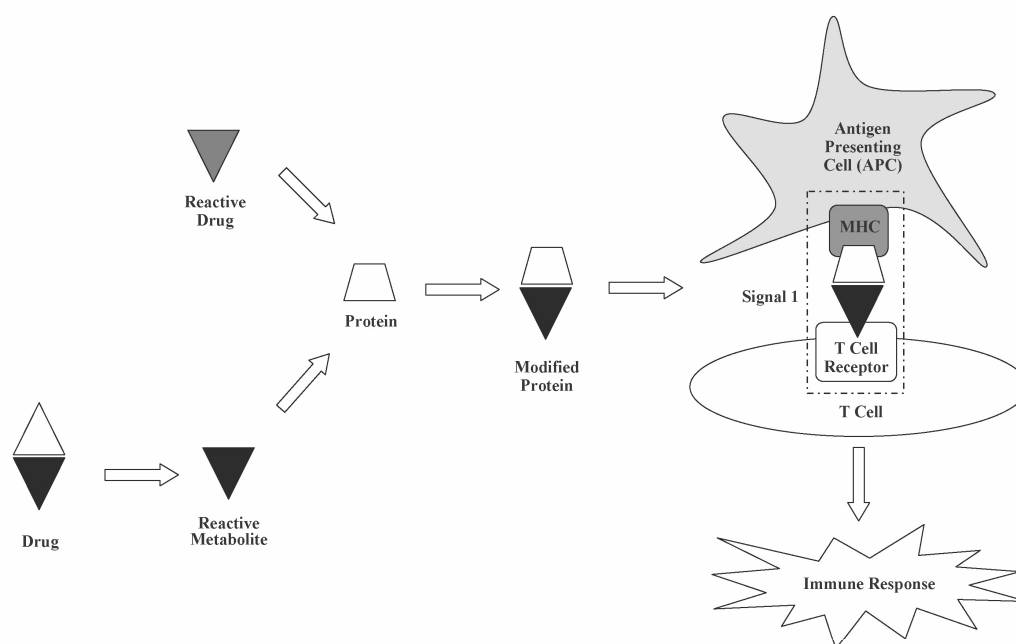


Figure 1. Hapten hypothesis. The reactive drug (hapten) or reactive metabolite of a chemically inert drug (pro-hapten) binds to a protein to form a drug-(metabolite)-protein adduct. The modified protein is taken up by antigen presenting cells (APCs), processed, and drug-modified peptides are presented in the context of the major histocompatibility complex (MHC) to help T cells via the T cell receptor. Recognition of processed antigens by the T cell receptor (also referred to as “Signal 1”) leads to an immune response. Adapted from [26].

Danger Hypothesis

The observation that reactive metabolites and covalent binding to proteins will not *per se* generate IDRs has led to the proposition of the danger hypothesis. This hypothesis states that damage to cells is needed to release “danger signals” that stimulate the innate immune system [26, 42]. Previous data has indeed shown that next to “Signal 1”, co-stimulation of T cells by activated APCs is required to generate an immune response. Without co-stimulation (also referred to as “Signal 2”), the immune response equals tolerance. Danger signals from stressed cells stimulate APCs, leading to up-regulation of co-stimulatory molecules, generation of “Signal 2” and an immune response. Consistently, next to their ability to function as haptens, reactive metabolites can damage cells leading to “danger signals” and up-regulation of “Signal 2” in order to induce IDRs. This theory could explain the increased incidence of some types of IDRs in patients having certain types of injuries and/or infections (e.g. HIV-positive patients) [13]. A general depiction of the danger hypothesis is given in Figure 2.

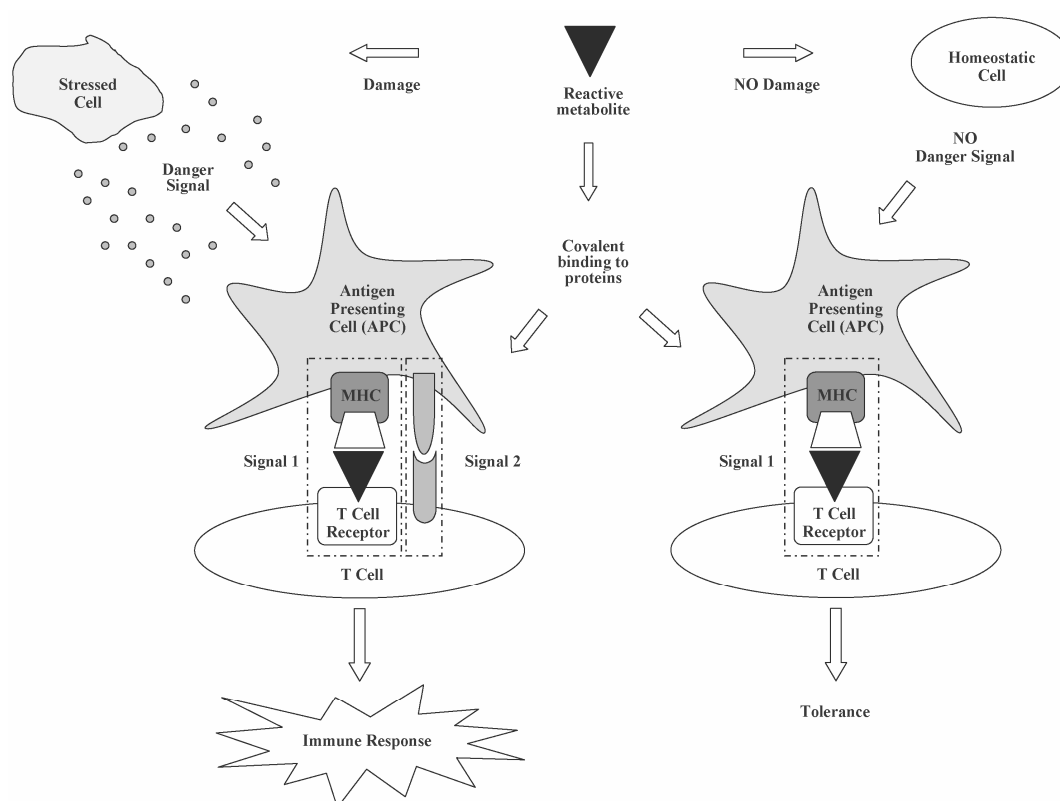


Figure 2. Danger hypothesis. The danger hypothesis states that next to covalent binding to proteins, reactive metabolites may damage cells, thereby releasing “danger signals” (also referred to as “Signal 2”) which are needed to activate APCs, up-regulate co-stimulatory molecules and generate an immune response. In absence of “Signal 2”, the immune response is tolerance. Adapted from [26].

Pharmacological Interaction Hypothesis

The pharmacological interaction hypothesis is based on the observation that clones of T cells from patients with a history of IDR to a specific drug were able to proliferate in presence of that drug, but in the absence of metabolism [26]. This observation suggests that T cells would recognize the parent drug, rather than modified peptides as proposed in the hapten hypothesis. This then would imply that covalent binding of reactive metabolites to proteins is not necessary to generate an IDR. It was proposed that chemically inert drugs may bind reversibly to the MHC-T cell receptor complexes and thereby stimulate a selective T cell immune response and possibly an IDR [26] (Figure 3). This theory fits with other clinical observations such as selective T cell stimulation without antibody response [43]. Both labile and hapten like presentations of drugs may take place simultaneously and lead to clinically distinct symptoms. Examples of compounds that may act by this mechanism include metals (e.g. nickel and beryllium) and drugs like sulfamethoxazole, carbamazepine and lidocaine [43].

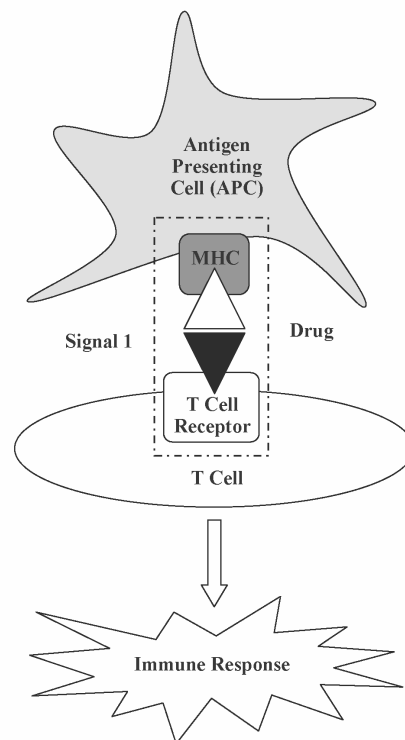


Figure 3. Pharmacological Interaction (PI) Hypothesis. This hypothesis suggests that the drug can reversibly bind to the MHC-T cell receptor complex, generate a “Signal 1” and thereby stimulate an immunological response to the parent drug. Adapted from [26].

Nonimmune Hypotheses

Although most of the evidence and symptoms of IDRs suggest an immune-mediated mechanism, some drugs and toxins could be considered as directly cytotoxic. For example, metabolic idiosyncrasy has been proposed to explain the absence of some typical immune-mediated symptoms of the IDR. However, none of these observations are very conclusive and a clear separation between immunologic and direct cytotoxic agents might not be possible as both mechanisms are probably closely related in the pathology [26].

Drug Metabolism and ADRs

Drug Metabolism

Metabolism of drugs

Although the exact mechanism is as yet unknown, drug metabolism and reactive metabolite formation seem to play an important role in ADRs and IDRs. Classically, the main role of drug metabolism is to convert lipophilic drug molecules to hydrophilic polar metabolites that are easier excreted from the body. Drug metabolic processes are typically divided into two types of reactions. Phase I metabolism include oxidation, reduction, hydrolysis, hydration and dehalogenation reactions [44]. Cytochrome P450 enzymes (P450s) constitute an important class of enzymes involved in the phase I metabolism of drugs. Due to their broad substrate specificity, P450s can catalyze a wide range of biotransformation reactions such as hydroxylation, dealkylation and oxidation reactions [44]. Other phase I metabolic enzymes include monoamine oxidases, flavin-containing oxygenases, amidases and esterases [44]. Phase II conjugation reactions mainly couple polar groups (e.g. glucuronic acid, sulfate and acetyl groups) to drugs and/or phase I drug metabolites to further increase their hydrophilicity. These biotransformation reactions involve sulfation, glucuronidation, GSH conjugation, acetylation, amino acid conjugation and methylation reactions [10, 45]. Phase II enzymes include UDP-Glucuronosyltransferase (UGTs), sulfotransferases (STs), N-acetyl transferases, methyl transferases and glutathione S-transferases (GSTs) [45].

Bioactivation of drugs

In some cases, however, metabolism can lead to the bioactivation of drugs and to the formation of reactive metabolites. Both phase I and phase II metabolic enzymes can be involved in the generation of reactive species. Different types of reactive metabolites exist such as electrophiles, radicals and reactive oxygen species. Electrophilic molecules, for example, are characterized as electron-deficient and will react with nucleophilic (electron rich) sites in proteins and/or in DNA. Free radicals possess unpaired electrons and can also lead to covalent binding to macromolecules. Additionally, they can abstract a hydrogen atom from macromolecules; a reaction that may lead to lipid peroxidation, oxidative stress and subsequent toxicity [10]. There is convincing evidence that reactive intermediates (RIs) are involved in the onset of many drug-related toxicities. Table 5 lists examples of drugs that are known to be bioactivated to reactive metabolites, give covalent

binding to proteins and have been associated with toxicity. Structures of RIs thought to be involved in ADRs are presented in Table 6.

Table 5. Examples of drugs and reactive metabolites possibly involved in ADRs.

Drug	Reactive metabolite	Toxicity	References
Carbamazepine	Epoxide	Skin rash	[15, 16, 46]
	Quinoneimine	Hepatotoxicity Blood dyscrasias	
Phenytoin	Catechol	Skin rash	[47, 48]
	Quinone		
Acetaminophen	Quinoneimine	Hepatotoxicity	[49-51]
Diclofenac	Quinoneimine	Hepatotoxicity	[52-55]
	Acyl glucuronide		
Amodiaquine	Quinoneimine	Hepatotoxicity	[21, 56]
		Agranulocytosis	
Troglitazone*	Isocyanate	Hepatotoxicity	[57, 58]
Bromfenac*	Acyl glucuronide	Hepatotoxicity	[7]
Halothane	Acyl halide	Hepatotoxicity	[59, 60]
Clozapine	Nitrenium ion	Agranulocytosis	[61, 62]
Tienilic acid*	Sulphoxide	Immunogenic hepatitis	[63-65]

* Drugs withdrawn from the market due to unacceptable safety profiles. Adapted from [13, 66].

Table 6. Examples of reactive intermediates (RIs) of drugs involved in ADRs.

Types of RIs	Structures and bioactivation pathways	Examples of drugs
Quinone		Bromobenzene Rifampin
Quinoneimine		Acetaminophen Diclofenac Carbamazepine
Catechol Quinone		Carbamazepine Phenytoin Fipexide
Arene oxide Epoxide		Furosemide Imipramine Bromobenzene Carbamazepine
Nitrenium ion Free radical		Clozapine Mianserin
Nitroso		Sulfamethoxazole
Acyl glucuronide		Diclofenac Benoxaprofen Bromfenac
Trichloromethyl radical Free radical		Carbon tetrachloride

Defense mechanisms

Organisms possess a wide range of defense mechanisms against reactive metabolites. The endogenous glutathione (GSH) peptide and enzymes such as GSTs, epoxide hydrolases (EH) and quinone reductases are efficient in detoxifying reactive electrophilic species whereas enzymes such as catalase, glutathione peroxidases and superoxide dismutases are mainly detoxifying by-products of metabolism (e.g. hydrogen peroxide) [10]. The nature and efficiency of the detoxification of reactive species is dependent on several factors including: the chemical nature/reactivity of the species, enzyme substrate-selectivity, tissue expression/localization and up-regulation of enzymes and co-factors [10].

The structure and chemical nature of electrophiles are also important factors determining the selectivity of their reactions with target nucleophilic macromolecules. For example, the “hard-soft” theory suggests that soft electrophiles will react more efficiently with soft nucleophiles, whereas hard electrophiles will more readily react with hard nucleophiles (Figure 4). “Hardness” and “softness” is determined by the polarizability of the electrophilic/nucleophilic center. Consistently, soft electrophiles such as quinones or polarized double bonds will react with soft nucleophiles such as GSH and thiol groups in proteins. Hard electrophiles (e.g. epoxides or alkyl carbonium ions) will react more promptly with hard nucleophiles such as basic groups in DNA and lysine residues in proteins. Consequently, the nature of the electrophile will also determine the toxic outcome. Hard electrophiles may react with DNA and be involved in mutagenicity and carcinogenicity whereas soft electrophiles reacting with thiol groups in proteins will most likely lead to protein disfunction and direct cytotoxicity. Ultra-reactive intermediates may react in their site of formation (e.g. P450) and thereby lead to mechanism-based inhibition of the enzyme involved. Intermediate-reactive electrophiles may react with nucleophilic sites in proteins being less critical for protein function but would thereby constitute antigens that might trigger an immune response and possibly an IDR (Figure 4).

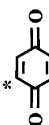
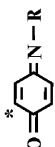
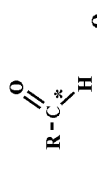

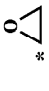

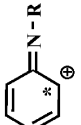
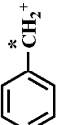
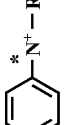
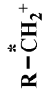
Electrophiles	Nucleophiles	Effect
Quinones 	Thiol-group (CYS)	Reactive to protein thiols = CYTOTOXIC
Quinoneimines 	Methylthiol-group (MET)	Ultra reactive = MECHANISM-BASED INHIBITION
Aldehydes 	Primary amino-group (LYS)	Reactive to protein lysines = No crucial targets = Not cytotoxic = May become antigenic = IMMUNE REACTION = IDRs ?
Activated alkyl halides 	Secondary amino-group (HIS)	
Epoxides 	Primary amino-group (DNA-bases: A, G)	
Acyl glucuronide 	Secondary amino-group (DNA-base: G, C, A, T)	
Aryl carbonium ion 	Oxygen atom (DNA-base: G, C, A, T)	
Benzyl carbonium ion 	Thiolate-group (GS-)	
Nitrenium ion 	Phosphate-group (DNA-backbone)	
Alkyl carbonium ion 		

Figure 4. "Hard-Soft" theory. Examples of "hard" and "soft" electrophiles and/or nucleophiles determining specific toxicological outcomes. * Possible sites of alkylation; X: halogen atoms.

Low-dose exposure to electrophiles can also induce protective mechanisms such as the endoplasmic reticulum (ER) stress response system and the induction of genes regulated by the antioxidant response element/electrophile response element (ARE/ERE). Electrophilic stress may lead to the induction of genes and proteins that express chaperone, antioxidant, xenobiotic detoxification and protein degradation functions [67]. For example, alkylation of cysteine residues of the thiol-rich Keap1 protein activates the transcription factor nrf2 which allows nuclear accumulation of nrf2 and activation of phase II and antioxidant genes.

Overall, the toxic outcome is a balance between drug bioactivation to potentially harmful metabolites and their detoxification by protection mechanisms of the body. Figure 5 proposes a general scheme summarizing different mechanisms and factors that are thought to be involved in this process.

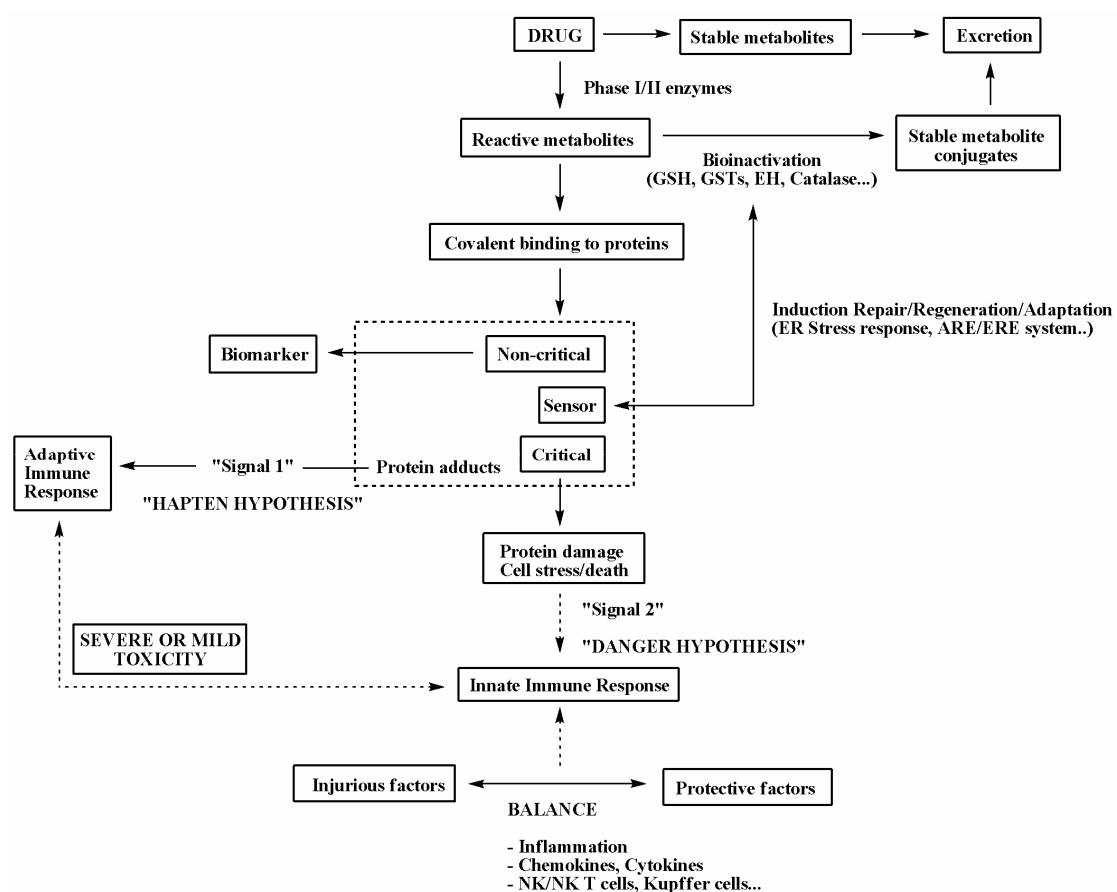


Figure 5. General scheme depicting the possible impact of drug metabolism and other factors in determining the toxic outcome in ADRs. Adapted from [68, 69]. NK (T): natural killer (T) cells.

Examples of bioactivation pathways

Below, the metabolism of some drugs involved in ADRs, and which have been subject of study in the research described in this thesis, will be discussed. The aim of this section is not to thoroughly describe the metabolism of those compounds but to focus on the major bioactivation pathways leading to reactive metabolites that have been suggested to play a role in observed drug-induced toxicities.

Acetaminophen

Acetaminophen (APAP) is a widely used analgesic agent. Although considered a safe drug, it is also a well known hepatotoxicant. It is estimated that APAP is the leading cause of acute hepatotoxicity in the United States upon overdose [70]. In the UK and Wales, about 500 deaths per year involving APAP were recorded between 1993 and 2002 [71].

The metabolism of APAP has been well studied (Figure 6). In therapeutic doses, APAP is mainly metabolized by phase II enzymes to glucuronidated and sulfated conjugates that are subsequently eliminated in the urine [72]. A small proportion of the drug is also converted by P450s to the reactive electrophilic N-acetyl-p-benzoquinoneimine metabolite (NAPQI) [73, 74]. NAPQI is usually detoxified by conjugation to GSH. However, in cases of APAP overdoses large amounts of NAPQI are formed, leading to the depletion of the GSH pools in the liver, covalent binding to liver proteins and subsequent hepatotoxicity [75].

Although covalent binding is thought to be the main mechanism involved in the hepatotoxicity of APAP, other hypotheses have been proposed as well. These include oxidative stress, alterations in the GSH/GSSG (reduced/oxidized glutathione) status, redox cycling resulting in lipid peroxidation, disruption of Ca^{2+} homeostasis, gene expression changes and activation of the antioxidant response element (ARE) [10]. These different pathways are most likely acting in combination resulting in hepatic apoptosis and necrosis.

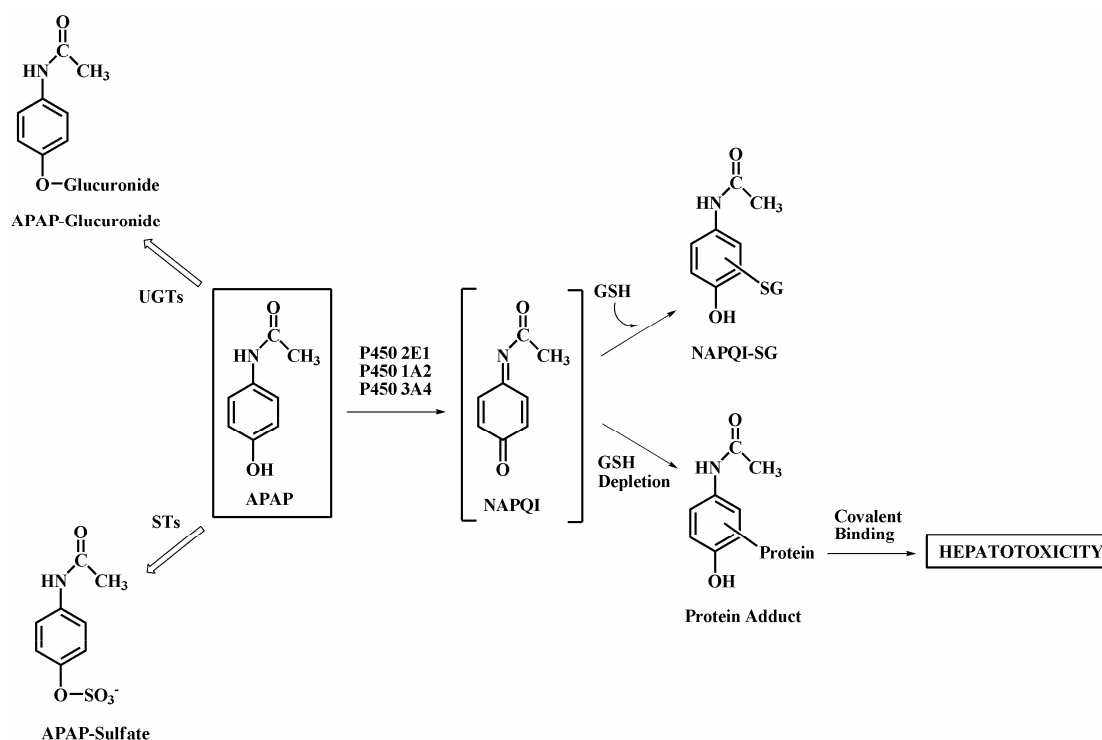


Figure 6. Scheme of the major metabolism and bioactivation pathways of APAP in humans. The reactive intermediate is depicted in brackets.

Recently, Kaplowitz proposed that APAP hepatotoxicity could be divided in two different group of events (Figure 7) [69]. “Upstream events” comprise the actual NAPQI formation, GSH depletion and covalent binding to proteins with subsequent mild hepatic injury. Up-regulation of transcription factor nrf2 may regulate the toxicity threshold. Mild hepatic injury would subsequently activate “downstream events” by stimulating the innate immune system which is controlling a tenuous balance between pro- versus anti-inflammatory cytokines and chemokines. Circumstances perturbing the factors of the innate immune system may consequently influence the outcome of the pathology from little (or no) injury to more severe hepatotoxicity [69]. This suggests that covalent binding to proteins and GSH depletion can not alone explain APAP-mediated hepatotoxicity, but that these processes are part of a more global and complicated process as discussed previously (Figure 5).

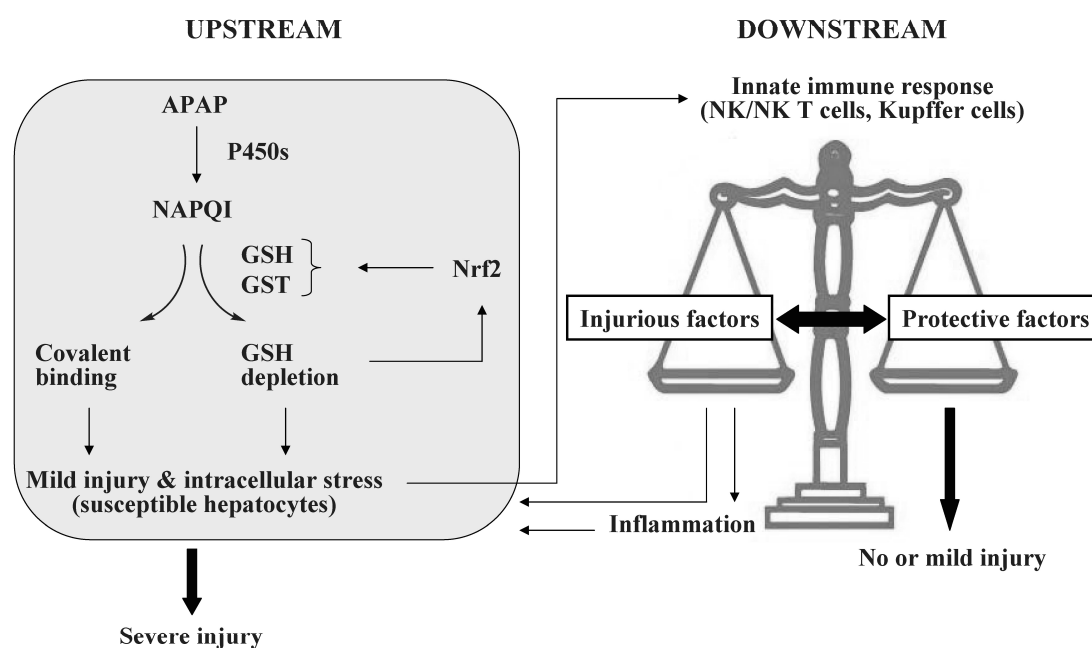


Figure 7. Current concepts of APAP hepatotoxicity. Adapted from [69].

3-Hydroxyacetanilide

In the context of covalent binding to proteins and its role in hepatotoxicity, it is interesting to discuss the case of 3-hydroxyacetanilide (AMAP), a non-toxic regioisomer of APAP. AMAP is known to be bioactivated to reactive metabolites by P450s, to give similar amounts of covalent binding to liver proteins as APAP but whereas APAP is hepatotoxic, AMAP is not [76, 77]. In mice, AMAP is mainly glucuronidated and sulfated by phase II enzymes (Figure 8) [77]. AMAP can also be hydroxylated by P450s [72, 78]. Although these hydroxylated metabolites are mainly glucuronidated and sulfated to the corresponding conjugates, a small proportion can be further oxidized to reactive benzoquinone intermediates that can alkylate proteins and/or be trapped by GSH to form GSH adducts [79, 80].

This example clearly shows that reactive metabolite formation and covalent binding to proteins is not sufficient for the development of toxicity. Consequently, it was proposed that alkylation of critical protein targets, with subsequent protein function disruption, could explain the different toxicity outcomes of the two compounds. In view of this, diminished mitochondrial function due to covalent binding to mitochondrial proteins may be of special importance in APAP hepatotoxicity since it is minimal with AMAP in comparison to APAP [81].

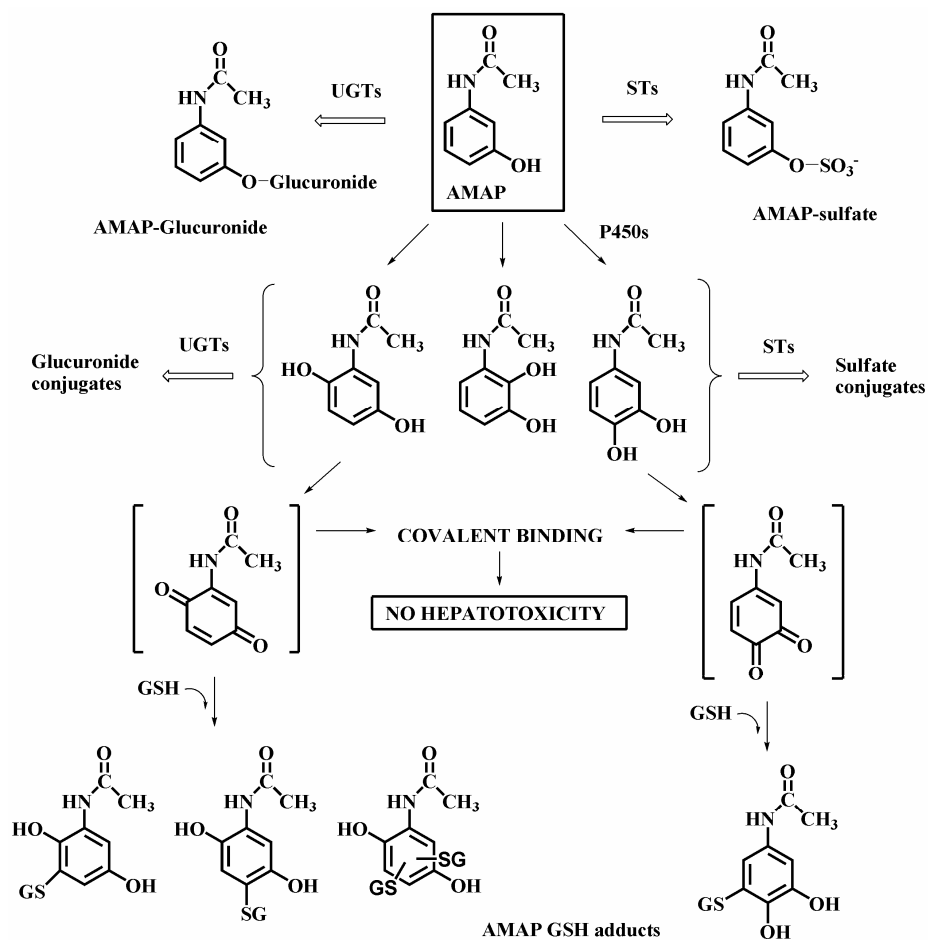


Figure 8. Scheme of the major metabolism and bioactivation pathways of AMAP in mice. Reactive intermediates are depicted in brackets.

Diclofenac

Diclofenac is a widely used non steroidal anti-inflammatory drug that has been involved in rare but severe hepatotoxicity cases. It has been estimated that 3.6 per 100.000 diclofenac users develop severe liver injury [22, 82, 83]. Although the exact mechanism is as yet unknown, formation of reactive metabolites has been suggested as a possible explanation for the idiosyncratic liver toxicity observed during diclofenac treatment.

Diclofenac is metabolized by P450s to the major 4'-OH-diclofenac metabolite, to 5-OH-diclofenac and other minor hydroxylated metabolites (Figure 9) [52, 53]. Further oxidation of 4'-OH-diclofenac and 5-OH-diclofenac can generate reactive quinoneimine intermediates which can be trapped by GSH [52, 54, 84, 85].

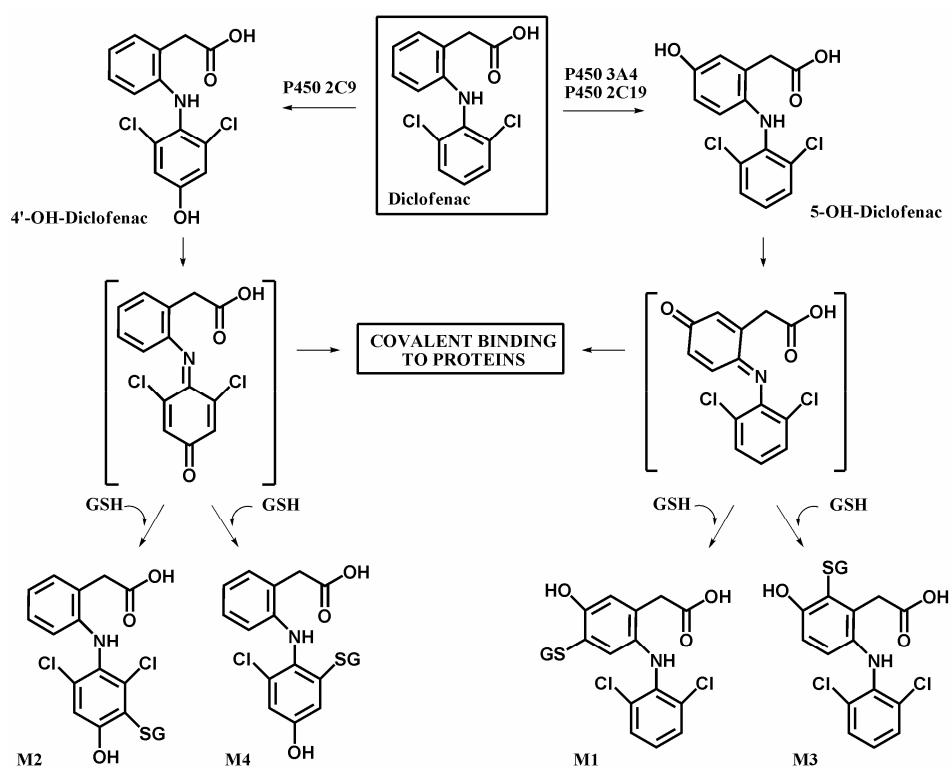


Figure 9. Scheme of P450-mediated bioactivation pathways of diclofenac in humans. Reactive intermediates are depicted in brackets.

Additionally, diclofenac and its hydroxylated metabolites can undergo phase II metabolism and be glucuronidated to the corresponding conjugates (Figure 10) [86, 87]. Attack at the carboxyl carbon of the labile ester bond of the acyl glucuronide by nucleophilic sites of proteins can lead to covalent binding to proteins. Moreover, acyl migration of unstable acyl glucuronides can generate reactive keto-groups that can alkylate nucleophilic sites on proteins [55, 88, 89]. Both types of RIs (originating from phase I and phase II metabolism) have been involved in covalent binding to proteins and are suggested to play a role in diclofenac-induced idiosyncratic hepatotoxicity reactions [90].

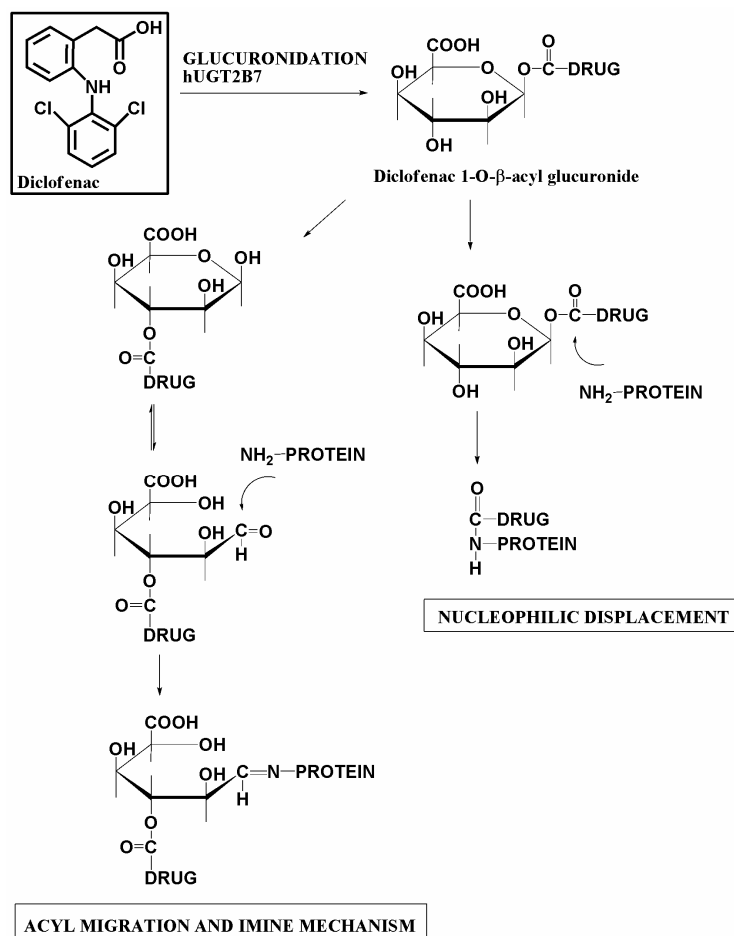


Figure 10. Scheme of the bioactivation pathways of diclofenac by phase II metabolism in humans. Two mechanisms of covalent binding of diclofenac acyl glucuronides to proteins are proposed. The first mechanism involves spontaneous acyl migration of the aglycone moiety with isomerization, ring opening, exposure of a reactive keto-group which can be attacked by nucleophilic sites on proteins. The second consists of the nucleophilic attack of the carboxy carbon of the acyl glucuronide by nucleophilic residues of proteins. hUGT2B7: human UDP-Glucuronosyltransferase-2B7 isoenzyme. Adapted from [23].

Clozapine

Clozapine is an antipsychotic agent that is used for the treatment of refractory schizophrenia [91]. Clozapine has also been associated with agranulocytosis and neutropenia reactions in approximately 1% of the patients using the drug [92]. Although the exact mechanism is not known yet, formation of reactive metabolites has been proposed as a possible explanation for the observed IDRs.

Clozapine is mainly biotransformed by the cytochrome P450 system to the N-demethylated and N-oxide metabolites (Figure 11) [93, 94]. A reactive nitrenium ion is also formed by P450s and by myeloperoxidases (MPOs) in activated neutrophils

and/or bone marrow cells [95-97]. Several GSH adducts have been identified in different types of *in vitro* enzymatic incubations [62, 93, 96, 98]. Moreover, this cytotoxic reactive metabolite was shown to covalently bind to cellular proteins and neutrophils [61, 62, 97].

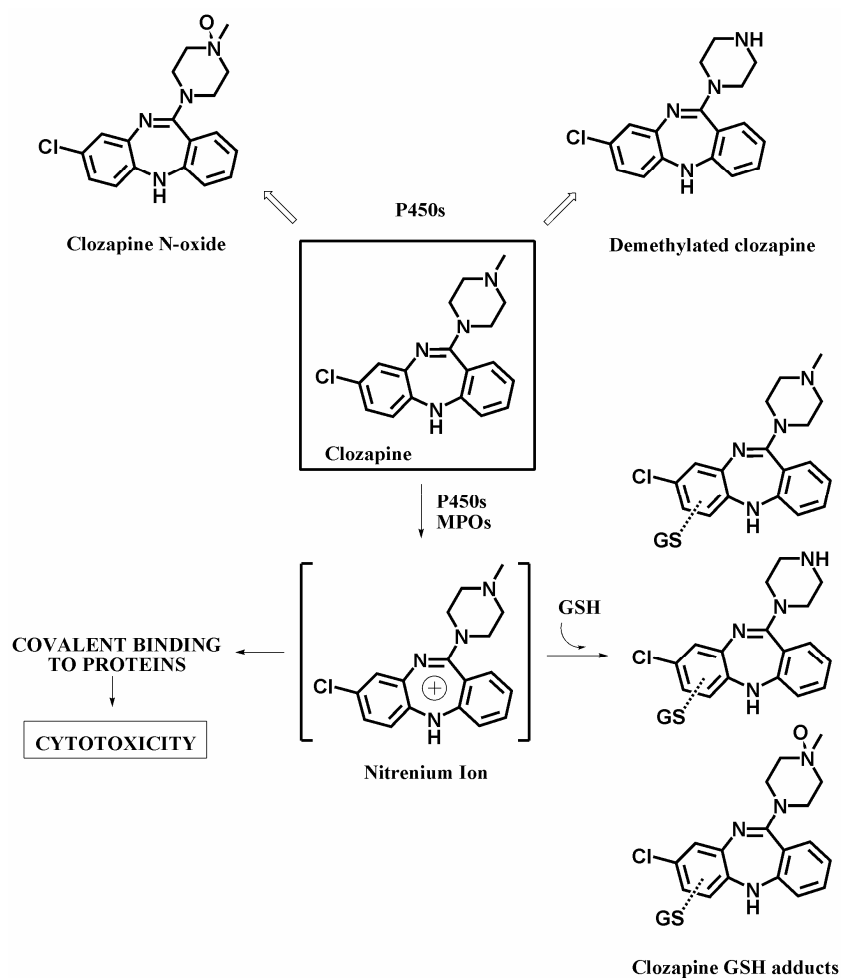


Figure 11. Scheme of the major metabolism and bioactivation pathways of clozapine in humans. The reactive intermediate is depicted in brackets.

Carbamazepine

Although carbamazepine is a widely used anticonvulsant agent, it has also been associated with severe hypersensitivity reactions in a minority of patients taking the drug. It has been estimated that 1 in 1000 to 1 in 10,000 exposures to carbamazepine might lead to hypersensitivity reactions [99, 100]. Reactions include skin rashes as well as blood, renal and hepatic disorders [101-103]. The exact mechanism of carbamazepine-induced hypersensitivity reactions is yet unknown. However, clinical manifestations suggest an immune etiology and a mechanism in

agreement with the “hapten hypothesis” described previously [101, 104-106]. Consequently, reactive metabolite formation has also been suggested as a potential cause for these adverse events [101, 107].

Carbamazepine is extensively metabolized in humans, with more than 30 metabolites identified in the urine of patients taking the drug [108]. Major metabolism pathways include hydroxylation of the side rings of carbamazepine, epoxidation towards the carbamazepine 10,11-epoxide (CE) metabolite and glucuronidation of the parent compound and/or of the hydroxylated metabolites [91, 109]. Several cytotoxic and protein-reactive metabolites of carbamazepine have also been identified [16, 46, 110-112]. For example, one of the major metabolite (e.g. 2-OH-carbamazepine) can be further metabolized to 2-hydroxyiminostilbene and to the reactive iminoquinone intermediate that has been shown to generate GSH and N-acetyl cysteine (NAc) adducts [15, 113]. Other GSH adducts have also been identified in human liver microsomes (HLM) incubations, including GSH adducts originating from the CE [114] and from the 2,3-arene oxide (Figure 12) [115]. Next to hepatic enzymes, carbamazepine can also be bioactivated by MPOs of activated neutrophils to reactive metabolites (e.g. 9-acridine carboxaldehyde) [116]. Covalent binding to neutrophils has also been observed, suggesting that this metabolite might also play a role in carbamazepine-induced IDRs [117].

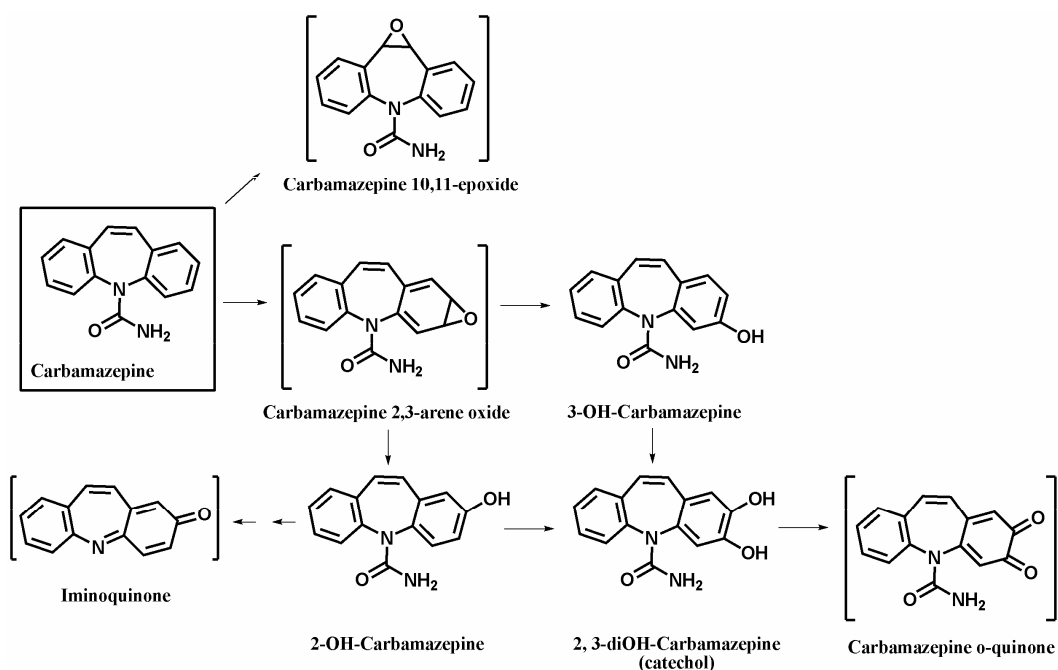


Figure 12. Structures of reactive metabolites (in brackets) of carbamazepine produced by P450s and which are possibly involved in carbamazepine-induced hypersensitivity reactions.

Screening methods for reactive intermediates

“Early phase/discovery” *in vitro* screening tools

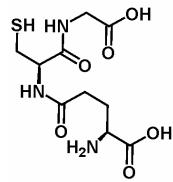
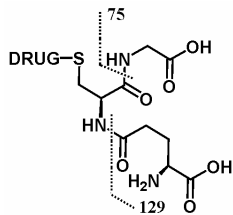
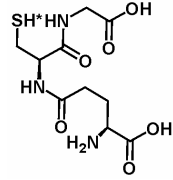
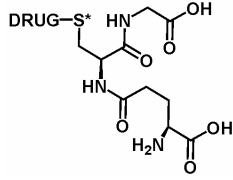
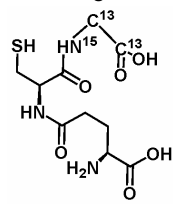
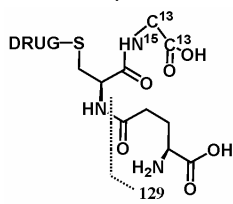
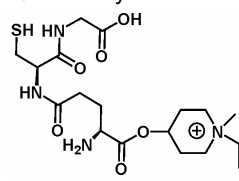
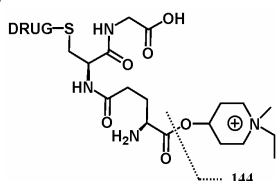
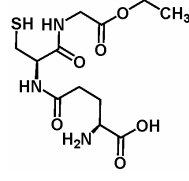
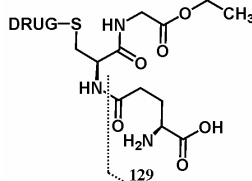
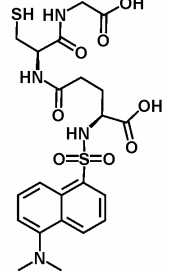
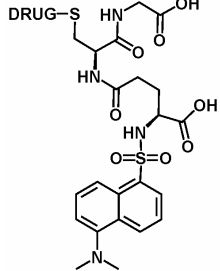
Although much effort has been spent on better understanding ADRs, the current mechanistic knowledge is still limited. The role of reactive metabolites of drugs in ADRs is however generally accepted. Therefore, strategies that are currently used for the safety assessment of novel drug candidates usually rely on screening and characterizing potentially reactive metabolites of drugs. A “panel screening” approach of well-characterized *in vitro* and/or *in vivo* toxicity assays is being used to profile novel drug candidates for their potential to form RIs and to be possibly involved in ADRs. Predicting ADRs will remain challenging but this combined approach may minimize and identify drug candidates showing unacceptable safety profiles [118].

Trapping experiments

Detection of reactive metabolites is difficult due to the chemical reactivity of the intermediates and to the usually low amounts present in incubations. Therefore, the most common way to screen for reactive metabolites is to perform trapping experiments with model nucleophiles and to analyze the formed adducts with spectroscopic techniques.

The endogenous tripeptide GSH is commonly used as trapping agent for soft electrophilic metabolites of drugs produced in microsomal incubations. As previously discussed, GSH can trap different types of RIs including quinones, quinoneimines, iminoquinone methides, epoxides, arene oxides and nitrenium ions [118]. The corresponding GSH adducts are typically analyzed by liquid-chromatography mass spectrometry (LC-MS). Usually, tandem mass spectrometry (MS/MS) is used to characterize GSH adducts since they show a characteristic fragmentation pattern consisting of losses of 75 and/or 129 Da corresponding to the peptidic side chains of the GSH moiety. This property has been exploited to develop sensitive and selective MS-based methodologies for the screening of GSH adducts; such as neutral loss, precursor ion and multiple reaction monitoring scanning techniques (Table 7) [119-121]. Although MS detection is usually performed in the positive mode, a recent report suggests that scanning for precursor ions in the negative mode might actually be more efficient in detecting GSH adducts [122].

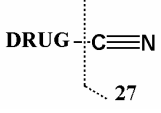
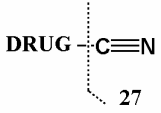
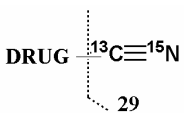
Table 7. Glutathione-based trapping agents and screening methods for “soft” reactive intermediates.

Trapping agent	Trapped drug-conjugate	Detection	Characteristics	References
Glutathione 		MS	+ Standard methodology + Structural information - Sensitivity and selectivity dependent on MS instrument	[119, 121]
Tritiated ³ H-glutathione 		Radio-activity MS	+ Quantitative + Structural information - Radioactivity - Still requires HPLC separation	[123]
Mixture glutathione and stable isotope-labeled glutathione 		MS	+ Unique isotopic MS signature + Unambiguous identification of GSH adducts + Structural information - Radioactivity	[98, 124]
Quaternary ammonium glutathione 		MS	+ Fixed positive charge + Semi-quantitative + Structural information	[125]
Glutathione ethyl ester 		MS	+ Extraction possible + Increased sensitivity + Structural information	[126]
Dansyl glutathione 		FLD MS	+ Quantitative + Fluorescence detection + Not MS-dependent + Structural information - Still requires HPLC separation	[127]

Examples of glutathione-based trapping agents and methods used to identify and characterize *in vitro*-generated “soft” reactive metabolites of drugs. Advantages (+) and disadvantages (-) of the methodologies are also indicated. MS: mass spectrometry; HPLC: high performance liquid chromatography; FLD: fluorescence detection.

Stable isotope trapping experiments (using a mixture of GSH and isotope-labeled GSH) and the use of GSH ethyl ester are other variants that have shown to increase the selectivity and sensitivity in GSH adduct detection [118, 124, 126, 128]. Attempts to quantify amounts of trapped RIs were done by developing novel trapping agents consisting of fluorescent, radio-labeled and quaternary ammonium GSH analogues [125, 127, 128]. An overview of the different glutathione-based trapping agents and methods discussed above are depicted in Table 7.

Table 8. Cyanide-based trapping agents and screening methods for “hard” reactive intermediates.

Trapping agent	Trapped drug-conjugate	Detection	Characteristics	References
Cyanide				
$\text{Na}^+ \text{C}\equiv\text{N}^-$		MS	+ Structural information	[129, 130]
¹⁴ C-Cyanide				
$\text{Na}^+ {}^{14}\text{C}\equiv\text{N}^-$	$\text{DRUG}-{}^{14}\text{C}\equiv\text{N}$	Radioactivity	+ Quantitative - No structural information - Radioactivity	[131, 132]
Mixture cyanide and stable isotope-labeled cyanide				
$\text{K}^+ \text{C}\equiv\text{N}^-$		MS	+ Unique isotopic MS signature + Unambiguous identification of CN adducts	[66, 133]
$\text{K}^+ {}^{13}\text{C}\equiv{}^{15}\text{N}^-$			+ Structural information - Radioactivity	

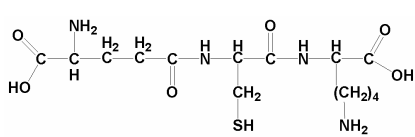
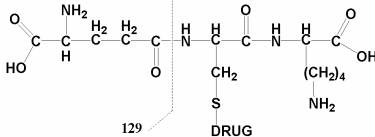

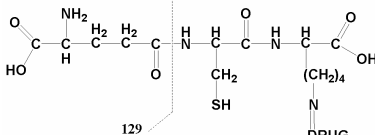
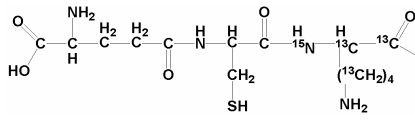
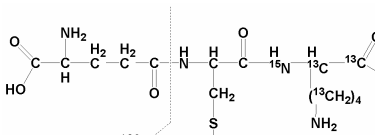

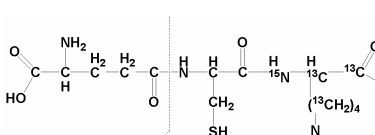
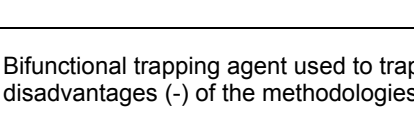
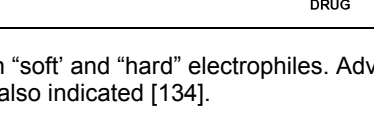
Examples of cyanide-based trapping agents and methods used to identify and characterize *in vitro*-generated “hard” reactive metabolites of drugs. Advantages (+) and disadvantages (-) of the methodologies are also indicated. CN: cyanide.

One generic limitation of the above mentioned methodologies is that GSH trapping experiments are unable to detect all types of RIs [133]. Some of the GSH adducts are unstable and GSH is known to have limited trapping efficiency towards “hard” electrophiles. The latter RIs will more readily react with lysine and histidine residues in proteins and/or with “hard” nucleophilic sites in membranes or DNA. These RIs can be trapped by hard nucleophiles such as the cyanide (CN) anion. Consistently, enzymatic incubations are often performed using sodium or potassium CN as trapping agents for “hard” electrophiles. Radio-labeled [¹⁴C] sodium CN was used to study the bioactivation of alicyclic amines towards reactive iminium intermediates [131]. Recently, a quantitative high-throughput method was set up to evaluate

reactive metabolite formation using [^{14}C] potassium CN [132]. CN adducts also show a typical fragmentation pattern allowing the development of sensitive and selective MS-based methodologies such as neutral loss scanning [66, 133]. The typical isotopic MS profile obtained when using a mixture of CN and radio-labeled [$^{13}\text{C}^{15}\text{N}$] CN may also facilitate adduct detection. A summary of cyanide-based trapping agents and screening methodologies is presented in Table 8.

Interestingly, a new bifunctional trapping agent containing both a cysteine and lysine residue was developed for the simultaneous screening of “hard” and “soft” electrophiles [134]. Neutral loss MS scanning can be performed since this trap also shows the typical 129 Da loss when fragmented. Combined with isotope trapping techniques, this approach could constitute an efficient high-throughput methodology for the screening of a wide variety of reactive metabolites of novel drug candidates (Table 9).

Table 9. Bifunctional trapping agent.

Trapping agent	Trapped drug-conjugate	Characteristics
Mixture bifunctional and stable isotope-labeled bifunctional traps		
		<ul style="list-style-type: none"> + Structural information + Can trap both “hard” and “soft” intermediates + Unique MS signature + Unambiguous identification of adducts - Not quantitative - Radioactivity
		
		
		
		

Bifunctional trapping agent used to trap both “soft” and “hard” electrophiles. Advantages (+) and disadvantages (-) of the methodologies are also indicated [134].

(Bio)synthesis of (reactive) metabolites

Mass spectrometry provides a highly sensitive readout of mass. A major disadvantage, however, is that structural information of the adducts obtained by LC-MS/MS experiments is to some extent limited. MS alone may be insufficient in identifying the exact position of oxidation, to differentiate isomers, or to provide the exact structure of the metabolite [135]. Moreover, excess of endogenous material in biological samples often suppresses the ionization of drug-related compounds, thereby complicating metabolite identification by MS. Novel MS strategies as well as derivatization techniques (e.g. accurate mass measurements, H/D-exchange) may however help to overcome some of the limitations mentioned above [135, 136].

Complementing MS data with Nuclear Magnetic Resonance (NMR) experiments usually allows the determination of the precise location(s) of compound modifications and the exact structural elucidation of drug metabolites and/or resulting adducts. In addition to being particularly good in providing structural information, NMR also has the advantages of being a non-destructive process, a quantitative technique, and to be relatively rapid. Major limitations, however, of classical NMR include its relative insensitivity and its inability of separating compound-dependent signals from those of sample matrices. As a consequence, large amounts of pure metabolite (≥ 1 mg) are necessary for high-quality NMR spectra; which requires laborious metabolite isolation, purification, concentration and sample reconstitution in deuteriated solvent. Although the development of LC-NMR and LC-NMR-MS techniques mitigates to some extent the need for sample purification, other challenges remain (e.g. lack of sensitivity, need of expensive deuteriated buffers) when using those techniques in routine metabolite identification processes [135, 137, 138].

Overall, the main bottleneck in NMR studies remains the need of high amounts of pure metabolites. Classical organic synthesis of drug metabolites may be problematic due to the lack of appropriate synthetic routes and usually only low amounts of metabolites can be generated by mammalian enzymes due to their low catalytic activities. An alternative approach is to use electrochemical oxidation of the parent drug to obtain large amounts of oxidative metabolites. While not all relevant enzymatic metabolites may be obtained, this method has the advantage of being suitable to up-scaling metabolite production, thereby allowing their structural elucidation by NMR as has been shown recently for GSH adducts of clozapine [139] and troglitazone [140].

Biosynthetic tools and fermentation techniques can also be used for the up-scaling of metabolite production [141]. For example, the biosynthesis of large amounts (up to 169 mg) of human-relevant P450 metabolites of diclofenac was demonstrated using microbial bioreactors, allowing their structural characterization by MS and NMR [142]. More recently, the concept of using microbial P450 enzymes (e.g. P450 BM3 also known as CYP102A1) for the production of high amounts of drug metabolites has been proposed. Advantages of bacterial P450s in comparison to human P450s are their stability, higher catalytic activity and their ability to be “engineered” towards the production of human-relevant metabolites [143]. Recently, several P450 BM3 mutants were obtained by a combination of random- and site-directed mutagenesis, and used to metabolize drug-like molecules such as APAP, dextromethorphan, amodiaquine and MDMA [144]. P450 BM3 mutants were also shown to generate high amounts of human metabolites of 7-ethoxycoumarin [145]. Moreover, when prodrugs are converted to “active metabolites” by human P450s, large quantities of the pure metabolites are required to further investigate the drug efficacy, possible toxic effects and pharmacokinetics. In this context P450 BM3 mutants were shown to be successful in generating high amounts of Piceatannol, the human active metabolite of the anticancer agent Resveratrol [146]. The properties of these P450 BM3 mutants could therefore also be used for the production of high amounts of reactive metabolites, thus facilitating their identification, characterization and structural elucidation. This concept will be further explored in the second part of this thesis.

Covalent Binding Studies

Although trapping experiments can give an indication of the intrinsic potential of a drug to be bioactivated to reactive metabolites, little is known about the degree of protein covalent binding *in vitro* and/or *in vivo*. Baillie *et al.* have adopted the measurement of *in vitro* covalent binding to liver microsomal proteins as an early screening tool for drug candidates. For compounds showing a high degree of efficacy and potency in animals, with good pharmacokinetic and physico-chemical properties, a radio-labeled drug analogue is synthesized. Levels of covalent binding are assessed by performing incubations with the radio-analogue *in vitro* with liver enzymatic preparations and *in vivo* in rats. Levels of covalent binding are then compared to a theoretical safety “threshold value of 50 pmol drug equivalent/mg total liver protein”; which is 20-fold less than the covalent binding observed in animals suffering from liver necrosis after administration of a model hepatotoxicant such as APAP [66]. Importantly, this threshold value was considered as a target upper level

more than as an absolute value not to be exceeded. Seeing that as yet no coherent link between reactive metabolite formation, covalent binding to proteins and onset of ADRs is available, covalent binding data should be considered along with other parameters (e.g. the intended clinical use, the severity of indication, dosing-regimen, intended clinical population, etc) in order to decide whether the development of the drug should be discontinued or not [66]. A major advantage of this method is that quantitative data on covalent binding to proteins of the drug and of its metabolites is possible. Major drawbacks, however, include the need of synthetic radio-labeled drug analogues and the complications related to working with radioactivity [118].

“Avoiding structural alerts”

A well-known strategy to decrease the potential of novel drug candidates to form reactive metabolites is to modify the chemical structure of the compounds [148]. This strategy includes the measurement of covalent binding levels of radio-labeled drug candidates in parallel with trapping experiments using GSH, NAc and/or CN.

Structural analysis of the trapped adducts allows, in principle at least, the elucidation of the underlying bioactivation routes of the drug candidate. Subsequent chemical modification of the compounds can be performed to avoid and/or minimize these bioactivation pathways as well as the adduct formation and covalent binding levels [66]. A major difference in comparison to traditional risk assessment strategies is that radioactivity studies are performed early in the drug discovery process, when structural changes in the structure of the new chemical entities are still feasible.

Worth mentioning is that a large amount of experimental data is currently available on the chemical motives that potentially can form reactive metabolites. A comprehensive listing of these potentially harmful chemical structures is available for medicinal chemists [149].

In summary, it is likely that a panel of screening assays has to be performed to assess and decrease the intrinsic potential of novel drug candidates to be bioactivated to reactive metabolites and to covalently modify proteins. A summary of some of the “early” *in vitro* and/or *in vivo* screening tools for RIs is presented in Figure 13.

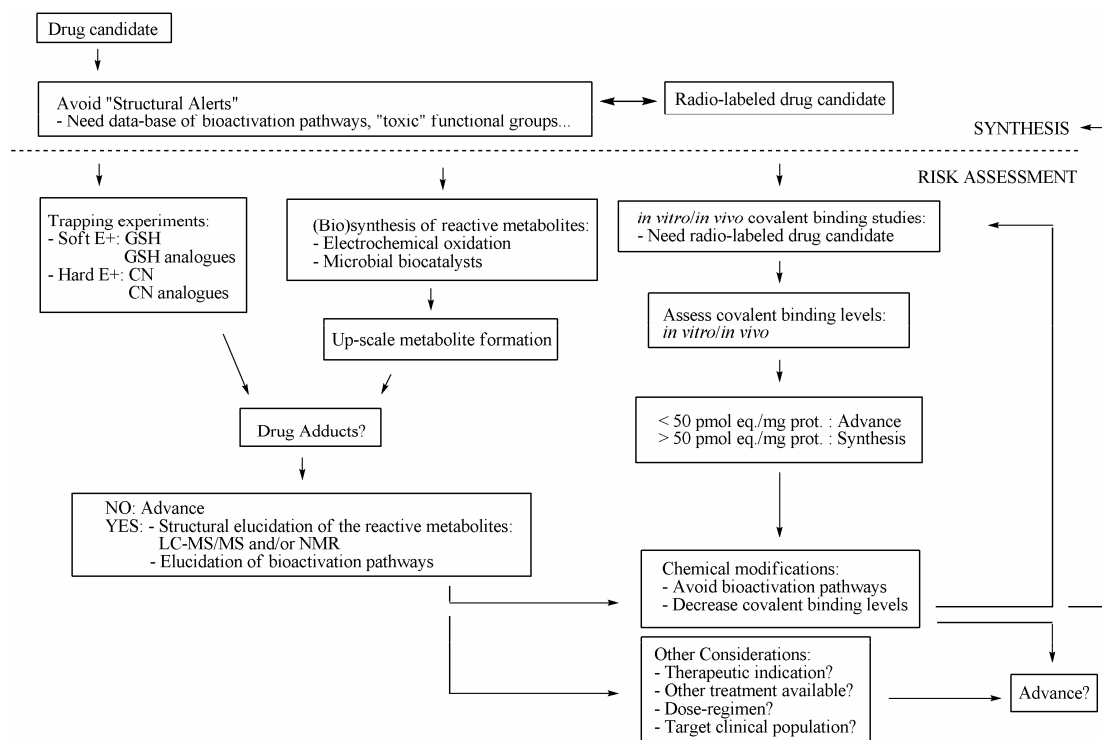


Figure 13. Examples of early screening methods for reactive metabolites. Based on [118, 138]. E⁺: electrophile.

“Late phase/development” *in vivo* biomonitoring tools

In vitro screening tools can assess the potential of novel compounds to be bioactivated to reactive electrophilic intermediates. However, *in vivo* data on covalent binding of drugs and/or drug metabolites to proteins are highly necessary to perform reliable risk assessments. While GSH adducts and/or their decomposition products (e.g. mercapturic acids) measured *in vivo* represent short-term exposure to reactive chemicals, protein adducts better reflect chronic exposure to electrophiles [150, 151]. As such, protein adducts may reflect the internal exposure to RIs *in vivo* which is more relevant for risk assessment purposes. However, as shown for example with the nonhepatotoxic regioisomer of APAP, AMAP, covalent binding to proteins *per se* is not sufficient to induce toxicity. So, next to dosimetry and quantitative considerations, identifying many, if not all, real protein targets of RIs is an important challenge to better understand the links between covalent binding to proteins and organ toxicity [67].

Protein adduct analysis

Protein adduct analysis is difficult and complicated since protein adduct structures are highly complex and variable; they have a short half-life and are usually in very low abundance in comparison to “parent” unmodified proteins [152]. This is typically due to low amounts of reactive metabolites, high concentrations of endogenous trapping agents (e.g. GSH) and to the presence of multiple protein targets [67].

Different methods and strategies have been applied for the investigation and/or detection of drug protein adducts *in vivo* [91, 152]. Briefly, the strategies usually involve first the isolation of drug-protein adducts from the tissue using chromatographic and/or electrophoretic techniques. Direct (semi-)quantitative analysis of protein adducts can be performed using radioisotope-based assays (when the drug is radio-labeled) or by immunological techniques (after raising antibodies against drug-protein adducts in animals) [153]. Adduct analysis can also be performed after chemical and/or enzymatic detachment of the drug moiety from the protein. Digestion of proteins by proteases, with subsequent isolation and purification steps of the peptides, may also facilitate adduct analysis. Adduct and/or drug moiety detection can be performed using different analytical techniques but usually involves chromatography in combination with MS. A scheme of general strategies that can be adopted for protein adduct analysis is depicted in Figure 14.

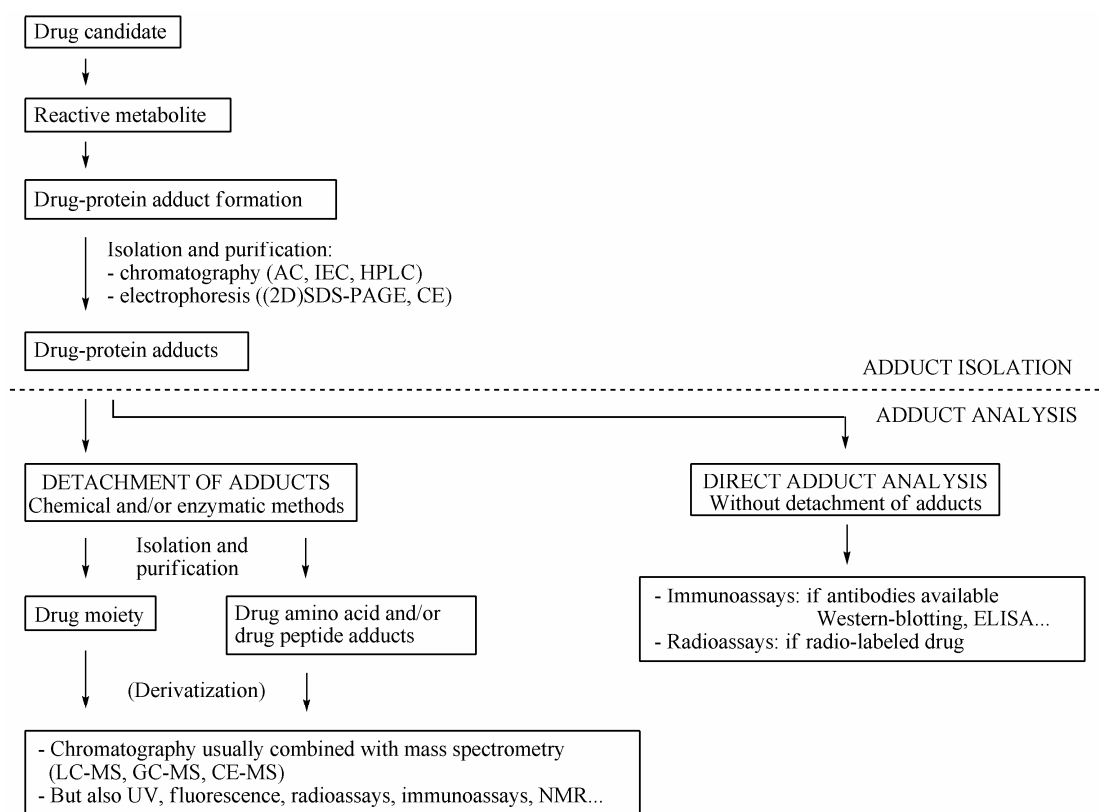


Figure 14. Scheme of general strategies that can be applied for drug-protein adduct analysis. Adapted from [146-148]. AC: affinity chromatography; IEC: ion exchange chromatography; (2D) SDS-PAGE: (two-dimension) sodium dodecyl sulfate polyacrylamide gel electrophoresis; CE: capillary electrophoresis; GC-MS: gas chromatography-mass spectrometry.

Initial work, using radioassays and immunochemical methods, succeeded in measuring covalent binding of several drugs to proteins and to relate it to toxicity. However, at the time, few protein targets of drugs (e.g. halothane, APAP, diclofenac and trichloroethylene) were identified [67]. Major advances in the proteomics technology (e.g. (2D) SDS-PAGE separation techniques combined with autoradiography, MS and/or immunoblotting techniques) have allowed for a more precise identification of proteins adducts. In 2007, more than 120 individual target proteins of drugs and/or other xenobiotics were identified [155]. A web-accessible Target Protein Database was subsequently created for the storage of such information and to facilitate the identification of common protein alkylation patterns of different drugs and/or toxicants [156]. The number of identified target proteins is rapidly expanding and, at the time of the writing of this thesis, this number had increased to 268 in that same database. For example, 32 target hepatic proteins of APAP, 32 target lung proteins of BHT (2,6-di-tert-butyl-4-hydroxytoluene), 17 target

proteins of naphthalene and more than 46 target proteins of bromobenzene have currently been identified. Table 10 depicts some of the identified proteins alkylated by reactive metabolites of drugs involved in ADRs.

Interestingly, recent developments in the proteomics technology (e.g. shotgun proteomics) and in protein functional assays have allowed the study of specific biological consequences of protein adduction (Table 11). For example, biotin-labeled model electrophilic probes (e.g. IAB, PEO-IAB and BMCC, Table 11) have been used for selective and efficient isolation of alkylated proteins and/or peptides by affinity capture. Using this technique, several protein alkylation sites were identified that could directly be related to specific alterations in protein function [175-178]. This approach could therefore be useful to better understand and establish predictive relationships between specific protein modifications and functional changes related to toxicity [67, 176].

Table 10. Examples of target proteins of reactive metabolites of drugs involved in ADRs.

Drug	Target organ/cells	Examples target proteins	Analytical methods	Potential toxicity	References
APAP	Liver Kidney	Glutamine synthetase, lamin A, selenium-binding protein, glutamate dehydrogenase, aldehyde dehydrogenase, N10-formyl tetrahydrofolate dehydrogenase, carbamyl phosphate synthetase I, sulfotransferase analog, GST π , glutathione peroxidase, osteoblast-specific factor 3, mitochondrial ATP synthetase α -subunit, protein initiation factor 4A, Hb	MS Immunoassays Radioisotope assays	Hepatic necrosis Renal toxicity	[72, 157-162]
Carbamazepine	Liver Skin Blood cells	CYP1A2, 2C, 3A4, MPO	MS Immunoassays	Agranulocytosis Aplastic anemia Drug-induced lupus	[16, 46, 111, 116, 117, 163-165]
Diclofenac	Liver	Albumin, CYP2C11, dipeptidyl peptidase IV (CD26), microsomal proteins, intestinal proteins	MS Radioisotope assays Immunoassays	Hepatotoxicity Bone marrow toxicity Gastrointestinal toxicity	[53, 55, 84, 88, 166, 167]
Halothane	Liver Skin	Protein disulfide isomerase, CYP2E1, carboxylesterase, calreticulin, ERp72, ERp99, UDP-glucose: glycoprotein glucosyl-transferase, GST	MS Immunoassays	Halothane hepatitis Skin rash Fever	[168-174]
Tienilic acid	Liver	CYP1A2, 2C9, 2C11 Kidney microsomes	SDS-PAGE Immunoassays MS	Hepatitis	[63, 64]

Examples of drugs involved in ADRs in humans that are known to form reactive metabolites by cytochromes P450 and to covalently bind to proteins. Adapted from [153].

Table 11. Examples of specific biological consequences of protein adduction.

Target protein	Chemical /model electrophile	Selective alkylation site(s)	Specific effect of protein alkylation	Potential toxic effect	References
Hsp90	4-HNE and 4-ONE	Cys572	Inhibition HSP90 activity?	Lipid peroxidation	[179]
Hsp72	4-HNE	Cys267	Inhibition of ATPase activity	Lipid peroxidation	[180]
Thioredoxin 1	Biotinylated 15-deoxy-PGJ2	Cys35 Cys69	n.d.	Intracellular redox alteration	[181]
b-actin	Biotinylated 15-deoxy-PGJ2	Cys374	Protein conformational change	Disruption actin cytoskeleton/ polymerization alterations	[182]
PP2A	PEO-IAB BMCC	- 4 Cys residues in C subunit	No effect Inhibition phosphatase activity	No effect Alteration cellular signaling processes	[177]
HLM	IAB BMCC	243 Cys residues (in 182 proteins) 223 Cys residues (in 151 proteins) ~ 25% common targets	BiP induction No effect	ER stress response up-regulation No effect	[176]
Keap1	tBHQ IAB BMCC	n.d. Central linker domain Other domains	Polyubiquitination Keap1/nrf2 activation Polyubiquitination Keap1/nrf2 activation No effect	ARE/ERE induction ARE/ERE induction No effect	[178]

4-HNE: 4-hydroxy-2-nonenal; 4-ONE: 4-oxo-2-nonenal; Hsp: heat shock protein; PP2A: serine-threonine phosphatase 2A; PEO-IAB: (+)-biotinyl-iodoacetamidyl-3, 6-dioxaoctanediamine; tBHQ: *tert*-butylhydroquinone; IAB: N-iodoacetyl-N-biotinylhexylenediamine; BMCC: 1-biotinamido-4-(4'-[maleimidoethyl-cyclohexane]-carboxamido)butane; n. d. not determined; Cys: cysteine residue; BiP: BIP/GRP78 chaperone; ER: endoplasmic reticulum; HLM: human liver microsomes.

In vivo biomonitoring methods

The methods for protein adduct analysis described previously are time-consuming and labor-intensive. Moreover, they are mainly aimed at the identification of protein targets of reactive metabolites of drugs and to study the biological consequences of protein adduction. In addition to these aspects, biomonitoring tools allowing the determination of internal exposures to reactive metabolites would greatly help risk assessment programs.

Previous work has shown that protein, DNA and mercapturic acid adducts can be used as biomarkers to reflect internal exposures to electrophilic chemicals *in vivo* in humans. Usually, adducts originated from occupational exposure of individuals to reactive, potentially genotoxic, chemicals. While DNA and protein adducts are reflecting (semi-)chronic exposures, mercapturic acid adducts are decomposition products of GSH adducts reflecting recent exposures to electrophilic compounds [150]. For instance, mercapturic acid adducts were measured in the urine of individuals exposed to 1,3-dichloropropene, acrylonitrile and/or benzene. Hemoglobin adducts were found in the erythrocytes of individuals exposed to ethylene oxide, propylene oxide and butadiene; albumin adducts in the blood of workers exposed to benzene and polycyclic aromatic hydrocarbons (e.g. naphthalene and benzo(a)pyrene), and DNA adducts were found in smokers and in individuals exposed to polycyclic aromatic hydrocarbons and butadiene (Table 12) [150].

Most adducts mentioned above arise from chemicals that can be considered as potential mutagens and/or carcinogens, and consequently characterized as “hard” electrophiles. In contrast, only few tools exist for the *in vivo* biomonitoring of protein adducts originating from RIs of drugs related to ADRs and IDRs. In animals, and as discussed previously, Baillie *et al.* have adopted an approach including *in vivo* studies with radio-labeled drug analogues early in the discovery process. Using this approach, pharmacokinetic parameters as well as covalent binding levels to both liver and plasma proteins can be determined *in vivo* in the presence of all bioactivation and/or detoxification pathways [66, 118]. Major disadvantages, however, include the necessity of synthesizing adequate radio-labeled drug analogues and the fact that these studies can not be performed in humans. Consequently, complicated extrapolation of *in vivo* animal data has to be performed subsequently for risk assessment purposes.

Few methodologies exist for the biomonitoring of protein adducts related to ADRs in humans (Table 12). Indeed, many methodologies are too in-sensitive to detect protein adducts *in vivo*. For instance, a Western immunoblotting assay using antisera against protein adducts of acetaminophen showed APAP protein adducts only in the sera of one patient showing the highest increase in liver enzyme levels (>6000 IU/L) and suffering from severe hepatocellular injury [183]. A more sensitive method was developed to detect APAP-cysteine adducts by HPLC with electrochemical detection [184]. In this case, APAP adducts were detected in patients with mild hepatic injury suggesting that this method could be a useful biomonitoring tool to follow exposure to NAPQI and APAP toxicity.

Because of the difficulty in identifying drug-protein adducts *in vivo* in humans, an alternative approach is the detection of plasma antibodies against drug metabolite-modified proteins adducts. For instance, this has allowed the biomonitoring of drug-protein adducts in patients suffering from diclofenac and/or halothane-induced toxicity [153]. Recently, an immunologic methodology was also developed for the biomonitoring of covalent binding of acyl glucuronide metabolites of mycophenolic acid to plasma proteins in renal pediatric patients. This method was used to assess *in vivo* exposure levels to acyl glucuronides that have immunosuppressive and pro-inflammatory activities [185]. This work shows how albumin can be used as model protein for the biomonitoring of reactive metabolites of drugs; a concept that is subject of study in the third part of this thesis.

Table 12. Examples of biomonitoring tools for electrophiles *in vivo* in humans.

Clinical Biomarker	Chemicals/drugs	Matrix	Analytical methods	References
Chemicals related to mutagenicity/carcinogenicity				
Mercapturic acid adducts	1,3-dichloropropene	Urine	GC-MS	[186, 187]
	Benzene	Urine		
Hemoglobin adducts	Butadiene	Blood	MS	[188, 189]
Albumin adducts	Benzene	Serum	GC-MS	[190, 191]
	Benzo(a)pyrene	Serum	Immunoassays	
DNA adducts	Butadiene		³² P-postlabelling	[192, 193]
Drugs related to ADRs/IDRs				
Protein adducts	Acetaminophen	Serum	Immunoassays	[183]
Albumin adducts	Mycophenolic acid	Plasma	Immunoassays	[185]
Cysteine adducts	Acetaminophen	Serum	HPLC with ECD	[184]
Antibodies against protein adducts	Diclofenac	Plasma	Immunoassays	[39, 194]
		Serum	Immunoassays	
	Halothane	Serum	Immunoassays	[60, 195]

ECD: electrochemical detection.

Aims and outline of the thesis

State of research when starting in 2003

When the research described in this thesis started, no reliable strategies were available to predict whether or not the formation of reactive metabolites in patients will result in an adverse drug reaction (ADR) and/or idiosyncratic drug reaction (IDR) to a specific drug. Previous and current *in vitro* and *in vivo* screening strategies usually consist of assessing the potential of novel drugs and drug candidates to generate reactive metabolites that may alkylate macromolecular targets (e.g. proteins) and as a consequence potentially induce ADRs and/or IDRs in humans. Although the causal link “reactive metabolite formation-covalent binding to proteins-onset of ADRs/IDRs” is still unclear, current knowledge supports the assumption that bioactivation to reactive metabolites, whether or not combined with immune-mediated responses, may pose a risk for patients or other drug users.

Nowadays, common strategies during drug discovery and development programs focus on the generation and the characterization of reactive metabolites of drugs, and their assessment *in vivo*. Reactive metabolites are usually initially detected in *in vitro* trapping experiments using different trapping agents (e.g. GSH and CN). These adducts typically reflect the potential of compounds/drugs to form electrophilic metabolites and are meant to better understand the bioactivation mechanisms of the

drug under study but also as a guidance to redesign drug candidate molecules. Major challenges with these experiments, however, are the varying reactivity of the intermediates, their limited extent of formation and consequently their low abundance which is complicating their detection and structural elucidation.

Another major issue for risk assessment purposes is the estimation of *in vivo* exposures to reactive metabolites generated from drugs and drug candidates. As previously discussed, one has meanwhile included *in vivo* experiments with radio-labeled drugs in animals as tool to assess *in vivo* covalent binding levels of drugs and/or their metabolites to proteins. In contrast, when the present research started, no appropriate methods existed for the assessment of the levels of protein adducts and covalent binding to proteins *in vivo* in humans.

Aims and scope of the thesis

The main aim of the research described in this thesis was the development of screening methods for reactive intermediates (RIs) of drugs. The main aim of this work can be divided in two specific aims. More specifically, the first aim of the research consisted of the development and/or improvement of early phase *in vitro* assays for the screening of reactive metabolites. These assays assess the potential of novel drugs and drug candidates to form RIs and GSH adducts *in vitro*. This part of the work therefore focused on the development of novel efficient tools for the generation of high amounts of “reference” reactive metabolites of drugs. The generation of high levels of RIs should enable the development of sensitive and more universal analytical methods for the screening of reactive metabolites. Next to the detection at low levels, higher amounts of reactive metabolites were aimed at to facilitate their characterization and/or structural elucidation by various spectroscopy techniques including NMR.

The second specific aim of the thesis consisted of the development of novel concepts and tools for the biomonitoring of reactive metabolites *in vivo* in humans. As protein adducts, in contrast to GSH-conjugates and mercapturic acids, are typical biomarkers reflecting longer-term exposure to reactive compounds, this strategy aimed at the determination of the *in vivo* human exposure to reactive metabolites. New analytical strategies were developed to assess the potential of drugs and novel drug candidates to be bioactivated to RIs and to covalently bind to proteins *in vivo*, using albumin as a prototype protein. This concept might help achieving more reliable risk assessments.

Outline of the thesis

In the first part of this thesis, **Chapter 1** concerns a general introduction describing the current knowledge about ADRs and IDRs, the role of metabolism and reactive metabolites in the onset of ADRs as well as the current strategies applied for the risk assessment of novel drug candidates.

The second part of the thesis concerns the development of novel *in vitro* tools for the generation, identification and characterization of reactive metabolites. In this section, **Chapter 2** focuses on the use of cytochrome P450 BM3 mutants as novel biocatalysts for the generation and characterization of reactive metabolites of drugs. This chapter shows how higher amounts of (reactive) metabolites of drugs can be generated by mutant bacterial cytochromes P450. This allowed the discovery of novel human-relevant GSH adducts of several marketed drugs. The potential role of glutathione S-transferases (GSTs) in catalyzing the conjugation of reactive metabolites of drugs with GSH was investigated in **Chapter 3**. Here, it was investigated whether GSH adduct formation could further be increased by the addition of GSTs in enzymatic incubations. Eventually, the tools developed in chapter 2 and 3 with several model drugs (e.g. acetaminophen, clozapine, diclofenac, carbamazepine and 3-hydroxyacetanilide) were evaluated with trimethoprim, a drug that has been involved in serious IDRs in humans but of which the involvement of cytochromes P450 in its bioactivation was still largely unknown. The overall bioactivation and GSH adduct formation of trimethoprim were investigated in **Chapter 4**.

The third part of the thesis concerns the development of novel tools for the biomonitoring of reactive metabolites *in vivo* in humans. Albumin adducts of acetaminophen were evaluated as *in vivo* biomarkers for reactive metabolites formed in humans in **Chapter 5**. A generic strategy for the generation of reference albumin adducts of acetaminophen, with subsequent adduct analysis in plasma of patients exposed to the drug, is proposed. An automated on-line LC-MS/MS system, allowing a higher throughput in albumin adducts analysis, was subsequently developed and is described in **Chapter 6**.

In the last part of this thesis, **Chapter 7** concerns an overall summary of the work described in the thesis including general conclusions and perspectives for future work.

References

- [1] Gomes, E. R. and Demoly, P. (2005) Epidemiology of hypersensitivity drug reactions. *Curr Opin Allergy Clin Immunol.* 5, 309-316.
- [2] Lazarou, J., Pomeranz, B. H. and Corey, P. N. (1998) Incidence of adverse drug reactions in hospitalized patients: a meta-analysis of prospective studies. *Jama.* 279, 1200-1205.
- [3] Askmark, H. and Wiholm, B. E. (1990) Epidemiology of adverse reactions to carbamazepine as seen in a spontaneous reporting system. *Acta Neurol Scand.* 81, 131-140.
- [4] Demoly, P. and Bousquet, J. (2001) Epidemiology of drug allergy. *Curr Opin Allergy Clin Immunol.* 1, 305-310.
- [5] Pirmohamed, M., James, S., Meakin, S., Green, C., Scott, A. K., Walley, T. J., Farrar, K., Park, B. K. and Breckenridge, A. M. (2004) Adverse drug reactions as cause of admission to hospital: prospective analysis of 18 820 patients. *Bmj.* 329, 15-19.
- [6] Einarson, T. R. (1993) Drug-related hospital admissions. *Ann Pharmacother.* 27, 832-840.
- [7] Lasser, K. E., Allen, P. D., Woolhandler, S. J., Himmelstein, D. U., Wolfe, S. M. and Bor, D. H. (2002) Timing of new black box warnings and withdrawals for prescription medications. *Jama.* 287, 2215-2220.
- [8] <http://www.fda.gov/>.
- [9] Smith, D. A. and Schmid, E. F. (2006) Drug withdrawals and the lessons within. *Curr Opin Drug Discov Devel.* 9, 38-46.
- [10] Williams, D. P., Kitteringham, N. R., Naisbitt, D. J., Pirmohamed, M., Smith, D. A. and Park, B. K. (2002) Are chemically reactive metabolites responsible for adverse reactions to drugs? *Curr Drug Metab.* 3, 351-366.
- [11] Li, A. P. (2002) A review of the common properties of drugs with idiosyncratic hepatotoxicity and the "multiple determinant hypothesis" for the manifestation of idiosyncratic drug toxicity. *Chem Biol Interact.* 142, 7-23.
- [12] Navarro, V. J. and Senior, J. R. (2006) Drug-related hepatotoxicity. *N Engl J Med.* 354, 731-739.
- [13] Park, B. K., Kitteringham, N. R., Powell, H. and Pirmohamed, M. (2000) Advances in molecular toxicology-towards understanding idiosyncratic drug toxicity. *Toxicology.* 153, 39-60.
- [14] Weiss, M. E. and Adkinson, N. F. (1988) Immediate hypersensitivity reactions to penicillin and related antibiotics. *Clin Allergy.* 18, 515-540.
- [15] Ju, C. and Uetrecht, J. P. (1999) Detection of 2-hydroxyimino stilbene in the urine of patients taking carbamazepine and its oxidation to a reactive iminoquinone intermediate. *J Pharmacol Exp Ther.* 288, 51-56.
- [16] Madden, S., Maggs, J. L. and Park, B. K. (1996) Bioactivation of carbamazepine in the rat in vivo. Evidence for the formation of reactive arene oxide(s). *Drug Metab Dispos.* 24, 469-479.
- [17] Alvir, J. M., Lieberman, J. A., Safferman, A. Z., Schwimmer, J. L. and Schaaf, J. A. (1993) Clozapine-induced agranulocytosis. Incidence and risk factors in the United States. *N Engl J Med.* 329, 162-167.
- [18] Ono, K., Kurohara, K., Yoshihara, M., Shimamoto, Y. and Yamaguchi, M. (1991) Agranulocytosis caused by ticlopidine and its mechanism. *Am J Hematol.* 37, 239-242.
- [19] Uetrecht, J. P., Zahid, N. and Whitfield, D. (1994) Metabolism of vesnarinone by activated neutrophils: implications for vesnarinone-induced agranulocytosis. *J Pharmacol Exp Ther.* 270, 865-872.
- [20] Jewell, H., Maggs, J. L., Harrison, A. C., O'Neill, P. M., Ruscoe, J. E. and Park, B. K. (1995) Role of hepatic metabolism in the bioactivation and detoxication of amodiaquine. *Xenobiotica.* 25, 199-217.
- [21] Maggs, J. L., Kitteringham, N. R., Breckenridge, A. M. and Park, B. K. (1987) Autoxidative formation of a chemically reactive intermediate from amodiaquine, a myelotoxin and hepatotoxin in man. *Biochem Pharmacol.* 36, 2061-2062.
- [22] Aithal, G. P. and Day, C. P. (2007) Nonsteroidal anti-inflammatory drug-induced hepatotoxicity. *Clin Liver Dis.* 11, 563-575, vi-vii.
- [23] Park, B. K., Pirmohamed, M. and Kitteringham, N. R. (1998) Role of drug disposition in drug hypersensitivity: a chemical, molecular, and clinical perspective. *Chem Res Toxicol.* 11, 969-988.
- [24] Bigby, M., Jick, S., Jick, H. and Arndt, K. (1986) Drug-induced cutaneous reactions. A report from the Boston Collaborative Drug Surveillance Program on 15,438 consecutive inpatients, 1975 to 1982. *Jama.* 256, 3358-3363.
- [25] Hyson, C. and Sadler, M. (1997) Cross sensitivity of skin rashes with antiepileptic drugs. *Can J Neurol Sci.* 24, 245-249.
- [26] Uetrecht, J. (2007) Idiosyncratic drug reactions: current understanding. *Annu Rev Pharmacol Toxicol.* 47, 513-539.
- [27] Pellock, J. M. (1999) Felbamate in epilepsy therapy: evaluating the risks. *Drug Saf.* 21, 225-239.

- [28] Goldkind, L. and Laine, L. (2006) A systematic review of NSAIDs withdrawn from the market due to hepatotoxicity: lessons learned from the bromfenac experience. *Pharmacoepidemiol Drug Saf.* 15, 213-220.
- [29] Graham, D. J., Drinkard, C. R. and Shatin, D. (2003) Incidence of idiopathic acute liver failure and hospitalized liver injury in patients treated with troglitazone. *Am J Gastroenterol.* 98, 175-179.
- [30] Olanow, C. W. and Watkins, P. B. (2007) Tolcapone: an efficacy and safety review (2007). *Clin Neuropharmacol.* 30, 287-294.
- [31] Kang, B. J., Cho, M. J., Oh, J. T., Lee, Y., Chae, B. J. and Ko, J. (2006) Long-term patient monitoring for clozapine-induced agranulocytosis and neutropenia in Korea: when is it safe to discontinue CPMS? *Hum Psychopharmacol.* 21, 387-391.
- [32] Mockenhaupt, M., Viboud, C., Dunant, A., Naldi, L., Halevy, S., Bouwes Bavinck, J. N., Sidoroff, A., Schneck, J., Roujeau, J. C. and Flahault, A. (2008) Stevens-Johnson syndrome and toxic epidermal necrolysis: assessment of medication risks with emphasis on recently marketed drugs. The EuroSCAR-study. *J Invest Dermatol.* 128, 35-44.
- [33] Smith, D. A., Obach, R. S., Williams, D. P. and Park, B. K. (2008) Clearing the MIST (metabolites in safety testing) of time: The impact of duration of administration on drug metabolite toxicity. *Chem Biol Interact.*
- [34] Rieder, M. J., Shear, N. H., Kanee, A., Tang, B. K. and Spielberg, S. P. (1991) Prominence of slow acetylator phenotype among patients with sulfonamide hypersensitivity reactions. *Clin Pharmacol Ther.* 49, 13-17.
- [35] Huang, Y. S., Chern, H. D., Su, W. J., Wu, J. C., Lai, S. L., Yang, S. Y., Chang, F. Y. and Lee, S. D. (2002) Polymorphism of the N-acetyltransferase 2 gene as a susceptibility risk factor for antituberculosis drug-induced hepatitis. *Hepatology.* 35, 883-889.
- [36] Mallal, S., Nolan, D., Witt, C., Masel, G., Martin, A. M., Moore, C., Sayer, D., Castley, A., Mamotte, C., Maxwell, D., James, I. and Christiansen, F. T. (2002) Association between presence of HLA-B*5701, HLA-DR7, and HLA-DQ3 and hypersensitivity to HIV-1 reverse-transcriptase inhibitor abacavir. *Lancet.* 359, 727-732.
- [37] Phillips, E. J. (2006) Genetic screening to prevent abacavir hypersensitivity reaction: are we there yet? *Clin Infect Dis.* 43, 103-105.
- [38] Hung, S. I., Chung, W. H., Liou, L. B., Chu, C. C., Lin, M., Huang, H. P., Lin, Y. L., Lan, J. L., Yang, L. C., Hong, H. S., Chen, M. J., Lai, P. C., Wu, M. S., Chu, C. Y., Wang, K. H., Chen, C. H., Fann, C. S., Wu, J. Y. and Chen, Y. T. (2005) HLA-B*5801 allele as a genetic marker for severe cutaneous adverse reactions caused by allopurinol. *Proc Natl Acad Sci U S A.* 102, 4134-4139.
- [39] Aithal, G. P., Ramsay, L., Daly, A. K., Sonchit, N., Leathart, J. B., Alexander, G., Kenna, J. G., Caldwell, J. and Day, C. P. (2004) Hepatic adducts, circulating antibodies, and cytokine polymorphisms in patients with diclofenac hepatotoxicity. *Hepatology.* 39, 1430-1440.
- [40] Walton, B., Simpson, B. R., Strunin, L., Doniach, D., Perrin, J. and Appleyard, A. J. (1976) Unexplained hepatitis following halothane. *Br Med J.* 1, 1171-1176.
- [41] Van Der Ven, A. J., Koopmans, P. P., Vree, T. B. and Van Der Meer, J. W. (1991) Adverse reactions to co-trimoxazole in HIV infection. *Lancet.* 338, 431-433.
- [42] Matzinger, P. (1994) Tolerance, danger, and the extended family. *Annu Rev Immunol.* 12, 991-1045.
- [43] Pichler, W. J., Beeler, A., Keller, M., Lerch, M., Posadas, S., Schmid, D., Spanou, Z., Zawodniak, A. and Gerber, B. (2006) Pharmacological interaction of drugs with immune receptors: the p-i concept. *Allergol Int.* 55, 17-25.
- [44] Woolf, T. F. and Jordan, R. A. (1987) Basic concepts in drug metabolism: Part I. *J Clin Pharmacol.* 27, 15-17.
- [45] Jordan, R. A. and Woolf, T. F. (1987) Basic concepts in drug metabolism: Part II. *J Clin Pharmacol.* 27, 87-90.
- [46] Lillibridge, J. H., Amore, B. M., Slattery, J. T., Kalthorn, T. F., Nelson, S. D., Finnell, R. H. and Bennett, G. D. (1996) Protein-reactive metabolites of carbamazepine in mouse liver microsomes. *Drug Metab Dispos.* 24, 509-514.
- [47] Cattle, L., Munns, A. J., Hogg, N. A., Scott, J. R., Hooper, W. D., Dickinson, R. G. and Gillam, E. M. (2000) Phenytoin metabolism by human cytochrome P450: involvement of P450 3A and 2C forms in secondary metabolism and drug-protein adduct formation. *Drug Metab Dispos.* 28, 945-950.
- [48] Munns, A. J., De Voss, J. J., Hooper, W. D., Dickinson, R. G. and Gillam, E. M. (1997) Bioactivation of phenytoin by human cytochrome P450: characterization of the mechanism and targets of covalent adduct formation. *Chem Res Toxicol.* 10, 1049-1058.
- [49] Cohen, S. D., Pumford, N. R., Khairallah, E. A., Boekelheide, K., Pohl, L. R., Amouzadeh, H. R. and Hinson, J. A. (1997) Selective protein covalent binding and target organ toxicity. *Toxicol Appl Pharmacol.* 143, 1-12.
- [50] Hinson, J. A., Pumford, N. R. and Roberts, D. W. (1995) Mechanisms of acetaminophen toxicity: immunochemical detection of drug-protein adducts. *Drug Metab Rev.* 27, 73-92.

- [51] Bartolone, J. B., Beierschmitt, W. P., Birge, R. B., Hart, S. G., Wyand, S., Cohen, S. D. and Khairallah, E. A. (1989) Selective acetaminophen metabolite binding to hepatic and extrahepatic proteins: an in vivo and in vitro analysis. *Toxicol Appl Pharmacol.* 99, 240-249.
- [52] Tang, W., Stearns, R. A., Bandiera, S. M., Zhang, Y., Raab, C., Braun, M. P., Dean, D. C., Pang, J., Leung, K. H., Doss, G. A., Strauss, J. R., Kwei, G. Y., Rushmore, T. H., Chiu, S. H. and Baillie, T. A. (1999) Studies on cytochrome P-450-mediated bioactivation of diclofenac in rats and in human hepatocytes: identification of glutathione conjugated metabolites. *Drug Metab Dispos.* 27, 365-372.
- [53] Shen, S., Marchick, M. R., Davis, M. R., Doss, G. A. and Pohl, L. R. (1999) Metabolic activation of diclofenac by human cytochrome P450 3A4: role of 5-hydroxydiclofenac. *Chem Res Toxicol.* 12, 214-222.
- [54] Poon, G. K., Chen, Q., Teffera, Y., Ngui, J. S., Griffin, P. R., Braun, M. P., Doss, G. A., Freedman, C., Stearns, R. A., Evans, D. C., Baillie, T. A. and Tang, W. (2001) Bioactivation of diclofenac via benzoquinone imine intermediates-identification of urinary mercapturic acid derivatives in rats and humans. *Drug Metab Dispos.* 29, 1608-1613.
- [55] Kretz-Rommel, A. and Boelsterli, U. A. (1994) Mechanism of covalent adduct formation of diclofenac to rat hepatic microsomal proteins. Retention of the glucuronic acid moiety in the adduct. *Drug Metab Dispos.* 22, 956-961.
- [56] Harrison, A. C., Kitteringham, N. R., Clarke, J. B. and Park, B. K. (1992) The mechanism of bioactivation and antigen formation of amodiaquine in the rat. *Biochem Pharmacol.* 43, 1421-1430.
- [57] Kassahun, K., Pearson, P. G., Tang, W., McIntosh, I., Leung, K., Elmore, C., Dean, D., Wang, R., Doss, G. and Baillie, T. A. (2001) Studies on the metabolism of troglitazone to reactive intermediates in vitro and in vivo. Evidence for novel biotransformation pathways involving quinone methide formation and thiazolidinedione ring scission. *Chem Res Toxicol.* 14, 62-70.
- [58] Tettey, J. N., Maggs, J. L., Rapeport, W. G., Pirmohamed, M. and Park, B. K. (2001) Enzyme-induction dependent bioactivation of troglitazone and troglitazone quinone in vivo. *Chem Res Toxicol.* 14, 965-974.
- [59] Satoh, H., Gillette, J. R., Davies, H. W., Schulick, R. D. and Pohl, L. R. (1985) Immunochemical evidence of trifluoroacetylated cytochrome P-450 in the liver of halothane-treated rats. *Mol Pharmacol.* 28, 468-474.
- [60] Kenna, J. G., Satoh, H., Christ, D. D. and Pohl, L. R. (1988) Metabolic basis for a drug hypersensitivity: antibodies in sera from patients with halothane hepatitis recognize liver neoantigens that contain the trifluoroacetyl group derived from halothane. *J Pharmacol Exp Ther.* 245, 1103-1109.
- [61] Gardner, I., Leeder, J. S., Chin, T., Zahid, N. and Uetrecht, J. P. (1998) A comparison of the covalent binding of clozapine and olanzapine to human neutrophils in vitro and in vivo. *Mol Pharmacol.* 53, 999-1008.
- [62] Williams, D. P., Pirmohamed, M., Naisbitt, D. J., Maggs, J. L. and Park, B. K. (1997) Neutrophil cytotoxicity of the chemically reactive metabolite(s) of clozapine: possible role in agranulocytosis. *J Pharmacol Exp Ther.* 283, 1375-1382.
- [63] Leceour, S., Bonierbale, E., Challine, D., Gautier, J. C., Valadon, P., Dansette, P. M., Catinot, R., Ballet, F., Mansuy, D. and Beaune, P. H. (1994) Specificity of in vitro covalent binding of tienilic acid metabolites to human liver microsomes in relationship to the type of hepatotoxicity: comparison with two directly hepatotoxic drugs. *Chem Res Toxicol.* 7, 434-442.
- [64] Koenigs, L. L., Peter, R. M., Hunter, A. P., Haining, R. L., Rettie, A. E., Friedberg, T., Pritchard, M. P., Shou, M., Rushmore, T. H. and Trager, W. F. (1999) Electrospray ionization mass spectrometric analysis of intact cytochrome P450: identification of tienilic acid adducts to P450 2C9. *Biochemistry.* 38, 2312-2319.
- [65] Valadon, P., Dansette, P. M., Girault, J. P., Amar, C. and Mansuy, D. (1996) Thiophene sulfoxides as reactive metabolites: formation upon microsomal oxidation of a 3-arylthiophene and fate in the presence of nucleophiles in vitro and in vivo. *Chem Res Toxicol.* 9, 1403-1413.
- [66] Evans, D. C., Watt, A. P., Nicoll-Griffith, D. A. and Baillie, T. A. (2004) Drug-protein adducts: an industry perspective on minimizing the potential for drug bioactivation in drug discovery and development. *Chem Res Toxicol.* 17, 3-16.
- [67] Liebler, D. C. (2008) Protein damage by reactive electrophiles: targets and consequences. *Chem Res Toxicol.* 21, 117-128.
- [68] Guengerich, F. P. (2005) Generation of reactive intermediates. *J Biochem Mol Toxicol.* 19, 173-174.
- [69] Kaplowitz, N. (2005) Idiosyncratic drug hepatotoxicity. *Nat Rev Drug Discov.* 4, 489-499.
- [70] Ostapowicz, G., Fontana, R. J., Schiodt, F. V., Larson, A., Davern, T. J., Han, S. H., McCashland, T. M., Shakil, A. O., Hay, J. E., Hynan, L., Crippin, J. S., Blei, A. T., Samuel, G., Reisch, J. and Lee, W. M. (2002) Results of a prospective study of acute liver failure at 17 tertiary care centers in the United States. *Ann Intern Med.* 137, 947-954.
- [71] Morgan, O., Griffiths, C. and Majeed, A. (2005) Impact of paracetamol pack size restrictions on poisoning from paracetamol in England and Wales: an observational study. *J Public Health (Oxf).* 27, 19-24.

- [72] Bessems, J. G. and Vermeulen, N. P. (2001) Paracetamol (acetaminophen)-induced toxicity: molecular and biochemical mechanisms, analogues and protective approaches. *Crit Rev Toxicol.* 31, 55-138.
- [73] Raucy, J. L., Lasker, J. M., Lieber, C. S. and Black, M. (1989) Acetaminophen activation by human liver cytochromes P450IIE1 and P450IA2. *Arch Biochem Biophys.* 271, 270-283.
- [74] Thummel, K. E., Lee, C. A., Kunze, K. L., Nelson, S. D. and Slattery, J. T. (1993) Oxidation of acetaminophen to N-acetyl-p-aminobenzoquinone imine by human CYP3A4. *Biochem Pharmacol.* 45, 1563-1569.
- [75] Jollow, D. J., Mitchell, J. R., Potter, W. Z., Davis, D. C., Gillette, J. R. and Brodie, B. B. (1973) Acetaminophen-induced hepatic necrosis. II. Role of covalent binding in vivo. *J Pharmacol Exp Ther.* 187, 195-202.
- [76] Roberts, S. A., Price, V. F. and Jollow, D. J. (1990) Acetaminophen structure-toxicity studies: in vivo covalent binding of a nonhepatotoxic analog, 3-hydroxyacetanilide. *Toxicol Appl Pharmacol.* 105, 195-208.
- [77] Rashed, M. S., Myers, T. G. and Nelson, S. D. (1990) Hepatic protein arylation, glutathione depletion, and metabolite profiles of acetaminophen and a non-hepatotoxic regioisomer, 3'-hydroxyacetanilide, in the mouse. *Drug Metab Dispos.* 18, 765-770.
- [78] Streeter, A. J., Bjorge, S. M., Axworthy, D. B., Nelson, S. D. and Baillie, T. A. (1984) The microsomal metabolism and site of covalent binding to protein of 3'-hydroxyacetanilide, a nonhepatotoxic positional isomer of acetaminophen. *Drug Metab Dispos.* 12, 565-576.
- [79] Rashed, M. S. and Nelson, S. D. (1989) Use of thermospray liquid chromatography-mass spectrometry for characterization of reactive metabolites of 3'-hydroxyacetanilide, a non-hepatotoxic regioisomer of acetaminophen. *J Chromatogr.* 474, 209-222.
- [80] Rashed, M. S. and Nelson, S. D. (1989) Characterization of glutathione conjugates of reactive metabolites of 3'-hydroxyacetanilide, a nonhepatotoxic positional isomer of acetaminophen. *Chem Res Toxicol.* 2, 41-45.
- [81] Myers, T. G., Dietz, E. C., Anderson, N. L., Khairallah, E. A., Cohen, S. D. and Nelson, S. D. (1995) A comparative study of mouse liver proteins arylated by reactive metabolites of acetaminophen and its nonhepatotoxic regioisomer, 3'-hydroxyacetanilide. *Chem Res Toxicol.* 8, 403-413.
- [82] Garcia Rodriguez, L. A., Williams, R., Derby, L. E., Dean, A. D. and Jick, H. (1994) Acute liver injury associated with nonsteroidal anti-inflammatory drugs and the role of risk factors. *Arch Intern Med.* 154, 311-316.
- [83] Banks, A. T., Zimmerman, H. J., Ishak, K. G. and Harter, J. G. (1995) Diclofenac-associated hepatotoxicity: analysis of 180 cases reported to the Food and Drug Administration as adverse reactions. *Hepatology.* 22, 820-827.
- [84] Tang, W., Stearns, R. A., Wang, R. W., Chiu, S. H. and Baillie, T. A. (1999) Roles of human hepatic cytochrome P450s 2C9 and 3A4 in the metabolic activation of diclofenac. *Chem Res Toxicol.* 12, 192-199.
- [85] Yan, Z., Li, J., Huebert, N., Caldwell, G. W., Du, Y. and Zhong, H. (2005) Detection of a novel reactive metabolite of diclofenac: evidence for CYP2C9-mediated bioactivation via arene oxides. *Drug Metab Dispos.* 33, 706-713.
- [86] Stierlin, H. and Faigle, J. W. (1979) Biotransformation of diclofenac sodium (Voltaren) in animals and in man. II. Quantitative determination of the unchanged drug and principal phenolic metabolites, in urine and bile. *Xenobiotica.* 9, 611-621.
- [87] Stierlin, H., Faigle, J. W., Sallmann, A., Kung, W., Richter, W. J., Kriemler, H. P., Alt, K. O. and Winkler, T. (1979) Biotransformation of diclofenac sodium (Voltaren) in animals and in man. I. Isolation and identification of principal metabolites. *Xenobiotica.* 9, 601-610.
- [88] Kretz-Rommel, A. and Boelsterli, U. A. (1994) Selective protein adducts to membrane proteins in cultured rat hepatocytes exposed to diclofenac: radiochemical and immunochemical analysis. *Mol Pharmacol.* 45, 237-244.
- [89] Boelsterli, U. A. (2003) Diclofenac-induced liver injury: a paradigm of idiosyncratic drug toxicity. *Toxicol Appl Pharmacol.* 192, 307-322.
- [90] Hargus, S. J., Amouzedeh, H. R., Pumford, N. R., Myers, T. G., McCoy, S. C. and Pohl, L. R. (1994) Metabolic activation and immunochemical localization of liver protein adducts of the nonsteroidal anti-inflammatory drug diclofenac. *Chem Res Toxicol.* 7, 575-582.
- [91] Zhou, S., Chan, E., Duan, W., Huang, M. and Chen, Y. Z. (2005) Drug bioactivation, covalent binding to target proteins and toxicity relevance. *Drug Metab Rev.* 37, 41-213.
- [92] Atkin, K., Kendall, F., Gould, D., Freeman, H., Liberman, J. and O'sullivan, D. (1996) Neutropenia and agranulocytosis in patients receiving clozapine in the UK and Ireland. *Br J Psychiatry.* 169, 483-488.
- [93] Pirmohamed, M., Williams, D., Madden, S., Templeton, E. and Park, B. K. (1995) Metabolism and bioactivation of clozapine by human liver in vitro. *J Pharmacol Exp Ther.* 272, 984-990.
- [94] Tugnait, M., Hawes, E. M., McKay, G., Eichelbaum, M. and Midha, K. K. (1999) Characterization of the human hepatic cytochromes P450 involved in the in vitro oxidation of clozapine. *Chem Biol Interact.* 118, 171-189.

- [95] Uetrecht, J. P. (1992) Metabolism of clozapine by neutrophils. Possible implications for clozapine-induced agranulocytosis. *Drug Saf.* 7 Suppl 1, 51-56.
- [96] Maggs, J. L., Williams, D., Pirmohamed, M. and Park, B. K. (1995) The metabolic formation of reactive intermediates from clozapine, a drug associated with agranulocytosis in man. *J Pharmacol Exp Ther.* 275, 1463-1475.
- [97] Liu, Z. C. and Uetrecht, J. P. (1995) Clozapine is oxidized by activated human neutrophils to a reactive nitrenium ion that irreversibly binds to the cells. *J Pharmacol Exp Ther.* 275, 1476-1483.
- [98] Yan, Z., Maher, N., Torres, R., Caldwell, G. W. and Huebert, N. (2005) Rapid detection and characterization of minor reactive metabolites using stable-isotope trapping in combination with tandem mass spectrometry. *Rapid Commun Mass Spectrom.* 19, 3322-3330.
- [99] Vittorio, C. C. and Muglia, J. J. (1995) Anticonvulsant hypersensitivity syndrome. *Arch Intern Med.* 155, 2285-2290.
- [100] Tennis, P. and Stern, R. S. (1997) Risk of serious cutaneous disorders after initiation of use of phenytoin, carbamazepine, or sodium valproate: a record linkage study. *Neurology.* 49, 542-546.
- [101] Leeder, J. S. (1998) Mechanisms of idiosyncratic hypersensitivity reactions to antiepileptic drugs. *Epilepsia.* 39 Suppl 7, S8-16.
- [102] Pellock, J. M. (1987) Carbamazepine side effects in children and adults. *Epilepsia.* 28 Suppl 3, S64-70.
- [103] Romero Maldonado, N., Sendra Tello, J., Raboso Garcia-Baquero, E. and Harto Castano, A. (2002) Anticonvulsant hypersensitivity syndrome with fatal outcome. *Eur J Dermatol.* 12, 503-505.
- [104] Shear, N. H. and Spielberg, S. P. (1988) Anticonvulsant hypersensitivity syndrome. In vitro assessment of risk. *J Clin Invest.* 82, 1826-1832.
- [105] Naisbitt, D. J., Britschgi, M., Wong, G., Farrell, J., Depta, J. P., Chadwick, D. W., Pichler, W. J., Pirmohamed, M. and Park, B. K. (2003) Hypersensitivity reactions to carbamazepine: characterization of the specificity, phenotype, and cytokine profile of drug-specific T cell clones. *Mol Pharmacol.* 63, 732-741.
- [106] Leeder, J. S., Gaedigk, A., Lu, X. and Cook, V. A. (1996) Epitope mapping studies with human anti-cytochrome P450 3A antibodies. *Mol Pharmacol.* 49, 234-243.
- [107] Park, B. K., Coleman, J. W. and Kitteringham, N. R. (1987) Drug disposition and drug hypersensitivity. *Biochem Pharmacol.* 36, 581-590.
- [108] Lertratanakoon, K. and Horning, M. G. (1982) Metabolism of carbamazepine. *Drug Metab Dispos.* 10, 1-10.
- [109] Schutz, H., Feldmann, K. F., Faigle, J. W., Kriemler, H. P. and Winkler, T. (1986) The metabolism of ¹⁴C-oxcarbazepine in man. *Xenobiotica.* 16, 769-778.
- [110] Riley, R. J., Kitteringham, N. R. and Park, B. K. (1989) Structural requirements for bioactivation of anticonvulsants to cytotoxic metabolites in vitro. *Br J Clin Pharmacol.* 28, 482-487.
- [111] Pirmohamed, M., Kitteringham, N. R., Guenther, T. M., Breckenridge, A. M. and Park, B. K. (1992) An investigation of the formation of cytotoxic, protein-reactive and stable metabolites from carbamazepine in vitro. *Biochem Pharmacol.* 43, 1675-1682.
- [112] Pirmohamed, M., Kitteringham, N. R., Breckenridge, A. M. and Park, B. K. (1992) The effect of enzyme induction on the cytochrome P450-mediated bioactivation of carbamazepine by mouse liver microsomes. *Biochem Pharmacol.* 44, 2307-2314.
- [113] Pearce, R. E., Uetrecht, J. P. and Leeder, J. S. (2005) Pathways of carbamazepine bioactivation in vitro: II. The role of human cytochrome P450 enzymes in the formation of 2-hydroxyiminostilbene. *Drug Metab Dispos.* 33, 1819-1826.
- [114] Bu, H. Z., Kang, P., Deese, A. J., Zhao, P. and Pool, W. F. (2005) Human in vitro glutathionyl and protein adducts of carbamazepine-10,11-epoxide, a stable and pharmacologically active metabolite of carbamazepine. *Drug Metab Dispos.* 33, 1920-1924.
- [115] Bu, H. Z., Zhao, P., Dalvie, D. K. and Pool, W. F. (2007) Identification of primary and sequential bioactivation pathways of carbamazepine in human liver microsomes using liquid chromatography/tandem mass spectrometry. *Rapid Commun Mass Spectrom.* 21, 3317-3322.
- [116] Furst, S. M. and Uetrecht, J. P. (1993) Carbamazepine metabolism to a reactive intermediate by the myeloperoxidase system of activated neutrophils. *Biochem Pharmacol.* 45, 1267-1275.
- [117] Furst, S. M., Sukhai, P., McClelland, R. A. and Uetrecht, J. P. (1995) Covalent binding of carbamazepine oxidative metabolites to neutrophils. *Drug Metab Dispos.* 23, 590-594.
- [118] Caldwell, G. W. and Yan, Z. (2006) Screening for reactive intermediates and toxicity assessment in drug discovery. *Curr Opin Drug Discov Devel.* 9, 47-60.
- [119] Baillie, T. A. and Davis, M. R. (1993) Mass spectrometry in the analysis of glutathione conjugates. *Biol Mass Spectrom.* 22, 319-325.
- [120] Castro-Perez, J., Plumb, R., Liang, L. and Yang, E. (2005) A high-throughput liquid chromatography/tandem mass spectrometry method for screening glutathione conjugates using exact mass neutral loss acquisition. *Rapid Commun Mass Spectrom.* 19, 798-804.

- [121] Zheng, J., Ma, L., Xin, B., Olah, T., Humphreys, W. G. and Zhu, M. (2007) Screening and identification of GSH-trapped reactive metabolites using hybrid triple quadrupole linear ion trap mass spectrometry. *Chem Res Toxicol.* 20, 757-766.
- [122] Dieckhaus, C. M., Fernandez-Metzler, C. L., King, R., Krolkowski, P. H. and Baillie, T. A. (2005) Negative ion tandem mass spectrometry for the detection of glutathione conjugates. *Chem Res Toxicol.* 18, 630-638.
- [123] Thompson, D. C., Perera, K. and London, R. (1995) Quinone methide formation from para isomers of methylphenol (cresol), ethylphenol, and isopropylphenol: relationship to toxicity. *Chem Res Toxicol.* 8, 55-60.
- [124] Yan, Z. and Caldwell, G. W. (2004) Stable-isotope trapping and high-throughput screenings of reactive metabolites using the isotope MS signature. *Anal Chem.* 76, 6835-6847.
- [125] Soglia, J. R., Contillo, L. G., Kalgutkar, A. S., Zhao, S., Hop, C. E., Boyd, J. G. and Cole, M. J. (2006) A semiquantitative method for the determination of reactive metabolite conjugate levels in vitro utilizing liquid chromatography-tandem mass spectrometry and novel quaternary ammonium glutathione analogues. *Chem Res Toxicol.* 19, 480-490.
- [126] Soglia, J. R., Harriman, S. P., Zhao, S., Barberia, J., Cole, M. J., Boyd, J. G. and Contillo, L. G. (2004) The development of a higher throughput reactive intermediate screening assay incorporating micro-bore liquid chromatography-micro-electrospray ionization-tandem mass spectrometry and glutathione ethyl ester as an in vitro conjugating agent. *J Pharm Biomed Anal.* 36, 105-116.
- [127] Gan, J., Harper, T. W., Hsueh, M. M., Qu, Q. and Humphreys, W. G. (2005) Dansyl glutathione as a trapping agent for the quantitative estimation and identification of reactive metabolites. *Chem Res Toxicol.* 18, 896-903.
- [128] Zhu, M., Zhao, W., Vazquez, N. and Mitroka, J. G. (2005) Analysis of low level radioactive metabolites in biological fluids using high-performance liquid chromatography with microplate scintillation counting: method validation and application. *J Pharm Biomed Anal.* 39, 233-245.
- [129] Gorrod, J. W. and Aislaitner, G. (1994) The metabolism of alicyclic amines to reactive iminium ion intermediates. *Eur J Drug Metab Pharmacokinet.* 19, 209-217.
- [130] Shetty, H. U. and Nelson, W. L. (1985) Attempts to use cyanide ion to trap imine intermediates in the microsomal N-dealkylation of propranolol: formation of alpha-aminonitriles as artifacts when using ether for extraction. *J Pharm Sci.* 74, 968-971.
- [131] Gorrod, J. W., Whittlesea, C. M. and Lam, S. P. (1991) Trapping of reactive intermediates by incorporation of ¹⁴C-sodium cyanide during microsomal oxidation. *Adv Exp Med Biol.* 283, 657-664.
- [132] Meneses-Lorente, G., Sakatis, M. Z., Schulz-Utermoehl, T., De Nardi, C. and Watt, A. P. (2006) A quantitative high-throughput trapping assay as a measurement of potential for bioactivation. *Anal Biochem.* 351, 266-272.
- [133] Argoti, D., Liang, L., Conteh, A., Chen, L., Bershas, D., Yu, C. P., Vouros, P. and Yang, E. (2005) Cyanide trapping of iminium ion reactive intermediates followed by detection and structure identification using liquid chromatography-tandem mass spectrometry (LC-MS/MS). *Chem Res Toxicol.* 18, 1537-1544.
- [134] Yan, Z., Maher, N., Torres, R. and Huebert, N. (2007) Use of a trapping agent for simultaneous capturing and high-throughput screening of both "soft" and "hard" reactive metabolites. *Anal Chem.* 79, 4206-4214.
- [135] Prakash, C., Shaffer, C. L. and Nedderman, A. (2007) Analytical strategies for identifying drug metabolites. *Mass Spectrom Rev.* 26, 340-369.
- [136] Liu, D. Q. and Hop, C. E. (2005) Strategies for characterization of drug metabolites using liquid chromatography-tandem mass spectrometry in conjunction with chemical derivatization and on-line H/D exchange approaches. *J Pharm Biomed Anal.* 37, 1-18.
- [137] Sandvoss, M., Bardsley, B., Beck, T. L., Lee-Smith, E., North, S. E., Moore, P. J., Edwards, A. J. and Smith, R. J. (2005) HPLC-SPE-NMR in pharmaceutical development: capabilities and applications. *Magn Reson Chem.* 43, 762-770.
- [138] Sandvoss, M., Roberts, A. D., Ismail, I. M. and North, S. E. (2004) Direct on-line hyphenation of capillary liquid chromatography to nuclear magnetic resonance spectroscopy: practical aspects and application to drug metabolite identification. *J Chromatogr A.* 1028, 259-266.
- [139] Madsen, K. G., Olsen, J., Skonberg, C., Hansen, S. H. and Jurva, U. (2007) Development and evaluation of an electrochemical method for studying reactive phase-I metabolites: correlation to in vitro drug metabolism. *Chem Res Toxicol.* 20, 821-831.
- [140] Madsen, K. G., Gronberg, G., Skonberg, C., Jurva, U., Hansen, S. H. and Olsen, J. (2008) Electrochemical oxidation of troglitazone: identification and characterization of the major reactive metabolite in liver microsomes. *Chem Res Toxicol.* 21, 2035-2041.
- [141] Chen, Y., Monshouwer, M. and Fitch, W. L. (2007) Analytical tools and approaches for metabolite identification in early drug discovery. *Pharm Res.* 24, 248-257.
- [142] Osorio-Lozada, A., Surapaneni, S., Skiles, G. L. and Subramanian, R. (2008) Biosynthesis of drug metabolites using microbes in hollow fiber cartridge reactors: case study of diclofenac metabolism by *Actinoplanes* species. *Drug Metab Dispos.* 36, 234-240.

- [143] Yun, C. H., Kim, K. H., Kim, D. H., Jung, H. C. and Pan, J. G. (2007) The bacterial P450 BM3: a prototype for a biocatalyst with human P450 activities. *Trends Biotechnol.* 25, 289-298.
- [144] Van Vugt-Lussenburg, B. M., Damsten, M. C., Maasdijk, D. M., Vermeulen, N. P. and Commandeur, J. N. (2006) Heterotropic and homotropic cooperativity by a drug-metabolising mutant of cytochrome P450 BM3. *Biochem Biophys Res Commun.* 346, 810-818.
- [145] Kim, D. H., Kim, K. H., Liu, K. H., Jung, H. C., Pan, J. G. and Yun, C. H. (2008) Generation of human metabolites of 7-ethoxycoumarin by bacterial cytochrome P450 BM3. *Drug Metab Dispos.* 36, 2166-2170.
- [146] Kim, D. H., Ahn, T., Jung, H. C., Pan, J. G. and Yun, C. H. (2009) Generation of the human metabolite piceatannol from the anticancer-preventive agent resveratrol by bacterial cytochrome P450 BM3. *Drug Metab Dispos.* 37, 932-936.
- [147] Day, S. H., Mao, A., White, R., Schulz-Utermoehl, T., Miller, R. and Beconi, M. G. (2005) A semi-automated method for measuring the potential for protein covalent binding in drug discovery. *J Pharmacol Toxicol Methods.* 52, 278-285.
- [148] Doss, G. A. and Baillie, T. A. (2006) Addressing metabolic activation as an integral component of drug design. *Drug Metab Rev.* 38, 641-649.
- [149] Kalgutkar, A. S., Gardner, I., Obach, R. S., Shaffer, C. L., Callegari, E., Henne, K. R., Mutlib, A. E., Dalvie, D. K., Lee, J. S., Nakai, Y., O'donnell, J. P., Boer, J. and Harriman, S. P. (2005) A comprehensive listing of bioactivation pathways of organic functional groups. *Curr Drug Metab.* 6, 161-225.
- [150] Van Welie, R. T., Van Dijck, R. G., Vermeulen, N. P. and Van Sittert, N. J. (1992) Mercapturic acids, protein adducts, and DNA adducts as biomarkers of electrophilic chemicals. *Crit Rev Toxicol.* 22, 271-306.
- [151] De Rooij, B. M., Boogaard, P. J., Commandeur, J. N., Van Sittert, N. J. and Vermeulen, N. P. (1997) Allylmercapturic acid as urinary biomarker of human exposure to allyl chloride. *Occup Environ Med.* 54, 653-661.
- [152] Zhou, S. (2003) Separation and detection methods for covalent drug-protein adducts. *J Chromatogr B Analyt Technol Biomed Life Sci.* 797, 63-90.
- [153] Yang, X. X., Hu, Z. P., Chan, S. Y. and Zhou, S. F. (2006) Monitoring drug-protein interaction. *Clin Chim Acta.* 365, 9-29.
- [154] Tornqvist, M., Fred, C., Haglund, J., Helleberg, H., Paulsson, B. and Rydberg, P. (2002) Protein adducts: quantitative and qualitative aspects of their formation, analysis and applications. *J Chromatogr B Analyt Technol Biomed Life Sci.* 778, 279-308.
- [155] Koen, Y. M., Gogichaeva, N. V., Alterman, M. A. and Hanzlik, R. P. (2007) A proteomic analysis of bromobenzene reactive metabolite targets in rat liver cytosol in vivo. *Chem Res Toxicol.* 20, 511-519.
- [156] Hanzlik, R. P., Koen, Y. M., Theertham, B., Dong, Y. and Fang, J. (2007) The reactive metabolite target protein database (TPDB)—a web-accessible resource. *BMC Bioinformatics.* 8, 95.
- [157] Pumford, N. R., Martin, B. M. and Hinson, J. A. (1992) A metabolite of acetaminophen covalently binds to the 56 kDa selenium binding protein. *Biochem Biophys Res Commun.* 182, 1348-1355.
- [158] Pumford, N. R., Halmes, N. C., Martin, B. M., Cook, R. J., Wagner, C. and Hinson, J. A. (1997) Covalent binding of acetaminophen to N-10-formyltetrahydrofolate dehydrogenase in mice. *J Pharmacol Exp Ther.* 280, 501-505.
- [159] Qiu, Y., Benet, L. Z. and Burlingame, A. L. (1998) Identification of the hepatic protein targets of reactive metabolites of acetaminophen in vivo in mice using two-dimensional gel electrophoresis and mass spectrometry. *J Biol Chem.* 273, 17940-17953.
- [160] Bulera, S. J., Birge, R. B., Cohen, S. D. and Khairallah, E. A. (1995) Identification of the mouse liver 44-kDa acetaminophen-binding protein as a subunit of glutamine synthetase. *Toxicol Appl Pharmacol.* 134, 313-320.
- [161] Hoivik, D. J., Manautou, J. E., Tveit, A., Mankowski, D. C., Khairallah, E. A. and Cohen, S. D. (1996) Evidence suggesting the 58-kDa acetaminophen binding protein is a preferential target for acetaminophen electrophile. *Fundam Appl Toxicol.* 32, 79-86.
- [162] Axworthy, D. B., Hoffmann, K. J., Streeter, A. J., Calleman, C. J., Pascoe, G. A. and Baillie, T. A. (1988) Covalent binding of acetaminophen to mouse hemoglobin. Identification of major and minor adducts formed in vivo and implications for the nature of the arylating metabolites. *Chem Biol Interact.* 68, 99-116.
- [163] Masubuchi, Y., Nakano, T., Ose, A. and Horie, T. (2001) Differential selectivity in carbamazepine-induced inactivation of cytochrome P450 enzymes in rat and human liver. *Arch Toxicol.* 75, 538-543.
- [164] Pearce, R. E., Vakkalagadda, G. R. and Leeder, J. S. (2002) Pathways of carbamazepine bioactivation in vitro I. Characterization of human cytochromes P450 responsible for the formation of 2- and 3-hydroxylated metabolites. *Drug Metab Dispos.* 30, 1170-1179.
- [165] Pirmohamed, M., Kitteringham, N. R., Breckenridge, A. M. and Park, B. K. (1992) Detection of an autoantibody directed against human liver microsomal protein in a patient with carbamazepine hypersensitivity. *Br J Clin Pharmacol.* 33, 183-186.

- [166] Hargus, S. J., Martin, B. M., George, J. W. and Pohl, L. R. (1995) Covalent modification of rat liver dipeptidyl peptidase IV (CD26) by the nonsteroidal anti-inflammatory drug diclofenac. *Chem Res Toxicol.* 8, 993-996.
- [167] Ware, J. A., Graf, M. L., Martin, B. M., Lustberg, L. R. and Pohl, L. R. (1998) Immunochemical detection and identification of protein adducts of diclofenac in the small intestine of rats: possible role in allergic reactions. *Chem Res Toxicol.* 11, 164-171.
- [168] Pumford, N. R. and Halmes, N. C. (1997) Protein targets of xenobiotic reactive intermediates. *Annu Rev Pharmacol Toxicol.* 37, 91-117.
- [169] Njoku, D. B., Greenberg, R. S., Bourdi, M., Borkowf, C. B., Dake, E. M., Martin, J. L. and Pohl, L. R. (2002) Autoantibodies associated with volatile anesthetic hepatitis found in the sera of a large cohort of pediatric anesthesiologists. *Anesth Analg.* 94, 243-249, table of contents.
- [170] Madan, A. and Parkinson, A. (1996) Characterization of the NADPH-dependent covalent binding of [¹⁴C]halothane to human liver microsomes: a role for cytochrome P4502E1 at low substrate concentrations. *Drug Metab Dispos.* 24, 1307-1313.
- [171] Pumford, N. R., Martin, B. M., Thomassen, D., Burris, J. A., Kenna, J. G., Martin, J. L. and Pohl, L. R. (1993) Serum antibodies from halothane hepatitis patients react with the rat endoplasmic reticulum protein ERp72. *Chem Res Toxicol.* 6, 609-615.
- [172] Brown, A. P. and Gandolfi, A. J. (1994) Glutathione-S-transferase is a target for covalent modification by a halothane reactive intermediate in the guinea pig liver. *Toxicology.* 89, 35-47.
- [173] Satoh, H., Martin, B. M., Schulick, A. H., Christ, D. D., Kenna, J. G. and Pohl, L. R. (1989) Human anti-endoplasmic reticulum antibodies in sera of patients with halothane-induced hepatitis are directed against a trifluoroacetylated carboxylesterase. *Proc Natl Acad Sci U S A.* 86, 322-326.
- [174] Butler, L. E., Thomassen, D., Martin, J. L., Martin, B. M., Kenna, J. G. and Pohl, L. R. (1992) The calcium-binding protein calreticulin is covalently modified in rat liver by a reactive metabolite of the inhalation anesthetic halothane. *Chem Res Toxicol.* 5, 406-410.
- [175] Wong, H. L. and Liebler, D. C. (2008) Mitochondrial protein targets of thiol-reactive electrophiles. *Chem Res Toxicol.* 21, 796-804.
- [176] Shin, N. Y., Liu, Q., Stamer, S. L. and Liebler, D. C. (2007) Protein targets of reactive electrophiles in human liver microsomes. *Chem Res Toxicol.* 20, 859-867.
- [177] Codreanu, S. G., Adams, D. G., Dawson, E. S., Wadzinski, B. E. and Liebler, D. C. (2006) Inhibition of protein phosphatase 2A activity by selective electrophile alkylation damage. *Biochemistry.* 45, 10020-10029.
- [178] Hong, F., Sekhar, K. R., Freeman, M. L. and Liebler, D. C. (2005) Specific patterns of electrophile adduction trigger Keap1 ubiquitination and Nrf2 activation. *J Biol Chem.* 280, 31768-31775.
- [179] Carbone, D. L., Doorn, J. A., Kiebler, Z., Ickes, B. R. and Petersen, D. R. (2005) Modification of heat shock protein 90 by 4-hydroxynonenal in a rat model of chronic alcoholic liver disease. *J Pharmacol Exp Ther.* 315, 8-15.
- [180] Carbone, D. L., Doorn, J. A., Kiebler, Z., Sampey, B. P. and Petersen, D. R. (2004) Inhibition of Hsp72-mediated protein refolding by 4-hydroxy-2-nonenal. *Chem Res Toxicol.* 17, 1459-1467.
- [181] Shibata, T., Yamada, T., Ishii, T., Kumazawa, S., Nakamura, H., Masutani, H., Yodoi, J. and Uchida, K. (2003) Thioredoxin as a molecular target of cyclopentenone prostaglandins. *J Biol Chem.* 278, 26046-26054.
- [182] Aldini, G., Carini, M., Vistoli, G., Shibata, T., Kusano, Y., Gamberoni, L., Dalle-Donne, I., Milzani, A. and Uchida, K. (2007) Identification of actin as a 15-deoxy-Delta^{12,14}-prostaglandin J₂ target in neuroblastoma cells: mass spectrometric, computational, and functional approaches to investigate the effect on cytoskeletal derangement. *Biochemistry.* 46, 2707-2718.
- [183] James, L. P., Farrar, H. C., Sullivan, J. E., Givens, T. G., Kearns, G. L., Wasserman, G. S., Walson, P. D., Hinson, J. A. and Pumford, N. R. (2001) Measurement of acetaminophen-protein adducts in children and adolescents with acetaminophen overdoses. *J Clin Pharmacol.* 41, 846-851.
- [184] Muldrew, K. L., James, L. P., Coop, L., McCullough, S. S., Hendrickson, H. P., Hinson, J. A. and Mayeux, P. R. (2002) Determination of acetaminophen-protein adducts in mouse liver and serum and human serum after hepatotoxic doses of acetaminophen using high-performance liquid chromatography with electrochemical detection. *Drug Metab Dispos.* 30, 446-451.
- [185] Shipkova, M., Armstrong, V. W., Weber, L., Niedmann, P. D., Wieland, E., Haley, J., Tonshoff, B. and Oellerich, M. (2002) Pharmacokinetics and protein adduct formation of the pharmacologically active acyl glucuronide metabolite of mycophenolic acid in pediatric renal transplant recipients. *Ther Drug Monit.* 24, 390-399.
- [186] Van Welie, R. T., Van Duyn, P., Brouwer, D. H., Van Hemmen, J. J., Brouwer, E. J. and Vermeulen, N. P. (1991) Inhalation exposure to 1,3-dichloropropene in the Dutch flower-bulb culture. Part II. Biological monitoring by measurement of urinary excretion of two mercapturic acid metabolites. *Arch Environ Contam Toxicol.* 20, 6-12.

- [187] Van Sittert, N. J., Boogaard, P. J. and Beulink, G. D. (1993) Application of the urinary S-phenylmercapturic acid test as a biomarker for low levels of exposure to benzene in industry. *Br J Ind Med.* 50, 460-469.
- [188] Osterman-Golkar, S., Peltonen, K., Anttinen-Klemetti, T., Landin, H. H., Zorcec, V. and Sorsa, M. (1996) Haemoglobin adducts as biomarkers of occupational exposure to 1,3-butadiene. *Mutagenesis.* 11, 145-149.
- [189] Swenberg, J. A., Koc, H., Upton, P. B., Georguieva, N., Ranasinghe, A., Walker, V. E. and Henderson, R. (2001) Using DNA and hemoglobin adducts to improve the risk assessment of butadiene. *Chem Biol Interact.* 135-136, 387-403.
- [190] Rappaport, S. M., Waidyanatha, S., Yeowell-O'connell, K., Rothman, N., Smith, M. T., Zhang, L., Qu, Q., Shore, R., Li, G. and Yin, S. (2005) Protein adducts as biomarkers of human benzene metabolism. *Chem Biol Interact.* 153-154, 103-109.
- [191] Omland, O., Sherson, D., Hansen, A. M., Sigsgaard, T., Autrup, H. and Overgaard, E. (1994) Exposure of iron foundry workers to polycyclic aromatic hydrocarbons: benzo(a)pyrene-albumin adducts and 1-hydroxypyrene as biomarkers for exposure. *Occup Environ Med.* 51, 513-518.
- [192] Zhao, C., Vodicka, P., Sram, R. J. and Hemminki, K. (2000) Human DNA adducts of 1,3-butadiene, an important environmental carcinogen. *Carcinogenesis.* 21, 107-111.
- [193] Zhao, C., Vodicka, P., Sram, R. J. and Hemminki, K. (2001) DNA adducts of 1,3-butadiene in humans: relationships to exposure, GST genotypes, single-strand breaks, and cytogenetic end points. *Environ Mol Mutagen.* 37, 226-230.
- [194] Bougie, D., Johnson, S. T., Weitekamp, L. A. and Aster, R. H. (1997) Sensitivity to a metabolite of diclofenac as a cause of acute immune hemolytic anemia. *Blood.* 90, 407-413.
- [195] Kenna, J. G., Neuberger, J. and Williams, R. (1987) Identification by immunoblotting of three halothane-induced liver microsomal polypeptide antigens recognized by antibodies in sera from patients with halothane-associated hepatitis. *J Pharmacol Exp Ther.* 242, 733-740.

PART II

NOVEL *IN VITRO* TOOLS FOR THE GENERATION, IDENTIFICATION AND CHARACTERIZATION OF REACTIVE METABOLITES

Chapter 2

Application of drug metabolising mutants of cytochrome P450 BM3 (CYP102A1) as biocatalysts for the generation of reactive metabolites

Adapted from: Micaela C. Damsten^{*}, Barbara M. van Vugt-Lussenburg^{*}, Tineke Zeldenthuis, Jon S. de Vlieger, Jan N. M. Commandeur, Nico P. E. Vermeulen.
Application of drug metabolising mutants of cytochrome P450 BM3 (CYP102A1) as biocatalysts for the generation of reactive metabolites.
Chemico-Biological Interactions 171, 2008, p: 96-107.

^{*} Both authors contributed equally to this work

Abstract

Recently, several mutants of cytochrome P450 BM3 (CYP102A1) with high activity toward drugs have been obtained by a combination of site-directed and random mutagenesis. In the present study, the applicability of these mutants as biocatalysts for the production of reactive metabolites from the drugs clozapine, diclofenac and acetaminophen was investigated. We showed that the four CYP102A1 mutants used in this study formed the same metabolites as human and rat liver microsomes, with an activity up to 70-fold higher compared to human enzymes. Using these CYP102A1 mutants, three novel GSH adducts of diclofenac were discovered which were also formed in incubations with human liver microsomes. This work shows that CYP102A1 mutants are very useful tools for the generation of high levels of reference metabolites and reactive intermediates of drugs. Producing high levels of those reactive metabolites, that might play a role in adverse drug reactions (ADRs) in humans, will facilitate their isolation, structural elucidation, and could be very useful for the toxicological characterisation of novel drugs and/or drug candidates.

Introduction

Cytochromes P450 (P450s) are involved in the metabolism of approximately 80% of the drugs currently on the market [1, 2]. Most often, metabolism by P450s increases solubility of the compound, facilitating urinary and biliary excretion. However, in some cases, metabolism of drugs by P450s leads to the formation of highly reactive electrophilic metabolites that can subsequently react with macromolecules, leading to covalent adducts to proteins. These events are thought to be related to serious adverse drug reactions (ADRs) and to rare idiosyncratic drug reactions (IDRs). Consequently, it is important to assess the potential of novel drug candidates to form reactive electrophilic metabolites early in the drug discovery process [3].

The most common way to determine the formation of electrophilic metabolites is to screen for the formation of glutathione (GSH) adducts by LC-MS/MS analysis. Currently, several methods exist for the sensitive and selective detection of GSH conjugates [4-6]. Reactive intermediates (RIs) are usually generated in *in vitro* incubations using rat or human liver microsomes in the presence of GSH. However, due to the relatively low activity of human P450s and the occurrence of suicide inhibition of the enzymes by the RIs, generally only low concentrations of reactive metabolites are formed by liver microsomes [7]. Consequently, only major GSH adducts can be identified easily while minor adducts might stay undetected.

The soluble cytochrome P450 BM3 (CYP102A1) from *Bacillus megaterium* is considered a good candidate for use as a biocatalyst in biotechnology, because this very stable enzyme has the highest catalytic activity ever recorded for a P450 [8]. In a previous study we described a site-directed mutant of CYP102A1, R47L/F87V/L188Q, that is able to metabolize various drug-like molecules, including acetaminophen. Acetaminophen is metabolized by this triple mutant into the reactive N-acetyl-p-benzoquinoneimine (NAPQI) intermediate, albeit with an activity still 15-fold lower than human P450 3A4 [9]. In a subsequent study, this mutant was subjected to several rounds of random mutagenesis, which resulted in four mutants with an up to 90-fold increased activity towards drug substrates compared to human P450 2D6 [10].

In the present study we evaluated whether these novel drug metabolising CYP102A1 mutants can be used as biocatalysts for the biosynthesis of high amounts of reactive metabolites of drugs. We chose clozapine, diclofenac and acetaminophen as model

compounds since these drugs have been involved in serious ADRs in humans [11-13]. These compounds are known to be bioactivated to several reactive electrophilic intermediates that can be trapped by GSH [14-18]. We therefore investigated whether the CYP102A1 mutants (Table 1) were able to metabolize these drugs and to produce GSH adducts. The metabolites formed were subsequently compared to those formed by rat liver microsomes (RLM) and human liver microsomes (HLM). It was determined whether the same metabolites were formed and it was studied whether the CYP102A1 mutants produce higher levels of GSH adducts when compared to human and/or rat enzymes. In previous studies, *E. coli* cytosolic fractions were used for metabolism studies with these CYP102A1 mutants. However, to prevent conjugation of the reactive metabolites to cytosolic components instead of GSH, for this study we used His-tagged CYP102A1 mutants, that were based on the mutants described in [10], which were purified by nickel column chromatography.

Table 1. Mutations present in the CYP102A1 mutants used in this study.

Mutant M01 _{his}	Mutant M02 _{his}	Mutant M05 _{his}	Mutant M11 _{his}
R47L	R47L	R47L	R47L
			E64G
		F81I	F81I
	L86I		
F87V	F87V	F87V	F87V
			E143G
L188Q	L188Q	L188Q	L188Q
			Y198C *
E267V		E267V	E267V
			H285Y *
	N319T		
G415S		G415S	G415S
	A964V *		
G1049E *			

Mutations indicated by asterisk are additional in comparison to the non-His-tagged CYP102A1 mutants M01, M02 and M11, as previously described in [10].

Experimental procedures

Enzymes and plasmids

The CYP102A1 mutants M01, M02, M05 and M11 were prepared in the pT1-P450BM3 plasmid as described previously [10]. These mutants were cloned into a pET28a+ vector system, which contains an N-terminal His-tag to allow purification by nickel column chromatography. The pET28a+ vector containing wild-type CYP102A1

as described in [19] was kindly provided by dr. V. Urlacher (Institut für Technische Biochemie, Universität Stuttgart, Germany). The genes of the mutants M01, M02, M05 and M11 were cloned into this pET28a+ vector as described in [19]. The resulting His-tagged CYP102A1 mutants M01_{his}, M02_{his}, M05_{his} and M11_{his} were used in this study. Sequencing showed that one or two extra mutations were introduced in the genes of M01_{his}, M02_{his} and M11_{his} during the cloning process (Table 1). Enzyme kinetic analysis of these mutants using benzoxyresorufin and dextromethorphan as substrates did not show significant differences when compared to the corresponding non-His-tagged mutants M01, M02, M05 and M11 (data not shown), suggesting that the extra mutations are without effect.

The plasmids pCWh3A4 and pLCMhOR, containing P450 3A4 and human NADPH P450 reductase, respectively, were a kind gift from dr. M. Kranendonk (Department of Genetics, Faculty of Medical Sciences, Universidade Nova de Lisboa, Portugal) and were expressed as described in [20]. The plasmid pCWh2C9/hOR, containing P450 2C9, bicistronically co-expressed with human NADPH P450 reductase, was a kind gift from dr. F. Guengerich and was expressed as described in [21].

Expression and purification

The His-tagged pET28a+ constructs were transformed into *E. coli* BL21 (DE3) cells using standard procedures. For expression, 300 ml Terrific Broth (TB) [22] medium (24 g/l yeast extract, 12 g/l tryptone, 4 ml/l glycerol) with 30 µg/ml kanamycin was inoculated with 15 ml of an overnight culture. The cells were grown at 150 rpm and 37°C until the OD₆₀₀ reached 0.8. Then, protein expression was induced by the addition of 0.6 mM isopropyl-β-D-thiogalactopyranoside (IPTG). The temperature was lowered to 30°C, and 0.5 mM of the heme precursor δ-aminolevulinic acid was added. Expression was allowed to proceed for 5 h. Cells were harvested by centrifugation (4000 g, 4°C, 15 minutes), and the pellet was resuspended in 15 ml KPi-glycerol buffer (100 mM potassium phosphate (KPi) pH 7.5, 10% glycerol, 0.5 mM EDTA and 0.25 mM dithiothreitol). Cells were disrupted using a French press (1000 psi, 2 repeats), and the cytosolic fraction was separated from the membrane fraction by ultracentrifugation of the lysate (120.000 g, 4°C, 60 minutes). The mutants were purified using Ni-NTA agarose (Sigma). To prevent aspecific binding, 1 mM histidine was added to the cytosolic fraction. 2 ml Ni-NTA slurry was added, and the cytosolic fraction was equilibrated at 4°C for 3 hours. The Ni-NTA agarose was retained in a polypropylene tube with porous disc (Pierce, Rockford, USA), and was washed 3 times with 5 ml KPi-glycerol buffer containing 2 mM histidine. The CYP102A1 mutants were eluted in 10 ml KPi-glycerol buffer containing 300 mM

histidine. The histidine was subsequently removed by repeated washing with KPi-glycerol buffer in a Vivaspin 20 filtration tube (10.000 MWCO PES, Sartorius) (4000 g) until the histidine concentration was below 300 nM.

Formation of GSH adducts from clozapine, diclofenac and acetaminophen

All incubations were performed at a final volume of 250 μ l and consisted of 100 mM potassium phosphate (KPi) buffer, pH 7.4, containing 250 nM of CYP102A1 mutant (M01_{his}, M02_{his}, M05_{his} or M11_{his}), 1 mM of substrate (clozapine, diclofenac or acetaminophen) and 5 mM GSH. Reactions were initiated by the addition of an NADPH regenerating system resulting in final concentrations of 0.4 mM NADPH, 0.3 mM glucose-6-phosphate and 0.4 units/ml glucose-6-phosphate dehydrogenase. The reactions were allowed to proceed for 60 minutes at 24°C, after which they were terminated by the addition of 25 μ l 10% HClO₄. The reactions containing diclofenac were terminated by the addition of 250 μ l cold methanol instead of HClO₄. Samples were centrifuged to remove precipitated protein (4000 g, 15 minutes), and the resulting supernatants were analysed on HPLC, as described below. To determine which peaks represent metabolites, control incubations without NADPH were performed. To establish which of the metabolites are GSH adducts, control incubations in the absence of GSH were also performed.

To compare the activity and the metabolic profile of the CYP102A1 mutants with those formed by mammalian P450s, incubations were also performed with pooled human liver microsomes (HLM) from BD Gentest™ (Cat. No.: 452161) and with non-induced rat liver microsomes (RLM) that were prepared as described in [23]. A final microsomal protein concentration of 1 mg/ml was used and these incubations were performed as described above, at 37°C instead of 24°C.

For positive identification of some of the GSH conjugates, diclofenac incubations were also performed with human P450 2C9 and P450 3A4. P450 2C9 and P450 3A4 produce different GSH-conjugates which have been characterised previously by a combination of mass spectrometry and NMR [16, 28, 29]. Diclofenac was incubated at a concentration of 1 mM in presence of 250 nM P450 2C9 or P450 3A4, 5 mM GSH and a NADPH-regenerating system (0.4 mM NADPH, 0.3 mM glucose-6-phosphate and 0.4 units/ml glucose-6-phosphate dehydrogenase). After incubating for 1 hour at 37°C, the reactions were terminated by the addition of 250 μ l of cold methanol. Samples were vortexed and centrifuged for 15 minutes at 4000 rpm in

order to precipitate proteins. Supernatants were analyzed with the chromatographic conditions as described below.

The time dependence of product formation was determined for the three substrates, each with one representative CYP102A1 mutant showing high levels of metabolite formation. For clozapine and acetaminophen, M11_{his} was used, and for diclofenac, M01_{his} was used. Incubations were performed as described above, with incubation times of 0, 15, 30, 45 and 60 minutes.

To determine whether drug metabolism by the four mutants could be further increased by the addition of caffeine, as was described previously for P450 3A and for CYP102A1 R47L/F87V/L188Q with acetaminophen [9, 24], incubations were performed as described above in the presence of 10 mM caffeine.

Analysis of metabolites by HPLC and LC-MS

Metabolites and parent compounds were analysed by reversed phase chromatography using a C18-column (Phenomenex, Luna 5 μ , 150 x 4.6 mm), which was eluted by a binary gradient, composed of solvent A (1% acetonitrile, 0.2% formic acid, 98.8% water) and solvent B (99% acetonitrile, 0.2% formic acid, 0.8% water). Total flow rate was 0.5 ml/min (in case of UV-detection) or 0.4 ml/min (in case of mass spectrometrical detection). The gradient was programmed as follows:

- 1) 0 to 5 minutes: isocratic at 0% solvent B (100% solvent A)
- 2) 5 to 30 minutes: linear increase from 0 to 100% solvent B
- 3) 30 to 35 minutes: linear decrease from 100% to 0% solvent B
- 4) 35 to 40 minutes: isocratic at 0% solvent B (100% solvent A).

Metabolites were detected using a UV/VIS detector for quantification, and by MS for identification. For quantification of metabolites, detection was performed using a UV/VIS-detector set at 254 nm. Standard curves of the substrates were used to estimate the concentrations of the metabolites, assuming that the extinction coefficients of the metabolites are equal to that of the corresponding substrates. The Shimadzu Class VP 4.3 software package was used to determine peak areas of the metabolites. Standard curves of the compounds were linear between 1 and 500 μ M; limits of detection were estimated to be 0.5 μ M (data not shown). Inter-experimental variation of the HPLC system was approximately 2-3%.

For identification of metabolites, two different mass spectrometers were used for the analyses. A Finnigan LCQ Deca mass spectrometer was used with positive electron spray ionisation (ESI). N₂ was used as sheath gas (60 psi) and auxiliary gas (10 psi),

the needle voltage was 5000 V and the heated capillary was at 150°C. To confirm the presence of very low-abundant metabolites, the more sensitive IT-TOF LC-MS instrument (Shimadzu) was used. In this case, electron spray ionisation (ESI) was also used in the positive mode. The interface voltage was 500 V, the nebulizer gas flow (N₂) was 1.5 l/min and the heated block temperature was 200°C. The LC-MS Solution software package from Shimadzu was used to determine peak areas of the metabolites in the corresponding extracted ion chromatograms. Inter-experimental variation of the LC-MS systems was always below 5%.

Results and discussion

Biotransformation of clozapine by HLM, RLM and CYP102A1 mutants

The CYP102A1 mutants were able to metabolize clozapine to three major GSH adducts (CG-1, CG-2 and CG-3; Figure 1-A; Table 2) and to four non GSH-dependent metabolites (C-1, C-2, C-3 and C-4; Figure 1-A; Table 2). The CYP102A1 mutants showed different metabolic profiles. Mutant M11_{his} had the highest overall activity and was the only mutant that formed C-4 ($t_r = 14.2$). On the contrary, M02_{his}, which showed the lowest overall activity, did not form CG-2 and C-1.

Table 2. Metabolism of clozapine by CYP102A1 mutants.

	t_r	M01 _{his}	M02 _{his}	M05 _{his}	M11 _{his}
GSH-conjugates					
CG-1	16.0	22.0 ± 1.8	9.1 ± 0.1	59.6 ± 7.3	168.3 ± 8.4
CG-2	15.8	9.0 ± 1.5	-	20.7 ± 4.0	53.4 ± 2.7
CG-3	15.5	1.3 ± 0.5	0.7 ± 0.2	2.5 ± 0.1	6.0 ± 2.4
Stable metabolites					
C-1	17.4	13.3 ± 2.4	-	44.7 ± 9.2	115.8 ± 7.9
C-2	16.4	95.5 ± 14.5	7.5 ± 1.9	171.2 ± 20.3	465.2 ± 77.0
C-3	15.7	7.9 ± 1.2	15.1 ± 2.6	10.1 ± 1.2	5.2 ± 1.1
C-4	14.2	-	-	-	5.0 ± 1.2

Metabolites formed from clozapine by four mutants of CYP102A1. Metabolites were analyzed by HPLC with UV detection at 254 nm. t_r is in minutes. Absence (-) of the metabolite is indicated. Product formation is expressed in nmol product/nmol enzyme/60 minutes, assuming that the extinction coefficients of the substrate and its metabolites are comparable. Values represent the mean ± standard deviation of triplicate experiments. All GSH adducts are indicated in **bold**.

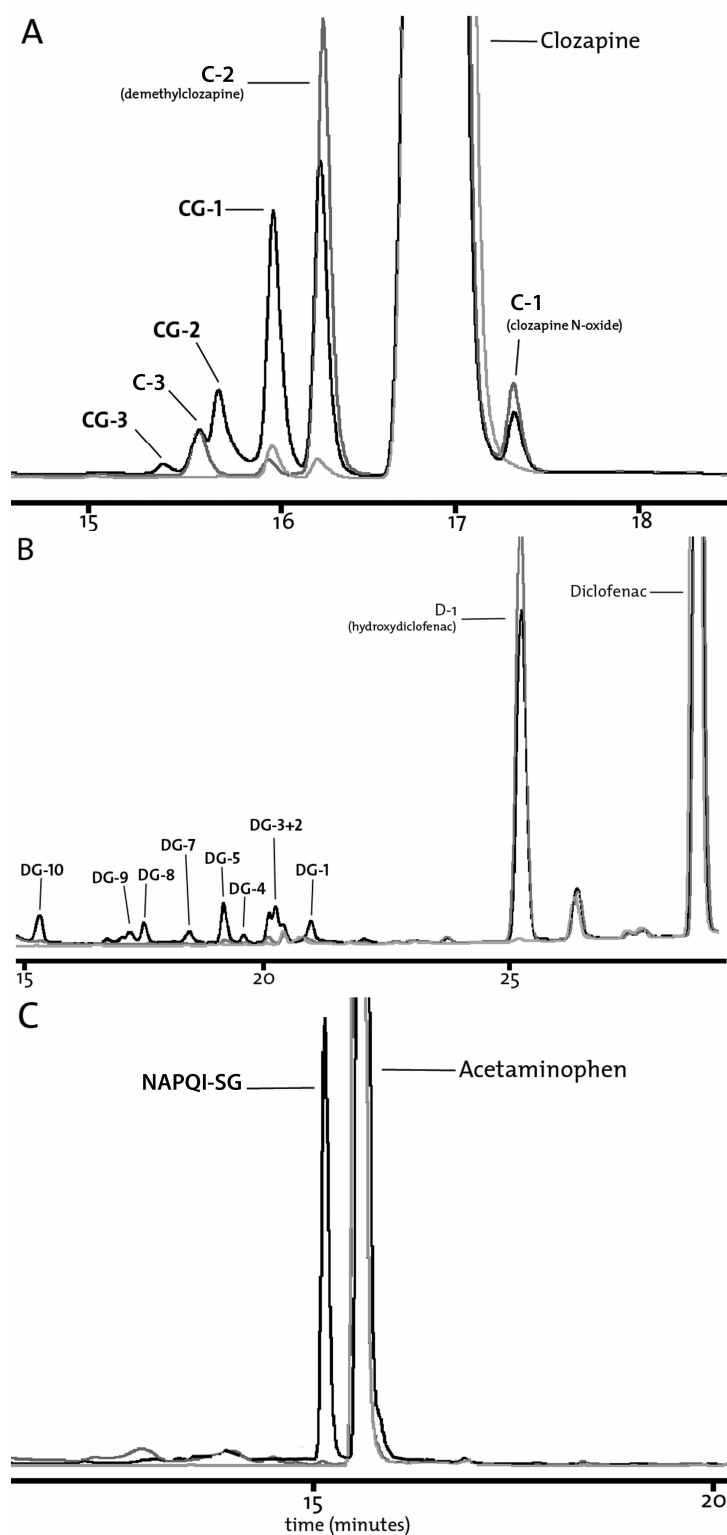


Figure 1. Chromatograms of clozapine, diclofenac and acetaminophen metabolized by CYP102A1 mutants. Black line: standard incubation. Grey line: incubation without GSH. Light grey line: incubation without NADPH (negative control). A: clozapine metabolized by mutant M05_{his}. B: diclofenac metabolized by mutant M01_{his}. C: acetaminophen metabolized by mutant M11_{his}. GSH adducts are indicated in **bold**.

LC-MS analysis showed that CYP102A1 mutant M11_{his} formed all the metabolites that were produced by RLM and HLM but at significantly higher levels (Table 3). Only one metabolite (C-5) was formed exclusively by M11_{his}. Two GSH adducts with an m/z value of 316.6 $[M+2H]^{2+}$, corresponding to clozapine coupled to GSH (Cloza+SG), were observed in the incubations performed with RLM (CG-1 and CG-3) and three adducts of this mass were found with HLM (CG-1, CG-3 and CG-4). M11_{his} was 7-, 17- and 22-fold more active than HLM in producing metabolites CG-1, CG-3 and CG-4 respectively (Table 3). Another GSH adduct, with an m/z value of 309.6 $[M+2H]^{2+}$, was also observed in the incubations performed with HLM (CG-2 in Table 3) but was not produced by RLM. M11_{his} showed to be 34-fold more active than HLM in producing this GSH adduct, that most likely corresponds to the N-demethylated GSH adduct of clozapine (Cloza-CH₂+SG). These results are in agreement with previous data from literature where three major GSH adducts of clozapine were identified in incubations with RLM and HLM [14, 15, 25]. Possible structures for these GSH adducts are proposed in Figure 2.

Table 3. Identification of the metabolites of clozapine.

Metabolites	t_r	HLM	RLM	M11 _{his}	m/z	Proposed structure
GSH-conjugates						
CG-1	16.2	100 ± 12	64 ± 3	722 ± 87	316.61²	Cloza+SG
CG-2	15.8	100 ± 10	-	3440 ± 338	309.59²	Cloza-CH₂+SG
CG-3	15.7	100 ± 13	127 ± 13	1721 ± 220	316.61²	Cloza+SG
CG-4	15.4	100 ± 9	-	2191 ± 240	316.61²	Cloza+SG
Stable Metabolites						
C-1	17.7	100 ± 9	427 ± 56	286 ± 40	343.13 ¹	Cloza+O
C-2	16.5	100 ± 10	181 ± 13	1257 ± 77	313.12 ¹	Cloza-CH ₂
C-3	15.1	100 ± 9	55 ± 4	574 ± 48	301.12 ¹	Cloza-C ₂ H ₂
C-4	14.9	100 ± 11	50 ± 6	1685 ± 201	287.11 ¹	Cloza-C ₃ H ₄
C-5	17.6	-	-	+	329 ¹	Cloza-CH ₂ +O

Qualitative and quantitative comparison of the metabolites formed from clozapine by HLM, RLM and CYP102A1 mutant M11_{his}. Results from duplicate experiments analyzed with the IT-TOF LC-MS instrument are shown in the table. t_r is in minutes. Presence (+) and/or absence (-) of the metabolite is indicated. Activities of the different enzymes are presented as percentages (\pm standard deviations of the differences) taking the incubation with HLM as reference (100%). m/z values corresponding to the singly-protonated molecule¹ $[M+H]^+$ and/or of the diprotonated molecule² $[M+2H]^{2+}$ are indicated and a possible metabolite structure is proposed. All GSH adducts are indicated in bold.

In addition, several non-GSH metabolites were also observed in the incubations performed with RLM and HLM. The RLM and HLM both formed clozapine N-oxide (Cloza+O) and N-demethylated clozapine (Cloza-CH₂) as major metabolites (C-1 and C-2; Table 3). They were identified by their *m/z* values (*m/z* 343 and 313; [M+H]⁺) as has been described previously in literature [14, 15]. Three minor peaks (*t_r* 14.6, 15.8 and 16.4; data not shown), also showing a chlorine isotope pattern and a *m/z* value of 343 [M+H]⁺, were observed in the RLM, HLM and M11_{his} incubations when analyzed on the IT-TOF LC-MS instrument. These peaks were not initially detected by UV or by using the less-sensitive LCQ LC-MS instrument. Whether these metabolites (C-6, C-7 and C-8) correspond to the structures proposed in Figure 2 remains to be established. Two other metabolites, C-3 and C-4 (*m/z* 301; Cloza-C₂H₂ and *m/z* 287; Cloza-C₃H₄; [M+H]⁺; Table 3), were also formed by RLM and HLM. These chlorine-containing metabolites might correspond to the structures depicted in Figure 2, originating from partial degradation of the piperazine ring of clozapine as has been described in [26]. Eventually, the M11_{his} metabolite C-5 might represent a N-demethylated metabolite of clozapine that is further hydroxylated (Cloza-CH₂+O; *m/z* 329; [M+H]⁺; Table 3) as proposed in the biotransformation scheme of clozapine in Figure 2. In general, M11_{his} was found to be 3- to 17-fold more active than HLM for the production of these stable metabolites.

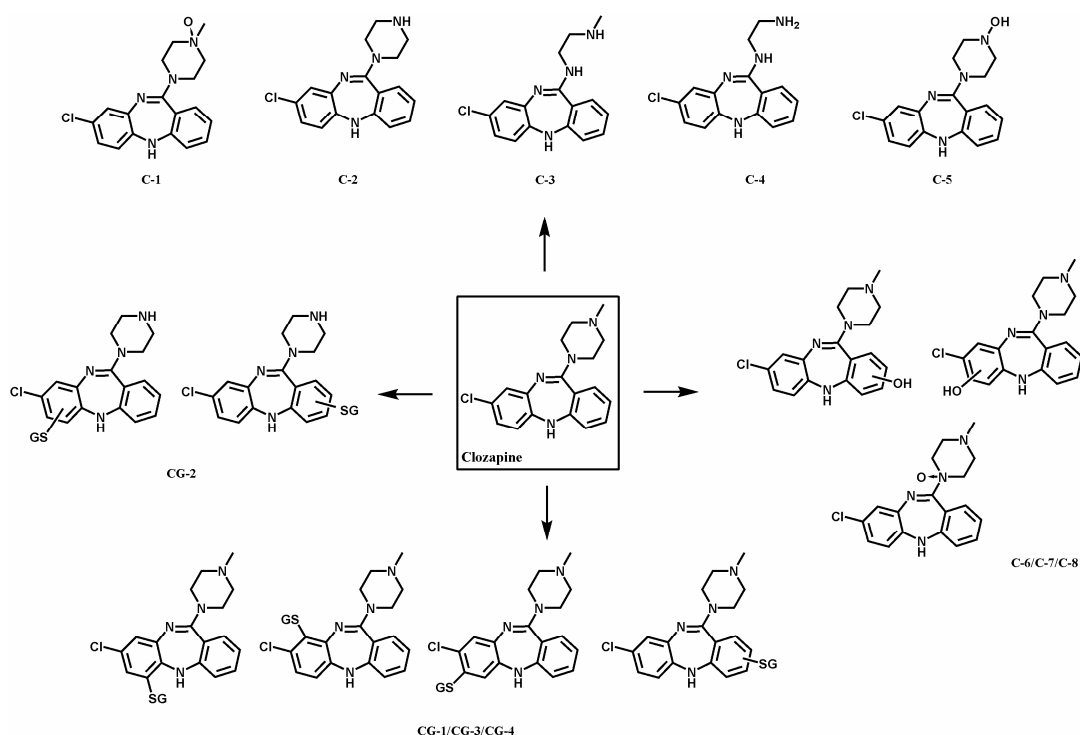


Figure 2. Proposed biotransformation scheme of clozapine

Biotransformation of diclofenac by HLM, RLM and CYP102A1 mutants

Diclofenac was metabolized by the CYP102A1 mutants to one non-GSH-dependent metabolite (D-1) and to ten different GSH adducts (Figure 1-B; Table 4). The activities of mutants M01_{his}, M05_{his} and M11_{his} were similar, whereas M02_{his} showed a significantly lower activity.

MS analysis shows that diclofenac is metabolized by the CYP102A1 mutants to hydroxylated diclofenac (Diclo+O) having an *m/z* of 312 (D-1; [M+H]⁺; Table 5). Mutant M11_{his} was 4-fold more active than HLM in the formation of this metabolite and 5.5-fold more active than RLM. This hydroxylated metabolite of diclofenac was also formed by human P450 2C9, which according to literature corresponds to 4'-hydroxydiclofenac [27] (data not shown). 5-hydroxydiclofenac, which has also been described in literature as a P450 3A4 metabolite [28, 29], was not observed in these incubations.

Table 4. Metabolism of diclofenac by CYP102A1 mutants.

	<i>t_r</i>	M0 _{his}	M02 _{his}	M05 _{his}	M11 _{his}
GSH-conjugates					
DG-1	20.9	48.5 ± 6.3	4.7 ± 1.5	51.8 ± 3.6	37.1 ± 11.6
DG-2	20.2	41.8 ± 4.8	14.1 ± 4.1	58.7 ± 4.6	39.2 ± 2.9
DG-3	20.1	86.2 ± 27.9	-	97.7 ± 9.0	115.3 ± 7.1
DG-4	19.5	11.5 ± 4.5	1.9 ± 0.2	4.8 ± 1.3	1.4 ± 0.2
DG-5	19.1	79.8 ± 6.0	10.1 ± 0.4	99.1 ± 5.9	82.3 ± 39.8
DG-6	18.5	3.7 ± 0.9	-	-	-
DG-7	18.4	25.2 ± 5.3	-	27.6 ± 7.7	34.6 ± 8.7
DG-8	17.5	40.2 ± 13.2	-	50.6 ± 5.2	61.8 ± 9.7
DG-9	17.2	20.6 ± 0.1	-	30.3 ± 3.2	22.2 ± 16.2
DG-10	15.4	39.0 ± 5.5	34.7 ± 6.2	39.0 ± 6.5	32.5 ± 7.2
Stable metabolites					
D-1	25.2	980.1 ± 148.5	137.6 ± 9.1	942.1 ± 43.2	1038.0 ± 53.8

Metabolites formed from diclofenac by four mutants of CYP102A1. Metabolites were analyzed by HPLC with UV detection at 254 nm. *t_r* is in minutes. Absence (-) of the metabolite is indicated. Product formation is expressed in nmol product/nmol enzyme/60 minutes, assuming that the extinction coefficients of the substrate and its metabolites are comparable. Values represent the mean ± standard deviation of triplicate experiments. All GSH adducts are indicated in bold.

Table 5. Identification of the metabolites of diclofenac.

Metabolites	t_r	HLM	RLM	M11 _{his}	m/z	Proposed structure
GSH-conjugates						
DG-1	19.6	-	100 ± 11	302 ± 41	617.08¹	Diclo+O+SG
DG-2	a. 19.2	+	+	+	617.08¹	Diclo+O+SG
	b. 19.1	+	+	+	617.08¹	Diclo+O+SG
Total		100 ± 12	530 ± 64	6860 ± 823		
DG-3	19.0	-	-	+	583.13¹	Diclo+O+SG-HCl
DG-4	n.i.	n.i.	n.i.	n.i.	n.i.	
DG-5	17.5	100 ± 10	326 ± 33	456 ± 41	461.59²	Diclo+O+2SG
DG-6	n.i.	n.i.	n.i.	n.i.	n.i.	
DG-7	16.9	100 ± 13	6.2 ± 0.8	243 ± 24	444.61²	Diclo+O+2SG-HCl
DG-8	16.3	100 ± 9	-	751 ± 80	427.62²	Diclo+O+2SG-2HCl
DG-9	n.i.	n.i.	n.i.	n.i.	n.i.	
DG-10	n.i.	n.i.	n.i.	n.i.	n.i.	
Stable Metabolites						
D-1	25.3	100 ± 9	74 ± 9	414 ± 48	312.02 ¹	Diclo+O

Qualitative and quantitative comparison of the metabolites formed from diclofenac by HLM, RLM and CYP102A1 M11_{his}. Results from duplicate experiments analyzed with the IT-TOF LC-MS instrument are shown in the table. t_r is in minutes. Presence (+), absence (-) and/or non-identified (n.i.) metabolites are indicated. The activities of the different enzymes are presented as percentages (\pm standard deviations of the differences) taking the incubation with HLM as reference (100%). m/z values corresponding to the protonated molecule¹ $[M+H]^+$ and/or of the diprotonated molecule² $[M+2H]^{2+}$ are indicated and a possible metabolite structure is proposed. All GSH adducts are indicated in bold.

The GSH adducts DG-1 and DG-2 ($t_r = 20.9$ and 20.2 min; Table 4) were formed by all four CYP102A1 mutants. According to MS analysis, DG-2 appeared to consist of two overlapping peaks of m/z 617 (DG-2a and DG-2b; $[M+H]^+$; Table 5) corresponding to hydroxylated GSH adducts of diclofenac (Diclo+O+SG). DG-1 is also a GSH adduct with the same m/z 617 value. RLM also produced all three GSH adducts of m/z 617, whereas HLM only produced DG-2a and DG-2b (Table 5). DG-3 was only formed by M01_{his}, M05_{his} and M11_{his} ($t_r = 20.1$; Table 4). This GSH adduct has an m/z value of 583 $[M+H]^+$, corresponding to the hydroxylated GSH adduct of diclofenac where one chlorine atom is substituted (Diclo+O+SG-HCl; Table 5). Neither RLM nor HLM did produce this metabolite. Incubations performed with human P450 3A4 produced two GSH adducts of m/z 617 co-eluting with DG-1 and DG-2b. Incubations with P450 2C9 only showed one GSH adduct with an m/z value of 617 co-eluting with DG-2a (data not shown). In the literature, three and four GSH adducts have been described for diclofenac metabolism by RLM and HLM,

respectively, generally referred to as M1-M4 [16, 29, 30]. Three of these adducts have an m/z of 617 (M1, M2 and M3) and one an m/z of 583 (M4). M1 and M3 have been described as P450 3A4 metabolites and therefore most likely correspond to DG-1 and DG-2b. DG-2a probably corresponds to the 4'-OH-3'-SG-diclofenac adduct, also referred to the P450 2C9 metabolite M2 [29]. DG-3 most likely corresponds to M4, as proposed in Figure 3. Mutant M11_{his} was 13-fold and 69-fold more active than RLM and HLM for the production of DG-2a and DG-2b and 3-fold more active than RLM in producing DG-1 (Table 5).

DG-4 and DG-5 (t_r = 19.5 and 19.1 min; Table 4) were formed by all mutants. Only mutant M01_{his} formed DG-6 (t_r = 18.5 min; Table 4). DG-7 to DG-9 (t_r = 18.4, 17.5 and 17.2 min; Table 4) were formed by all mutants except M02_{his}, and DG-10 (t_r = 15.4 min; Table 4) was formed by all CYP102A1 mutants. For DG-5, an m/z value of 461.6 $[M+2H]^{2+}$ with a dichlorine isotope pattern was found, which corresponds to a double conjugated GSH adduct of diclofenac (Diclo+O+2SG; Table 5). For DG-7, an m/z value of 444.6 $[M+2H]^{2+}$ with a monochlorine isotope pattern was found. For DG-8, an m/z value of 427.6 $[M+2H]^{2+}$ without chlorine isotope pattern was observed in the MS spectra. These masses correspond to double conjugated GSH adducts of diclofenac where one (DG-7; Diclo+O+2SG-HCl; Table 5) or two atoms of chlorine have been displaced (DG-8; Diclo+O+2SG-2HCl; Table 5). The masses of DG-4, DG-6, DG-9 and DG-10 could not be determined with certainty under the conditions used.

The discovery of three double GSH adduct of diclofenac is interesting because it implicates secondary bioactivation of initially formed GSH-conjugates. Using the less sensitive LCQ LC-MS instrument, DG-5, DG-7 and DG-8 could only be found in the M11_{his} incubations and were therefore initially considered to be exclusive CYP102A1 metabolites. However, when measuring with the more sensitive IT-TOF LC-MS instrument, it could be demonstrated that DG-5, DG-7 and DG-8 were also present in the human and rat liver microsomes incubations (Table 5; Figure 3). Interestingly, Yu *et al.* [31] recently mentioned the presence of GSH adducts of diclofenac in incubations with HLM that correspond to the m/z values of DG-7 and DG-8 found in this study. Mutant M11_{his} was able to generate DG-5, DG-7 and DG-8 at 5-, 2.5- and 7.5-fold higher amounts than HLM, respectively. A biotransformation scheme of diclofenac is presented in Figure 4, proposing several possible structures for the metabolites detected in this study.

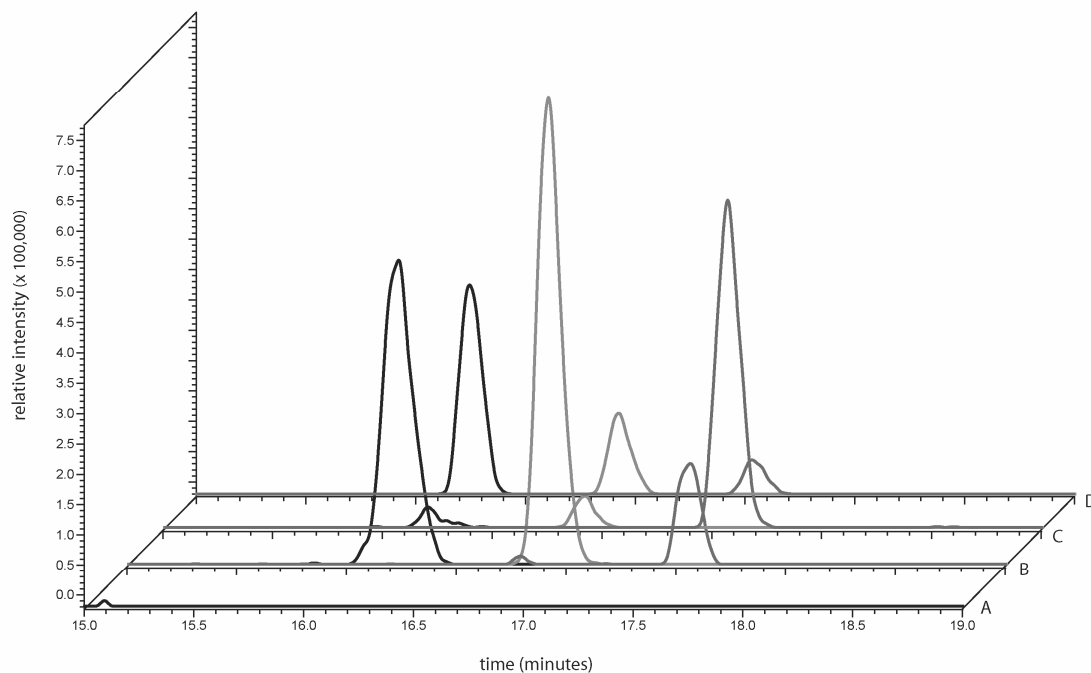


Figure 3. LC-MS analysis of the double GSH adducts of diclofenac. Incubations were analyzed with the IT-TOF LC-MS instrument and correspond to: (A) incubation with HLM without NADPH (negative control; 75 μ l injection); (B) standard incubation with HLM (75 μ l injection); (C) standard incubation with RLM (75 μ l injection) and (D) standard incubation with CYP102A1 M11_{his} (5 μ l injection). Black line: Extracted ion chromatograms (EIC) of m/z 427.62 (DG-8); light grey line: EIC of m/z 444.61 (DG-7) and dark grey line: EIC of m/z 461.59 (DG-5).

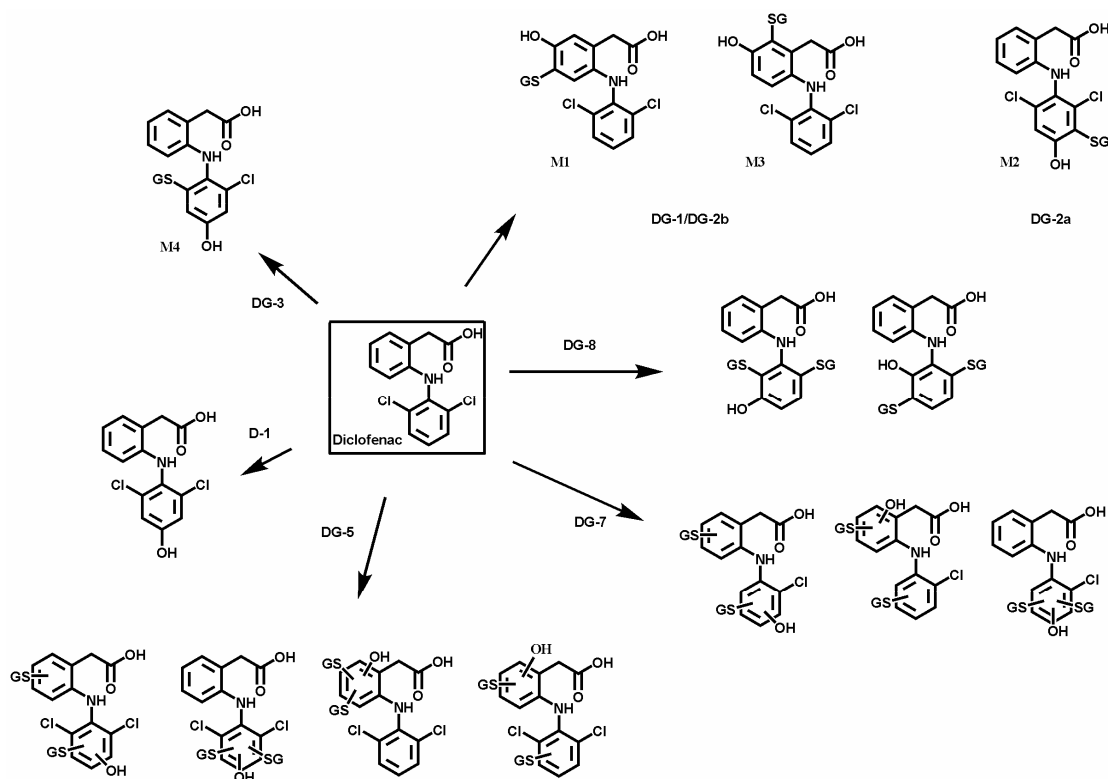


Figure 4. Proposed biotransformation scheme of diclofenac.

Biotransformation of acetaminophen by HLM, RLM and CYP102A1 mutants

All CYP102A1 mutants were able to generate the GSH adduct of acetaminophen (Figure 1-C; Table 6). M11_{his} showed the highest activity for the NAPQI-SG formation. Similar to what has been described previously [17], acetaminophen was also metabolized by HLM and RLM into NAPQI (Table 6). NAPQI-SG (m/z 457; $[M+H]^+$) was formed with the highest specific activity by mutant M11_{his}, which was 41-fold more active than HLM and 53-fold more active than RLM for the formation of this GSH adduct.

Table 6. Bioactivation of acetaminophen by CYP102A1 mutants and mammalian liver microsomes.

Enzyme fraction	NAPQI-SG formation
M01 _{his}	150.0 ± 43.7
M02 _{his}	38.0 ± 3.5
M05 _{his}	417.0 ± 77.4
M11 _{his}	904.5 ± 189.3
HLM	21.77 ± 4.6
RLM	17.1 ± 3.6

Formation of glutathione conjugate of NAPQI (NAPQI-SG) was quantified by HPLC with UV detection at 254 nm (t_r 15.1 minutes). Product formation is expressed in nmol product/nmol enzyme/60 minutes, assuming that the extinction coefficients of the substrate and its metabolites are comparable. Values represent the mean ± standard deviation of triplicate experiments. Identity of NAPQI-SG was confirmed by LCQ Deca LC-MS instrument, showing a m/z value of 457.1 corresponding to the singly-protonated molecule $[M+H]^+$.

Time dependence of metabolite formation

It is known that the rate of metabolite production by enzymes sometimes is strongly decreasing in time due to spontaneous enzyme inactivation, suicide inhibition (mechanism-based inhibition) or product inhibition. For example, mechanism-based inhibition was observed previously with rat P450 2C11 with diclofenac [7]. We previously demonstrated that several CYP102A1 mutants show non-linear time courses; after an initial fast phase lasting 0.5-2 minutes, the reaction continued at a lower activity [10]. Because the aim of the present study was to produce high levels of metabolites using CYP102A1, it was studied for how long metabolite production still continues. The product formation was linear from 15 to 60 minutes (data not shown).

Heterotropic cooperativity: activation by caffeine

In a previous study, we showed that acetaminophen metabolism by the CYP102A1 triple mutant R47L/F87V/L188Q was activated up to 70-fold by the addition of

caffeine [9]. To determine whether this activation also occurs for the present CYP102A1 mutants, incubations with clozapine, diclofenac and acetaminophen were performed in the presence of 10 mM caffeine. Activation of acetaminophen metabolism was only observed with mutant M02_{his}: this activation was approximately 10-fold (Figure 5). For mutant M01_{his}, 80% inhibition was observed in the presence of 10 mM caffeine, whereas for mutant M05_{his} and M11_{his}, the presence of caffeine did not have any effect on the catalytic activity. For the other two substrates, no activation or inhibition was observed in the presence of caffeine (data not shown). The reason why the different mutants do not respond in the same way cannot yet be rationalised because the underlying mechanism of the heterotropic cooperativity remains to be established. Also, because the different mutants always differ in three or more amino acids it is not possible yet to know which of these modifications might have affected the heterotropic cooperativity.

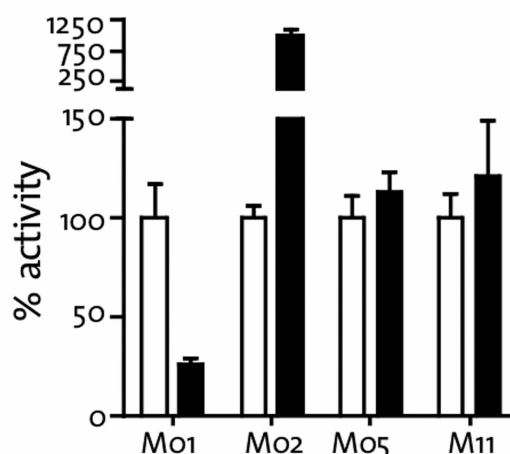


Figure 5. Effect of caffeine on acetaminophen metabolism by CYP102A1 mutants. % Activity in the absence (white bars) and presence (black bars) of 10 mM caffeine.

Conclusions

The present study demonstrates the applicability of drug metabolising mutants of CYP102A1 for the biosynthesis of high amounts of toxicologically relevant reactive metabolites of drugs, using clozapine, diclofenac and acetaminophen as model compounds. For all of these three substrates, the CYP102A1 mutants were indeed capable to generate the relevant reactive metabolites which are formed by human and rat liver microsomes but at significantly higher (up to 70-fold) levels. Formation of high levels of multiple metabolites by these enzymes will strongly facilitate the optimisation of analytical methods, structural identification and

pharmacological/toxicological characterisation of both major and minor drug metabolites formed by human P450s. The initial discovery of three novel GSH adducts of diclofenac in incubations of CYP102A1 mutants allowed us to demonstrate their presence in human incubations by using a more sensitive LC-MS system (Figure 3). Although quantitatively present at very low levels, it still cannot be ruled out that also minor reactive intermediates contribute to the mechanism leading to toxicity, for example by being very selective towards critical cellular target-molecules.

Recently, Madsen *et al.* [32] described an electrochemical method for the generation of reactive intermediates. This method showed to be successful in forming several GSH adducts formed by rat and human liver microsomes. However, it also showed limitations because not all relevant human and rat metabolites were produced. This can be explained by the fact that the regioselectivity of drug oxidation is often governed by the topology of the active site of P450s, rather than oxidation energies of the different positions. Therefore, CYP102A1 mutants, which also can orient metabolism to energetically less favorable positions, may constitute a more generic system for the generation of high levels of drug metabolites.

Acknowledgements

The authors would like to acknowledge Ben Bruyneel (Division of Biomolecular Analysis, Vrije Universiteit, Amsterdam) for his assistance in performing the LC-MS analyses.

References

- [1] Evans, W. E. and Relling, M. V. (1999) Pharmacogenomics: translating functional genomics into rational therapeutics. *Science*. 286, 487-491.
- [2] Shimada, T., Yamazaki, H., Mimura, M., Inui, Y. and Guengerich, F. P. (1994) Interindividual variations in human liver cytochrome P-450 enzymes involved in the oxidation of drugs, carcinogens and toxic chemicals: studies with liver microsomes of 30 Japanese and 30 Caucasians. *J Pharmacol Exp Ther*. 270, 414-423.
- [3] Baillie, T. A. (2006) Future of toxicology-metabolic activation and drug design: challenges and opportunities in chemical toxicology. *Chem Res Toxicol*. 19, 889-893.
- [4] Caldwell, G. W. and Yan, Z. (2006) Screening for reactive intermediates and toxicity assessment in drug discovery. *Curr Opin Drug Discov Devel*. 9, 47-60.
- [5] Yan, Z. and Caldwell, G. W. (2004) Stable-isotope trapping and high-throughput screenings of reactive metabolites using the isotope MS signature. *Anal Chem*. 76, 6835-6847.
- [6] Baillie, T. A. and Davis, M. R. (1993) Mass spectrometry in the analysis of glutathione conjugates. *Biol Mass Spectrom*. 22, 319-325.
- [7] Masubuchi, Y., Ose, A. and Horie, T. (2001) Mechanism-based inactivation of CYP2C11 by diclofenac. *Drug Metab Dispos*. 29, 1190-1195.
- [8] Munro, A. W., Leys, D. G., Mclean, K. J., Marshall, K. R., Ost, T. W., Daff, S., Miles, C. S., Chapman, S. K., Lysek, D. A., Moser, C. C., Page, C. C. and Dutton, P. L. (2002) P450 BM3: the very model of a modern flavocytochrome. *Trends Biochem Sci*. 27, 250-257.
- [9] Van Vugt-Lussenburg, B. M., Damsten, M. C., Maasdijk, D. M., Vermeulen, N. P. and Commandeur, J. N. (2006) Heterotropic and homotropic cooperativity by a drug-metabolising mutant of cytochrome P450 BM3. *Biochem Biophys Res Commun*. 346, 810-818.
- [10] Van Vugt-Lussenburg, B. M., Stjerschantz, E., Lastdrager, J., Oostenbrink, C., Vermeulen, N. P. and Commandeur, J. N. (2007) Identification of critical residues in novel drug metabolizing mutants of cytochrome P450 BM3 using random mutagenesis. *J Med Chem*. 50, 455-461.
- [11] Banks, A. T., Zimmerman, H. J., Ishak, K. G. and Harter, J. G. (1995) Diclofenac-associated hepatotoxicity: analysis of 180 cases reported to the Food and Drug Administration as adverse reactions. *Hepatology*. 22, 820-827.
- [12] Bjornsson, E., Jerlstad, P., Bergqvist, A. and Olsson, R. (2005) Fulminant drug-induced hepatic failure leading to death or liver transplantation in Sweden. *Scand J Gastroenterol*. 40, 1095-1101.
- [13] Idanpaan-Heikkila, J., Alhava, E., Olkinuora, M. and Palva, I. P. (1977) Agranulocytosis during treatment with clozapine. *Eur J Clin Pharmacol*. 11, 193-198.
- [14] Maggs, J. L., Williams, D., Pirmohamed, M. and Park, B. K. (1995) The metabolic formation of reactive intermediates from clozapine, a drug associated with agranulocytosis in man. *J Pharmacol Exp Ther*. 275, 1463-1475.
- [15] Pirmohamed, M., Williams, D., Madden, S., Templeton, E. and Park, B. K. (1995) Metabolism and bioactivation of clozapine by human liver in vitro. *J Pharmacol Exp Ther*. 272, 984-990.
- [16] Yan, Z., Li, J., Huebert, N., Caldwell, G. W., Du, Y. and Zhong, H. (2005) Detection of a novel reactive metabolite of diclofenac: evidence for CYP2C9-mediated bioactivation via arene oxides. *Drug Metab Dispos*. 33, 706-713.
- [17] Patten, C. J., Thomas, P. E., Guy, R. L., Lee, M., Gonzalez, F. J., Guengerich, F. P. and Yang, C. S. (1993) Cytochrome P450 enzymes involved in acetaminophen activation by rat and human liver microsomes and their kinetics. *Chem Res Toxicol*. 6, 511-518.
- [18] Bessems, J. G. and Vermeulen, N. P. (2001) Paracetamol (acetaminophen)-induced toxicity: molecular and biochemical mechanisms, analogues and protective approaches. *Crit Rev Toxicol*. 31, 55-138.
- [19] Steffen C. Maurer, H. S., Rolf D. Schmid, Vlada Urlacher, (2003) Immobilisation of P450 BM-3 and an NADP+ Cofactor Recycling System: Towards a Technical Application of Heme-Containing Monooxygenases in Fine Chemical Synthesis. *Publ*802-810.
- [20] Kranendonk, M., Carreira, F., Theisen, P., Laires, A., Fisher, C. W., Rueff, J., Estabrook, R. W. and Vermeulen, N. P. (1999) Escherichia coli MTC, a human NADPH P450 reductase competent mutagenicity tester strain for the expression of human cytochrome P450 isoforms 1A1, 1A2, 2A6, 3A4, or 3A5: catalytic activities and mutagenicity studies. *Mutat Res*. 441, 73-83.
- [21] Sandhu, P., Baba, T. and Guengerich, F. P. (1993) Expression of modified cytochrome P450 2C10 (2C9) in Escherichia coli, purification, and reconstitution of catalytic activity. *Arch Biochem Biophys*. 306, 443-450.
- [22] Tartof, K. D. and Hobbs, C. A. (1988) New cloning vectors and techniques for easy and rapid restriction mapping. *Gene*. 67, 169-182.
- [23] Bessems, J. G., Te Koppele, J. M., Van Dijk, P. A., Van Stee, L. L., Commandeur, J. N. and Vermeulen, N. P. (1996) Rat liver microsomal cytochrome P450-dependent oxidation of 3,5-disubstituted analogues of paracetamol. *Xenobiotica*. 26, 647-666.

- [24] Lee, C. A., Manyike, P. T., Thummel, K. E., Nelson, S. D. and Slattery, J. T. (1997) Mechanism of cytochrome P450 activation by caffeine and 7,8-benzoflavone in rat liver microsomes. *Drug Metab Dispos.* 25, 1150-1156.
- [25] Tugnait, M., Hawes, E. M., Mckay, G., Eichelbaum, M. and Midha, K. K. (1999) Characterization of the human hepatic cytochromes P450 involved in the in vitro oxidation of clozapine. *Chem Biol Interact.* 118, 171-189.
- [26] Schaber, G., Wiatr, G., Wachsmuth, H., Dachtler, M., Albert, K., Gaertner, I. and Breyer-Pfaff, U. (2001) Isolation and identification of clozapine metabolites in patient urine. *Drug Metab Dispos.* 29, 923-931.
- [27] Leemann, T., Transon, C. and Dayer, P. (1993) Cytochrome P450TB (CYP2C): a major monooxygenase catalyzing diclofenac 4'-hydroxylation in human liver. *Life Sci.* 52, 29-34.
- [28] Shen, S., Marchick, M. R., Davis, M. R., Doss, G. A. and Pohl, L. R. (1999) Metabolic activation of diclofenac by human cytochrome P450 3A4: role of 5-hydroxydiclofenac. *Chem Res Toxicol.* 12, 214-222.
- [29] Tang, W., Stearns, R. A., Wang, R. W., Chiu, S. H. and Baillie, T. A. (1999) Roles of human hepatic cytochrome P450s 2C9 and 3A4 in the metabolic activation of diclofenac. *Chem Res Toxicol.* 12, 192-199.
- [30] Tang, W., Stearns, R. A., Bandiera, S. M., Zhang, Y., Raab, C., Braun, M. P., Dean, D. C., Pang, J., Leung, K. H., Doss, G. A., Strauss, J. R., Kwei, G. Y., Rushmore, T. H., Chiu, S. H. and Baillie, T. A. (1999) Studies on cytochrome P-450-mediated bioactivation of diclofenac in rats and in human hepatocytes: identification of glutathione conjugated metabolites. *Drug Metab Dispos.* 27, 365-372.
- [31] Yu, L. J., Chen, Y., Deninno, M. P., O'connell, T. N. and Hop, C. E. (2005) Identification of a novel glutathione adduct of diclofenac, 4'-hydroxy-2'-glutathion-deschloro-diclofenac, upon incubation with human liver microsomes. *Drug Metab Dispos.* 33, 484-488.
- [32] Madsen, K. G., Olsen, J., Skonberg, C., Hansen, S. H. and Jurva, U. (2007) Development and Evaluation of an Electrochemical Method for Studying Reactive Phase-I Metabolites: Correlation to in Vitro Drug Metabolism. *Chem Res Toxicol.* 20, 821-831.

Chapter 3

The role of glutathione S-transferases in the trapping of reactive intermediates of drugs

Abstract

Conjugation to glutathione (GSH) is an important protection mechanism against reactive electrophilic metabolites of drugs that are thought to be involved in adverse drug reactions (ADRs). These conjugation reactions can be spontaneous or mediated by glutathione S-transferases (GSTs). Although previous clinical data suggest that GSTs could play a role in defining individual susceptibilities towards ADRs, only few *in vitro* studies have been performed to confirm these observations. The aim of this work was therefore to investigate if GSTs contribute to the conjugation of reactive intermediates of drugs with GSH. Five model compounds (acetaminophen, 3-hydroxyacetanilide, clozapine, diclofenac and carbamazepine) were incubated with rat liver microsomes and/or with the highly active bacterial P450 BM3 mutant M11_{his}; and the impact of the presence of rat GSTs on the GSH adduct levels was assessed by LC-MS. Although GSTs were found to have little effect on the amounts of GSH adducts for most drugs under study, they significantly increased the levels of the GSH adducts of carbamazepine. More specifically, GSTs catalyzed the GSH conjugation of the most reactive arene oxide intermediates of the drug. While further experiments with human GST isoforms are required, these results may support previous clinical observations suggesting that GST genetic polymorphisms could be a risk factor in carbamazepine-induced ADRs.

Introduction

Drug metabolism mainly consists of the conversion of lipophilic drug molecules to hydrophilic metabolites that can be eliminated from the body. Cytochromes P450 (P450s) are the phase I enzymes that are most frequently involved in this process. Functionalised metabolites can subsequently be conjugated to more polar groups by phase II enzymes, which further increase their solubility and excretion. Although these transformations are usually part of detoxification processes, P450s can also lead to the formation of reactive metabolites that can react with macromolecules in the body and cause toxicity. Covalent binding to DNA is usually related to mutagenicity and carcinogenicity; while the formation of protein adducts is generally thought to be associated with several forms of adverse drug reactions (ADRs) [1, 2].

Conjugation to glutathione (GSH) is an important defence mechanism which protects the organism against toxic effects of reactive intermediates (RIs). This reaction can occur spontaneously and/or be catalyzed by the glutathione S-transferases (GSTs) [3, 4]. Although these enzymes have different activities depending on their specific class and/or sub-type, their main reaction is to catalyze the reaction of GSH with electrophilic intermediates in order to form stable GSH conjugates that can be eliminated from the body, mainly by processing to mercapturic acids [5].

Known substrates of GSTs include insecticides, herbicides, environmental pollutants, carcinogens, by-products of lipid peroxidation but also a wide range of drugs including cancer chemotherapeutic agents (e.g. adriamycin, cyclophosphamide, melphalan) [6-8]. Still little is known, however, about the role of GSTs in the detoxification of RIs of drugs involved in ADRs and in rare idiosyncratic drug reactions (IDRs). Clinical studies have recently demonstrated a significant prevalence of the combined GSTM1-T1 double-null genotype in patients suffering from tacrine and troglitazone-induced liver injury [9, 10]. Similar findings were obtained for other types of drugs (e.g. diclofenac, carbamazepine) [11, 12] suggesting that GST polymorphisms could be one of the factors determining inter-individual differences in susceptibility to ADRs.

Remarkably, as yet, only few *in vitro* studies have been conducted to confirm these clinical observations. Coles *et al.* previously showed that GSTs can catalyze the coupling of the reactive metabolite of acetaminophen (NAPQI) to GSH [13]. In the case of carbamazepine, GSTs were suggested to play a protective role by

decreasing the rate of irreversible protein binding of ^{14}C -carbamazepine to mouse microsomal proteins [14].

Since the role of GSTs in ADRs remains unclear, the main goal of this study was to evaluate if GSTs could improve the GSH trapping efficiency of RIs of drugs in *in vitro* enzymatic incubations. Incubations were performed with rat liver microsomes and/or with the highly active bacterial P450 BM3 mutant M11_{his} [15]; and the effect of rat GSTs on GSH adduct levels was assessed by LC-MS. Acetaminophen, 3-hydroxyacetanilide, clozapine, diclofenac and carbamazepine were chosen as model compounds since they are all known to be bioactivated by P450s to RIs; to give covalent binding to proteins [16-21] and/or have been previously associated with ADRs [22-25].

Experimental procedures

Enzymes

The P450 BM3 mutant M11_{his} (M11_{his}) was prepared and expressed as described previously [15]. Control rat liver microsomes (RLM) were prepared as described in [26]. Rat liver glutathione S-transferases (GSTs) were purified as follows. Rat liver cytosol (24 ml) was first dialyzed overnight against 2 liters of 10 mM KPi buffer (pH 7.4). The dialyzed cytosol was centrifuged (13.000 rpm, 4°C, 10 minutes) and the supernatant was filtered using 0.45 µm Acrodisc filters. GSTs were subsequently isolated from the cytosolic fraction using pre-packed Glutathione-agarose columns (G 3907 from Sigma). The columns were first equilibrated with 5 x 2.5 ml of 10 mM KPi buffer containing 150 mM NaCl (pH 7.4). Then, 7.5 ml of the cytosolic fraction was loaded onto the equilibrated columns under gravity flow. The flow-through was collected, applied a second time onto the columns and the loaded columns were allowed to stand for 1 hour. The columns were subsequently washed with 3 x 2.5 ml of 10 mM KPi buffer containing 150 mM NaCl (pH 7.4) and washing fractions were collected. Elution of bound GSTs took place with 8 x 2.5 ml of 50 mM Tris-HCl buffer pH 8.0 containing 10 mM of reduced glutathione. Collected fractions were checked for GST activity using the CDNB assay described below and the fractions showing activity were pooled to constitute the GST batch. GSH was subsequently removed from the GST batch by repeated washing with 50 mM Tris-HCl buffer (pH 8.0) in Vivaspin 20 filtration tubes at 4000 rpm (10.000 MWCO PES, Sartorius). A final GST protein concentration of 0.5 mg/ml was determined by the Bradford method using bovine serum albumin (BSA) as standard [27].

GST enzymatic activities were determined using the standard CDNB assay as described in [28]. Briefly, 50 μl of 1-chloro-2,4-dinitrobenzene (CDNB; 10 mM in ethanol) was added to 50 μl of reduced glutathione (GSH; 10 mM in KPi buffer pH 6.5) in a 3 ml cuvet containing 1 ml of 10 mM KPi buffer (pH 6.5). A 10 μl aliquot of a 20 times diluted enzymatic fraction was added to the mixture, the cuvet was shaken and the absorbance was monitored at 340 nm for 2 minutes at room temperature. When using $\Delta\epsilon = 9.6 \text{ mM}^{-1}\text{cm}^{-1}$, a specific activity of 28.7 $\mu\text{mol product}/\text{min}/\text{mg}$ protein was found for the GST batch.

Enzymatic incubations

Incubations had a final volume of 250 μl and usually consisted of 100 mM KPi buffer pH 7.4, 1 mM of substrate and 5 mM of GSH (final concentrations). Stock solutions of 100 mM were prepared for the different substrates. Acetaminophen (APAP) and 3-hydroxyacetanilide (AMAP) were dissolved in H_2O ; clozapine and diclofenac in DMSO and carbamazepine in ethanol. Final organic modifier concentrations in the incubation mixtures were always below 1%. A final enzymatic concentration of 1 mg/ml RLM and 250 nM of purified M11_{his} were used in the incubations. Reactions were initiated by the addition of 2 mM NADPH (final concentration). The reactions were allowed to proceed for 60 minutes at 37°C for RLM and at 24°C for M11_{his}. Incubations were subsequently terminated by the addition of 25 μl 10% HClO_4 (APAP, AMAP and clozapine) or 250 μl cold methanol (diclofenac and carbamazepine). Samples were centrifuged to remove precipitated protein (4000 rpm, 15 minutes) and supernatants were analysed by LC-MS. Control incubations consisted of reactions performed without NADPH and/or without GSH. For positive identification of some of the possible GSH adducts of carbamazepine, incubations with 10,11-carbamazepine epoxide (CE; final concentration of 250 μM) were performed in 100 mM KPi buffer pH 7.4, for 60 minutes, at 37°C and with 5 mM of GSH (final concentration). Samples were subsequently analyzed by LC-MS. Control incubations were performed without GSH.

To determine the effects of GSTs on the GSH adduct formation, incubations were performed like described above with and without GSTs (final protein concentration: 94 $\mu\text{g}/\text{ml}$; final specific activity: 5.4 $\mu\text{mol prod}/\text{min}/\text{mg prot}$). To better discriminate enzymatic versus non-enzymatic reactions, experiments were performed with two different GSH concentrations: 1 mM and 5 mM (final concentrations). Since the K_m of GSTs for GSH is approximately 100 μM [13], performing incubations with 1 mM GSH instead of 5 mM was expected to reduce non-enzymatic reactions five-fold

while not impacting GST-dependent reactions. This may assist the identification of GST-dependent catalytic effects on the levels of GSH adducts. Furthermore, experiments with ethacrynic acid (EA) were performed to evaluate whether GST effects could be inhibited. Enzymatic incubations were performed as described above with and without GSTs and different concentrations of EA were added to the mixture (0, 0.5 and 1 mM). High concentrations of EA were chosen as to ensure that all GST activity would be inhibited. All samples were treated like described above and analyzed by LC-MS.

Analytical methods

LC-MS analysis was performed using a LCQ Deca mass spectrometer instrument (Thermo Finnigan). Metabolites were separated by reversed chromatography using a C18 column (Phenomenex, Luna 5 μ , 150 x 4.6 mm). The following gradient was used at a flow rate of 0.4 ml/min: from 0 to 5 minutes 0% solvent B, followed by an increase to 100% solvent B from 5 to 30 minutes, followed by a decrease to 0% solvent B from 30 to 35 minutes, and finally 0% solvent B from 35 to 40 minutes. Solvent A consisted of 1% acetonitrile, 98.8% H₂O and 0.2% formic acid; solvent B consisted of 99% acetonitrile, 0.8% H₂O and 0.2% formic acid. MS analysis was performed in the positive mode using electrospray ionisation (ESI). N₂ was used as sheath gas (60 psi) and auxiliary gas (10 psi), the needle voltage was 5000 V and the heated capillary was at 150°C. The LC-MS Solution software package from Shimadzu was used to determine peak areas of the GSH adducts in the corresponding extracted ion chromatograms. Data analysis was performed using GraphPad Prism 4.0 and statistically significant differences were determined by Student t-test analysis.

Results

Bioactivation of acetaminophen

Incubations performed with RLM produced one major GSH adduct (AG-1; t_r 15.74 min; Table 1) with a m/z of 457.1 [M+H]⁺ corresponding to NAPQI coupled to GSH. In addition, a minor GSH adduct, with a m/z of 473.1 [M+H]⁺, was also present in the incubation mixture (AG-2; t_r 15.40 min). This adduct most likely originates from an ortho-quinone metabolite of APAP (Figure 1). When GSTs were added to the incubations, no significant changes were observed in the GSH adduct levels.

Table 1. GST effects on the GSH adducts of acetaminophen.

GSH adducts	t_r	m/z	Structure	RLM		M11 _{his}	
				- GSTs	+ GSTs	- GSTs	+ GSTs
AG-1	15.74	457.1	APAP+SG	100 ± 2	86 ± 25	100 ± 2	137 ± 24
AG-2	15.40	473.1	APAP+O+SG	100 ± 2	112 ± 20	-	-
AG-3	15.42	457.1	APAP+SG	-	-	100 ± 4	79 ± 18
AG-4	15.10	473.1	APAP+O+SG	-	-	100 ± 2	133 ± 69

LC-MS analysis of the GSH adducts of APAP produced by RLM and BM3 mutant M11_{his}. Peak areas were determined in the corresponding extracted ion chromatograms. Areas of the GSH adducts in the incubations without GSTs were arbitrary set to 100 % and changes after addition of 94 µg/ml GSTs were determined (\pm standard deviation of the differences). t_r is in minutes; m/z corresponds to the mass of the protonated molecule $[M+H]^+$ and possible GSH adduct structures are proposed. Absence (-) of the GSH adduct is indicated in the table.

The P450 BM3 mutant M11_{his} metabolized APAP to the same major GSH adduct as RLM (AG-1; Table 1). This is in agreement with previous data obtained in our laboratory [15]. M11_{his} also produced two minor GSH adducts: one additional GSH adduct of m/z of 457.1 $[M+H]^+$ (AG-3; t_r 15.42 min) and one GSH adduct of m/z of 473.1 $[M+H]^+$ (AG-4; t_r 15.10 min). M11_{his} did not produce GSH adduct AG-2 (Figure 1). When incubated in presence of GSTs, no statistically significant changes were observed in the amounts of GSH adducts produced.

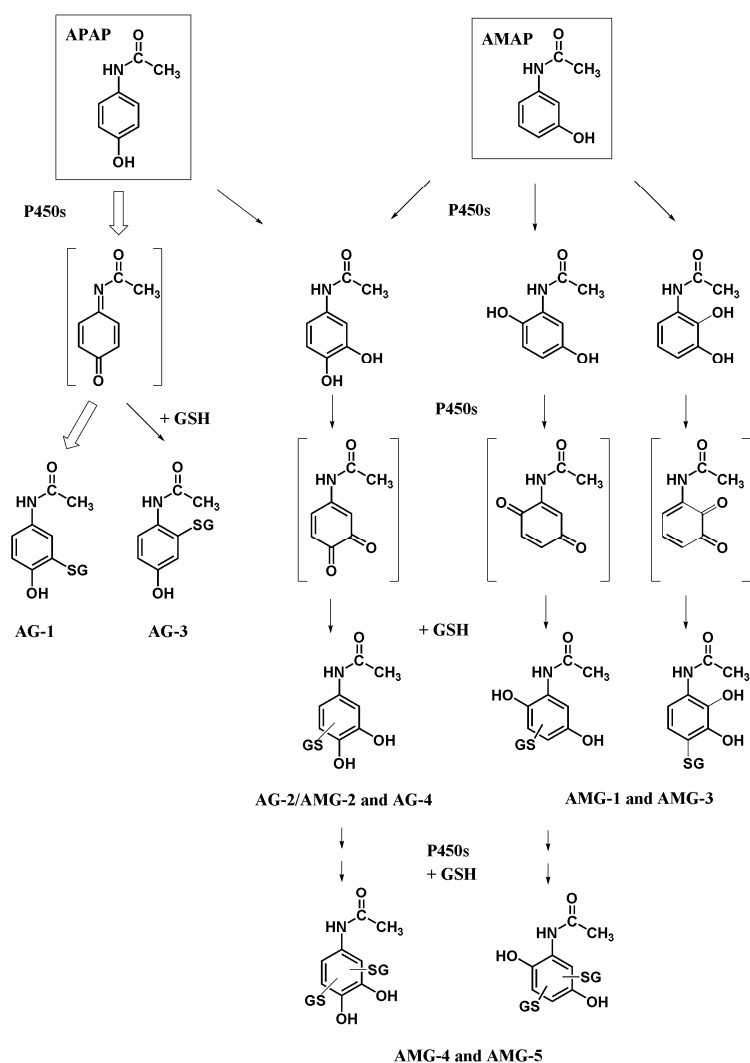


Figure 1. Scheme of the possible GSH adducts of APAP and AMAP.

Bioactivation of 3-hydroxyacetanilide

Incubations performed with AMAP and RLM produced four GSH adducts (Table 2). Three GSH adducts had a m/z of 473.1 $[M+H]^+$ (AMG-1, AMG-2 and AMG-3; t_r 14.64, 15.40 and 15.64 min respectively) corresponding to ortho- and para-quinone metabolites of AMAP conjugated to GSH (Figure 1). One adduct had a m/z of 778.2 $[M+H]^+$ (AMG-4; t_r 14.60; Table 2) corresponding to a doubly conjugated GSH adduct of AMAP. This metabolism pattern is in agreement with previous data from literature [29, 30]. By co-elution, we found that one of the GSH adducts of AMAP (AMG-2; Table 2) corresponds to one hydroxylated GSH adduct of APAP (AG-2; Table 1). Therefore, this GSH adduct must originate from the 3,4-ortho-catechol reactive metabolite of APAP and AMAP (Figure 1). Interestingly, levels of this GSH adduct were 20-fold higher in AMAP incubations compared to those performed with APAP

(data not shown). In general, GSTs did slightly decrease GSH adduct levels in RLM incubations but these changes were not statistically significant.

Table 2. GST effects on the metabolism of 3-hydroxyacetanilide.

GSH adducts	t_r	m/z	Structure	RLM		M11 _{his}	
				- GSTs	+ GSTs	- GSTs	+ GSTs
AMG-1	14.64	473.1	AMAP+O+SG	100 ± 4	92 ± 31	-	-
AMG-2	15.40	473.1	AMAP+O+SG	100 ± 2	86 ± 19	100 ± 4	81 ± 9
AMG-3	15.64	473.1	AMAP+O+SG	100 ± 3	83 ± 17	-	-
AMG-4	14.60	778.2	AMAP+O+2xSG	100 ± 2	99 ± 23	100 ± 3	121 ± 35
AMG-5	14.87	778.2	AMAP+O+2xSG	-	-	100 ± 2	89 ± 7

LC-MS analysis of the GSH adducts of AMAP produced by RLM and BM3 mutant M11_{his}. Peak areas were determined in the corresponding extracted ion chromatograms. Areas of the GSH adducts in the incubations without GSTs were arbitrary set to 100 % and changes after addition of 94 µg/ml GSTs were determined (± standard deviation of the differences). t_r is in minutes; m/z corresponds to the mass of the protonated molecule $[M+H]^+$ and possible GSH adduct structures are proposed. Absence (-) of the GSH adduct is indicated in the table.

AMAP was metabolized to three GSH adducts by M11_{his} (Table 2). One GSH adduct corresponds to AMG-2 (t_r 15.40 min), originating from the common RI of APAP and AMAP described above. The two other GSH adducts had a m/z of 778.2 $[M+H]^+$ (AMG-4 and AMG-5; t_r 14.60 and 14.87 min respectively) corresponding to doubly-conjugated GSH adducts of AMAP. AMG-4 was also found in RLM incubations, whereas AMG-5 is an exclusive M11_{his}-dependent GSH adduct (Figure 1). Again, GSTs did not significantly alter the levels of these GSH adducts.

Bioactivation of clozapine

RLM produced two GSH adducts having a m/z of 632.2 $[M+H]^+$ corresponding to clozapine coupled to GSH (CG-1 and CG-2; t_r 16.75 and 17.23 min; Table 3).

Addition of GSTs did not significantly affect the GSH adduct levels.

When clozapine was incubated with M11_{his}, four major GSH adducts were produced (Table 3). Two were also formed by RLM (CG-1 and CG-2). The two additional adducts had a m/z of 618.2 $[M+H]^+$ corresponding to N-demethylated clozapine coupled to GSH (CG-3 and CG-4; t_r 16.30 and 17.01). This metabolic profile is consistent with that observed previously [15]. As with RLM, GSTs did not significantly influence GSH adduct levels in M11_{his} incubations.

Table 3. GST effects on the metabolism of clozapine.

GSH adducts	t_r	m/z	Structure	RLM		M11 _{his}	
				- GSTs	+ GSTs	- GSTs	+ GSTs
CG-1	16.75	632.2	Cloza+SG	100± 5	118 ± 60	100± 2	104 ± 20
CG-2	17.23	632.2	Cloza+SG	100± 2	101 ± 8	100± 1	107 ± 8
CG-3	16.30	618.2	Cloza-CH ₂ +SG	-	-	100± 3	87 ± 18
CG-4	17.01	618.2	Cloza-CH ₂ +SG	-	-	100± 2	113 ± 21

LC-MS analysis of the GSH adducts of clozapine produced by RLM and BM3 mutant M11_{his}. Peak areas were determined in the corresponding extracted ion chromatograms. Areas of the GSH adducts in the incubations without GSTs were arbitrary set to 100 % and changes after addition of 94 µg/ml GSTs were determined (\pm standard deviation of the differences). t_r is in minutes; m/z corresponds to the mass of the protonated molecule $[M+H]^+$ and possible GSH adduct structures are proposed. Absence (-) of the GSH adduct is indicated in the table.

Bioactivation of diclofenac

Three GSH adducts of diclofenac were produced by RLM (Table 4). Two adducts had a m/z 617.1 $[M+H]^+$ corresponding to quinoneimine(s) of diclofenac coupled to GSH (DG-1 and DG-2; t_r 20.18 and 20.78 min respectively). One minor GSH adduct had a m/z 583.1 $[M+H]^+$ (DG-3; t_r 20.22 min) and most likely correspond to a quinoneimine or epoxide intermediate of diclofenac where a chlorine atom has been substituted by GSH. No statistically significant changes in the GSH adduct levels were observed when GSTs were added to the incubation mixtures.

M11_{his} metabolized diclofenac to seven GSH adducts (Table 4). This metabolism pattern is in agreement with previous data obtained in our laboratory [15]. Briefly, M11_{his} produced the same GSH adducts as RLM (DG-1, DG-2 and DG-3). The P450 BM3 mutant also generated a third GSH adduct having a m/z 617.1 $[M+H]^+$ (DG-4; t_r 20.32). Furthermore, three double GSH adducts of diclofenac were found in the M11_{his} incubations (DG-5, DG-6 and DG-7; t_r 18.74, 18.16 and 17.51 min respectively), corresponding to quinoneimine(s) of diclofenac, doubly-conjugated to GSH, where no (DG-5), one (DG-6) or two (DG-7) chlorine atoms have been displaced. Addition of GSTs to the incubations did not significantly change the GSH adduct levels observed.

Table 4. GST effects on the metabolism of diclofenac.

GSH adducts	t_r	m/z	Structure	RLM		M11 _{his}	
				- GSTs	+ GSTs	- GSTs	+ GSTs
DG-1	20.18	617.1	Diclo+O+SG	100 ± 2	99 ± 9	100 ± 1	90 ± 9
DG-2	20.78	617.1	Diclo+O+SG	100 ± 4	123 ± 11	100 ± 5	91 ± 21
DG-3	20.22	583.1	Diclo+O+SG-HCl	100 ± 3	142 ± 40	100 ± 2	85 ± 28
DG-4	20.32	617.1	Diclo+O+SG	-	-	100 ± 4	167 ± 55
DG-5	18.74	922.1	Diclo+O+2xSG	-	-	100 ± 4	90 ± 39
DG-6	18.16	888.1	Diclo+O+2xSG-HCl	-	-	100 ± 1	86 ± 27
DG-7	17.51	854.1	Diclo+O+2xSG-2xHCl	-	-	100 ± 2	96 ± 24

LC-MS analysis of the GSH adducts of diclofenac produced by RLM and BM3 mutant M11_{his}. Peak areas were determined in the corresponding extracted ion chromatograms. Areas of the GSH adducts in the incubations without GSTs were arbitrary set to 100 % and changes after addition of 94 µg/ml GSTs were determined (\pm standard deviation of the differences). t_r is in minutes; m/z corresponds to the mass of the protonated molecule $[M+H]^+$ and possible GSH adduct structures are proposed. Absence (-) of the GSH adduct is indicated in the table.

Bioactivation of carbamazepine

Carbamazepine was metabolized to three GSH adducts of m/z 560.2 $[M+H]^+$ by RLM (CAG-1, CAG-2 and CAG-3; t_r 18.23, 17.50 and 16.95 min respectively; Table 5).

These adducts most likely originate from epoxide intermediates of carbamazepine that have been coupled to GSH. This is in agreement with previous data from literature [19, 31]. Addition of GSTs to the incubation mixture did not affect the levels of CAG-1 but significantly increased the amounts of CAG-2 and CAG-3 formed (1.9- and 3.4- fold higher respectively; Table 5).

In absence of GSTs, only two of the GSH adducts described above (CAG-1 and CAG-2; Table 5) were found in M11_{his} incubations. But, interestingly, when GSTs were added to the incubations, a third GSH adduct was detected which most likely correspond to CAG-3 previously observed in the RLM incubations (Figure 2).

Comparatively, amounts of CAG-1 and CAG-2 were not significantly affected by the addition of GSTs to the M11_{his} incubations.

Table 5. GST effects on the metabolism of carbamazepine.

GSH adducts	t_r	m/z	Structure	RLM		M11 _{his}	
				- GSTs	+ GSTs	- GSTs	+ GSTs
CAG-1	18.23	560.2	Carb+O+2H+SG	100 ± 2	81 ± 9	100 ± 3	91 ± 5
CAG-2	17.50	560.2	Carb+O+2H+SG	100 ± 5	191 ± 26 *	100 ± 2	98 ± 13
CAG-3	16.95	560.2	Carb+O+2H+SG	100 ± 4	343 ± 40 **	-	+ [#]

LC-MS analysis of the GSH adducts of carbamazepine produced by RLM and BM3 mutant M11_{his}. Peak areas were determined in the corresponding extracted ion chromatograms. Areas of the GSH adducts in the incubations without GSTs were arbitrary set to 100 % and changes after addition of 94 µg/ml GSTs were determined (± standard deviation of the differences). t_r is in minutes; m/z corresponds to the mass of the protonated molecule $[M+H]^+$ and possible GSH adduct structures are proposed. Absence (-) and presence (+) of the GSH adduct is indicated in the table. Statistically-significant changes are depicted as: * p-value < 0.05; ** p-value < 0.01 and [#] GSH adduct only formed in presence of GSTs.

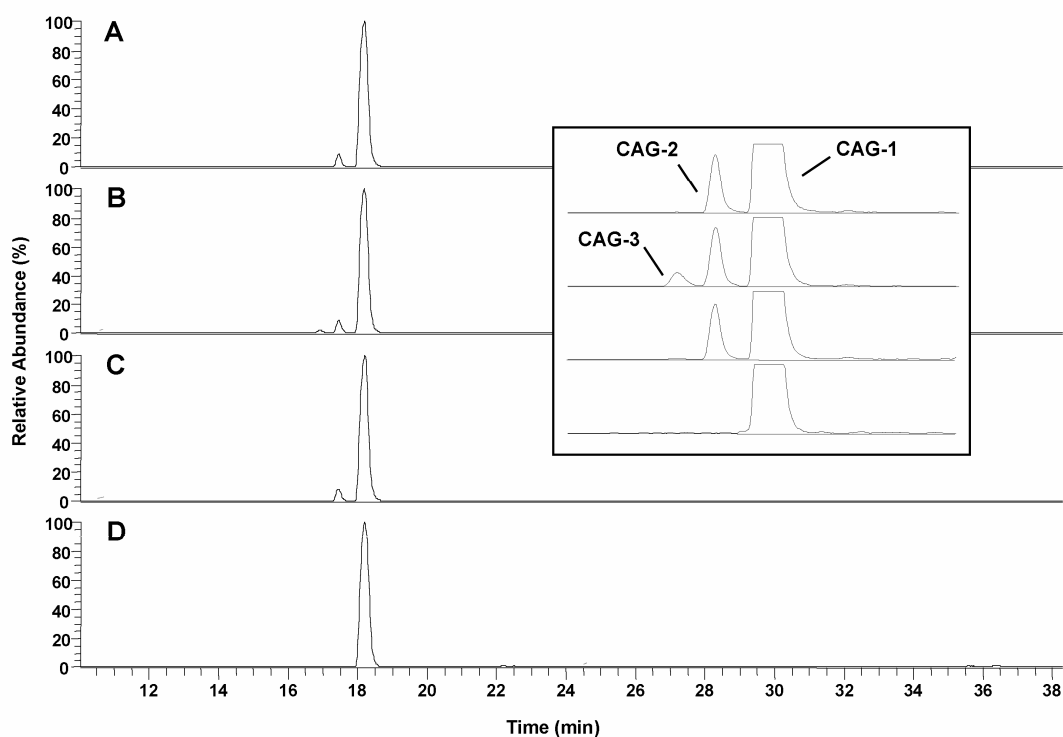


Figure 2. GSH adducts of carbamazepine. LC-MS analysis of the GSH adducts of carbamazepine in P450 BM3 mutant M11_{his} incubations. Extracted Ion Chromatograms of m/z 560.2 are presented: (A) carbamazepine incubation performed without GSTs; (B) carbamazepine incubation performed with 94 µg/ml GSTs; (C) carbamazepine incubation performed with 94 µg/ml GSTs and 1 mM of EA and (D) GSH adduct originating from CE.

Incubations with carbamazepine 10,11-epoxide (CE) were performed to identify some of the GSH adducts of carbamazepine. By co-elution, we found that the major CAG-1 adduct in carbamazepine incubations originates from CE (Figure 2). Previous data from literature described the formation of two GSH adduct diastereoisomers when reacting CE with GSH [32]. This discrepancy most likely reflects differences in chromatographic systems and suggests that CAG-1 may actually consist of two GSH adduct diastereoisomers. Consequently, CAG-2 and CAG-3 must originate from arene oxides located on the side rings of carbamazepine (Figure 3). Although conjugation of CE to GSH occurred to some extent spontaneously, GSTs were also found to significantly catalyze this reaction (3.5-fold increase; Figure 4B).

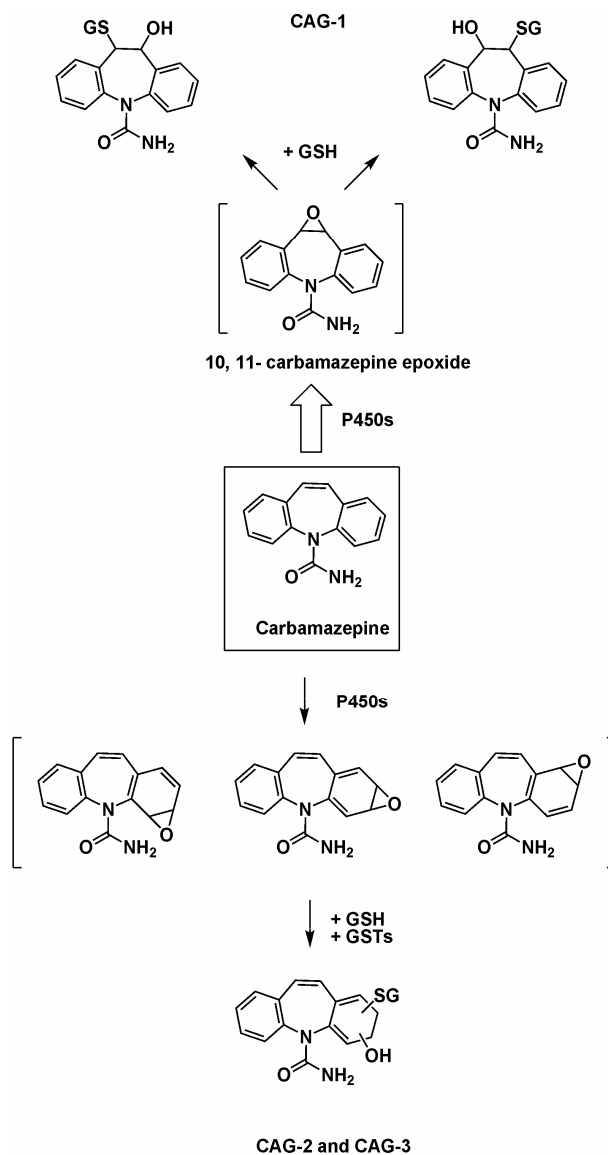
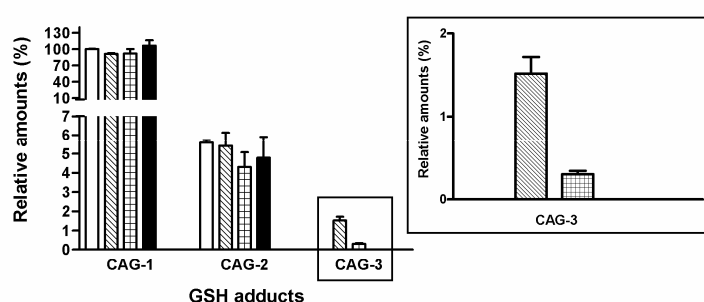


Figure 3. GSH adducts of carbamazepine and GST effects with rat enzymes.

Ethacrynic acid (EA) significantly inhibited the observed GST effects. In M11_{his} incubations, a concentration of 0.5 mM EA decreased CAG-3 levels by 80% whereas 1 mM of EA totally inhibited the formation of this adduct (Figure 2 and Figure 4). CAG-1 and CAG-2 levels were not significantly affected by EA (Figure 4). The catalytic effect of GSTs in the formation of CAG-1 in CE incubations was also fully inhibited by EA (Figure 4). No evaluation could be performed in RLM incubations since EA appeared to inhibit the rat liver P450s at both concentrations (data not shown).

A. M11_{his} carbamazepine incubations



B. 10,11 - carbamazepine epoxide incubations

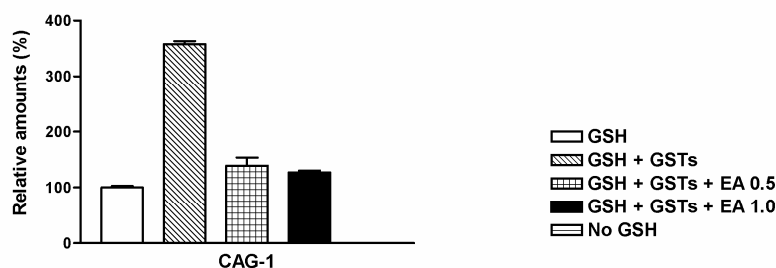


Figure 4. GST and EA effects on the GSH adducts of carbamazepine: (A) in M11_{his} carbamazepine incubations; (B) GSH adduct CAG-1 in incubations performed with CE. Incubations with GSH only (GSH; set arbitrary to 100%); with GSH and 94 $\mu\text{g/ml}$ GSTs (GSH + GSTs); with GSH, 94 $\mu\text{g/ml}$ GSTs and 0.5 mM EA (GSH + GSTs + EA 0.5); with GSH, 94 $\mu\text{g/ml}$ GSTs and 1.0 mM EA (GSH + GSTs + EA 1.0) and control incubation performed without GSH (No GSH) are depicted in the figures.

M11_{his} was found to be more active than RLM in producing CAG-1 and CAG-2 (10- and 1.7-fold higher, respectively; Figure 5). Interestingly, catalytic effects of GSTs were only observed for the minor GSH adducts (e.g. CAG-2 and CAG-3 in RLM incubations and CAG-3 in M11_{his} incubations; Figure 5). The formation of the major CAG-1 GSH adduct was only catalyzed by GSTs in CE incubations. This apparent inconsistency may originate from the different concentrations and/or types of RIs present in both enzymatic systems. It is indeed likely that the high levels of the 10,11-

epoxide intermediate present in CE incubations has triggered GSTs to catalyze its conjugation to GSH. However, in a more physiologically-relevant situation (e.g. carbamazepine incubations), GSTs appear to have a higher affinity for arene oxide-type of intermediates than for CE.

Finally, and as for the other compounds under study, varying the GSH concentration (1 mM or 5 mM; final concentrations) did not significantly change the GST effects observed in carbamazepine incubations (data not shown).

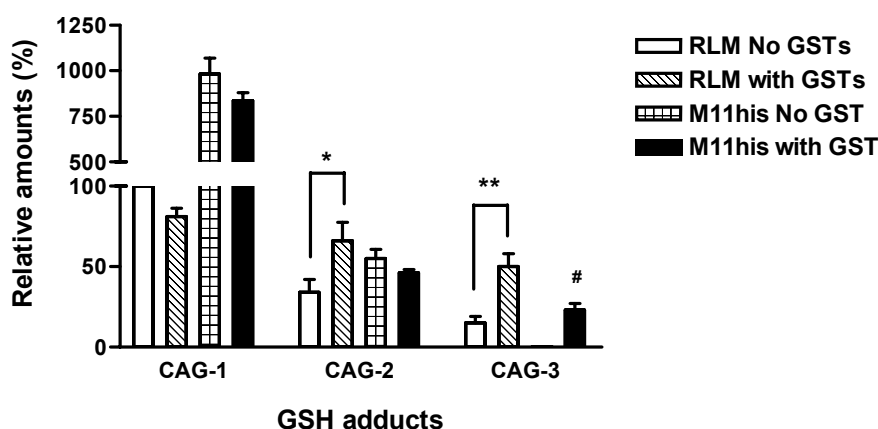


Figure 5. GST effects on the GSH adducts of carbamazepine produced by RLM and P450 BM3 mutant M11_{his}. Relative amounts of GSH adducts are presented in the figure (with standard deviations of the differences) in incubations performed with and without 94 $\mu\text{g/ml}$ GSTs. Levels of GSH adducts are compared after setting arbitrary the amounts of CAG-1 produced by RLM without GSTs as reference (100%). Statistically-significant changes are depicted as: * p-value < 0.05; ** p-value < 0.01 and # GSH adduct only formed in presence of GSTs.

Discussion

Although previous clinical studies suggest that GSTs could be involved in the detoxification of reactive metabolites of drugs involved in adverse and idiosyncratic drug reactions, as yet few *in vitro* studies have been performed to confirm these observations. The aim of this study was therefore to investigate if GSTs can catalyze the coupling of RIs of drugs to GSH, and thereby increase GSH adduct levels in *in vitro* incubation mixtures. Five model compounds were chosen based on previous studies indicating bioactivation towards RIs, covalent binding to proteins and/or because they have been associated with ADRs.

For most compounds under study, we found that the presence of rat GSTs had little effect on GSH adduct levels. Previous reports, however, showed that GSH

conjugation of the reactive metabolite of APAP (NAPQI) can be catalyzed by GSTs [13]. These discrepancies can be explained by the very different experimental conditions used in both studies. While Coles *et al.* monitored GST activities in a very short time-frame by stopped-flow kinetics using synthetic NAPQI, low GSH concentrations (0.1 mM) and low pH (6.5); we have investigated the role of GSTs in catalyzing GSH adduct formation in enzymatic incubations performed for a longer period of time, with physiologically-relevant pH value (pH 7.4) and GSH concentration (5 mM). In their discussion, Coles *et al.* finally concluded that at physiological concentrations, rapid non-enzymatic reaction of NAPQI with GSH would predominate [13]. This is in agreement with our observations.

Interestingly, we found that GSTs catalyzed the GSH conjugation of arene oxide intermediates of carbamazepine (CAG-2 and CAG-3; Table 5 and Figure 3). Comparatively, levels of the major GSH adduct CAG-1, originating from the stable 10,11-carbamazepine epoxide, were not affected by GSTs in carbamazepine incubations. Several reactive metabolites and GSH adducts of carbamazepine have been identified previously [19, 32-34] and GSTs were already suggested to play a protective role by decreasing covalent binding levels to mouse microsomal proteins *in vivo* [14]. Interestingly, Pirmohamed *et al.* proposed that arene oxides, more than the stable 10,11-carbamazepine epoxide, may be the chemical reactive metabolites responsible for carbamazepine-induced IDRs [34]. In view of this, our results may indicate that GSTs could play a significant protective role by catalyzing the conjugation of these reactive arene oxide intermediates with GSH.

Consequently, this may also suggest that variations in GST activities, possibly from genetic polymorphisms, could have an impact on individual susceptibilities towards the drug. This may be in line with the observation that GST M1 null genotype was found to be a risk factor in carbamazepine-induced hepatotoxicity in humans [12]. One major limitation of our study, however, is the lack of human data and the resulting difficulties related to interpreting and extrapolating *in vitro* animal data to human clinical observations. It is indeed known that the relative amounts and activities of GST enzymes are species-dependent and may thus give rise to significant inter-species differences in susceptibility to toxic effects of xenobiotics [3]. In order to perform accurate human risk assessments, knowledge of the differences and similarities of the enzymes involved in bio(in)activation processes is very important. This was highlighted for example for aflatoxin B₁, where significant species

differences were found both in the bioactivation and in the detoxification pathways of the chemical [35].

In summary, the role of GSTs in catalyzing the coupling of RIs of drugs to GSH seems to be highly substrate-dependent and most likely depends on the type and/or levels of intermediates involved. Indeed, while GSTs significantly increased GSH adduct levels in carbamazepine incubations, no catalytic effects were observed in APAP, AMAP, clozapine or diclofenac incubations. Glutathione concentrations might have been too high to fully discriminate enzymatic versus non-enzymatic GSH conjugation reactions. Additionally, experiments with human enzymes and/or purified GST isoforms are required to further confirm clinical observations and to validate the potential impact of GST genetic polymorphisms in ADRs. More generally, it should be emphasized that in addition to mercapturic acids, many other thioether adducts derived from GSH-conjugates may be formed and excreted in urine (e.g. cysteine S-conjugates, 3-mercaptopyruvic acid S-conjugates, 3-mercaptolactic acid S-conjugates, methylthioether compounds, etc). The relative amounts of these products will depend on the specific activities of more than 15 enzymatic systems which may also play a role in detoxification and bioactivation mechanisms of xenobiotics [3].

References

- [1] D.C. Liebler, F.P. Guengerich, Elucidating mechanisms of drug-induced toxicity, *Nat Rev Drug Discov* 4 (2005) 410-420.
- [2] D.C. Evans, A.P. Watt, D.A. Nicoll-Griffith, T.A. Baillie, Drug-protein adducts: an industry perspective on minimizing the potential for drug bioactivation in drug discovery and development, *Chem Res Toxicol* 17 (2004) 3-16.
- [3] J.N. Commandeur, G.J. Stijntjes, N.P. Vermeulen, Enzymes and transport systems involved in the formation and disposition of glutathione S-conjugates. Role in bioactivation and detoxication mechanisms of xenobiotics, *Pharmacol Rev* 47 (1995) 271-330.
- [4] D. Sheehan, G. Meade, V.M. Foley, C.A. Dowd, Structure, function and evolution of glutathione transferases: implications for classification of non-mammalian members of an ancient enzyme superfamily, *Biochem J* 360 (2001) 1-16.
- [5] C. Frova, Glutathione transferases in the genomics era: new insights and perspectives, *Biomol Eng* 23 (2006) 149-169.
- [6] J.D. Hayes, J.U. Flanagan, I.R. Jowsey, Glutathione transferases, *Annu Rev Pharmacol Toxicol* 45 (2005) 51-88.
- [7] D.L. Eaton, T.K. Bammler, Concise review of the glutathione S-transferases and their significance to toxicology, *Toxicol Sci* 49 (1999) 156-164.
- [8] H.A. Dirven, B. Van Ommen, P.J. Van Bladeren, Glutathione conjugation of alkylating cytostatic drugs with a nitrogen mustard group and the role of glutathione S-transferases, *Chem Res Toxicol* 9 (1996) 351-360.
- [9] T. Simon, L. Becquemont, M. Mary-Krause, I. De Waziers, P. Beaune, C. Funck-Brentano, P. Jaillon, Combined glutathione-S-transferase M1 and T1 genetic polymorphism and tacrine hepatotoxicity, *Clin Pharmacol Ther* 67 (2000) 432-437.
- [10] I. Watanabe, A. Tomita, M. Shimizu, M. Sugawara, H. Yasumo, R. Koishi, T. Takahashi, K. Miyoshi, K. Nakamura, T. Izumi, Y. Matsushita, H. Furukawa, H. Haruyama, T. Koga, A study to survey susceptible genetic factors responsible for troglitazone-associated hepatotoxicity in Japanese patients with type 2 diabetes mellitus, *Clin Pharmacol Ther* 73 (2003) 435-455.
- [11] M.I. Lucena, R.J. Andrade, C. Martinez, E. Ulzurrun, E. Garcia-Martin, Y. Borraz, M.C. Fernandez, M. Romero-Gomez, A. Castiella, R. Planas, J. Costa, S. Anzola, J.A. Agundez, Glutathione S-transferase m1 and t1 null genotypes increase susceptibility to idiosyncratic drug-induced liver injury, *Hepatology* 48 (2008) 588-596.
- [12] K. Ueda, T. Ishitsu, T. Seo, N. Ueda, T. Murata, M. Hori, K. Nakagawa, Glutathione S-transferase M1 null genotype as a risk factor for carbamazepine-induced mild hepatotoxicity, *Pharmacogenomics* 8 (2007) 435-442.
- [13] B. Coles, I. Wilson, P. Wardman, J.A. Hinson, S.D. Nelson, B. Ketterer, The spontaneous and enzymatic reaction of N-acetyl-p-benzoquinonimine with glutathione: a stopped-flow kinetic study, *Arch Biochem Biophys* 264 (1988) 253-260.
- [14] J.H. Lillibridge, B.M. Amore, J.T. Slattery, T.F. Kalhorn, S.D. Nelson, R.H. Finnell, G.D. Bennett, Protein-reactive metabolites of carbamazepine in mouse liver microsomes, *Drug Metab Dispos* 24 (1996) 509-514.
- [15] M.C. Damsten, B.M. Van Vugt-Lussenburg, T. Zeldenthuis, J.S. De Vlieger, J.N. Commandeur, N.P. Vermeulen, Application of drug metabolising mutants of cytochrome P450 BM3 (CYP102A1) as biocatalysts for the generation of reactive metabolites, *Chem Biol Interact* (2007)
- [16] D.J. Jollow, J.R. Mitchell, W.Z. Potter, D.C. Davis, J.R. Gillette, B.B. Brodie, Acetaminophen-induced hepatic necrosis. II. Role of covalent binding in vivo, *J Pharmacol Exp Ther* 187 (1973) 195-202.
- [17] J.L. Maggs, D. Williams, M. Pirmohamed, B.K. Park, The metabolic formation of reactive intermediates from clozapine, a drug associated with agranulocytosis in man, *J Pharmacol Exp Ther* 275 (1995) 1463-1475.
- [18] W. Tang, R.A. Stearns, R.W. Wang, S.H. Chiu, T.A. Baillie, Roles of human hepatic cytochrome P450s 2C9 and 3A4 in the metabolic activation of diclofenac, *Chem Res Toxicol* 12 (1999) 192-199.
- [19] S. Madden, J.L. Maggs, B.K. Park, Bioactivation of carbamazepine in the rat in vivo. Evidence for the formation of reactive arene oxide(s), *Drug Metab Dispos* 24 (1996) 469-479.
- [20] S.A. Roberts, V.F. Price, D.J. Jollow, Acetaminophen structure-toxicity studies: in vivo covalent binding of a nonhepatotoxic analog, 3-hydroxyacetanilide, *Toxicol Appl Pharmacol* 105 (1990) 195-208.
- [21] A.J. Streeter, S.M. Bjorge, D.B. Axworthy, S.D. Nelson, T.A. Baillie, The microsomal metabolism and site of covalent binding to protein of 3'-hydroxyacetanilide, a nonhepatotoxic positional isomer of acetaminophen, *Drug Metab Dispos* 12 (1984) 565-576.

- [22] A.T. Banks, H.J. Zimmerman, K.G. Ishak, J.G. Harter, Diclofenac-associated hepatotoxicity: analysis of 180 cases reported to the Food and Drug Administration as adverse reactions, *Hepatology* 22 (1995) 820-827.
- [23] E. Bjornsson, P. Jerlstad, A. Bergqvist, R. Olsson, Fulminant drug-induced hepatic failure leading to death or liver transplantation in Sweden, *Scand J Gastroenterol* 40 (2005) 1095-1101.
- [24] J. Idanpaan-Heikkila, E. Alhava, M. Olkinuora, I.P. Palva, Agranulocytosis during treatment with chlozapine, *Eur J Clin Pharmacol* 11 (1977) 193-198.
- [25] P.S. Friedmann, I. Strickland, M. Pirmohamed, B.K. Park, Investigation of mechanisms in toxic epidermal necrolysis induced by carbamazepine, *Arch Dermatol* 130 (1994) 598-604.
- [26] M. Rooseboom, J.N. Commandeur, G.C. Floor, A.E. Rettie, N.P. Vermeulen, Selenoxidation by flavin-containing monooxygenases as a novel pathway for beta-elimination of selenocysteine Se-conjugates, *Chem Res Toxicol* 14 (2001) 127-134.
- [27] M.M. Bradford, A rapid and sensitive method for the quantitation of microgram quantities of protein utilizing the principle of protein-dye binding, *Anal Biochem* 72 (1976) 248-254.
- [28] W.H. Habig, M.J. Pabst, W.B. Jakoby, Glutathione S-transferases. The first enzymatic step in mercapturic acid formation, *J Biol Chem* 249 (1974) 7130-7139.
- [29] M.S. Rashed, S.D. Nelson, Characterization of glutathione conjugates of reactive metabolites of 3'-hydroxyacetanilide, a nonhepatotoxic positional isomer of acetaminophen, *Chem Res Toxicol* 2 (1989) 41-45.
- [30] M.S. Rashed, T.G. Myers, S.D. Nelson, Hepatic protein arylation, glutathione depletion, and metabolite profiles of acetaminophen and a non-hepatotoxic regioisomer, 3'-hydroxyacetanilide, in the mouse, *Drug Metab Dispos* 18 (1990) 765-770.
- [31] J. Zheng, L. Ma, B. Xin, T. Olah, W.G. Humphreys, M. Zhu, Screening and identification of GSH-trapped reactive metabolites using hybrid triple quadrupole linear ion trap mass spectrometry, *Chem Res Toxicol* 20 (2007) 757-766.
- [32] H.Z. Bu, P. Kang, A.J. Deese, P. Zhao, W.F. Pool, Human in vitro glutathionyl and protein adducts of carbamazepine-10,11-epoxide, a stable and pharmacologically active metabolite of carbamazepine, *Drug Metab Dispos* 33 (2005) 1920-1924.
- [33] H.Z. Bu, P. Zhao, D.K. Dalvie, W.F. Pool, Identification of primary and sequential bioactivation pathways of carbamazepine in human liver microsomes using liquid chromatography/tandem mass spectrometry, *Rapid Commun Mass Spectrom* 21 (2007) 3317-3322.
- [34] M. Pirmohamed, N.R. Kitteringham, T.M. Guenther, A.M. Breckenridge, B.K. Park, An investigation of the formation of cytotoxic, protein-reactive and stable metabolites from carbamazepine in vitro, *Biochem Pharmacol* 43 (1992) 1675-1682.
- [35] A.S. Wilson, D.P. Williams, C.D. Davis, M.D. Tingle, B.K. Park, Bioactivation and inactivation of aflatoxin B1 by human, mouse and rat liver preparations: effect on SCE in human mononuclear leucocytes, *Mutat Res* 373 (1997) 257-264.

Chapter 4

Trimethoprim: novel reactive intermediates and bioactivation pathways by cytochromes P450

Adapted from: Micaela C. Damsten, Jon S. de Vlieger, Wilfried M. Niessen, Hubertus Irth, Nico P. E. Vermeulen and Jan N. M. Commandeur.
Trimethoprim: Novel Reactive Intermediates and Bioactivation Pathways by Cytochrome P450s.
Chemical Research in Toxicology, 2008, Nov 21 (11), p: 2181-7.

Abstract

Trimethoprim (TMP) is a widely used antibacterial agent that is usually considered as a safe drug. TMP has, however, been implicated in rare adverse drug reactions (ADRs) in humans. Bioactivation to a reactive iminoquinone methide intermediate has been proposed as a possible cause for the toxicity of the drug. However, little is known about the cytochromes P450 (P450s) involved in this bioactivation and in the metabolism of TMP in general. In this study, we have investigated the metabolism and bioactivation of TMP by human liver microsomes (HLM), rat liver microsomes (RLM), by recombinant human cytochromes P450, and by the bacterial P450 BM3 mutant M11_{his}. In addition to non GSH-dependent metabolites, five GSH adducts were identified in the HLM incubations. Next to two major GSH adducts probably originating from the iminoquinone methide intermediate described previously, three minor GSH adducts were also identified, indicating that other types of reactive intermediates are formed by HLM, such as ortho-quinones and para-quinone methide intermediates. The major GSH adducts were produced by P450 1A2 and P450 3A4, while the minor GSH adducts were mainly formed by P450 1A2, P450 3A4 and P450 2D6. Although preliminary, these results might indicate that genetic polymorphisms in P450 enzymes could play a role in the onset of TMP-related ADRs in humans.

Introduction

Trimethoprim (TMP) is a broad-spectrum antibacterial agent that is frequently used in combination with sulphonamides as the combined drug cotrimoxazole [1]. Although generally considered safe, cotrimoxazole has also been involved in rare but severe adverse drug reactions (ADRs) in humans [2-8]. Of the two components of cotrimoxazole, hypersensitivity reactions were thought to be related to the sulphonamide component due to its bioactivation to a reactive nitroso metabolite [7]. However, skin rashes (i.e. toxic epidermal necrolysis) and neutropenia reactions have also been reported when TMP is used alone [9-11]. Therefore, it was hypothesized that the combination of two drugs with intrinsic bioactivation potential might explain the increased risks in developing cotrimoxazole-induced ADRs.

As summarized in Figure 1, it has been shown that TMP is biotransformed to several metabolites by human and rat enzymes. O-demethylation of TMP, yielding the 3'-OH-TMP and 4'-OH-TMP metabolites, is the major metabolism route in rats and in humans [12-14]. O-demethylated metabolites can be further conjugated to glucuronic acid by phase II enzymes, yielding the corresponding glucuronides [12]. Minor metabolism pathways include N-oxidation of TMP yielding TMP-1-N-oxide (1-NO-TMP) and TMP-3-N-oxide (3-NO-TMP). Hydroxylation of the methylene carbon of TMP to C α -OH-TMP, with further oxidation to the carbonyl metabolite, has also been reported [12-15]. Next to the stable metabolites mentioned above, Lai *et al.* have shown that TMP can also be bioactivated by human and/or rat liver microsomes (HLM and/or RLM) to a reactive iminoquinone methide intermediate that can be trapped by N-acetyl cysteine (NAC) [16] (Figure 1). It was proposed that the formation of this reactive metabolite might be responsible for the TMP-induced ADRs observed in humans.

So far, however, no information is available on the individual human cytochrome P450 enzymes (P450s) involved in this bioactivation pathway and in the oxidative metabolism of TMP in general. Inhibition studies with selective marker substrate reactions of specific human cytochrome P450 isoforms have only shown that TMP is a strong and relatively selective inhibitor of P450 2C8 [17]. In this study, we have therefore investigated the oxidative metabolism of TMP by HLM, RLM, recombinant human P450 enzymes, and the cytochrome P450 BM3 mutant M11_{his} (M11_{his}). The bacterial P450 BM3 mutant was previously shown to bioactivate several drugs to higher amounts of reactive intermediates than mammalian P450s, which facilitated

their identification and structural elucidation [18]. Experiments with recombinant human P450 enzymes were performed to identify the enzymes involved in the metabolism and/or bioactivation of TMP. Bioactivation of TMP to reactive metabolites was evaluated by detecting and characterizing the corresponding GSH adducts by LC-MS/MS analysis [19]. Incubations with rat liver glutathione S-transferases (GSTs) were performed to assess the effect of GSTs on GSH adduct levels. Ultimately, results from these experiments will be discussed in the perspective of TMP-induced ADRs.

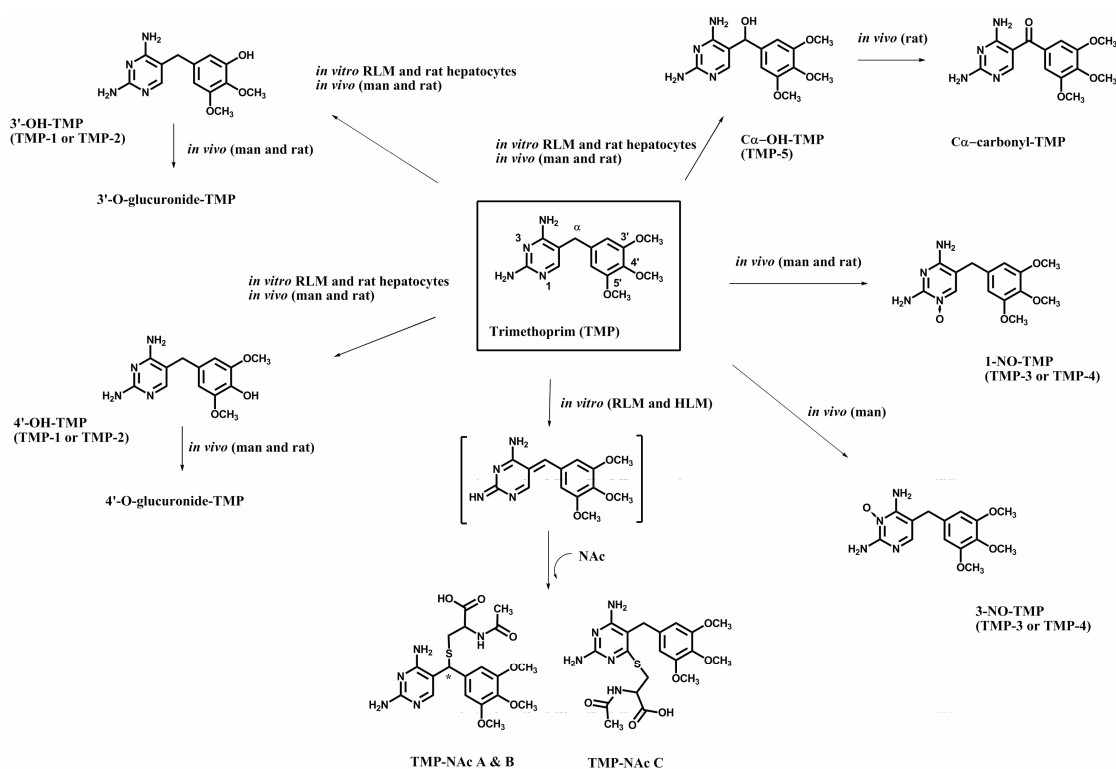


Figure 1. Scheme of the known human and rat metabolism of TMP. A scheme of the known metabolites of TMP originating from *in vitro* and/or *in vivo* experiments is presented in the figure. The proposed reactive intermediate of TMP is depicted in brackets and the corresponding NAc adducts are presented as described in ref [16].

Material and Methods

Enzymes and plasmids

Control RLM were prepared according to the standard protocol used in our laboratory [20]. The bacterial P450 BM3 mutant M11_{his} (M11_{his}) was prepared and purified as described in [18]. Pooled HLM were obtained from BD GentestTM (Cat. No.: 452161). Recombinant human cytochrome P450 enzymes P450 1A2, P450 2C9, P450 2D6

and P450 3A4 were prepared as described in [21]. Expression of human recombinant P450 2E1 was done as described in [22]. Recombinant human P450 2C8 and P450 2C19 were purchased from BD Gentest (Cat. No. 456252 and No. 456259, respectively). Rat liver GSTs were isolated as described in Chapter 3.

Enzymatic incubations with HLM, RLM, recombinant human P450s and P450 BM3 mutant M11_{his}

Incubations had a final volume of 250 μ l and consisted of 100 mM potassium phosphate buffer (pH 7.4), 500 μ M TMP (in DMSO) and 5 mM GSH. Final DMSO concentrations in the incubations were always below 1%. A final protein concentration of 1 mg/ml HLM or RLM was used in the incubations. Incubations with recombinant human P450 enzymes (P450 1A2, P450 2C8, P450 2C9, P450 2C19, P450 2D6, P450 2E1 and P450 3A4) were performed with a final P450 concentration of 250 nM and incubations with the P450 BM3 mutant with 250 nM of purified M11_{his}. Reactions were initiated by the addition of 2 mM NADP(H) and were incubated for 60 minutes at 37°C for the HLM, RLM and recombinant P450s and at 24°C for M11_{his}. To differentiate high- vs low-affinity enzymes, incubations with recombinant human P450s were also performed for 20 minutes at a final TMP concentration of 50 μ M. To assess the effects of GSTs on GSH adduct levels, RLM and M11_{his} incubations were performed as described above with and without GSTs (final protein concentration: 94 μ g/ml; final specific activity: 5.4 μ mol prod/min/mg prot). Incubations were subsequently terminated with 250 μ l cold methanol. Samples were centrifuged to remove precipitated protein (4000 rpm, 15 minutes), and the supernatants were analysed by LC-MS/MS. Control incubations in absence of enzymes were performed to determine which peaks represent metabolites. To establish which of the metabolites are GSH adducts, control incubations in the absence of GSH were also performed.

A large-scale incubation of trimethoprim with RLM was performed to determine amounts of TMP metabolites. Briefly, 100 μ M TMP was incubated with 1 mg/ml RLM, 5 mM GSH and 2 mM NADP(H) (final concentrations) in a total volume of 5 ml 100 mM potassium phosphate buffer (pH 7.4). Incubations were performed at 37°C for 3 hours and were subsequently stopped with 10 ml of cold methanol. Proteins were removed by centrifugation (15 minutes at 4000 rpm), and the supernatant was dried overnight under N₂. The sample was reconstituted in 1.25 ml of 20% acetonitrile (in H₂O) and analyzed by LC-UV/MS. On the basis of the assumption that the extinction coefficient of TMP and its metabolites are similar at 254 nm, amounts of metabolites

in the RLM incubation were assessed by determining peak areas in the UV chromatogram. Levels of metabolites present in the HLM incubation were subsequently extrapolated from the MS data. Amounts of metabolites (depicted in parentheses in Table 1) are expressed as percentages relative to the total amount of metabolites present in the incubation (100%).

Analytical methods

Metabolites were separated by reversed-phase liquid chromatography using a C18 column from Phenomenex (Luna 5 μ , 150 x 4.6 mm). The following gradient was used at a flow rate of 0.4 ml/min: from 0 to 5 minutes, isocratic at 0% solvent B; from 5 to 30 minutes, linear increase from 0 to 100 % solvent B; from 30 to 35 minutes, linear decrease from 100 to 0 % solvent B and re-equilibration at 0 % solvent B from 35 to 40 minutes. Solvent A consisted of 1% acetonitrile, 98.8% H₂O and 0.2% formic acid; solvent B consisted of 98.8% acetonitrile, 1% H₂O and 0.2% formic acid. Samples were analyzed on two LC-MS instruments. Metabolites were identified on the IT-TOF LC-UV/MS instrument (Shimadzu). Full MS analysis was performed with electrospray ionisation (ESI) in the positive mode. The interface voltage was 5 kV, the nebulizer gas flow (N₂) was 1.5 l/min, and the heated block temperature was 200°C. The LC-MS solution software package from Shimadzu was used to determine peak areas of the metabolites in the corresponding extracted ion chromatograms. Accurate mass data allowed us to propose structures on the metabolites detected in the incubation mixtures. MS/MS experiments were performed to further characterize the GSH adducts of TMP. Experiments were performed with an isolation width of 2.0, a collision energy of 25% and an ion accumulation time of 10 msec. UV detection was performed using a Shimadzu SPD20A UV detector set at 254 nm. Full MS analysis and MS/MS experiments were also performed on the LCQ Deca LC-MS instrument (Thermo Finnigan) in the positive mode using ESI. N₂ was used as sheath gas (60 psi) and auxiliary gas (10 psi), the needle voltage was 5 kV, and the heated capillary was at 150°C. MS/MS experiments were performed with an isolation width of 2.0, a collision energy of 25%, an activation energy of 0.25, and an activation time of 30 msec. Injection volumes were 40 μ l, and inter-experimental variation of the LC-MS systems was always below 5%.

Results and Discussion

Biotransformation of trimethoprim by HLM

TMP was first incubated with HLM to identify its main metabolites and biotransformation pathways. All incubations were analysed with the IT-TOF LC-MS instrument, allowing accurate mass data to be obtained (Table 1). The relative error of “measured” vs “calculated” m/z values for each metabolite and/or GSH adduct was always below 5 ppm and therefore supports the identity of the metabolites proposed in Table 1.

HLM produced eleven metabolites of which five were dependent on the presence of GSH (Table 1). Two metabolites (TMP-1 and TMP-2; Table 1) with m/z 277.130 $[M+H]^+$ correspond to O-demethylated TMP. This is in agreement with previous data from literature [14] and, by analogy, we assumed that TMP-1 and TMP-2 most likely correspond to 3'-OH-TMP and 4'-OH-TMP, as depicted in Figure 1. Three metabolites with m/z 307.140 $[M+H]^+$ correspond to oxygenated TMP (TMP-3, TMP-4 and TMP-5; Table 1). Similarly, three oxygenated metabolites have been reported previously in humans [14, 15]. Accordingly, we postulated that TMP-3 and TMP-4 correspond to the N-oxides and the minor TMP-5 metabolite to α -OH-TMP (Figure 1). HLM also produced a metabolite with m/z 263.115 $[M+H]^+$ (TMP-6; Table 1). This m/z might correspond to double O-demethylated trimethoprim. Double O-demethylation can take place either on the 3'- and 4'- and/or on the 3'- and 5'- positions of TMP, yielding the structures proposed in Figure 2.

In presence of GSH, five GSH-dependent metabolites were observed in the HLM incubations (Table 1). Two GSH adducts with m/z 596.213 $[M+H]^+$ and/or m/z 298.610 $[M+2H]^{2+}$ indicate that TMP has been coupled to GSH (TMPG-1 and TMPG-2; Table 1). MS/MS experiments were performed with the LCQ and IT-TOF LC-MS instruments to confirm and further characterize these GSH adducts. The fragmentation pattern of the TMPG-1 and TMPG-2 adducts was similar (Table 2). The fragments observed with the LCQ LC-MS system were as follows: m/z 596 $[M+H]^+$; m/z 578 [loss of H_2O]; m/z 486 [loss of the pyrimidine ring of TMP]; m/z 467 [loss of the glutamyl moiety of GSH]; m/z 357 [m/z 486 – glutamyl moiety of GSH] and m/z 289 [iminoquinone methide intermediate]. The major fragment in the MS/MS spectra (m/z 289) is the iminoquinone methide intermediate originating from the loss of the whole GSH moiety. On the IT-TOF LC-MS system, the major iminoquinone

methide fragment (m/z 289.130) and fragments originating for the peptide moiety of the GSH adducts were found (m/z 179.049 and m/z 130.049). This fragmentation pattern is consistent with that of two N-acetyl cysteine adducts previously described by Lai *et al.*; where the major fragment is the iminoquinone methide intermediate originating from the loss of the whole NAc moiety. Therefore, we postulate that TMPG-1 and TMPG-2 are adduct diastereoisomers originating from the reactive iminoquinone methide intermediate described in [16] and where the GSH moiety is attached on C α of TMP (Figure 2).

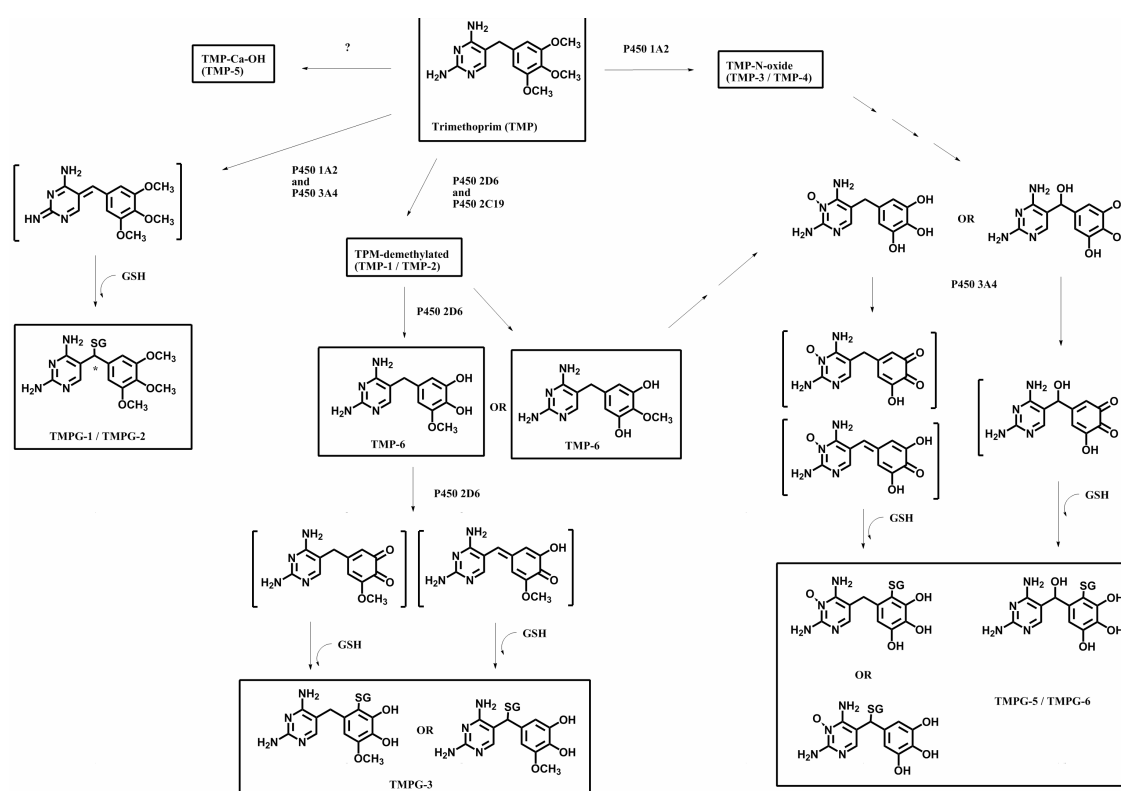


Figure 2. Scheme of the proposed human metabolism of TMP. Scheme of the possible *in vitro* human metabolites of TMP. Metabolites and/or GSH adducts proposed in this study are highlighted in rectangles; while possible reactive metabolites of TMP are depicted in brackets. Human P450 isoforms involved in the metabolite formation are also indicated in the figure.

Table 1. Metabolites of TMP formed by HLM, RLM and BM3 mutant M11_{his}.

Metabolites	t _r (min)	HLM	RLM	M11 _{his}	Elemental composition	Calculated mass (m/z)	Measured mass (m/z)	Relative error (in ppm)	Change to parent drug (TMP)
Not GSH-dependent									
TMP-1	14.2	100 ± 3 (17.9%)	354 ± 18 (23.2%)	179 ± 12	C ₃ H ₁₆ N ₄ O ₃	277.129 ¹	277.130 ¹	0.4	TMP-CH ₂
TMP-2	14.7	100 ± 4 (50.3%)	318 ± 23 (58.8%)	464 ± 12	C ₃ H ₁₆ N ₄ O ₃	277.129 ¹	277.130 ¹	1.4	TMP-CH ₂
TMP-3	14.8	100 ± 1 (12.7%)	196 ± 33 (9.2%)	159 ± 112	C ₄ H ₁₈ N ₄ O ₄	307.140 ¹	307.139 ¹	2.3	TMP+O
TMP-4	15.8	100 ± 2 (8.8%)	177 ± 16 (5.7%)	7 ± 1	C ₄ H ₁₈ N ₄ O ₄	307.140 ¹	307.141 ¹	2.0	TMP+O
TMP-5	16.8	100 ± 2 (6.5%)	22 ± 2 (0.5%)	-	C ₄ H ₁₈ N ₄ O ₄	307.140 ¹	307.140 ¹	0.0	TMP+O
TMP-6	13.6	100 ± 4 (2.5%)	180 ± 15 (1.6%)	21 ± 5	C ₂ H ₁₄ N ₄ O ₃	263.114 ¹	263.115 ¹	2.7	TMP-2xCH ₂
TMP-7	16.0	-	-	+	C ₄ H ₁₈ N ₄ O ₅	323.135 ¹	323.136 ¹	3.1	TMP+2xO
TMP-8	16.5	-	-	+	C ₄ H ₁₈ N ₄ O ₅	323.135 ¹	323.137 ¹	4.6	TMP+2xO
TMP-9	13.8	-	-	+	C ₃ H ₁₆ N ₄ O ₄	293.124 ¹	293.125 ¹	2.7	TMP+O-CH ₂
GSH-dependent									
TMPG-1	14.4	100 ± 4 (0.6%)	212 ± 15 (0.5%)	222 ± 34	C ₂₄ H ₃₃ N ₇ O ₈ S	596.213 ¹	596.213 ¹	0.0	TMP+SG
TMPG-2	14.5	100 ± 2 (0.7%)	196 ± 21 (0.5%)	145 ± 21	C ₂₄ H ₃₃ N ₇ O ₈ S	298.610 ²	298.610 ²	0.0	TMP+SG
TMPG-3	13.6	100 ± 3 (ND)	52452 ± 10536 (ND)	-	C ₂₂ H ₂₉ N ₇ O ₈ S	298.610 ²	298.611 ²	1.0	TMP-2xCH ₂ +SG
TMPG-4	13.7	-	-	+	C ₂₃ H ₃₁ N ₇ O ₁₀ S	568.182 ¹	284.595 ²	0.0	TMP+O-CH ₂ +SG
TMPG-5	13.5	100 ± 3 (ND)	-	73 ± 37	C ₂₁ H ₂₇ N ₇ O ₁₀ S	299.599 ²	299.601 ²	2.0	TMP+O-3xCH ₂ +SG
TMPG-6	13.6	100 ± 5 (ND)	61 ± 23 (ND)	111 ± 67	C ₂₁ H ₂₇ N ₇ O ₁₀ S	285.584 ²	285.583 ²	4.9	TMP+O-3xCH ₂ +SG
						570.159 ¹	570.159 ¹	4.0	TMP+O-3xCH ₂ +SG
						285.584 ²	285.584 ²	0.0	

Bold figures between brackets represent the percentage of each TMP metabolite to the total of TMP metabolites produced by each enzyme fraction. Quantification is based on LC-UV chromatograms with the assumption that the extinction coefficient for each metabolite is the same at 254 nm (ND, peaks are below the limit of detection by UV). Elemental compositions, m/z for "calculated exact masses" and "measured masses" of the protonated molecule¹ [M+H]⁺ and/or diprotonated molecule² [M+2H]²⁺ are presented in the table. Errors (in ppm) of "calculated exact mass" vs "measured mass" were determined for each metabolite and possible structures are proposed.

Table 2. Fragmentation pattern of the GSH adducts of TMP.

GSH adducts	<i>m/z</i> (di)protonated molecule and fragments		Elemental composition	Proposed structure
	LCQ	IT-TOF		
TMPG-1	596.1 ¹		C ₂₄ H ₃₃ N ₇ O ₉ S	[M+H] ⁺
		298.612 ² (2.3 ppm)	C ₂₄ H ₃₃ N ₇ O ₉ S	[M+2H] ²⁺
	577.9		C ₂₄ H ₃₁ N ₇ O ₈ S	Loss H ₂ O
	486.3		C ₂₀ H ₂₈ N ₃ O ₉ S	Loss pyrimidine ring of TMP
	467.0		C ₁₉ H ₂₆ N ₆ O ₆ S	Loss glutamyl moiety of GSH
	357.2		C ₁₅ H ₂₀ N ₂ O ₆ S	<i>m/z</i> 486 - glutamyl moiety of GSH
	289.1	289.132 (5.5 ppm)	C ₁₄ H ₁₇ N ₄ O ₃	Loss GSH: iminoquinone methide
		179.049 (2.8 ppm)	C ₅ H ₁₁ N ₂ O ₃ S	[cysteinylglycine+H] ⁺
	130.049 (0.1 ppm)	C ₅ H ₈ N ₁ O ₃	[pyroglutamic acid+H] ⁺	
TMPG-2	596.1 ¹		C ₂₄ H ₃₃ N ₇ O ₉ S	[M+H] ⁺
		298.613 ² (4.7 ppm)	C ₂₄ H ₃₃ N ₇ O ₉ S	[M+2H] ²⁺
	578.0		C ₂₄ H ₃₁ N ₇ O ₈ S	Loss H ₂ O
	486.0		C ₂₀ H ₂₈ N ₃ O ₉ S	Loss pyrimidine ring of TMP
	356.9		C ₁₅ H ₂₀ N ₂ O ₆ S	<i>m/z</i> 486 - glutamyl moiety of GSH
	289.1	289.130 (4.8 ppm)	C ₁₄ H ₁₇ N ₄ O ₃	Loss GSH: iminoquinone methide
		179.048 (0.6 ppm)	C ₅ H ₁₁ N ₂ O ₃ S	[cysteinylglycine+H] ⁺
		130.049 (0.8 ppm)	C ₅ H ₈ N ₁ O ₃	[pyroglutamic acid+H] ⁺
TMPG-3	ND	568.187 ¹ (8.1 ppm)	C ₂₂ H ₂₉ N ₇ O ₉ S	[M+H] ⁺
		439.139 (1.8 ppm)	C ₁₇ H ₂₂ N ₆ O ₆ S	Loss glutamyl moiety of GSH
TMPG-4	598.1 ¹	598.188 ¹ (7 ppm)	C ₂₃ H ₃₁ N ₇ O ₁₀ S	[M+H] ⁺
		299.599 ² (4.3 ppm)	C ₂₃ H ₃₁ N ₇ O ₁₀ S	[M+2H] ²⁺
	580.1		C ₂₃ H ₂₉ N ₇ O ₉ S	Loss H ₂ O
	523.0		C ₂₁ H ₂₆ N ₆ O ₈ S	Loss glycine moiety of GSH
	469.1	469.149 (2.6 ppm)	C ₁₈ H ₂₄ N ₆ O ₇ S	Loss glutamyl moiety of GSH
	325.0		C ₁₃ H ₁₆ N ₄ O ₄ S	[TMP+O-CH ₂ +SH] ⁺
TMPG-5	ND	285.583 ² (4.9 ppm)	C ₂₁ H ₂₇ N ₇ O ₁₀ S	[M+2H] ²⁺
		130.051 (8.5 ppm)	C ₅ H ₈ N ₁ O ₃	[pyroglutamic acid+H] ⁺
		179.048 (2.2 ppm)	C ₅ H ₁₁ N ₂ O ₃ S	[cysteinylglycine+H] ⁺
TMPG-6	ND	285.584 ² (0.4 ppm)	C ₂₁ H ₂₇ N ₇ O ₁₀ S	[M+2H] ²⁺
		130.049 (1.5 ppm)	C ₅ H ₈ N ₁ O ₃	[pyroglutamic acid+H] ⁺

Characteristics of the electrospray product ion spectra of the GSH adducts of TMP obtained on the LCQ and IT-TOF LC-MS instruments. *m/z* corresponding to the protonated molecule¹ [M+H]⁺; diprotonated molecule² [M+2H]²⁺ and/or of the protonated fragments are presented. Non-detected adducts are also indicated (ND). When measured on the IT-TOF LC-MS instrument, relative errors (in ppm) of “calculated exact mass” versus “measured mass” are indicated. Elemental compositions and possible structures of the protonated molecules and/or fragments are shown in the table.

On the IT-TOF LC-MS system, one GSH adduct with m/z 284.595 $[M+2H]^{2+}$ was observed in the HLM incubations (TMPG-3; Table 1). However, because of the low amounts of conjugates, TMPG-3 could not be detected on the LCQ LC-MS instrument, and the fragmentation pattern on the IT-TOF LC-MS instrument only showed the loss of the glutamyl moiety of GSH (m/z 439.139; Table 2). Accurate mass data of both the protonated molecule and fragment might indicate that TMP has been doubly O-demethylated and conjugated to GSH. Double O-demethylation of TMP may lead to a catechol metabolite (TMP-6) that can be activated to reactive ortho-quinone and para-quinone methide intermediates that can react with GSH and lead to GSH adduct TMPG-3 (Figure 2).

Two GSH adducts with m/z 285.583 $[M+2H]^{2+}$ were also identified in the HLM incubation (TMPG-5 and TMPG-6; Table 1). This m/z might correspond to oxygenated and triple O-demethylated TMP coupled to GSH. Levels of TMPG-5 and TMPG-6 were, however, too low to obtain representative MS/MS spectra with the LCQ LC-MS instrument. On the IT-TOF LC-MS instrument, only fragments originating from the peptide moiety of the adducts were observed (m/z 130.050 and m/z 179.048; Table 2). These adducts might derive from reactive ortho-quinone and para-quinone methide intermediates originating from multiple O-demethylation reactions of TMP (Figure 2). However, considering the multiple metabolic reactions needed to obtain these adducts, it is likely that TMPG-5 and TMPG-6 only represent *in vitro* experimental artefacts that would be of little relevance for *in vivo* situations.

Biotransformation of trimethoprim by RLM and P450 BM3 mutant M11_{his}

RLM produced the same metabolites as HLM but at different levels (Table 1). The O-demethylated metabolites TMP-1 and TMP-2 were produced at more than 3-fold higher levels compared to HLM. The N-oxidative metabolites of TMP (TMP-3 and TMP-4) were produced in approximately 2-fold higher levels compared to HLM while C α -OH-TMP (TMP-5) was present in significantly lower amounts (5 times lower; Table 1). The double O-demethylated metabolite TMP-6 was produced in 1.8-fold higher levels compared to HLM. All GSH-dependent metabolites formed by HLM were also observed in the incubations with RLM, except for TMPG-5 which was not produced by the rat enzymes. Significantly higher amounts of TMPG-3 were produced by RLM (520 times higher; Table 1). TMPG-1 and TMPG-2 were formed in approximately 2-fold higher levels than HLM. In contrast, only small amounts of TMPG-6 were present in the RLM incubations (Table 1).

Recently, we have demonstrated that a mutant of the bacterial cytochrome P450 BM3 enzyme (M11_{his}) was able to convert drugs to similar metabolites as rat and human enzymes but at significantly higher levels [18]. To investigate whether M11_{his} is also able to produce large amounts of TMP metabolites, TMP incubations with M11_{his} were also performed. It was found that M11_{his} was able to metabolize TMP to 13 metabolites (Table 1). The amounts of metabolites produced, however, were in general only slightly higher than those observed in HLM incubations. The single O-demethylated metabolites of TMP (TMP-1 and TMP-2) were produced in higher levels than HLM (factors of 1.8 and 4.6, respectively; Table 1). M11_{his} also formed the two N-oxide metabolites (TMP-3 and TMP-4) but not the C α -OH-TMP metabolite TMP-5. TMP-3 was present in higher levels (1.6 times higher than HLM), whereas TMP-4 was formed in significantly lower amounts by M11_{his}. TMP-6 was produced in 5-fold lower levels compared to HLM. Additionally, three novel metabolites were observed in the incubations with M11_{his}. Two metabolites with m/z 323.135 [M+H]⁺ (TMP-7 and TMP-8; Table 1) most likely correspond to double oxygenated metabolites of TMP. The third novel metabolite with m/z 293.124 [M+H]⁺ might correspond to oxygenated and O-demethylated TMP (TMP-9; Table 1).

Next to non-GSH-dependent metabolites, M11_{his} also produced four of the five GSH adducts that were formed by HLM (Table 1). TMPG-1 and TMPG-2 were produced at 2.2 and 1.5 times higher levels than HLM, respectively. TMPG-5 and TMPG-6 were formed in similar amounts as with HLM, while TMPG-3 was not found in the M11_{his} incubations. The BM3 mutant also generated a unique GSH adduct with m/z 299.601 [M+2H]²⁺ (TMPG-4; Table 1). Accurate mass measurements indicate that this adduct could correspond to oxygenated and O-demethylated TMP coupled to GSH. The fragmentation pattern observed with the LCQ LC-MS system is consistent with this structure: m/z 598 [M+H]⁺; m/z 580 [loss of H₂O]; m/z 523 [loss of the glycine moiety of GSH]; m/z 469 [loss of the glutamyl moiety of GSH] and m/z 325 [TMP+O-CH₂+SH] (Table 2). On the IT-TOF LC-MS instrument, only one fragment was observed originating from the loss of the glutamyl moiety of the GSH adduct (m/z 469.149; Table 2). This GSH adduct might originate from a reactive para-quinone methide intermediate of TMP, as described previously for TMPG-3, TMPG-5 and TMPG-6.

Addition of GSTs to RLM and M11_{his} incubations did not significantly alter GSH adduct levels (data not shown).

Quantification of TMP metabolites in microsomal incubations

Because metabolite levels produced on analytical scale were too low to be detected by UV, a large-scale incubation of TMP with RLM was performed, and relative amounts of TMP metabolites were determined based on their UV absorbance at 254 nm. When assuming that the extinction coefficient of the metabolites at this wavelength is comparable, it is estimated that about 15% of TMP is metabolized by RLM after 3 hours of incubation (Table 1). TMP-1 and TMP-2 were identified as major metabolites representing 23 and 59% of total TMP metabolites, respectively. This is in agreement with previous studies where O-demethylation of TMP was also shown to be the major oxidative pathway in rats [12, 13]. The oxygenated trimethoprim metabolites TMP-3 and TMP-4 represented 9 and 6% of the total amounts of metabolites. TMP-5, TMP-6, TMPG-1 and TMPG-2 are all minor metabolites roughly accounting for 3% of total metabolites. Levels of TMPG-3 and TMPG-6 could not be quantified because they are below the limit of detection by UV.

When compared to RLM, HLM produce the same oxidative TMP metabolites at approximately the same percentages (Table 1). Only TMP-5 was found to be produced at significantly higher levels by HLM when compared to RLM, 6.5 vs 0.5% of total TMP metabolites. On the basis of our data, GSH adducts accounted for approximately 1.5% of total TMP metabolites. It can therefore be concluded that bioactivation and GSH adduct formation only represent a minor metabolism pathway of TMP in rats and in humans.

Incubations with recombinant human P450s

Incubations were performed with different recombinant human P450s to determine which P450 isoforms are involved in the oxidative metabolism of TMP. First, TMP was incubated at a final concentration of 500 μ M for 60 minutes. Using these conditions, several P450s were able to produce the same metabolites as observed in the HLM incubations (Table 3). To discriminate between possible high-affinity vs low-affinity enzymes, incubations were also performed at a final TMP concentration of 50 μ M, since this concentration was previously shown to be physiologically relevant [17]. Although at lower concentrations, the same metabolism pattern was observed.

Consistently, it was found that all the P450 isoforms tested formed the major O-demethylated metabolites (TMP-1 and TMP-2; Table 3). P450 2C19 and P450 2D6 showed the highest activity in producing TMP-1, while P450 2D6 had the highest activity in generating TMP-2. P450 1A2 and P450 2E1 were mainly responsible for

Table 3. Metabolism of TMP by recombinant human P450s.

Metabolites	t _r (min)	1A2 13.3%*	2C8 6.2%*	2C9 18.7%*	2C19 3.6%*	2D6 2.1%*	2E1 15.6%*	3A4 28.5%*
Oxidative metabolites								
TMP-1	14.2	66.7 ± 3.4	41.0 ± 2.6	46.6 ± 19.7	100.0 ± 14.5	89.3 ± 20.5	70.5 ± 1.7	76.1 ± 12.4
TMP-2	14.5	6.7 ± 2.4	1.5 ± 0.3	20.8 ± 4.6	44.0 ± 8.9	100.0 ± 17.4	8.3 ± 1.2	5.2 ± 2.4
TMP-3	14.6	100.0 ± 35.8	ND	33.7 ± 8.4	ND	29.5 ± 5.3	81.1 ± 9.5	63.2 ± 8.4
TMP-4	15.6	100.0 ± 57.9	ND	21.1 ± 14.0	7.0 ± 8.8	5.3 ± 7.0	19.3 ± 12.3	54.4 ± 7.0
TMP-5	16.7	ND	ND	ND	ND	ND	ND	ND
TMP-6	13.6	18.3 ± 2.6	ND	ND	ND	100.0 ± 13.7	ND	16.3 ± 2.6
GSH-dependent metabolites								
TMPG-1	14.3	100.0 ± 1.9	ND	ND	ND	ND	ND	47.2 ± 7.5
TMPG-2	14.5	100.0 ± 6.8	ND	ND	ND	ND	ND	72.7 ± 11.4
TMPG-3	13.6	11.4 ± 0.5	ND	ND	ND	100.0 ± 3.8	ND	ND
TMPG-5	13.5	ND	ND	ND	ND	ND	ND	100.0 ± 12.3
TMPG-6	13.6	ND	ND	ND	ND	ND	ND	100.0 ± 6.8

Results from duplicate experiments analyzed with the IT-TOF LC-MS instrument are presented in the table. TMP was incubated for 60 minutes with 250 nM recombinant P450 and 2 mM NADPH. Activities (only to be compared in the horizontal direction) are presented as percentages (\pm standard deviations of the differences) taking the most active enzyme as reference (100%). * Relative P450 isoform content in HLM, taken from [23]. ND, not determined.

the formation of TMP-3 and P450 1A2 for the production of TMP-4. None of the enzymes tested was able to generate TMP-5. P450 2D6 mainly produced the double O-demethylated metabolite TMP-6. Regarding GSH-dependent metabolites, P450 1A2 and P450 3A4 appear to be the enzymes responsible for the production of TMPG-1 and TMPG-2 (Table 3). P450 3A4 also generated TMPG-5 and TMPG-6. Next to P450 1A2, P450 2D6 showed to be a major enzyme involved in the formation of TMPG-3 (Figure 2).

Conclusions

The aim of this study was to investigate the metabolism of TMP by different P450s and to determine the types of reactive intermediates formed by characterizing the corresponding GSH adducts. Consistently, we found that next to six stable metabolites, trimethoprim is metabolized to five GSH-dependent metabolites by HLM (Table 1 and Figure 2). The major GSH adducts (TMPG-1 and TMPG-2) most likely originate for the iminoquinoneimine intermediate of TMP previously described in [16]. Interestingly, the other GSH adducts (TMPG-3, TMPG-5 and TMPG-6) probably derive from other reactive metabolites such as ortho-quinones and para-quinone methide intermediates most likely originating from O-demethylation reactions of TMP. For instance, TMPG-3 might result from GSH conjugation of a reactive intermediate originating from oxidation of the novel double O-demethylated metabolite TMP-6 (Figure 2).

When considering the different expression levels of cytochromes P450 in human liver [23], it is likely that P450 3A4 will be the major enzyme involved in the generation of most stable TMP metabolites. P450 1A2 and P450 3A4 will mainly contribute to the formation of reactive intermediates of TMP (Table 3). Interestingly, P450 2D6 is also involved in the formation of both the TMP-6 and TMPG-3 metabolites (Table 3). As this enzyme is known to be polymorphic in humans [24], one can speculate that variations in P450 2D6 activities might alter levels of (reactive) metabolites of TMP, and thereby influence risks in developing ADRs [25].

Previous work has also highlighted inter-species differences in the metabolism of TMP towards non-GSH-dependent metabolites [14, 15]. This is in agreement with our observations. Rat enzymes were generally found to be more efficient than HLM in metabolising TMP, except for TMP-5 and TMPG-6 (Table 1). Noticeably, TMPG-3 was formed in significantly higher levels by RLM compared to HLM (520-fold higher) and TMPG-5 was not produced by rat enzymes (Table 1).

This indicates that significant inter-species differences in the bioactivation of TMP are also taking place and suggests that rats might not constitute a representative model for risk assessment purposes in the case of TMP.

In summary, we have shown that TMP is bioactivated by HLM to multiple reactive intermediates that might contribute to the observed ADRs in humans. While this represents a minor metabolism pathway, these reactions seem to partly rely on polymorphic enzymes. Although no clear relationship between genetic polymorphisms and the onset of ADRs has been shown until now [25, 26], this study suggests that variations in cytochrome P450 enzyme activities could be one factor amongst multiple others predisposing to TMP-induced ADRs.

References

- [1] Niemi, M., Kajosaari, L. I., Neuvonen, M., Backman, J. T. and Neuvonen, P. J. (2004) The CYP2C8 inhibitor trimethoprim increases the plasma concentrations of repaglinide in healthy subjects. *Br J Clin Pharmacol.* 57, 441-447.
- [2] Frisch, J. M. (1973) Clinical experience with adverse reactions to trimethoprim-sulfamethoxazole. *J Infect Dis.* 128, Suppl:607-612 p.
- [3] Haaverstad, R. and Kannelonning, K. S. (1984) [Fatal agranulocytosis and toxic liver damage after use of trimethoprim-sulfamethoxazole]. *Tidsskr Nor Laegeforen.* 104, 741-742.
- [4] Keisu, M., Wiholm, B. E. and Palmblad, J. (1990) Trimethoprim-sulphamethoxazole-associated blood dyscrasias. Ten years' experience of the Swedish spontaneous reporting system. *J Intern Med.* 228, 353-360.
- [5] Williamson, G. D. and Crowe, G. R. (1972) Trimethoprim-sulphamethoxazole mixtures and agranulocytosis. *Med J Aust.* 2, 1506-1507.
- [6] Medina, I., Mills, J., Leoung, G., Hopewell, P. C., Lee, B., Modin, G., Benowitz, N. and Wofsy, C. B. (1990) Oral therapy for *Pneumocystis carinii* pneumonia in the acquired immunodeficiency syndrome. A controlled trial of trimethoprim-sulfamethoxazole versus trimethoprim-dapsone. *N Engl J Med.* 323, 776-782.
- [7] Pirmohamed, M., Alfirevic, A., Vilar, J., Stalford, A., Wilkins, E. G., Sim, E. and Park, B. K. (2000) Association analysis of drug metabolizing enzyme gene polymorphisms in HIV-positive patients with co-trimoxazole hypersensitivity. *Pharmacogenetics.* 10, 705-713.
- [8] Kielhofner, M. A. (1990) Trimethoprim- sulfamethoxazole: pharmacokinetics, clinical uses, and adverse reactions. *Tex Heart Inst J.* 17, 86-93.
- [9] Nwokolo, C., Byrne, L. and Misch, K. J. (1988) Toxic epidermal necrolysis occurring during treatment with trimethoprim alone. *Br Med J (Clin Res Ed).* 296, 970.
- [10] Das, G., Bailey, M. J. and Wickham, J. E. (1988) Toxic epidermal necrolysis and trimethoprim. *Br Med J (Clin Res Ed).* 296, 1604-1605.
- [11] Hawkins, T., Carter, J. M., Romeril, K. R., Jackson, S. R. and Green, G. J. (1993) Severe trimethoprim induced neutropenia and thrombocytopenia. *N Z Med J.* 106, 251-252.
- [12] Meshi, T. and Sato, Y. (1972) Studies on sulfamethoxazole-trimethoprim. Absorption, distribution, excretion and metabolism of trimethoprim in rat. *Chem Pharm Bull (Tokyo).* 20, 2079-2090.
- [13] Van 'T Klooster, G. A., Kolker, H. J., Woutersen-Van Nijnanten, F. M., Noordhoek, J. and Van Miert, A. S. (1992) Determination of trimethoprim and its oxidative metabolites in cell culture media and microsomal incubation mixtures by high-performance liquid chromatography. *J Chromatogr.* 579, 354-360.
- [14] Schwartz, D. E., Vetter, W. and Englert, G. (1970) Trimethoprim metabolites in rat, dog and man: qualitative and quantitative studies. *Arzneimittelforschung.* 20, 1867-1871.
- [15] Brooks, M. A., De Silva, J. A. and D'aroconte, L. (1973) Determination of trimethoprim and its N-oxide metabolites in urine of man, dog, and rat by differential pulse polarography. *J Pharm Sci.* 62, 1395-1397.
- [16] Lai, W. G., Zahid, N. and Uetrecht, J. P. (1999) Metabolism of trimethoprim to a reactive iminoquinone methide by activated human neutrophils and hepatic microsomes. *J Pharmacol Exp Ther.* 291, 292-299.
- [17] Wen, X., Wang, J. S., Backman, J. T., Laitila, J. and Neuvonen, P. J. (2002) Trimethoprim and sulfamethoxazole are selective inhibitors of CYP2C8 and CYP2C9, respectively. *Drug Metab Dispos.* 30, 631-635.
- [18] Damsten, M. C., Van Vugt-Lussenburg, B. M., Zeldenthuis, T., De Vlieger, J. S., Commandeur, J. N. and Vermeulen, N. P. (2008) Application of drug metabolising mutants of cytochrome P450 BM3 (CYP102A1) as biocatalysts for the generation of reactive metabolites. *Chem Biol Interact.* 171, 96-107.
- [19] Baillie, T. A. and Davis, M. R. (1993) Mass spectrometry in the analysis of glutathione conjugates. *Biol Mass Spectrom.* 22, 319-325.
- [20] Rooseboom, M., Commandeur, J. N., Floor, G. C., Rettie, A. E. and Vermeulen, N. P. (2001) Selenoxidation by flavin-containing monooxygenases as a novel pathway for beta-elimination of selenocysteine Se-conjugates. *Chem Res Toxicol.* 14, 127-134.
- [21] Appiah-Opong, R., Commandeur, J. N., Van Vugt-Lussenburg, B. and Vermeulen, N. P. (2007) Inhibition of human recombinant cytochrome P450s by curcumin and curcumin decomposition products. *Toxicology.* 235, 83-91.
- [22] Gillam, E. M., Guo, Z. and Guengerich, F. P. (1994) Expression of modified human cytochrome P450 2E1 in *Escherichia coli*, purification, and spectral and catalytic properties. *Arch Biochem Biophys.* 312, 59-66.
- [23] Rostami-Hodjegan, A. and Tucker, G. T. (2007) Simulation and prediction of in vivo drug metabolism in human populations from in vitro data. *Nat Rev Drug Discov.* 6, 140-148.

- [24] Ingelman-Sundberg, M. (2001) Pharmacogenetics: an opportunity for a safer and more efficient pharmacotherapy. *J Intern Med.* 250, 186-200.
- [25] Pirmohamed, M. and Park, B. K. (2003) Cytochrome P450 enzyme polymorphisms and adverse drug reactions. *Toxicology.* 192, 23-32.
- [26] Pirmohamed, M. and Park, B. K. (2001) Genetic susceptibility to adverse drug reactions. *Trends Pharmacol Sci.* 22, 298-305.

PART III

NOVEL TOOLS FOR THE BIOMONITORING OF REACTIVE METABOLITES *IN VIVO* IN HUMANS

Chapter 5

Liquid chromatography/tandem mass spectrometry detection of covalent binding of acetaminophen to human serum albumin

Adapted from: Micaela C. Damsten, Jan N. M. Commandeur, Alex Fidler, Albert G. Hulst, Daan Touw, Daan Noort, and Nico P. E. Vermeulen.
Liquid Chromatography/Tandem Mass Spectrometry Detection of Covalent Binding of Acetaminophen to Human Serum Albumin.
Drug Metabolism and Disposition, 2007, 35 (8), p: 1408-1417.

Abstract

Covalent binding of reactive electrophilic intermediates to proteins is considered to play an important role in the processes leading to adverse drug reactions and idiosyncratic drug reactions. Consequently, both for the discovery and the development of new drugs, there is a great interest in sensitive methodologies that enable the detection of covalent binding of drugs and drug candidates *in vivo*. In this work, we present a strategy for the generation and analysis of drug adducts to human serum albumin. Our methodology is based on the isolation of albumin from blood, its digestion to peptides by pronase E, and the sensitive detection of adducts to the characteristic cysteine-proline-phenylalanine (CPF) tripeptide by liquid chromatography/tandem mass spectrometry. We chose acetaminophen (APAP) as a model compound because this drug is known to induce covalent binding to proteins when bioactivated by cytochromes P450 to its reactive N-acetyl-p-benzoquinoneimine metabolite. First, by microsomal incubations of acetaminophen in presence of CPF and/or intact albumin, *in vitro* reference adducts were generated in order to determine the mass spectrometric characteristics of the expected CPF adducts and to confirm their formation upon pronase E digestion of the alkylated protein. When applying this methodology to albumin isolated from blood of patients exposed to APAP, we were indeed able to detect the corresponding CPF adducts. Therefore, this strategy could be seen as a potential biomonitoring tool to detect *in vivo* reactive intermediates of drugs and drug candidates, e.g. in the preclinical and clinical development phase.

Introduction

Although much effort has been made in the development of predictive animal models useful for the early assessment of toxicity of drugs and drug candidates, the prediction of drug toxicity in humans stays difficult. While some adverse drug reactions (ADRs) can be predicted from preclinical safety studies, others are idiosyncratic in nature and only show up after the drug has been introduced on the market. These idiosyncratic types of drug reactions can lead to severe, in some cases fatal, toxicities in several organs, in particular the liver, skin and blood [1, 2].

Even though the underlying mechanisms of most ADRs are as yet poorly understood, formation of reactive metabolites is considered to be a major trigger in the cascade of events leading to these adverse events [3]. Drugs can be bioactivated both by phase I and by phase II enzymes to reactive electrophilic intermediates, which subsequently react with nucleophilic sites in macromolecules to form covalent adducts to proteins [4, 5]. Covalent binding to proteins with subsequent inactivation of enzymes and/or disruption of cellular signaling processes are events that are thought to be related to the onset of ADRs [5]. By serving as haptens, drug-protein adducts may also trigger the auto-immune reactions which are often observed in case of idiosyncratic drug reactions (IDRs) [6, 7].

As reviewed by Caldwell and Zhou [8, 9], different methodologies are used for the detection of adducts resulting from the formation of reactive intermediates. Briefly, these methods involve *in silico* screening of potentially toxic motives in molecules, the use of small nucleophilic trapping agents followed by mass spectrometric analysis of adducts formed *in vitro* and mechanism-based inhibition of cytochrome P450. An estimation of the levels of total covalent binding to proteins, *in vitro* and/or *in vivo*, can eventually be obtained by using radio-labeled drugs in animal experiments. However, because extrapolation of animal data to evaluate potential risks in humans stays complicated [2, 10], there is still a need for sensitive and selective methods for the assessment of covalent binding to proteins *in vivo* in humans. In the present study, a recently developed liquid chromatography/tandem mass spectrometry (LC-MS/MS) methodology will be applied to monitor covalent binding of acetaminophen (APAP) to the blood protein albumin.

The concept of using blood protein adducts as biomarkers of human exposure to electrophilic compounds dates back to the 1970's and was originally applied for the *in vivo* monitoring of occupational exposures to reactive, potentially genotoxic, compounds [11, 12]. Consistently, adducts to human serum albumin (HSA) have been found in populations exposed to several environmental contaminants [13-16].

The aim of the present study is to evaluate the applicability of a recently developed LC-MS/MS methodology for the *in vivo* biomonitoring of reactive drug metabolites to the blood protein albumin. This methodology, which has been applied successfully for the biomonitoring of exposure of humans to chemical warfare agents [17, 18], is based on the digestion of albumin by pronase E and subsequent selective detection of covalent adducts to the tripeptide cysteine³⁴-proline-phenylalanine (CPF) by LC-MS/MS. Cysteine³⁴ is the only free thiol-group in HSA and is capable of reacting with electrophiles. In this work, we evaluated the applicability of this methodology for the monitoring of reactive drug metabolites using APAP as model compound. At therapeutic doses, APAP is primarily metabolized by phase II enzymes to stable glucuronic acid and sulfate conjugates. A small proportion of the drug is bioactivated by cytochromes P450 to a reactive N-acetyl-p-benzoquinoneimine (NAPQI) intermediate that under normal conditions is detoxified by conjugation to glutathione (GSH) [19-21]. When taken in overdoses, the high levels of NAPQI produced will deplete the GSH stores resulting in strongly increased covalent binding to liver proteins, oxidative stress and ultimately to severe hepatotoxicity [22].

We propose a general strategy which consists of the biosynthesis of reference adducts to CPF and albumin to determine the mass spectrometric characteristics of the CPF-adducts and to determine whether pronase E treatment of alkylated albumin is able to generate the corresponding CPF-adducts (Figure 1). The analytical procedure was subsequently applied for the measurement of adducts in the blood of humans exposed to high doses of APAP.

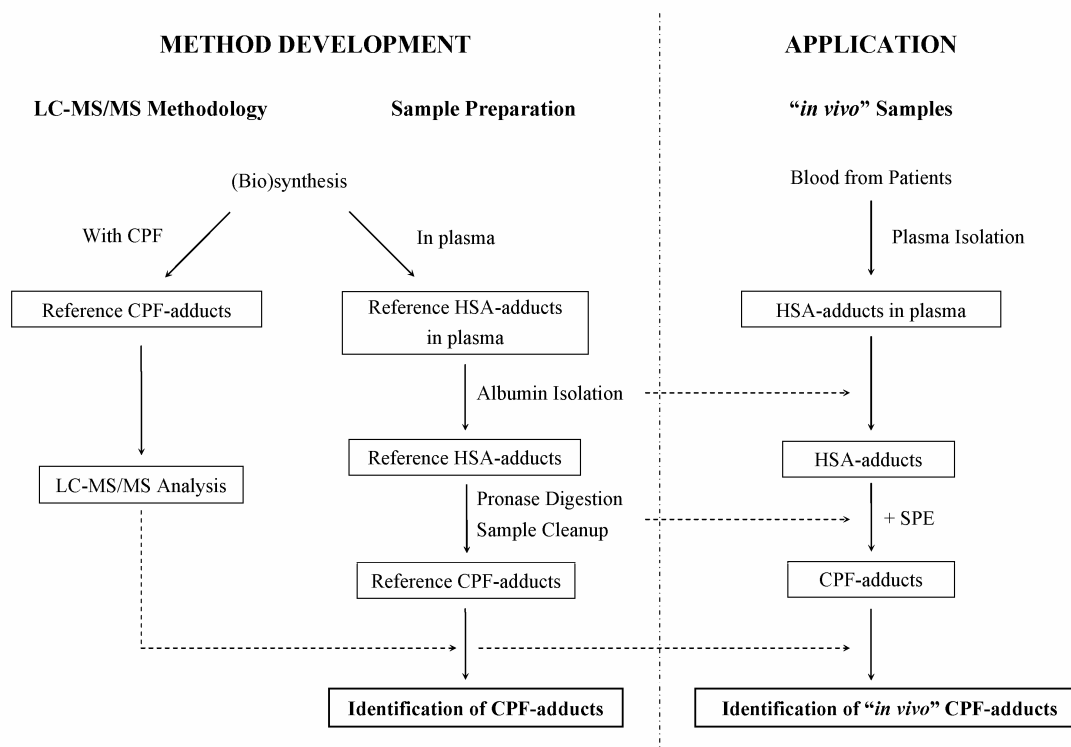


Figure 1. Scheme of the strategy proposed for the generation and detection of drug adducts to HSA.

Material and Methods

Materials

Pronase E (protease from *Streptomyces griseus*, Type XIV, 3.4.24.31), GSH (reduced glutathione, 98%) and NAc (*N*-acetyl-L-cysteine, 98%) were purchased from Sigma (Deisenhofen, Germany). NADPH-tetrasodium salt was obtained from AppliChem BioChemica (Darmstadt, Germany). Amicon Ultra-4 (10-kDa molecular mass cutoff) centrifugal filters were purchased from Millipore (Bedford, USA). The HiTrap™ Blue HP affinity columns (1 ml; prepacked with blue Sepharose high performance, with Cibacron Blue F3G-A as the ligand) and the PD-10 columns (containing 10 ml of Sephadex G 25 material) were obtained from Amersham Biosciences (Uppsala, Sweden). The Acrodisc LC polyvinylidene difluoride filters (0.45 μm , 25 mm) were obtained from Waters Corporation, and the Strata-X columns (33 μm Polymeric Sorbent) were from Phenomenex. β -Naphthoflavone-induced rat liver microsomes (RLM) were prepared according to the standard protocol of our laboratory [23]. Control human blood was obtained from healthy volunteers, and blood samples from patients overdosed with APAP were provided to us by Dr. D.

Touw (Apotheek Haagse Ziekenhuizen in The Hague, The Netherlands). Blood sampling was performed using 3.5 or 7 ml vacuum containers without anticlot or gel. Blood samples were subsequently centrifuged at 3000g in order to separate plasma from erythrocytes. The obtained plasma was stored at -70°C until further analysis. Sampling for aspartate transaminase (AST) and alanine aminotransferase (ALT) analyses was generally performed using heparin gel tubes. Analysis was performed after a centrifugation step, within 30 minutes after sampling. Human plasma exposed to perdeuterated sulfur mustard was used as internal standard to control the digestion procedure and to quantify the peptide adducts, and was prepared as described in [24]. All other chemicals were of the highest grade and were obtained from standard providers.

Instrumentation

LC/electrospray (ES)-MS(/MS) analyses were conducted on a Q-TOF™ hybrid instrument (Micromass, Altrincham, UK) equipped with a standard Z-spray™ ES interface (Micromass) and an Alliance, type 2690 liquid chromatograph (Waters, Milford, MA). The chromatographic hardware for this system consisted of a pre-column splitter (type Acurate; LC Packings, Amsterdam, The Netherlands), a six-port valve (Valco, Schenkon, Switzerland) with a 50 µl injection loop mounted, and a PepMap C18 column (15 cm x 1 mm i.d., 3-µm particles; LC Packings). A gradient of solvent A (H₂O with 0.2% formic acid) and B (acetonitrile with 0.2% formic acid) was used to achieve separation, following: 100% A (at time 0 min, 0.1 ml/min flow) to 100% A (at 5 min, 0.6 ml/min flow) to 30% A and 70% B (at 60 min, 0.6 ml/min flow). The flow delivered by the liquid chromatograph was split pre-column to allow a flow of approximately 40 µl/min through the column and into the ES-MS interface. The Q-TOF was operated at a cone voltage of 20 to 30 V, using nitrogen as the nebulizer and desolvation gas (at a flow of 20 and 400 l/h, respectively). MS/MS product ion spectra were recorded using a collision energy between 20 and 30 eV, with argon as the collision gas (at an indicated pressure of 10⁻⁴ mBar).

Standard tripeptide assay

Adducts to HSA were analyzed using a slightly modified methodology that has been described previously [24]. Briefly, human blood was first centrifuged and the obtained plasma (500 µl) was diluted with 2 ml of buffer A (50 mM KH₂PO₄, pH 7.00). To control the procedure and to allow the quantification of the peptide adducts in the human serum samples, the samples were spiked with 50 µl of an internal standard consisting of plasma isolated from human blood exposed to 100 µM of perdeuterated

sulfur mustard gas. The pronase E digest of albumin alkylated with perdeuterated sulfur mustard gas is known to produce the characteristic d_8 -S-(2-hydroxyethylthioethyl)-Cys-Pro-Phe (d_8 -HETE-CPF) adduct, as has been described in [24]. The samples were then filtered with 0.45 μ m Acrodisc filters, and the albumin was subsequently isolated from the filtrate using HiTrapTM Blue HP affinity columns. These columns were firstly conditioned with 10 ml of buffer A. The whole sample (2.55 ml) was then applied on the columns and washed with 10 ml of buffer A. Elution took place with 3 ml of buffer B (50 mM KH_2PO_4 with 1.5M KCl). The HiTrap columns were regenerated by washing with 10 ml of buffer A. PD-10 columns were used to desalt the obtained albumin fractions. After equilibration of the PD-10 columns with 25 ml of 50 mM NH_4HCO_3 , the samples were applied on the columns (3 ml) and eluted with 3 ml of the same bicarbonate buffer. The digestion procedure of the desalted albumin solution with pronase E was as follows: 100 μ l of a freshly prepared pronase E solution (10 mg/ml stock solution in aqueous 50 mM NH_4HCO_3) was added to 750 μ l of the albumin fraction (in 50 mM NH_4HCO_3). After 2 hours of incubation at 37°C, the mixture was passed through molecular mass cutoff filters (10 kDa) under centrifugation at 2772 x g in order to remove the enzyme. Under these conditions, pronase E digestion of albumin adducts is optimized [17, 24]. The filtrate was subsequently analyzed by LC-MS/MS. If not analyzed immediately, all samples were stored at -20°C until analysis.

Synthesis and purification of NAPQI-CPF adducts

The reactive metabolite of APAP, NAPQI, was synthesized according to a previously described method [25]. Briefly, fresh silver oxide was prepared by adding a silver nitrate solution (170 mg in 10 ml H_2O) to a solution of potassium hydroxide (100 mg in 18 ml H_2O). The mixture was left for 15 minutes on ice in order to yield the highest amounts of the silver oxide precipitate. After filtration of the solution and three washing steps with acetone, the obtained silver oxide powder was added to a solution of APAP (10 mg in 10 ml of chloroform). This reaction mixture was stirred at room temperature for 1 hour in order to obtain 10 ml of a yellowish NAPQI solution (in chloroform). A portion of this NAPQI solution (2 ml) was filtered, evaporated to dryness by rotaevaporation at room temperature, and further taken-up in 10 μ l of acetonitrile. This concentrated NAPQI solution was then reacted with 100 μ l of synthetic CPF tripeptide solution (stock concentration 2.5 mM in 50 mM NH_4HCO_3) in a total volume of 1.5 ml of a 30% acetonitrile solution (in bicarbonate buffer). After 2 hours of reaction at 37°C, the sample was measured by LC-MS/MS. LC-MS/MS analysis of the reaction mixture showed the presence of a product having the

molecular mass of the expected NAPQI-CPF adduct (Figure 2). The product ion spectrum of this protonated molecule (m/z 515.18 $[M+H]^+$) had characteristic fragments at m/z 497.18 ($[M+H]^+ - H_2O$), m/z 350.11 (b_2), m/z 322.13 (a_2), m/z 263.16 (y_2''), m/z 225.07 (a_1), m/z 208.06 (a_1-NH_3), m/z 166.06 (y_1''), m/z 152.07 $[APAP+H]^+$ and m/z 120.07 (immonium ion of phenylalanine).

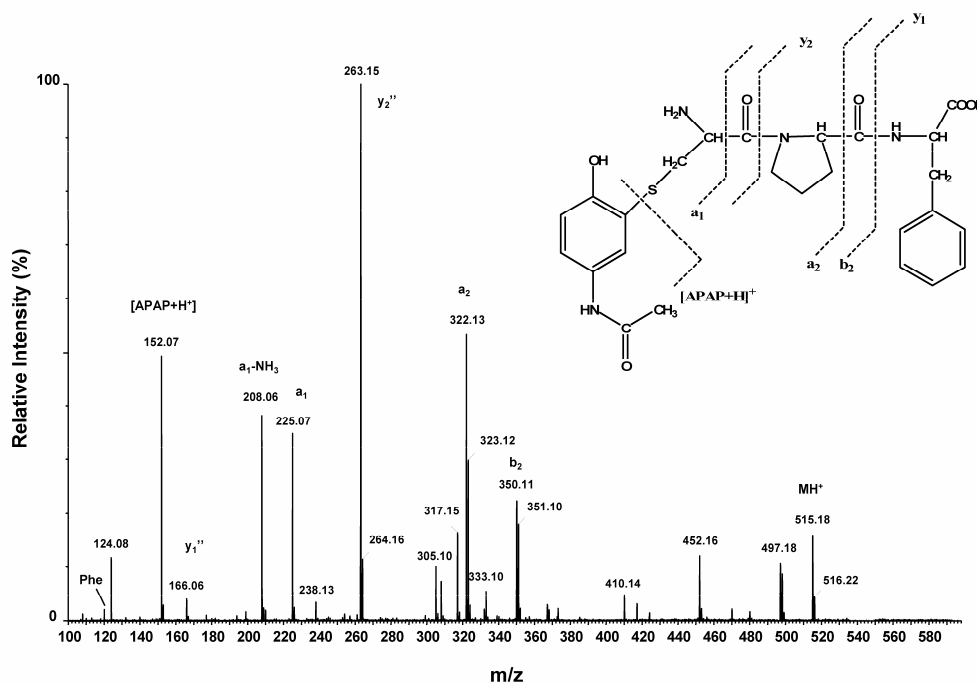


Figure 2. Electrospray product ion spectrum of the NAPQI-CPF adduct. The reference NAPQI-CPF adduct was obtained from the reaction of synthetic NAPQI with synthetic tripeptide CPF. The electrospray product ion spectrum of the adduct (m/z 515.18; $[M+H]^+$) was obtained with a collision energy of 24 eV.

To further characterize the NAPQI-CPF product and to enable quantification of NAPQI-CPF in patient samples, a large scale synthesis was performed. APAP (32 mg) was oxidised to NAPQI in 75 ml chloroform, as described above, and stirred vigorously for 2 hours at room temperature with 25 mg CPF in 30 ml 100 mM potassium phosphate buffer (pH 7.4). The resulting water phase was isolated and washed three times with a mixture of chloroform/isopropanol (3:1 v/v) in order to remove excess NAPQI and lipophilic side products. The water phase was subsequently dried overnight by nitrogen stream. The residue was taken up in 1 ml of 10% acetonitrile and applied to preparative HPLC to purify NAPQI-CPF-adducts.

The preparative HPLC consisted of a Luna C18 column (250 x 10 mm; 5 μ m particles) eluted at a flow-rate of 2 ml/min. A gradient of solvent A (1% acetonitrile/0.2% formic acid/98.8% water) and B (99% acetonitrile/0.2% formic

acid/0.8% water) was used to achieve separation of analytes. The gradient used started at 15% B (0 minutes) and was followed by a linear increase to 25% B (50 minutes). Peaks absorbing at 254 nm were collected and screened for presence of NAPQI-CPF by LC-MS. Two peaks at 21.9 (minor, 5%) and 23.6 minutes (major, 95%) were shown to contain NAPQI-CPF. The fractions containing purified NAPQI-CPF were pooled, dried by nitrogen stream and taken up in 500 μ l deuterium oxide. The $^1\text{H-NMR}$ spectrum was recorded on a Bruker MSL 400 system operating at 376.43 Hz. The $^1\text{H-NMR}$ -spectrum of the major NAPQI-CPF-isomer was consistent with a NAPQI-CPF adduct, although protons could not be assigned individually because of the complexity and overlap of the $^1\text{H-NMR}$ -signals. Because aromatic protons of the phenylalanine-residue interfere with the signals of the APAP-residue, the position of the thioether-bond could not be assigned. $^1\text{H-NMR}$ -spectrum: 6.8-7.6 ppm (aromatic protons; multiplet; 8H), 3.8-4.5 ppm (methine protons of phenylalanine, cysteine and proline; multiplet; 3H), 2.8-3.55 ppm (methylene protons of phenylalanine and cysteine; four methylene protons of proline; multiplet; 8H), 1.65-2.3 ppm (two methylene protons of proline and acetyl protons of APAP; multiplet; 5H). The concentration of the minor NAPQI-CPF-isomer was too low to obtain a good $^1\text{H-NMR}$ -spectrum.

To calibrate the concentration of NAPQI-CPF-solution, difluoroacetic acid (final concentration 720 μM) was added to the solution of NAPQI-CPF and analysed by $^1\text{H-NMR}$. Difluoroacetic acid was selected as internal standard because its signals (triplet at 5.82 ppm, $^2J_{\text{FH}}$ 51 Hz) do not interfere with the signals of NAPQI-CPF. By integrating the signals of aromatic protons of NAPQI-CPF ([8H]) and that of difluoroacetic acid ([1H]), the concentration of the NAPQI-CPF solution was estimated to be 650 μM . This solution was used for the quantification of NAPQI-CPF adducts formed by pronase E treatment of patient samples.

Incubation of synthetic NAPQI in human plasma

The synthetic NAPQI solution described above was used to expose human plasma to the reactive alkylating compound. In these experiments, 3 ml of the NAPQI solution (in chloroform) was evaporated to dryness by rotaevaporation at room temperature and further taken-up in 10 μ l of acetonitrile. The concentrated NAPQI solution was then reacted with 2 ml of human plasma for 2 hours at 37°C. Subsequently, 500 μ l of that incubation mixture was diluted with 2 ml of buffer A and spiked with 50 μ l of the internal standard. The sample was consistently passed through the Acrodisc filter and the albumin was isolated on the HiTrap column as described above. The albumin

fraction was then desalted on PD-10 columns and 750 μ l of that filtrate were treated with pronase E for 2 hours at 37°C. After a centrifugation step with the molecular mass cutoff filters, the filtrate was analyzed by LC-MS/MS.

Microsomal incubations of APAP in presence of synthetic CPF

Microsomal incubations of APAP and CPF had a final volume of 500 μ l and were conducted at 37°C in a heated shaking water bath. The incubation occurred in a 100 mM KH_2PO_4 buffer (pH 7.4) and the mixture was composed as follows (in final concentrations): 1 mM of APAP, β -naphthoflavone-induced RLM (2 mg protein/ml), and 1 mM of the synthetic Cysteine–Proline–Phenylalanine (CPF) tripeptide solution. After 5 minutes of pre-incubation, the co-factor NADP(H) (final concentration 2 mM) was added to the mixture, and the samples were incubated for 1 hour at 37°C. After the incubation time, the samples were placed on ice, and 200 μ l of 2.00 M HClO_4 was added in order to stop the incubations and precipitate proteins. The samples were vortexed and kept on ice for 5 additional minutes. The tubes were subsequently centrifuged for 15 minutes at 4000 rpm and a 400- μ l aliquot of the supernatant was neutralized by the addition of an equal volume of K_2HPO_4 1.00 M. The samples were vortexed, centrifuged again for 15 minutes at 4000 rpm, and the supernatant was analyzed by LC-MS/MS. An incubation performed without APAP was processed in parallel and served as control.

Microsomal incubations of APAP in presence of human plasma

Microsomal incubations of APAP in human plasma were performed similarly as described above. Briefly, 75 μ l of APAP (20 mM stock in H_2O) and 150 μ l of RLM (10 mg of protein/ml stock) were added to 500 μ l of human plasma. After 5 minutes of pre-incubation at 37°C, 150 μ l of NADP(H) (10 mM stock in 100 mM KPi buffer, pH 7.4) was added to the incubation mixture. The mixture was incubated for 1 hour at 37°C. After the incubation time, 2 ml of buffer A and 50 μ l of the internal standard were added to the samples. The albumin isolation, pronase E digestion, and peptide filtration steps were performed similar to the procedure described for the exposure of human plasma to synthetic NAPQI. The samples were subsequently analyzed by LC-MS/MS. Incubation performed without substrate served as control.

Analysis of human serum samples

Consistently, 500 μ l of human serum of patients exposed to high levels of APAP was diluted with 2 ml of buffer A and the samples were spiked with 50 μ l of the internal standard. The rest of the procedure was similar to that described earlier. Blood from

healthy volunteers, not being exposed to either APAP or NAc, was taken as control and processed in parallel.

Initial measurements of the patient's blood samples revealed a significant background signal interfering with the expected NAPQI-CPF adducts. Therefore, to increase the sensitivity in the albumin adduct detection, the protocol was slightly adapted by including a solid phase extraction step in the procedure. The human serum samples were analyzed with the modified protocol as follows. After isolation and desalting of albumin as described above, 300 μ l of a fresh pronase E solution (10 mg/ml) was added to approximately 2 ml of the albumin solution. After 2 hours of incubation at 37°C, the samples were centrifuged at 2772 x g to eliminate the excess of enzyme. The freshly digested samples were acidified with TFA (final concentration 0.1% TFA) and Strata X columns were used for the solid phase extraction procedure. The columns were first activated with 10 ml of methanol and then equilibrated with 10 ml of 100% H₂O with 0.1% TFA. The samples were applied on the column and subsequently eluted with 2-ml fractions of 0, 10, 20, 30, 40, 50, 60, 70, 80, 90 and 100% acetonitrile solutions containing 0.1% TFA. These different fractions were collected, freeze-dried, taken-up in 120 μ l of 100 % H₂O with 0.2% formic acid and analyzed by LC-MS/MS. The NAPQI-CPF adducts were eluted by the 30% acetonitrile/0.1% TFA fraction.

To quantify NAPQI-CPF-adducts formed by pronase E treatment of albumin, the albumin fractions isolated from the plasma samples were also spiked with 65 nmol of purified synthetic NAPQI-CPF (major isomer), prior to the treatment with pronase E. By measuring the increase in the ratio of the peak area of NAPQI-CPF to that of the internal standard (d₈-HETE-CPF), the amount of NAPQI-CPF in the non-spiked albumin-fraction was estimated.

To analyze small molecular weight adducts, the eluates obtained from the application of the serum samples on the HiTrap columns were collected, filtered with molecular mass cutoff filters (10 kDa) under centrifugation at 2772 x g and analyzed by LC-MS/MS.

Results

Incubation of synthetic NAPQI with human plasma

To assess whether NAPQI is also reactive towards the free cysteine³⁴ residue of HSA and whether the pronase E digest of alkylated albumin is leading to the

formation of NAPQI-CPF, human plasma was incubated *in vitro* with freshly synthesized NAPQI. Full MS analysis was used to screen the fragments obtained after fragmentation of the selected molecular ion with an m/z of 515.2 $[M+H]^+$. The reconstructed ion chromatogram of the summed ions corresponding to specific fragments of the synthetic adduct revealed the presence of two NAPQI-CPF adducts in the reaction mixture (Peak 1 and Peak 2 in Figure 3-A). Their product ion spectra were comparable to that of our reference adduct. Only slight differences in the fragmentation pattern of the two peaks were observed suggesting the formation of two regioisomeric NAPQI-CPF adducts (Figure 4).

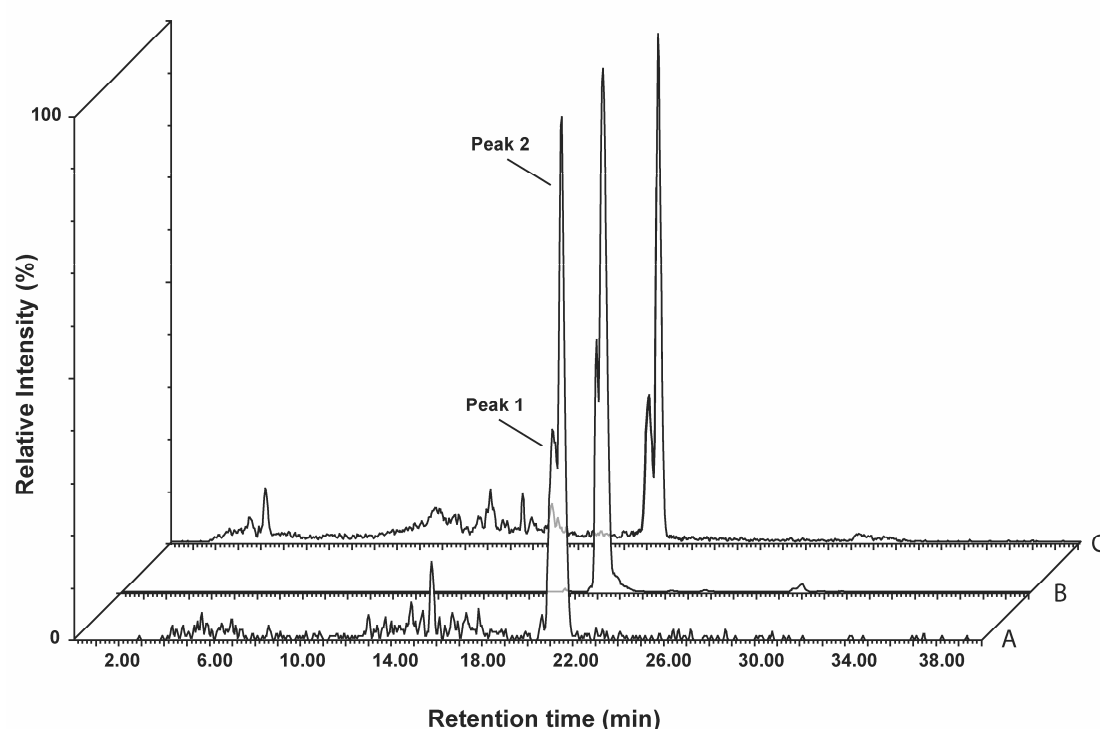


Figure 3. Analysis of NAPQI-CPF adducts ($[M+H]^+$; m/z 515.2) generated in different *in vitro* systems. Ion chromatograms of summed ions: m/z 152.1, 208.1, 225.1, 322.1, 350.2 in (A) a pronase digest of alkylated HSA isolated from human plasma exposed to synthetic NAPQI, (B) an APAP microsomal incubation performed with synthetic CPF and (C) a pronase digest of alkylated HSA isolated from an APAP microsomal incubation performed in human plasma.

Incubations of acetaminophen with rat liver microsomes

Next to the chemical synthesis of the albumin and CPF-adducts of NAPQI, it was also investigated whether *in vitro* incubations of APAP in presence of albumin or CPF produced the same adducts. We therefore used β -Naphthoflavone-induced rat liver microsomes (RLM) to bioactivate APAP to NAPQI in a biological system. By

performing incubations using synthetic CPF as trapping agent for NAPQI, two NAPQI-CPF adducts were found by LC-MS/MS analysis (Figure 3-B).

When APAP was incubated with RLM in presence of human plasma, two NAPQI-CPF adduct isomers were observed after pronase E digestion of the albumin fraction. The adducts had the same characteristic differences in their product ion spectra as observed in the products formed by synthetic NAPQI (Figure 3C).

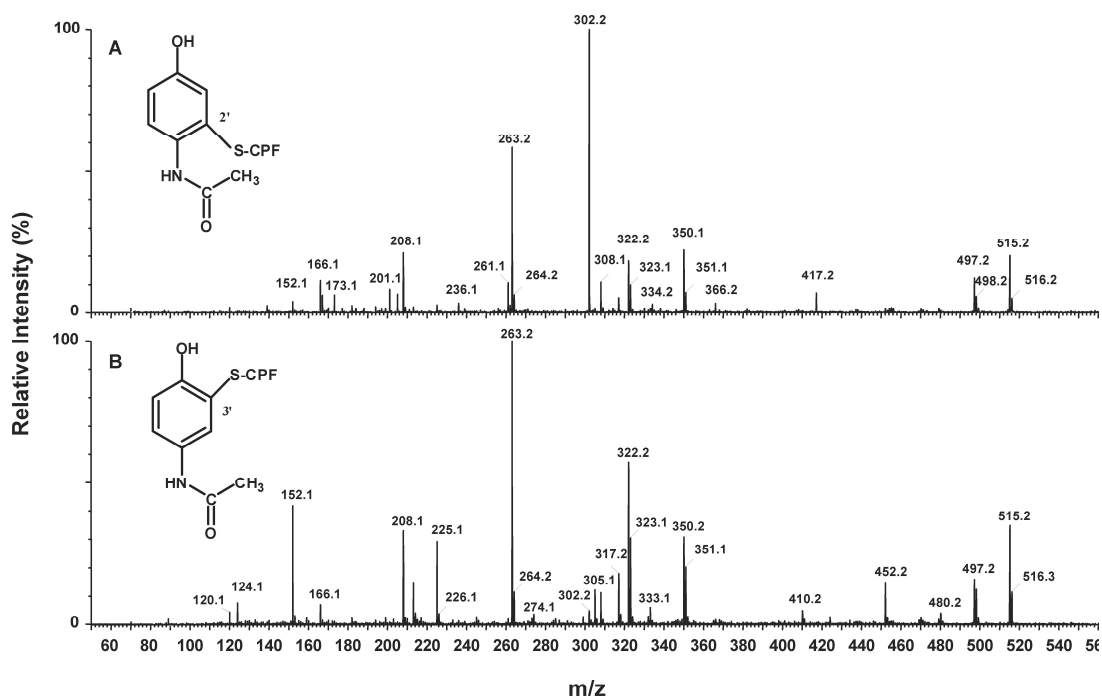


Figure 4. Electro spray product ion spectra of two NAPQI-CPF adduct regioisomers ($[M+H]^+$; m/z 515.2) with proposed structures: (A) NAPQI-CPF adduct corresponding to peak 1 in Figure 3 and (B) NAPQI-CPF adduct corresponding to peak 2 in Figure 3.

Analysis of human serum samples

The developed methodology was applied to analyze blood of patients exposed to high levels of APAP. Three patients were selected with the characteristics presented in Table 1. Patient TOX 444 suffered from severe hepatotoxicity as indicated by increased plasma aspartate transaminase and alanine aminotransferase levels. The two other patients (TOX 438 and TOX 440) had normal plasma transaminase levels and were therefore considered to be in a nonhepatotoxic condition.

Table 1. Characteristics of the patients overdosed with acetaminophen.

Patient	APAP dose (g)	Time after intake (h)	[APAP] (mg/l)	NAC treatment	ALT (U/l)	AST (U/l)
TOX 438	12	5	130	Yes	11	12
		23	4.5		n.d.	n.d.
TOX 440	10	2	150	No	16	30
		4	92		n.d.	n.d.
TOX 444	40	16	12	Yes	373	3150
		25	< 1		229	2282
		31	< 1		194	1683

The table includes the ingested dose of APAP; the time after APAP intake; the blood concentration of APAP in time; whether the patient was treated with N-acetyl cysteine (NAC), and the levels of hepatic enzymes alanine aminotransferase (ALT) and aspartate aminotransferase (AST) in time.

Initially, the serum samples of these patients were analyzed with the standard tripeptide assay as described in [24]. However, by this assay no NAPQI-CPF adducts were observed in the sera of patients TOX 438 and TOX 440 as a result of background interference, whereas two weak NAPQI-CPF signals were found in the serum of patient TOX 444 (data not shown). By using the solid-phase extraction step in the procedure, it was found that the NAPQI-CPF peaks eluted in the 30% acetonitrile/0.1 % TFA fraction. The signal-to-noise ratio of the NAPQI-CPF signals was significantly increased using this clean-up step. Two NAPQI-CPF adducts were observed in the sera of patient TOX 444, and signals corresponding to the major NAPQI-CPF adduct were now also observed in the sera of patients TOX 438 and TOX 440. The product ion spectra of these adducts were identical to those obtained in our previous *in vitro* experiments. No NAPQI-CPF adducts were present in the control subjects (Figure 5).

By spiking the isolated albumin fractions of patient TOX 444 with 65 nmol of synthetic NAPQI-CPF, before pronase E treatment, the amount of NAPQI-CPF in the pronase E digest was quantified. By comparing the peak areas of NAPQI-CPF in samples of patient TOX 444 with and without spiking with synthetic NAPQI-CPF, the amount of NAPQI-CPF in the unspiked sample was estimated to be 35 ± 15 pmol/ml serum. Based on the 10-fold lower peak areas in patient samples TOX 438 and 440 (Figure 5), the levels of NAPQI-CPF in these serum samples are estimated to be approximately 3 to 4 pmol/ml serum.

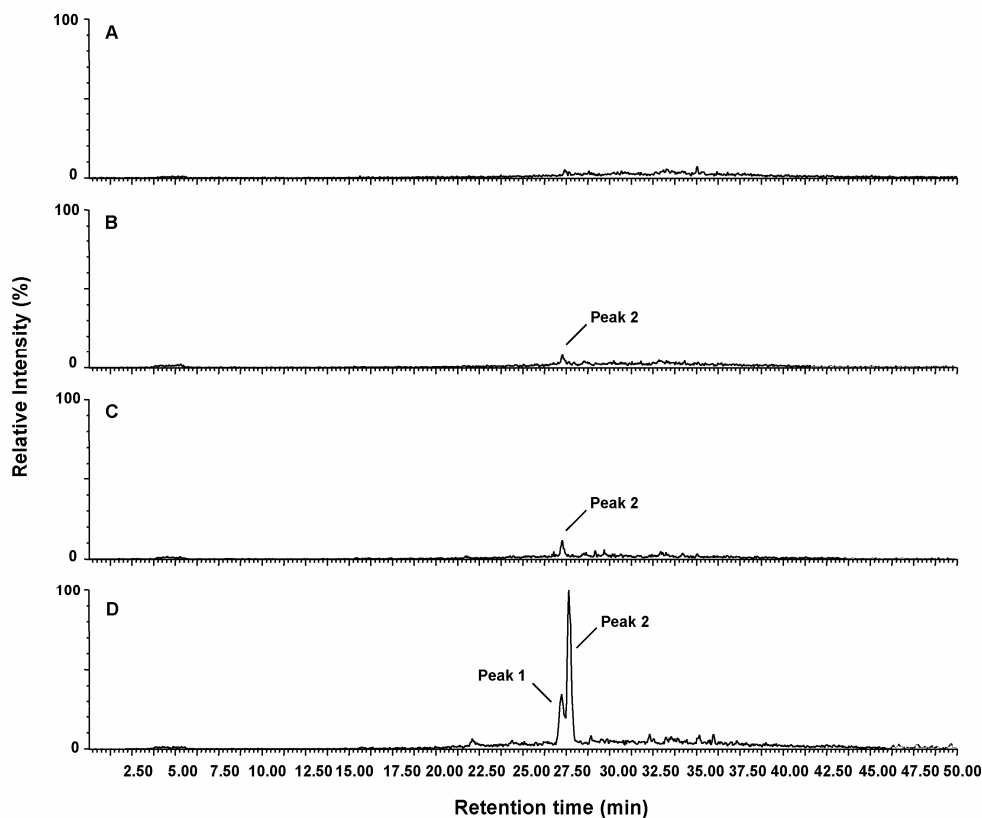


Figure 5. LC-MS/MS analysis of NAPQI-CPF adducts in human serum samples ($[M+H]^+$; m/z 515.2). Ion chromatograms of summed ions: m/z 152.1, 208.1, 225.1, 322.2, 323.2, 351.2 in (A) the control subject, (B) patient TOX 438, (C) patient TOX 440 and (D) patient TOX 444. The analyses of the 23-, 4- and 25-h time point samples of patients TOX 438, 440, and 444 respectively, are shown in the figure.

The eluates obtained during the albumin isolation step were also screened for the presence of other NAPQI-derived adducts. No GSH conjugates were observed in the human plasma samples. However, very high amounts of NAPQI-cysteine (NAPQI-Cys) and NAPQI-N-acetyl cysteine (NAPQI-NAc) adducts were found in the sera of these patients (Figure 6). Their specific fragmentation pattern confirmed the identity of these adducts of which the characteristics are presented in Table 2.

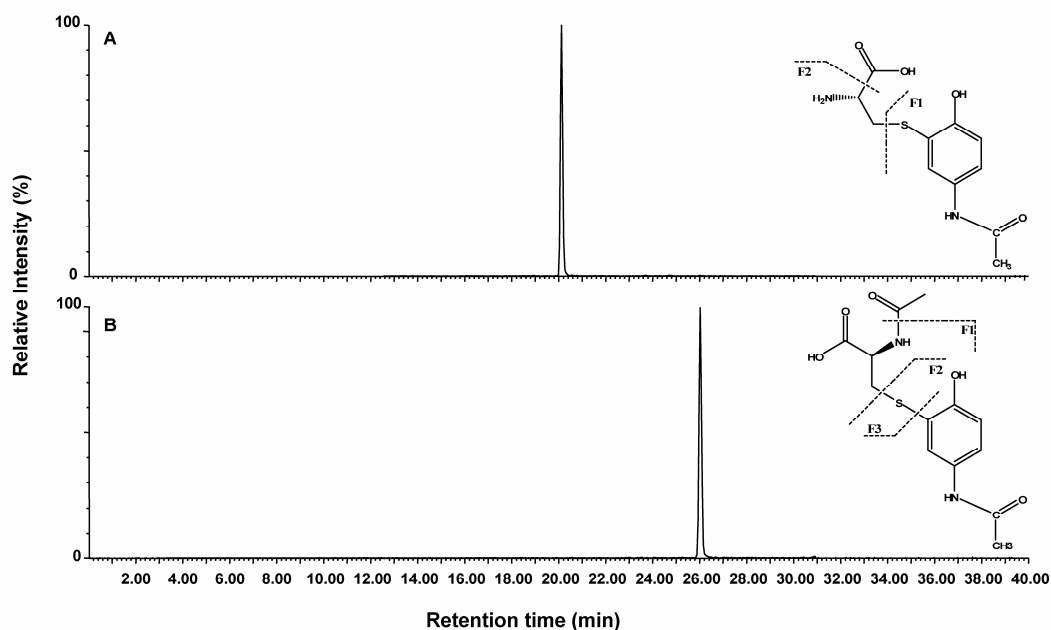


Figure 6. Analysis of NAPQI-NAC and NAPQI-Cys adducts in the human serum samples. LC-MS/MS analysis of (A) the NAPQI-Cys adduct ($[M+H]^+$; m/z 271.1; ion chromatogram of summed ions: m/z 140.0, 182.1) and (B) the NAPQI-NAC adduct ($[M+H]^+$; m/z 313.1; ion chromatogram of summed ions: m/z 208.1, 271.1), with proposed structures, analyzed in the 4-h time point sample of patient TOX 440.

Table 2. Characterization of the NAPQI-Cys and NAPQI-NAC adducts.

Adduct	t_r (min)	Parent ion	Fragments
NAPQI-Cys	20.12	m/z 271.1 $[M+H]^+$	m/z 254.1 ($[M+H]^+-NH_3$); m/z 225.1 [F2]; m/z 208.1 [F2- NH_3]; m/z 182.1 [F1]; m/z 140.0 [F1-acetyl]
NAPQI-NAC	26.02	m/z 313.1 $[M+H]^+$	m/z 271.1 [F1]; m/z 253.1 [F1- H_2O]; m/z 225.1 [F1-HCOOH]; m/z 208.1 [m/z 225.1- NH_3]; m/z 182.1 [F2]; m/z 166.1 [m/z 208.1-acetyl]; m/z 162 [F3]; m/z 140.1 [F2-acetyl]

Characteristics of the electrospray product ion spectra of the NAPQI-Cys and of the NAPQI-NAC adducts detected in the human serum samples. Product ion spectra's were obtained with a collision energy of 15 eV.

Interestingly, another high signal was found in the pronase E digest of the isolated albumin fraction of patient TOX 444 suggesting that another albumin adduct is formed *in vivo*. The ion chromatogram of the protonated molecule (m/z 655.4; $[M+H]^+$) is depicted in Figure 7A. The product ion spectrum of this ion showed characteristic signals at m/z 637.4 ($[M+H]^+ - H_2O$), m/z 527.3 (y_3''), m/z 490.3 (b_3), m/z 393.2 (b_2), m/z 375.2 ($b_2 - H_2O$), m/z 347.2 ($a_2 - H_2O$), m/z 263.2 (y_2''), m/z 230.1 ($b_2 - NAc$), m/z 162.1 $[NAc-H]^+$ and m/z 101.1 (a_1). This fragmentation pattern is consistent with the Glutamine-CPF (QCPF) tetrapeptide, from which the cysteine³⁴ residue formed a mixed disulfide with N-acetyl cysteine (Figure 7B). This adduct was also found in the serum of patient TOX 438 but was absent in patient TOX 440. Because the formation of a tetrapeptide instead of the CPF tripeptide was surprising, we checked the enzymatic activity of pronase E by analyzing the internal standard that was systematically added to the serum samples. The expected d_8 -HETE-CPF tripeptide adduct was consistently found in the samples thereby confirming a correct activity of the protease (data not shown). The human samples were also screened for the possible formation of NAPQI-QCPF adducts but no signals corresponding to these adducts were observed suggesting a complete digestion towards NAPQI-CPF adducts and no missed cleavages. Eventually, the levels of the different adducts analyzed for each patient were found to be constant in time.

Table 3 summarizes the different adducts identified in the human serum samples and gives a semi-quantitative overview of their relative concentrations.

Table 3. Overview of the adducts detected in the human serum samples.

Patient	APAP dose (g)	NAc treatment	NAPQI-CPF	NAPQI-NAc	NAPQI-Cys	QCPF-NAc
TOX 444	40	Yes	++	++++	++++	+++
TOX 440	10	No	+	++++	++++	-
TOX 438	12	Yes	+	++++	++++	+++
Blank	0	No	-	-	-	-

Levels of analytes are ranked as: very abundant (++++); abundant (+++); average (++); present (+); absent (-). Because levels are based on peak areas of summed ion chromatograms of each analyte, only levels from the same column should be compared.

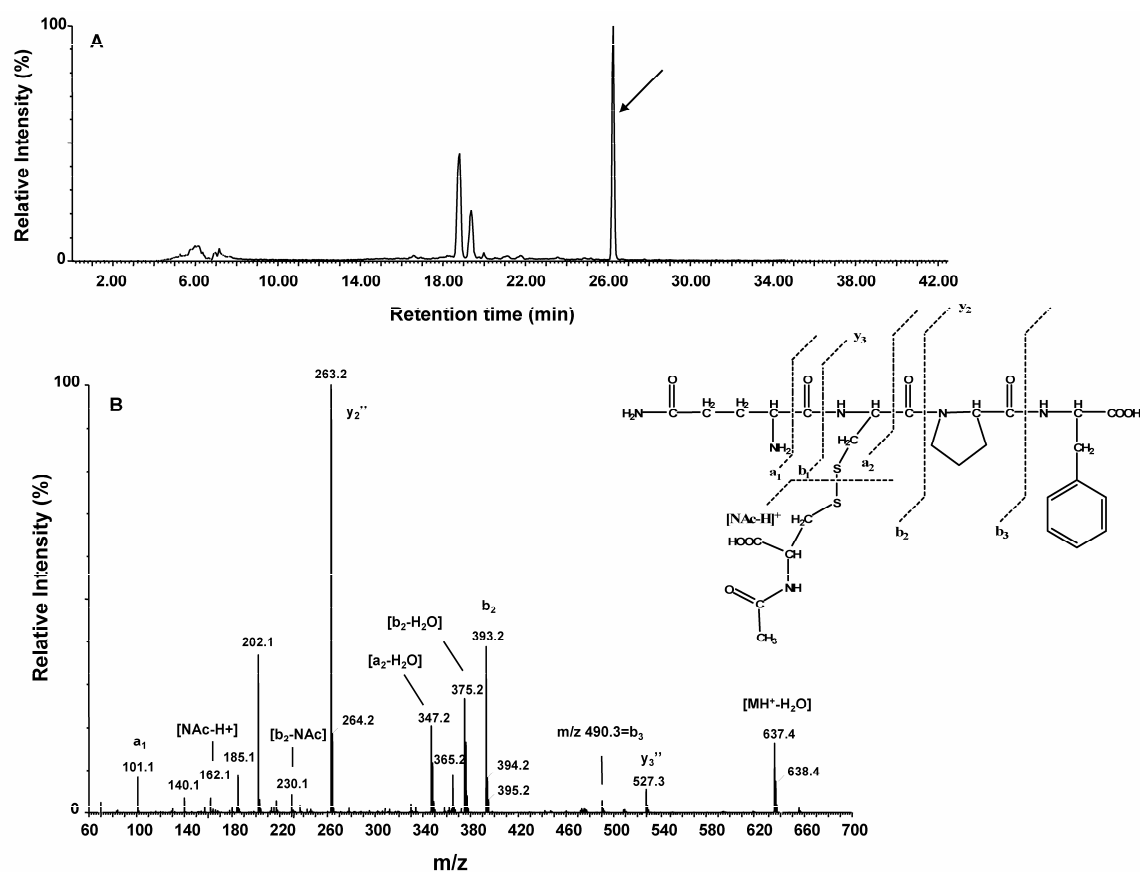


Figure 7. Analysis of the QCPF-NAc adduct in the human serum samples. LC-MS/MS analysis of the QCPF-NAc adduct ($[M+H]^+$; m/z 655.4) in a pronase digest of alkylated HSA isolated from the 25-h time point sample of patient TOX 444: (A) ion chromatogram of m/z 655.4 and (B) its product ion spectra with proposed structure.

Discussion

Predicting the potential of drugs and drug candidates to lead to adverse drug reactions in humans via electrophilic reactive intermediates is still a difficult and speculative task. Whereas the current way to assess this issue is usually to combine *in vitro* data on reactive intermediate formation with protein covalent binding studies *in vivo* in animals with radio-labeled drugs, extrapolation of these data to assess potential risks for humans remains complicated [2, 8]. In this study, we evaluated the use of albumin adducts as biomarkers of bioactivation of drugs to reactive metabolites *in vivo* in humans. An overall strategy for the generation and analysis of those adducts is proposed. The methodology used is based on LC-MS/MS analysis of covalent adducts to free cysteine³⁴ residue of HSA by detecting an alkylated CPF tripeptide obtained after pronase E digestion of the protein. APAP was chosen as model compound to study this concept [22, 26].

We have shown that microsomal incubations were able to generate the same albumin adducts as those obtained with synthetic NAPQI (Figure 3), indicating that the biosynthesis of reference adducts is possible. Therefore, this biosynthetic approach allows the development of sensitive and selective analytical methods for the detection of CPF adducts without the requirement for chemical synthesis of reference adducts. The NAPQI-CPF adducts observed had slightly different product ion spectra and consequently suggested the formation of two isomers. Based on literature, we assume that the major peak is most likely the 3'-NAPQI-S-CPF adduct because several studies have shown that conjugation of thiols to NAPQI predominantly takes place at the 3'-position of NAPQI [27-30]. As for the minor NAPQI-CPF adduct, two different products can be considered: a thioether ipso adduct and a 2'-NAPQI-S-CPF-adduct. Chen *et al.* [30] showed that the ipso-adduct was formed at slightly higher levels than the 2'-isomer, after reaction of NAPQI with GSH at pH 6. However, the ipso-adduct was shown to be highly unstable at lower pH, with a half live of 0.5 minutes at pH 4. Because of the lengthy procedure, involving albumin isolation and pronase E digestion, and the fact that the solid phase extraction was performed at acid pH (~ pH 2), it seems unlikely that the minor NAPQI-CPF adduct will correspond to the ipso-adduct. Therefore, we propose that the minor NAPQI-CPF adduct corresponds to the 2'-regioisomer.

When applying the developed methodology to blood samples from patients exposed to high doses of APAP, the major NAPQI-CPF isomer was observed in all patients (Figure 5). The patient with severe hepatotoxicity, TOX 444, showed an approximately 10-fold higher level of NAPQI-CPF adduct when compared to the patients without hepatotoxicity. The minor NAPQI-CPF isomer could only be observed in the blood sample of patient TOX 444. To our best knowledge, this is the first time that two NAPQI-HSA adduct regioisomers have been observed *in vivo* in humans. The levels of NAPQI-CPF adduct present in the serum of patient 444 were estimated to be about 35 pmol/ml of serum. It has been reported previously, that significantly higher levels of NAPQI-protein adducts can be found in serum in patients showing severe hepatotoxicity in comparison with serum of patients without or with low hepatotoxicity [31, 32]. However, because a different methodology was used in these studies, measuring total NAPQI-Cys adducts after complete hydrolysis of whole serum, the levels of our NAPQI-CPF adducts were not compared quantitatively to the adduct levels reported previously.

Besides the NAPQI-CPF adducts, very high levels of NAPQI-Cys and NAPQI-NAc adducts were found in the sera of all patients. These adducts probably originate either from the direct trapping of NAPQI by the antidote N-acetyl cysteine (NAc) and/or from the catabolism of corresponding GSH adducts [22, 33]. However, the fact that patient 440, who did not receive NAc, forms equal amounts of NAPQI-NAc suggests that the major amount may be derived from GSH adduct catabolism. The formation of the QCPF-NAc adduct can be explained by mixed disulfide formation between the cysteine thiol of HSA and NAc, as has been shown *in vivo* in the plasma of rats treated with NAc [34]. Because NAPQI is a strong oxidizing agent [20] and the formation of mixed disulfides is a known indicator of oxidation [35], the QCPF-NAc adduct could therefore be considered as a marker of oxidative stress. However, because human blood samples from patients exposed to NAc and not to APAP are not available, the precise impact of NAPQI on QCPF-NAc adduct formation could not be directly assessed.

From the present results it is clear that, although the doses of acetaminophen were extremely high, the levels of NAPQI-HSA adducts in the human samples were unexpectedly low. One explanation may be the extensive mixed disulfide formation due to the oxidative properties of NAPQI that may have prevented the formation of NAPQI-CPF adducts by blocking the free cysteine³⁴-thiol group of HSA. The fact that lower amounts of NAPQI-CPF adducts were observed in the blood of patient TOX

438, who ingested similar amounts of APAP than TOX 440 but was treated with NAc, might support this hypothesis. Another explanation is that alkylation is taking place to prealbumin in the liver and that the NAPQI-CPF adducts found in plasma result from the leakage of albumin adducts into the blood stream in cases of overt liver damage. This is consistent with the observation that much higher levels of NAPQI-CPF adducts were found in patient TOX 444, which showed high leakage of transaminases, in comparison to the adduct levels detected in patients TOX 438 and 440. Figure 8 summarizes the proposed interaction between NAPQI and the various trapping reactions involved.

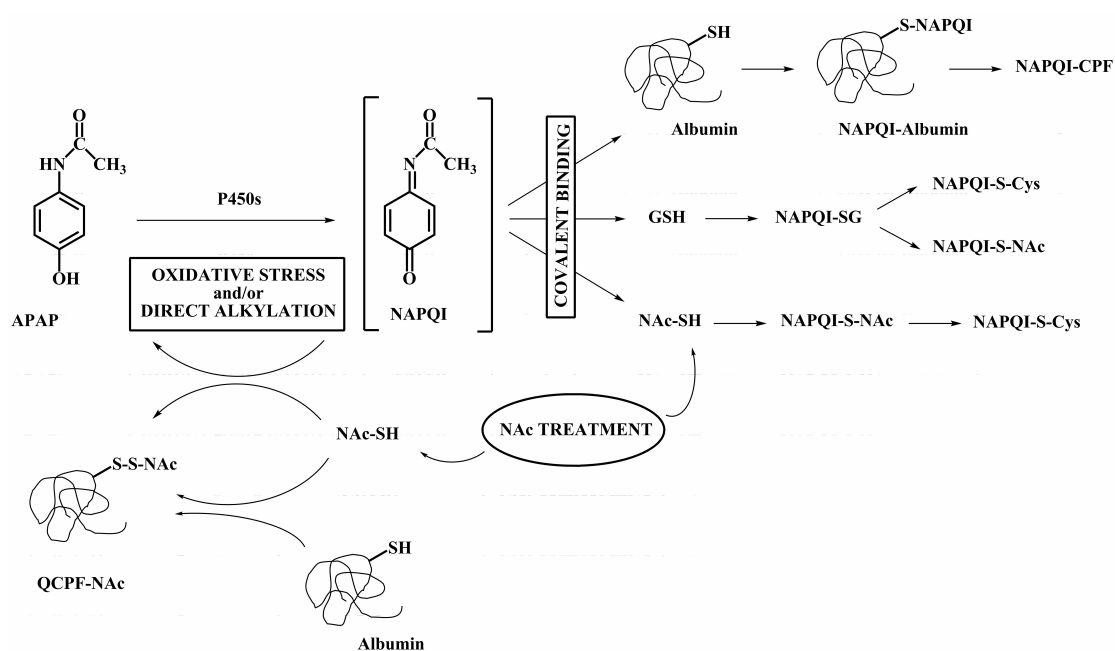


Figure 8. General scheme proposing the different trapping reactions involved in the formation of the adducts detected in the human serum samples.

Previous methods that have been used in order to investigate covalent binding of APAP to proteins *in vivo* include several immunoassays [36-39] and the use of radio-labeled APAP [19, 21, 28]. Still, these methods often lack the necessary sensitivity when concerning human serum samples [9]. More recently, a HPLC/electrochemical detection methodology was developed by Muldrew *et al.* [32] to quantify covalent protein binding of APAP. The methodology involves the dialysis of serum protein samples, subsequent digestion with protease, and the measurement of the NAPQI-Cys adducts formed. Although the sensitivity of the HPLC/electrochemical detection method was increased compared to the previously mentioned technologies, it remains a long and labor-intensive procedure. Comparatively, our LC-MS/MS methodology is quicker, sensitive, particularly selective and can provide precise structural information on the adducts formed to HSA as proven by the detection of two regioisomeric NAPQI adducts. This method also proved valuable to quantify the amounts of NAPQI-CPF adducts measured in the human serum samples. However, when the synthesis of the reference drug-CPF adduct is not possible, this methodology can already as such be applied for the retrospective and/or relative comparison of drug-albumin adduct levels between individuals. Eventually, the possibility of scanning for neutral losses corresponding to “non-drug related” fragments of drug-CPF adducts (e.g. the y_2 ” fragment corresponding to the PF part of the drug-CPF adduct) would allow the detection of novel, yet uncharacterized, drug-protein adducts.

In summary, we propose a generic strategy to assess the potential of drugs to be bioactivated to reactive electrophilic metabolites and to covalently bind to proteins *in vivo* (Figure 1). The strategy consists first in the biosynthesis of reference drug-albumin adducts for method development purposes. This biosynthetic approach is of particular importance because the synthesis of reactive metabolites of drugs is generally not feasible. Second, the developed analytical methodology is applied in the “*in vivo* approach” where serum samples of patients exposed to the drug are analyzed for the presence of similar albumin adducts. Smaller adducts, such as N-acetyl cysteine and cysteine adducts, can be measured as well hereby further confirming the bioactivation potential of the drug *in vivo*. While many adverse drug reactions seem not to be directly related to the concentration of the parent drug, it is likely that the onset of ADRs is related to the levels of reactive metabolites formed *in vivo*. Consequently, information on blood levels of “drug-protein adducts” will give an indication of the potential of a drug to be bioactivated to reactive electrophilic metabolites *in vivo*, and consequently on potential ADRs. Because of the fact that

HSA has a half-life of approximately 20 days, these drug-HSA adducts might accumulate in time. This could be of interest since IDRs usually have a delayed onset of occurrence and seem to take place essentially in patients taking a drug in relatively high doses, for a longer period of time. In this perspective, this strategy might also be seen as an *in vivo* dosimetry methodology to assess levels of covalent binding to proteins [40]. Consequently, this technology could constitute a potential biomonitoring tool that could improve the risk assessment of ADRs and IDRs of novel drugs and/or drug candidates.

References

- [1] Park, K., Williams, D. P., Naisbitt, D. J., Kitteringham, N. R. and Pirmohamed, M. (2005) Investigation of toxic metabolites during drug development. *Toxicol Appl Pharmacol.* 207, 425-434.
- [2] Smith, D. A. and Schmid, E. F. (2006) Drug withdrawals and the lessons within. *Curr Opin Drug Discov Devel.* 9, 38-46.
- [3] Williams, D. P., Kitteringham, N. R., Naisbitt, D. J., Pirmohamed, M., Smith, D. A. and Park, B. K. (2002) Are chemically reactive metabolites responsible for adverse reactions to drugs? *Curr Drug Metab.* 3, 351-366.
- [4] Evans, D. C., Watt, A. P., Nicoll-Griffith, D. A. and Baillie, T. A. (2004) Drug-protein adducts: an industry perspective on minimizing the potential for drug bioactivation in drug discovery and development. *Chem Res Toxicol.* 17, 3-16.
- [5] Zhou, S., Chan, E., Duan, W., Huang, M. and Chen, Y. Z. (2005) Drug bioactivation, covalent binding to target proteins and toxicity relevance. *Drug Metab Rev.* 37, 41-213.
- [6] Uetrecht, J. P. (1999) New concepts in immunology relevant to idiosyncratic drug reactions: the "danger hypothesis" and innate immune system. *Chem Res Toxicol.* 12, 387-395.
- [7] Park, B. K., Kitteringham, N. R., Powell, H. and Pirmohamed, M. (2000) Advances in molecular toxicology-towards understanding idiosyncratic drug toxicity. *Toxicology.* 153, 39-60.
- [8] Caldwell, G. W. and Yan, Z. (2006) Screening for reactive intermediates and toxicity assessment in drug discovery. *Curr Opin Drug Discov Devel.* 9, 47-60.
- [9] Zhou, S. (2003) Separation and detection methods for covalent drug-protein adducts. *J Chromatogr B Analyt Technol Biomed Life Sci.* 797, 63-90.
- [10] Olson, H., Betton, G., Robinson, D., Thomas, K., Monro, A., Kolaja, G., Lilly, P., Sanders, J., Sipes, G., Bracken, W., Dorato, M., Van Deun, K., Smith, P., Berger, B. and Heller, A. (2000) Concordance of the toxicity of pharmaceuticals in humans and in animals. *Regul Toxicol Pharmacol.* 32, 56-67.
- [11] Van Welie, R. T., Van Dijck, R. G., Vermeulen, N. P. and Van Sittert, N. J. (1992) Mercapturic acids, protein adducts, and DNA adducts as biomarkers of electrophilic chemicals. *Crit Rev Toxicol.* 22, 271-306.
- [12] Tornqvist, M., Fred, C., Haglund, J., Helleberg, H., Paulsson, B. and Rydberg, P. (2002) Protein adducts: quantitative and qualitative aspects of their formation, analysis and applications. *J Chromatogr B Analyt Technol Biomed Life Sci.* 778, 279-308.
- [13] Sherson, D., Sabro, P., Sigsgaard, T., Johansen, F. and Autrup, H. (1990) Biological monitoring of foundry workers exposed to polycyclic aromatic hydrocarbons. *Br J Ind Med.* 47, 448-453.
- [14] Wild, C. P., Jiang, Y. Z., Sabbioni, G., Chapot, B. and Montesano, R. (1990) Evaluation of methods for quantitation of aflatoxin-albumin adducts and their application to human exposure assessment. *Cancer Res.* 50, 245-251.
- [15] Rappaport, S. M., Waidyanatha, S., Yeowell-O'connell, K., Rothman, N., Smith, M. T., Zhang, L., Qu, Q., Shore, R., Li, G. and Yin, S. (2005) Protein adducts as biomarkers of human benzene metabolism. *Chem Biol Interact.* 153-154, 103-109.
- [16] Omland, O., Sherson, D., Hansen, A. M., Sigsgaard, T., Autrup, H. and Overgaard, E. (1994) Exposure of iron foundry workers to polycyclic aromatic hydrocarbons: benzo(a)pyrene-albumin adducts and 1-hydroxypyrene as biomarkers for exposure. *Occup Environ Med.* 51, 513-518.
- [17] Noort, D., Hulst, A. G., De Jong, L. P. and Benschop, H. P. (1999) Alkylation of human serum albumin by sulfur mustard in vitro and in vivo: mass spectrometric analysis of a cysteine adduct as a sensitive biomarker of exposure. *Chem Res Toxicol.* 12, 715-721.
- [18] Noort, D., Hulst, A. G. and Jansen, R. (2002) Covalent binding of nitrogen mustards to the cysteine-34 residue in human serum albumin. *Arch Toxicol.* 76, 83-88.
- [19] Zhou, L., McKenzie, B. A., Eccleston, E. D., Jr., Srivastava, S. P., Chen, N., Erickson, R. R. and Holtzman, J. L. (1996) The covalent binding of [¹⁴C]acetaminophen to mouse hepatic microsomal proteins: the specific binding to calreticulin and the two forms of the thiol:protein disulfide oxidoreductases. *Chem Res Toxicol.* 9, 1176-1182.
- [20] Gibson, J. D., Pumford, N. R., Samokyszyn, V. M. and Hinson, J. A. (1996) Mechanism of acetaminophen-induced hepatotoxicity: covalent binding versus oxidative stress. *Chem Res Toxicol.* 9, 580-585.
- [21] Qiu, Y., Benet, L. Z. and Burlingame, A. L. (1998) Identification of the hepatic protein targets of reactive metabolites of acetaminophen in vivo in mice using two-dimensional gel electrophoresis and mass spectrometry. *J Biol Chem.* 273, 17940-17953.
- [22] Bessems, J. G. and Vermeulen, N. P. (2001) Paracetamol (acetaminophen)-induced toxicity: molecular and biochemical mechanisms, analogues and protective approaches. *Crit Rev Toxicol.* 31, 55-138.

- [23] Rooseboom, M., Commandeur, J. N., Floor, G. C., Rettie, A. E. and Vermeulen, N. P. (2001) Selenoxidation by flavin-containing monooxygenases as a novel pathway for beta-elimination of selenocysteine Se-conjugates. *Chem Res Toxicol.* 14, 127-134.
- [24] Noort, D., Fidder, A., Hulst, A. G., Woolfitt, A. R., Ash, D. and Barr, J. R. (2004) Retrospective detection of exposure to sulfur mustard: improvements on an assay for liquid chromatography-tandem mass spectrometry analysis of albumin-sulfur mustard adducts. *J Anal Toxicol.* 28, 333-338.
- [25] Bessems, J. G., Te Koppele, J. M., Van Dijk, P. A., Van Stee, L. L., Commandeur, J. N. and Vermeulen, N. P. (1996) Rat liver microsomal cytochrome P450-dependent oxidation of 3,5-disubstituted analogues of paracetamol. *Xenobiotica.* 26, 647-666.
- [26] James, L. P., Mayeux, P. R. and Hinson, J. A. (2003) Acetaminophen-induced hepatotoxicity. *Drug Metab Dispos.* 31, 1499-1506.
- [27] Pumford, N. R., Halmes, N. C., Martin, B. M., Cook, R. J., Wagner, C. and Hinson, J. A. (1997) Covalent binding of acetaminophen to N-10-formyltetrahydrofolate dehydrogenase in mice. *J Pharmacol Exp Ther.* 280, 501-505.
- [28] Axworthy, D. B., Hoffmann, K. J., Streeter, A. J., Calleman, C. J., Pascoe, G. A. and Baillie, T. A. (1988) Covalent binding of acetaminophen to mouse hemoglobin. Identification of major and minor adducts formed in vivo and implications for the nature of the arylating metabolites. *Chem Biol Interact.* 68, 99-116.
- [29] Hoffmann, K. J., Streeter, A. J., Axworthy, D. B. and Baillie, T. A. (1985) Structural characterization of the major covalent adduct formed in vitro between acetaminophen and bovine serum albumin. *Chem Biol Interact.* 53, 155-172.
- [30] Chen, W., Shockcor, J. P., Tonge, R., Hunter, A., Gartner, C. and Nelson, S. D. (1999) Protein and nonprotein cysteinyl thiol modification by N-acetyl-p-benzoquinone imine via a novel ipso adduct. *Biochemistry.* 38, 8159-8166.
- [31] James, L. P., Alonso, E. M., Hynan, L. S., Hinson, J. A., Davern, T. J., Lee, W. M. and Squires, R. H. (2006) Detection of acetaminophen protein adducts in children with acute liver failure of indeterminate cause. *Pediatrics.* 118, e676-681.
- [32] Muldrew, K. L., James, L. P., Coop, L., Mccullough, S. S., Hendrickson, H. P., Hinson, J. A. and Mayeux, P. R. (2002) Determination of acetaminophen-protein adducts in mouse liver and serum and human serum after hepatotoxic doses of acetaminophen using high-performance liquid chromatography with electrochemical detection. *Drug Metab Dispos.* 30, 446-451.
- [33] Commandeur, J. N., Stijntjes, G. J. and Vermeulen, N. P. (1995) Enzymes and transport systems involved in the formation and disposition of glutathione S-conjugates. Role in bioactivation and detoxication mechanisms of xenobiotics. *Pharmacol Rev.* 47, 271-330.
- [34] Harada, D., Naito, S. and Otagiri, M. (2002) Kinetic analysis of covalent binding between N-acetyl-L-cysteine and albumin through the formation of mixed disulfides in human and rat serum in vitro. *Pharm Res.* 19, 1648-1654.
- [35] Eaton, P. (2006) Protein thiol oxidation in health and disease: techniques for measuring disulfides and related modifications in complex protein mixtures. *Free Radic Biol Med.* 40, 1889-1899.
- [36] Roberts, D. W., Pumford, N. R., Potter, D. W., Benson, R. W. and Hinson, J. A. (1987) A sensitive immunochemical assay for acetaminophen-protein adducts. *J Pharmacol Exp Ther.* 241, 527-533.
- [37] Bartolone, J. B., Birge, R. B., Sparks, K., Cohen, S. D. and Khairallah, E. A. (1988) Immunochemical analysis of acetaminophen covalent binding to proteins. Partial characterization of the major acetaminophen-binding liver proteins. *Biochem Pharmacol.* 37, 4763-4774.
- [38] Matthews, A. M., Roberts, D. W., Hinson, J. A. and Pumford, N. R. (1996) Acetaminophen-induced hepatotoxicity. Analysis of total covalent binding vs. specific binding to cysteine. *Drug Metab Dispos.* 24, 1192-1196.
- [39] James, L. P., Farrar, H. C., Sullivan, J. E., Givens, T. G., Kearns, G. L., Wasserman, G. S., Walson, P. D., Hinson, J. A. and Pumford, N. R. (2001) Measurement of acetaminophen-protein adducts in children and adolescents with acetaminophen overdoses. *J Clin Pharmacol.* 41, 846-851.
- [40] Yang, X. X., Hu, Z. P., Chan, S. Y. and Zhou, S. F. (2006) Monitoring drug-protein interaction. *Clin Chim Acta.* 365, 9-29.

Chapter 6

Automated detection of covalent adducts to human serum albumin by immunoaffinity chromatography, on-line solution phase digestion and liquid chromatography-mass spectrometry

Adapted from: Johannes S. Hoos^{*}, Micaela C. Damsten^{*}, Jon S. de Vlieger, Jan N.M. Commandeur, Nico P.E. Vermeulen, Wilfried M. Niessen, Henk Lingeman and Hubertus Irth.
Automated detection of covalent adducts to human serum albumin by immunoaffinity chromatography, on-line solution phase digestion and liquid chromatography–mass spectrometry.
Journal of Chromatography B, 2007, 859 (2), Nov 15; p: 147-56.

^{*} Both authors contributed equally to this work.

Abstract

A generic method for the detection of covalent adducts to the cysteine³⁴ residue of human serum albumin (HSA) has been developed, based on an on-line combination of immunoaffinity chromatography for selective sample pre-treatment, solution phase digestion, liquid chromatography and tandem mass spectrometry. Selective anti-HSA antibodies immobilized on agarose were used for sample pre-concentration and purification of albumin from the chemically produced alkylated HSA. After elution, HSA and HSA adducts are mixed with pronase and directed to a reaction capillary kept at a digestion temperature of 70°C. The digestion products were trapped on-line on a C18 SPE cartridge. The peptides were separated on a reversed-phase column using a gradient of organic modifier and subsequently detected using tandem mass spectrometry. Modified albumin samples consisted of synthetically alkylated HSA by the reactive metabolite of acetaminophen, N-acetyl-p-benzoquinoneimine (NAPQI), and using the alkylating agent 1-chloro-2,4-dinitrobenzene (CDNB) as reference. The resulting mixture of alkylated vs non-modified albumin has been applied to the on-line system, and alkylation of HSA is revealed by the detection of the modified marker tetrapeptide Glutamine-Cysteine-Proline-Phenylalanine (QCPF) adducts NAPQI-QCPF and CDNB-QCPF. Detection of alkylated species was enabled by the use of data comparison algorithms to distinguish between unmodified and modified HSA samples. The in-solution digestion proved to be a useful tool for enabling fast (less than 2 minutes) and reproducible on-line digestion of HSA. A detection limit of 1.5 µmol/l of modified HSA could be obtained by applying 10 µl of NAPQI-HSA sample.

Introduction

Covalent binding of reactive electrophilic metabolites of drugs to proteins has been suggested to be involved in the onset of serious adverse drug reactions (ADRs) and idiosyncratic drug reactions (IDRs) in humans [1]. Therefore, methods that can detect covalent adducts to proteins are of great interest for risk assessment purposes, e.g. during the development of novel drugs and/or drug candidates [2, 3]. Several methodologies exist for the quantitative and qualitative analysis of protein adducts [4]. Briefly, these methods consist first in the isolation of protein adducts with chromatographic and/or electrophoretic techniques (e.g. immunoaffinity chromatography, ion-exchange chromatography or HPLC), and the subsequent adduct analysis using immunological, radioactivity and/or mass spectrometry methodologies [5]. Although successful to some extent, these techniques usually remain labor-intensive and none of these answer the need for automated on-line isolation and detection of protein adducts.

Recently, we have described a concept where human serum albumin (HSA) is used as an *in vivo* biomarker for bioactivation of drugs towards reactive intermediates and for covalent binding to proteins [6]. The methodology consists of the isolation of albumin from blood, its digestion with pronase and the LC-Tandem MS detection of alkylated and/or unalkylated peptides containing the free cysteine³⁴ residue of HSA. This site is the only free cysteine residue of albumin and has already been shown to be alkylated by several electrophilic compounds [7-12].

In the present paper we demonstrate the full automation of the mass spectrometric detection of covalent adducts to the cysteine³⁴ residue of HSA, integrating several sample pre-treatment and separation steps. First, immunoaffinity chromatography (IAC) was performed for selective purification of albumin from the alkylated HSA samples using specific antibodies against human serum albumin. The modified and non-alkylated albumin was retained and concentrated by immobilized antibodies while matrix components (i.e. remains from the alkylation reaction) can be flushed to waste. Purified albumin was subsequently eluted using a low pH buffer and further digested using pronase which is known to form small peptides containing the cysteine³⁴ residue of HSA [6]. In this way, adducts to cysteine³⁴ could be monitored by LC-MS analysis on relatively small peptides. Pronase consists of a mixture of different enzymes, and cleaves in a relatively non-specific way compared to trypsin, chymotrypsin and pepsin. Recently, on-line digestion using immobilized enzyme

reactors (IMERs) has been reported in various research areas [13-16] and trypsin is most frequently applied for proteolysis. Developments and applications of IMERs immobilized with trypsin have been reviewed by Massolini *et al.* [17]. Using IMERs is a very elegant way to perform on-line digestion; the reactors are relatively stable and re-useable when used under suitable conditions. Although the first application of a pronase immobilized IMER has been shown recently by Temporini *et al.* [18], their applicability is limited by the ability to immobilize the proteolytic enzyme without affecting its activity. Furthermore, the validation and characterization of IMERs prior to application in quantitative protein bioanalysis is a delicate task. In the present paper, we report the use of an on-line, pre-column solution-phase digestion method that overcomes the need for immobilization. Recently, a comparable approach has been utilized in our group to perform in-flow digestion using pepsin for post-column digestion of protein mixtures [19]. We have integrated the solution-phase digestion module in an automated methodology that allows the detection of NAPQI-QCPF and CDNB-QCPF, i.e. two peptide-adducts formed after pronase digestions of HSA that previously was incubated with the chemically-produced reactive metabolite of acetaminophen (NAPQI) and with the direct alkylating agent CDNB (1-chloro-2,4-dinitrobenzene).

Material and Methods

Reagents

Sodium di-hydrogen phosphate, glycine hydrochloride, silver nitrate, human serum albumin, 1-chloro-2,4-dinitrobenzene, Tris base, Tris hydrochloride and pronase (protease type XIV from *Streptomyces griseus*, EC 3.4.24.31) were purchased from Sigma (Germany). Activity of the enzyme was 5.2 units per mg solid (units in amount of enzyme activity which will catalyze the transformation of 1 μ mole of the substrate per minute under conditions given by the supplier). Disodium hydrogenphosphate was obtained from Fluka (Buchs, Switzerland) and sodium chloride and formic acid came from Riedel-de-Haën (Seelze, Germany). Acetonitrile, acetone, diethyl ether, chloroform, potassium chloride and hydrochloric acid (36-38%) were supplied by J.T. Baker (Deventer, The Netherlands). Water was purified by a Millipore (Bedford, MA, USA) Milli-Q unit. Sodium hydroxide was obtained from Merck (Darmstadt, Germany). A 2 liters stock of a 10-fold concentrated PBS buffer was made by dissolving 57.30 g of $\text{Na}_2\text{HPO}_4 \cdot 12\text{H}_2\text{O}$, 137.99 g of NaH_2PO_4 , 175.30 g NaCl and 4.03 g KCl in 2 liters of water. This stock was used to prepare the PBS by diluting 100 ml of the concentrate with 900 ml of water. The resulting PBS buffer consists of

10 mM sodium phosphate, 150 mM sodium chloride and 3.4 mM potassium chloride. The pH was set to the required value with 8 M sodium hydroxide or hydrochloric acid.

Synthesis of albumin adducts

A general scheme of the synthesis of the reactive intermediate of acetaminophen (APAP), N-acetyl-p-benzoquinoneimine (NAPQI), and of the formation of NAPQI-HSA adducts is depicted in Figure 1A. For the formation of NAPQI, fresh silver oxide was synthesized as follows [20]. While stirring, 50 ml of a 2 M sodium hydroxide solution was added to 12.5 ml of a 0.4 M silver nitrate solution. The reaction mixture was kept on ice and stirred for 30 minutes. Isolation of silver oxide was performed by filtration over a Büchner funnel and the product was subsequently washed with 60 ml water, 60 ml acetone and 60 ml diethyl ether. The freshly prepared silver oxide was added to 10 ml of a 6.6 mM acetaminophen solution in chloroform and purged with nitrogen. The glass vial was sealed and the solution was stirred for 1.5 hour at room temperature. After filtration of the mixture, 4 ml of the yellowish NAPQI solution was added drop wise under stirring to 5 ml of HSA (2.5 mg/ml) in PBS (pH 7.4). This mixture was stirred for 1 hour at room temperature. The layers were allowed to settle for 10 minutes and the water layer containing NAPQI-HSA was stored at -80°C until further analysis.

As NAPQI can also react with other nucleophilic residues of HSA (e.g. lysines and histidines), the degree of alkylation of the free cysteine³⁴ residue of NAPQI-HSA was assessed. Two HSA syntheses were performed in parallel as described above; one HSA solution (2.5 mg/ml) was reacted with 4 ml of NAPQI (in chloroform) and one HSA solution (2.5 mg/ml) with 4 ml of chloroform. After 1 hour of reaction, water layers were isolated and free thiols were determined using a modification of Ellman's method [21]. Ellman reagent consisted in 10 mM DTNB in buffer 7.0 (100 mM NaH₂PO₄ containing 0.2 mM EDTA, adjusted to pH 7). Briefly, HSA samples were prepared in PBS (137 mM NaCl, 10.1 mM Na₂HPO₄, 1.76 mM KH₂PO₄ and 1 mM EDTA, adjusted to pH 7.4) by mixing 1000, 800, 600, 400, 200 and 0 µl of the HSA syntheses with PBS to a final volume of 1000 µl. Then, 200 µl of a strong buffer (100 mM boric acid and 0.2 mM EDTA, adjusted to pH 8.2 with NaOH) and 20 µl of Ellman reagent were added to each HSA sample. The mixtures were immediately vortexed, incubated for 15 minutes at room temperature and the absorbance was read at 412 nm (A_s) on a Pharmacia Biotech Ultrospec 2000 UV/Vis spectrophotometer. Control incubations consisted of incubations performed without HSA sample (A_p) and/or

without Ellman reagent (A_{er}). The amounts of free thiols in the samples were determined according to equation 1 [21]:

$$\text{Mol SH} = 0.00122 \text{ L} \times (A_s - A_p - A_{er}) / (\Delta\epsilon_{412} \times 1 \text{ cm}) \quad (1)$$

$$\text{with } \Delta\epsilon_{412} = 14150 \text{ M}^{-1} \text{ cm}^{-1}$$

All measurements were performed in triplicate.

It was found that both HSA ($Abs = 0.0562 \times [\text{HSA}]$ (in mg/ml)) and NAPQI-HSA samples ($Abs = 0.0041 \times [\text{HSA}]$ (in mg/ml)) gave a linear response in the dilution series described above (data not shown). Standard deviations were consistently below 1.5% absorbance units. From equation (1), the free thiol concentration measured in the HSA sample was determined to be 0.32 ± 0.002 mol SH/mol HSA, which is in agreement with previous data from literature [22]. The degree of alkylation of the cysteine³⁴ residues of NAPQI-HSA was determined with the ratio of the slopes of HSA versus NAPQI-HSA. Consequently, it was found that NAPQI-HSA contained approximately 7.3% of free thiols compared to the HSA sample, which was set to 100% as reference. This suggests that more than 90% of the cysteine³⁴ residues of HSA have been alkylated by NAPQI and that the NAPQI-HSA synthesis can be considered as complete.

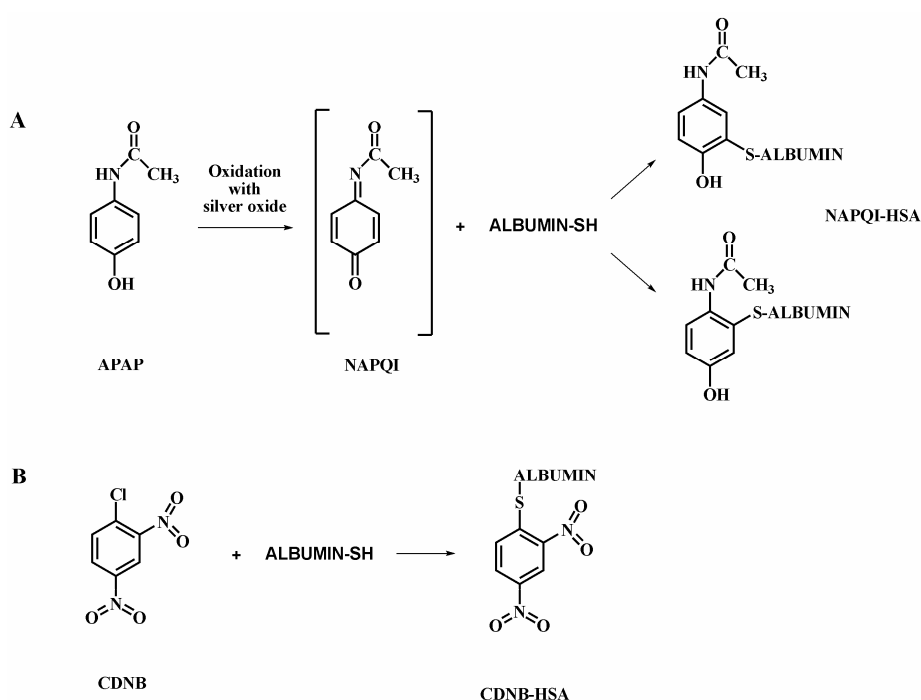


Figure 1. Synthesis of HSA protein adducts. (A) Synthesis of NAPQI-HSA protein adduct: APAP is oxidized by silver oxide to the reactive NAPQI intermediate which can subsequently react with the free cysteine³⁴ residue of HSA to form two possible adduct isomers. (B) Synthesis of CDNB-HSA protein adduct: CDNB reacts with the free cysteine³⁴ residue of HSA to form the CDNB-HSA adduct.

The CDNB-HSA adduct was produced by reacting HSA with the direct alkylating agent 1-chloro-2,4-dinitrobenzene (CDNB). The reaction scheme is shown in Figure 1B. Briefly, a total 80 μ l of a 100 mM CDNB solution in methanol was added drop wise under continuous stirring to 1 ml of a 5 mg/ml solution of HSA in 100 mM Tris buffer (pH 8.0). The mixture was allowed to react for 4 hours at 40°C. The obtained yellowish solution was subsequently stored at -80°C until further analysis.

Columns

The immunoaffinity chromatography column was produced in-house (1.0 mm x 15 mm I.D., peek material). Column frits were purchased from VICI AG international (peek alloyed with Teflon, PAT, 1/32" thick x 1/16" diameter, porosity 5 μ m). Immunoaffinity material was used from the HSA removal kit purchased from Vivascience (Sartorius, Goettingen, Germany). This kit includes agarose slurry containing immobilized antibody fractions for specific removal of albumin from biological samples. The material (particle size, 45-185 μ m) was used for on-line sample pre-treatment in this research. The column was filled with the anti-HSA agarose slurry using an in-house built packing device, which allows packing under low-pressure conditions. This packing device consisted of a column holder and a connector fitting with a common luer tip connection. Before packing, the column was closed on one end with a PAT frit. The column was packed with the slurry using a 1 ml syringe and the excess of material was carefully removed. The column was closed using a second PAT frit, and subsequently placed into an in-house built column holder. The column was flushed with PBS (pH 7.4) for 20 minutes at a flow rate of 0.040 ml/min. The SPE cartridge (C18, 5 μ m particles, 2.0 mm x 4.0 mm I.D.), used for pre-concentration and desalination, and the analytical column (Luna C18 (2), 5 μ m particles, 2.0 x 150 mm I.D.) were both supplied by Phenomenex (Torrance, CA, USA).

Apparatus

IAC was performed with a binary pump (Agilent, Amstelveen, The Netherlands) in combination with a MUST multiport switch from Spark Holland (Emmen, The Netherlands) which was triggered using a contact closure of the same Agilent binary pump. Elution was done using a Gilson 302 (Middleton, WI, USA) pump and enzyme solution was delivered by a Knauer (Berlin, Germany) pump. Injection was done by a temperature controllable autoinjector from Agilent which was kept at 8°C. Continuous flow digestion was performed by using an in-house built tee-piece infusing both elution solution and pronase solution into a reaction capillary (PEEK,

polyetheretherketone) with an I.D. of 0.50 mm and an inner volume of 140 μl and was supplied by Bester BV (Amstelveen, The Netherlands). The reaction capillary was kept inside a column oven to control the digestion reaction temperature. Analysis of the reaction mixture was performed by switching the reaction capillary in-line with a SPE cartridge which was equilibrated by a second Agilent 1100 (Amstelveen, The Netherlands) micro flow pump. This pump also performed separation of the digest products including a gradient over an analytical column, which was switched in-line with the SPE column after desalination. Both the latter switching events were operated by two temperature controlled column switches from Agilent. All Agilent apparatus were controlled by Chemstation version 10.02, and analysis was done by an Agilent 1100 MSD VL-series ion-trap. Positive ESI LC-MS was performed in full-spectrum acquisition mode in the range of m/z 200-1000. For identification purposes, tandem MS or MS^n experiments were performed using the smart-frag option. The spray voltage was set at 4.5 kV with a drying temperature of 350°C, nitrogen drying gas flow at 8 l/min and nebulizer pressure at 40 psi. The maximum accumulation time was 100 ms and the ICC target was set to 30.000, two spectra were averaged. Data processing was performed using LC-MSD trap software version 5.2, build 382 or ACD/SpecManager software version 9.15. Extracted ion chromatograms were generated for relevant m/z values and the peaks were integrated.

System set-up

Off-line digestion procedure

The pronase digestion of NAPQI-HSA was first evaluated by performing off-line batch experiments. The digestion products were analyzed and characterized by MS^2 experiments on the SPE-LC-MS system. This was done by addition of 10 μl of a pronase solution (1 mg/ml in PBS, pH 7.4) to a sample of 1000 μl containing 100 $\mu\text{g/ml}$ of NAPQI adducted albumin in PBS, pH 7.4. The mixture was immediately incubated at 37°C in a water bath and incubated for 8 hours. After this, 20 μl of the reacted sample was injected onto a SPE-LC-MS system consisting of a gradient pump, a conditioning pump and a switching valve. The sample was injected onto the SPE cartridge and desalinated for 5 minutes using the equilibration solution (99.3% water, 0.5% acetonitrile and 0.2% of formic acid). The analytical C18 column was switched in-line by switching the valve. A gradient was run from 0% of the equilibration solution up to 40% of the elution solution (99.3% acetonitrile, 0.5% water and 0.2% formic acid) within 20 minutes. After this, the column was flushed by applying 80% of this elution solution for 2 minutes. After the sample valve was switched back, both columns were reconditioned for the next run. The analytical

column was reconditioned by a Gilson 302 pump. The flow rate of both pumps was set to 0.2 ml/min, and total run-time including the reconditioning step was 35 minutes. Full scan mass spectrometric analysis was done using an m/z range between 100 and 1000 unless mentioned otherwise. MS^2 and MS^3 experiments were performed with the isolation window set to 4.0 and product ions were scanned in a range between m/z values 100 and 750.

Immunoaffinity chromatography procedure

The capacity of the IAC column was estimated by a method which has been previously published [23]. A 1 mg/ml solution of HSA was made in PBS (pH 7.4) solution. Different amounts of protein were applied by injecting an increasing volume of this solution onto the column using an Agilent 1100 autoinjector. The IAC was operated at a flow rate of 0.040 ml/min using PBS (pH 7.4). After 5 minutes, the column was flushed with 0.400 ml of 0.15 M NaCl to flush matrix components to waste. The elution of the protein was performed for 10 minutes using 10 mM glycine-HCl containing 150 mM NaCl (pH 2.7). The effluent was directed towards an Agilent 1100 series UV/VIS spectrometer and detection was done by using UV detection at 280 nm. The elution peak was integrated and the data were evaluated as reported in previous work.

On-line system

A detailed scheme of the entire on-line set-up is depicted in Figure 2 and a table with the detailed chromatographic conditions of the entire analytical process can be found in Table 1.

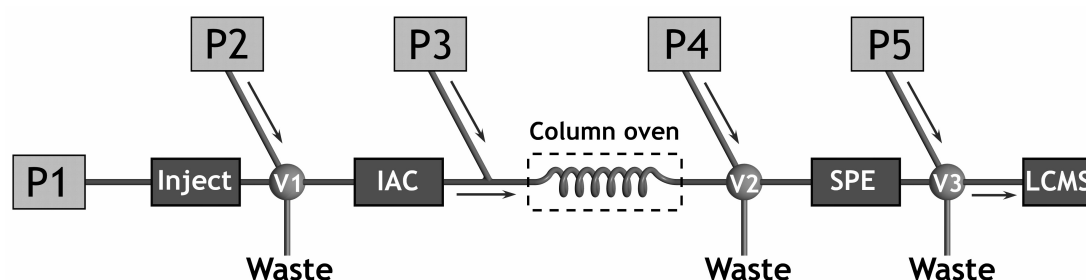


Figure 2. Scheme of the on-line setup used for this research. Protein is injected onto immunoaffinity chromatography (IAC) column by pump 1 (P1). Pump 2 (P2) elutes the protein by switching valve 1 (V1). Pump 3 (P3) adds protease in solution. The digested product is captured on a solid phase extraction (SPE) cartridge by switching valve 2 (V2). Pump 4 (P4) desalinates the trapped peptides and elutes the peptides over the liquid chromatography–mass spectrometry (LC-MS) system by switching valve 3 (V3). Pump 5 (P5) equilibrates the LC-MS system.

Table 1. Table with the detailed chromatographic conditions of the entire analytical process.

time (min)	IAC action	SPE action	LC-MS action
0-5	Sample application		
5-15	flushing		
15-25	elution		
18-23	elution	capturing	
23-26		flushing	
26-42		Gradient	Gradient
42-44		Flushing	Flushing

The IAC column was operated by pump 1 (P1) at a flow rate of 0.040 ml/min. This column was conditioned using PBS (pH 7.4). Albumin samples were introduced by the injector and the sample was delivered by pump 1 (P1) using PBS (pH 7.4). After 5 minutes, the column was flushed with 0.400 ml of a 0.15 M NaCl solution to remove matrix components to waste. After this, the protein was eluted from the column by switching valve 1 (V1) to pump 2 (P2) for 10 minutes with a solution of 10 mM glycine-HCl containing 150 mM of NaCl (pH 2.7). The protein fraction eluting between 17 and 21 minutes was delivered to the SPE cartridge via the reaction capillary. A UV chromatogram of the IAC procedure can be found in Figure 3. In the reaction capillary, the eluate from the IAC column was allowed to react with pronase dissolved in a PBS (pH 10.8) solution, delivered by pump 3 (P3, Figure 2) at a flow rate of 0.040 ml/min. Compatibility of the elution conditions using low pH with the on-line solution phase digestion was achieved by neutralizing the elution fraction by mixing the effluents from the immunoaffinity chromatography column continuously with pronase solution in PBS at a pH of 10.8. The resulting pH will be between pH 6 and 8, which is compatible with the pH optimum for the pronase activity. The digestion temperature was controlled by using the temperature controlled column switch, which also delivered the digested eluate from the IAC column to the SPE column by switching valve 2 (V2). When the protein was eluted, valve 1 (V1) was switched back and the IAC column was equilibrated for analysis of the next sample. When the digested protein effluent was delivered to the SPE cartridge via the reaction capillary, valve 2 (V2) was switched back and solvent delivered by gradient pump 4 (P4) desalinated the captured effluent for 3 minutes using a solvent consisting of 99.3% water, 0.5% acetonitrile and 0.2% of formic acid at a flow rate of 0.2 ml/min. After desalination, valve 3 (V3) was switched and a gradient was run to 50% within 16 minutes using a second solution consisting of 99.3% acetonitrile, 0.5%

water and 0.2% formic acid to separate the digest products from the originally captured protein. The columns were washed with 80% of the elution solution for 2 minutes, and subsequently the analytical column was re-equilibrated by pump 5 (P5) after switching back valve 3 (V3) using 99.3% water, 0.5% acetonitrile and 0.2% formic acid. The total run-time was 44 minutes. During separation of the digest products and re-equilibration of the SPE cartridge, the next sample could already be applied onto the immunoaffinity column. Hereby, the overall run-time could be reduced to 25 minutes, in principle enabling a sample throughput of almost 60 samples per day.

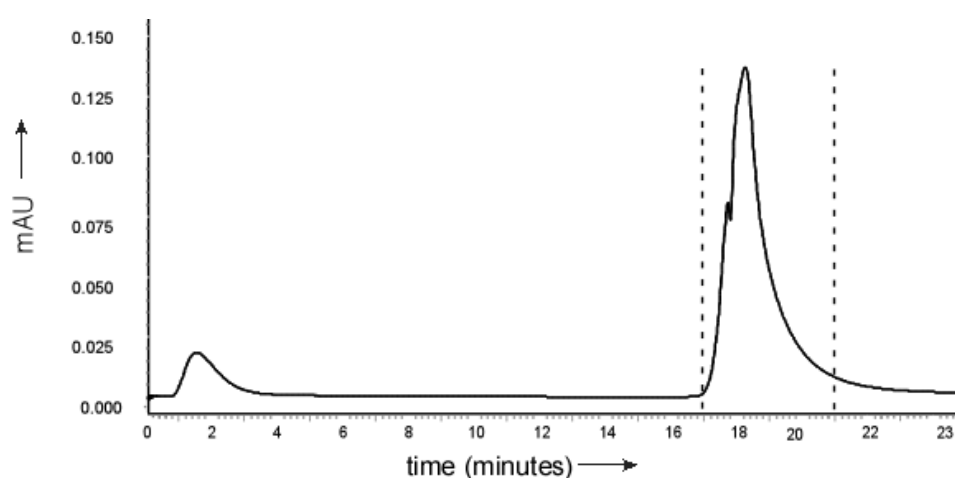


Figure 3. UV (280nm) monitoring of the immunoaffinity chromatography procedure. The elution peak (between dashed lines) is directed towards the on-line solution phase digestion procedure.

On-line digestion procedure optimization

For the evaluation of the continuous flow digestion procedure, protein was injected into the previously described system whereas the concentration of pronase in the delivered solution (P3, Figure 2) and the temperature of the reaction capillary were varied. Both the concentration of the protease as well as the thermal denaturation of albumin are important factors in protein digestion, as has been studied by Picó *et al.* [24]. The reaction time was kept constant at 1.75 minutes.

Chromatogram evaluation

Software assisted data comparison of chromatograms was done in the ACD/Specmanager software package as follows. The Agilent chemstation file (*.d) file was exported to netCDF file format (*.cdf). As a result, the mass spectral data are automatically converted to centroided mass spectra. The chromatograms were

imported to the software and the chromatograms were processed using the COMPARE algorithm. Data processing accuracy was set to 0.1, other settings were set to default. The program picks the differences between the chromatograms and highlights these in reconstructed extracted ion chromatograms.

Results and Discussion

The analytical system for the on-line detection of covalent adducts to human serum albumin comprises several pre-column steps, including immunoaffinity purification, solution phase on-line digestion, and C18 solid phase extraction with the subsequent determination of peptide adducts using liquid chromatography-mass spectrometry. During method development main attention was paid to achieve compatibility of the optimum conditions of the different steps.

Identification of NAPQI-peptide adducts

The pronase digestion of NAPQI-HSA was first studied by performing in-batch off-line digestion experiments. In principle, adduct formation by NAPQI results in a mass shift of 149.1 Dalton. Since NAPQI is known to be reactive towards the cysteine³⁴ residue of HSA, the full scan MS chromatogram was screened for peptides containing that cysteine residue with an m/z value shifted by 149.1 Dalton. A series of peptides containing this cysteine³⁴ residue has already been published [9]. The analyzed NAPQI-HSA and unmodified HSA digest sample traces were compared using ACD/SpecManager. Two peaks of m/z 643.3 corresponding to the m/z of NAPQI-glutamine-cysteine-proline-phenylalanine (NAPQI-QCPF) were found in the NAPQI-HSA sample and were not present in the unmodified HSA sample. Figure 4A shows an extracted ion chromatogram from a NAPQI-HSA digest at m/z 643.3. MS² experiments were subsequently performed on the ion at m/z 643.3 and the identity of the NAPQI-QCPF adducts could be confirmed (Figure 4B). Both compounds show almost identical product-ion mass spectra in MS² and MS³ experiments. This suggests the formation of two NAPQI-QCPF isomers. The two adduct isomers may result from two different reactions of NAPQI with the cysteine³⁴ group in HSA, either through electrophilic addition of thiolate to the carbonyl-carbon to yield a thio-hemiketal intermediate or by nucleophilic addition to the imine-carbon via an ipso intermediate [25]. Both structures may fragment to a product ion with m/z 208 forming the isomeric structures (1,4-benzothiazine and 1,4-benzooxathiine derivatives). Since it is not possible to distinguish between these isomeric structures in MS² mode, further attempts were done to assign the resulting spectra. MS³

fragmentation of both ions with m/z 208 yield fragment ions with m/z 166, due to the loss of $\text{H}_2\text{C}=\text{C}=\text{O}$ from the acetyl group. Although the results of the MS^2 and MS^3 experiments support the theory of isomer formation, further experiments especially including NMR have to be performed to confirm this phenomenon.

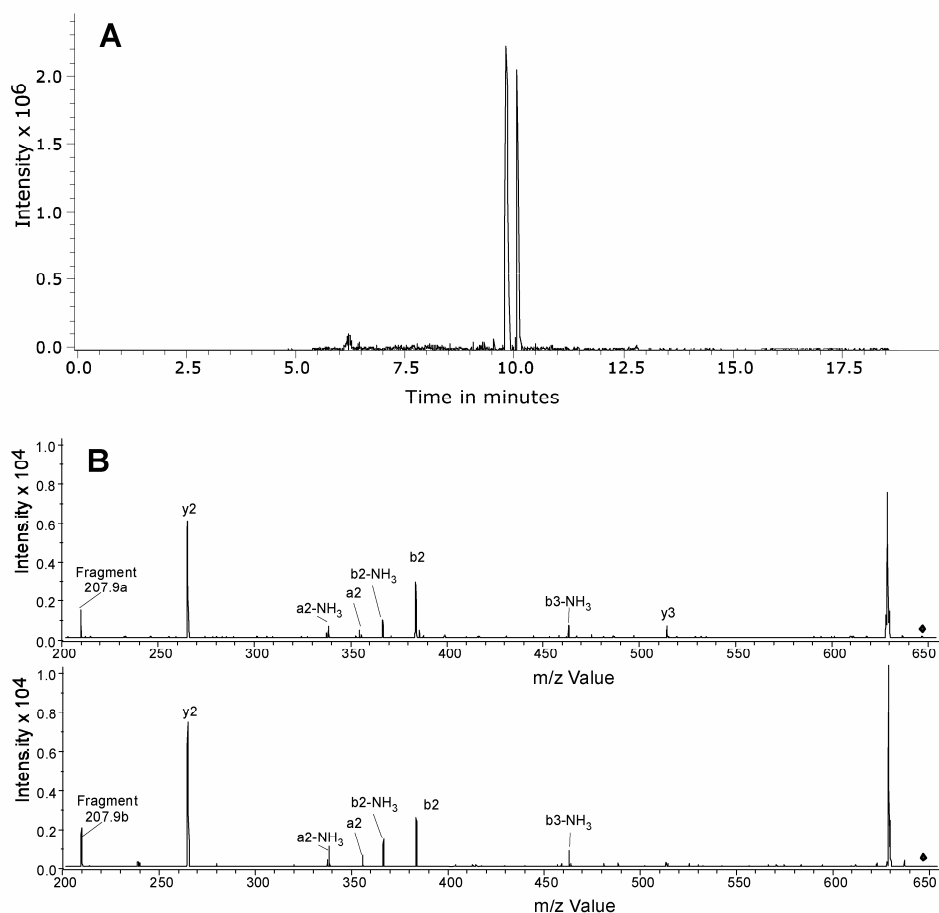


Figure 4. Analysis of NAPQI-HSA: (A) Reconstructed extracted ion chromatogram of the NAPQI-QCPF adducts ($[\text{M}+\text{H}]^+$; m/z 643.3) in a pronase digest of NAPQI-HSA and (B) Tandem MS product ion spectra of m/z 643.3 of the first peak (upper) and of the second peak (lower).

Immunoaffinity chromatography

An UV chromatogram of the IAC procedure can be found in Figure 3. The effluent from the IAC column was continuously delivered via the in-solution digestion reaction capillary. There was no need to pre-select the protein fraction from the IAC procedure for digestion since the effluent (both matrix components and purified protein) is continuously mixed with fresh enzyme. The eluting albumin fraction from the IAC column (between dashed lines) has been heart-cut towards the SPE cartridge via the reaction capillary by switching valve 2 (V2) (Figure 2) for subsequent

separation and analysis. The capacity of the IAC column is an important issue for the sample purification step. By means of a binding capacity curve [23], it was found that the capacity (390 pmol or 26 μg HSA) of the IAC column (inner volume of 12 μl) is in accordance with the specifications given by the supplier (2 mg/ml). Although a fixed sample volume with increasing sample concentrations would be analytically more appropriate, the use of a varying sample volume has not been of concern in our previous project [23]. Therefore, this approach has been used for the estimation of column capacity. By this experiment, the application in an on-line format could be realized. If a higher column capacity is needed, other column dimensions might be considered, e.g. by increasing the I.D. from 1 mm to 3 mm, enhancing the total capacity about 10-fold for both modified and unmodified HSA.

To assure that matrix components can be successfully removed at chosen conditions, a solution of Myoglobine has been injected and analyzed (data not shown). For this, 50 μl of a solution of PBS (pH 7.4) containing 1 mg/ml myoglobine has been injected onto the anti-HSA immunoaffinity column. Apart from the breakthrough of myoglobine from the anti-HSA immunoaffinity column, the elution profile did not differ from a blank (PBS, pH 7.4) injection. This indicates that proteins, which are not supposed to bind to the material, are successfully removed during the flushing process using 0.15 M NaCl.

Another important aspect is the immunoaffinity of the immobilized antibodies towards modified proteins. In order to prove that modified HSA binds to the immobilized anti-HSA antibodies, the following experiments were performed. First, a number of native (unmodified) peptides from HSA were identified using the complete on-line system (IAC, solution phase digestion, LC and MS). The mass spectrometer was set to full scan mode. 30 μl of a blank (PBS, pH 7.4) and HSA sample (0.1 mg/ml in PBS, pH 7.4) were injected and the results were compared. Since pronase generates significant background signals, comparison was performed with help of the ACD/SpecManager as described in the "Materials and Methods" section. Using ACD/SpecManager we were able to search for specific differences between blank samples (i.e., without HSA) with a rather high background and samples containing low abundant HSA within this background. The m/z signals with the highest intensity (those which were not present in the blank chromatogram) were selected for further MS/MS experiments. From the most intense m/z values, two peptides could be easily identified as native HSA peptides, i.e. VLIAF and DEFKPL. No further attempts were done to identify other peptides. The peptide DEFKPL (m/z 748.4) is present in

modified as well as in the unmodified HSA and will therefore be used as marker for human serum albumin. The MS was subsequently set to the Selected Reaction Monitoring (SRM) mode and continuous MS/MS was done on precursors 643.3 and 748.4, both with an isolation width of 4.0. After the analysis, an extracted ion chromatogram of the identified product ion traces of the modified peptide and the unmodified peptide were generated. 10 μ l of a 1 mg/ml solution of modified HSA was injected on the system. After a sample of NAPQI modified HSA was analyzed, the sample was spiked in a 1:1 ratio with unmodified HSA (1 mg/ml in PBS; pH 7.4). From this mixture also 10 μ l were injected and the same product ion traces were summed for a reconstructed chromatogram. The peaks of both experiments were integrated and the results are shown in Table 2. The first line represents only the modified protein and the second line the modified and unmodified protein mixed in a 1:1 ratio. The same sample volume was injected. The area of the unmodified peptide marker is consistent with the area of the previously analyzed sample and the control sample since the same amount of peptide marker can be produced whereas the amount of modified peptide was reduced by 50% as half of the amount was injected compared to the first experiment. In the unmodified HSA sample, no NAPQI modified peptide could be found. From these results it can be concluded that NAPQI-HSA was not displaced from the immunoaffinity column by native HSA, since the area of the native HSA marker peptide remained the same whereas the peak area of the modified peptide was reduced by approximately 50%. This indicates that it is possible to extract both the modified and the unmodified HSA using the anti-HSA immunoaffinity support. Although this experiment indicates sufficient affinity for both protein species, a dilution series will have to be considered for biological samples containing an excess of non-modified albumin. This is important to assure full recovery of (very) low levels of modified albumin.

Table 2. Relative intensities of marker peptides.

Sample type	Area <i>m/z</i> 748.4 DEFKPL	Area <i>m/z</i> 643.3 NAPQI-QCPF
Modified HSA	1510048	122595
Modified + unmodified HSA 1:1	1409927	56220
Unmodified HSA	1301998	Not detectable

Relative intensities of reconstructed extracted daughter ion peak areas of HSA and NAPQI-HSA peptides originating from samples consisting in modified HSA, of a 1:1 mixture of modified and unmodified HSA and of a control sample of unmodified HSA.

Continuous flow digestion

In previous work, Damsten *et al.* [6] described a method to analyze NAPQI adducts to albumin in human serum samples. Briefly, albumin from serum samples of patients exposed to high levels of acetaminophen was isolated and digested with pronase. The resulting mixture was analyzed by LC-MS/MS after removal of the enzyme. In the present study, albumin was isolated by immunoaffinity chromatography including an elution step using a low pH buffer. As previously published [23], it was found that the elution solution used (10 mM Glycine HCl and 0.15 M NaCl, pH 2.7) could be neutralized by mixing with PBS (pH 10.8) in a 1:1 ratio. Pronase was dissolved in this neutralizing buffer and mixed with the effluent from the immunoaffinity chromatography using the same flow rate. In this way, the neutralizing solution was applied and the protease could also be delivered using a single pump (P2, Figure 2). A schematic overview of this on-line system can be found in Figure 2. In the reaction capillary, the enzyme interacts with the eluted protein to form marker peptide(s) for NAPQI adducted albumin. The influence of the enzyme concentration was evaluated by varying the concentration of pronase between 0.1 and 2.0 mg/ml. Analysis was done using the completely on-line system. Extracted ion chromatograms of the MS² product ions of NAPQI-QCPF were constructed, the results being shown in Figure 5. The maximum amount of product ions was found at a concentration of 1.5 mg/ml of pronase. This concentration has been used for further analysis. It has to be kept in mind that the reaction concentration of pronase in the reaction capillary differs from the concentration in the buffered solution which was delivered by pump3 (P3, Figure 2). Since the effluent from the IAC column is mixed with the pronase solution in a 1:1 ratio, a dilution of 50% has to be taken into account. This means that a maximum amount of NAPQI-QCPF has been found at a pronase concentration in the reaction capillary of 0.8 mg/ml at given conditions.

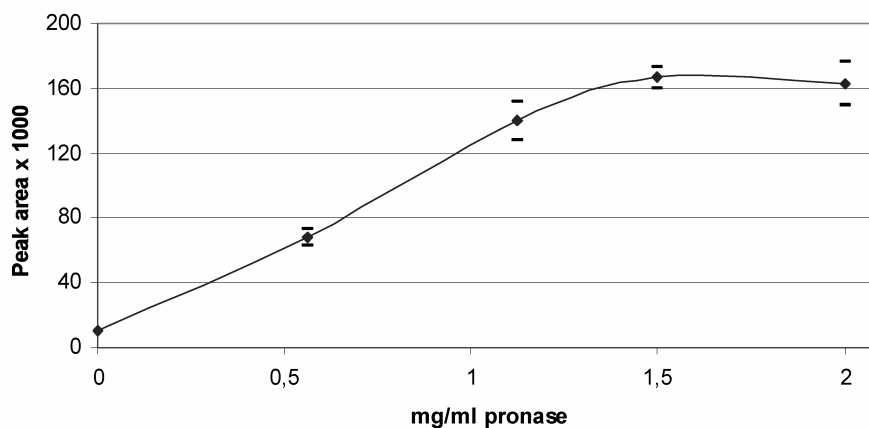


Figure 5. Influence of the pronase concentration on the NAPQI-QCPF peptide formation (peak areas of reconstructed extracted ion chromatograms of m/z 643.3) during the in-solution digestion procedure.

After this, the temperature of the reaction capillary (which was kept until this time at 37°C) was varied between 8 and 80°C. The reaction was monitored in a similar way as described for the enzyme concentration optimization, the results being depicted in Figure 6. A maximum product formation was found at 70°C, probably caused by both a higher activity of pronase and the thermal denaturation of albumin [24]. Further optimization studies were performed at a reaction capillary temperature of 70°C.

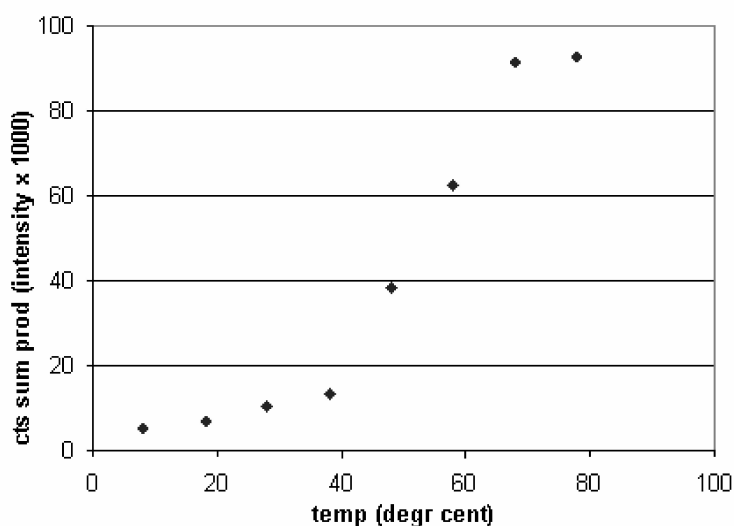


Figure 6. Influence of the solution phase digestion capillary temperature on the NAPQI-QCPF peptide formation (peak areas of reconstructed extracted ion chromatograms of m/z 643.3).

Since it can be expected that both the peptides from the protein and the protease itself are trapped on the C18 SPE column, we were interested to assess whether on-column digestion significantly contributes to the digestion of the HSA adducts. In order to study the contribution of on-column digestion, the temperature of the reaction capillary was kept constant at 8°C in order to minimize the in-solution formation of products in the reaction capillary, while the SPE column temperature was raised to 70°C to enhance possible on-column digestion. No significant traces of NAPQI-QCPF could be found using these settings and it can therefore be concluded that on-column digestion does not contribute in a significant way to the digestion of HSA adducts.

An estimation of the detection limit for NAPQI-QCPF was obtained by injection of a sample containing 0.1 mg/ml NAPQI-HSA into the complete on-line system using the optimized parameters. When 10 µl of a 1.5 µmol/l NAPQI-HSA solution were injected on the system, a signal-to-noise ratio was between 3 and 4 was obtained, resulting in an absolute detection limit of 15 pmol NAPQI adducted albumin via the cysteine³⁴ functionality. It should be kept in mind that the modification of the cysteine³⁴ residue by NAPQI is not a specific one, and other amino acid residues might be alkylated in a similar way. However, specific attention was paid to modifications of the cysteine³⁴ residue in this work because this site has often been suggested as an attractive biomarker of exposure to electrophiles [8, 26].

CDNB adducted HSA

Next to the detection NAPQI adducts to the cysteine³⁴ residue of human serum albumin, we also investigated the possibility to detect other albumin adducts. As 1-chloro-2,4-dinitrobenzene (CDNB) is known as an electrophilic and thiol-reactive compound, it was chosen for the synthesis of a different albumin adduct. The synthesized CDNB-HSA adduct was used to evaluate the general applicability of the system. The albumin was reacted with CDNB and the resulting mixture was injected onto the on-line analysis system. The reaction with CDNB results in a mass shift 166.0 Dalton to the peptide QCPF resulting in an expected m/z ratio of 660.3. In Figure 7A, three peaks can be observed in the extracted ion trace with m/z 660.3. Next, a tandem MS experiment was performed in an attempt to identify these peaks (Figure 7B). The last peak was identified as the CDNB-QCPF peptide adduct. The product ion spectrum of this peak is presented in Figure 7B. The two other peaks (Figures 7C and 7D) were not identified in this work, since the product ions differ significantly from the fragments of the CDNB-QCPF peptide adduct.

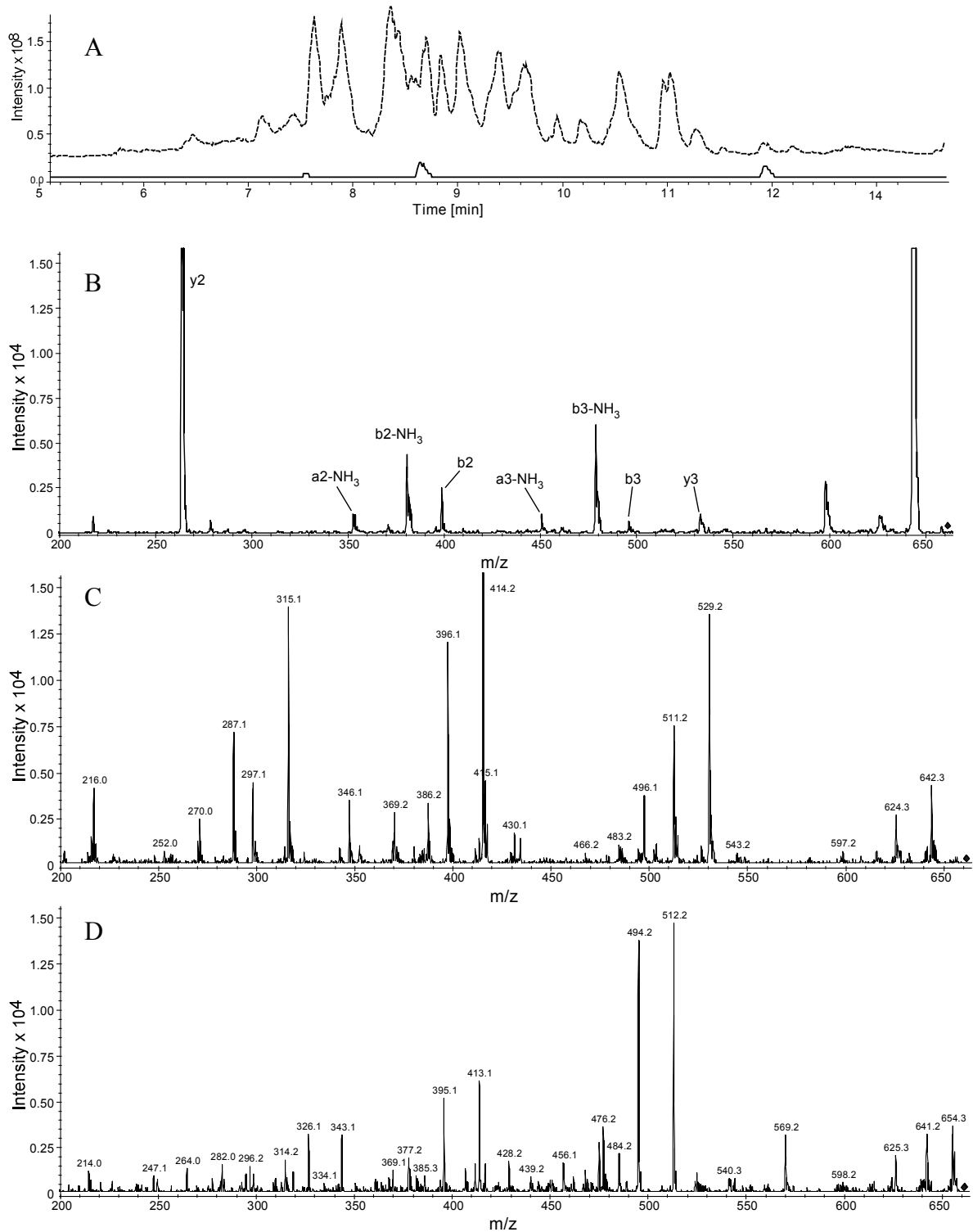


Figure 7. Analysis of CDNB-HSA: (A) The total ion current chromatogram of a pronase digest of CDNB adducted HSA shown by the dashed trace; the reconstructed extracted ion chromatogram of m/z 660.3 is shown by the solid trace (blow-up 3 fold); (B) Tandem MS product ion scan of m/z 660.3 (blow-up 6 fold) at retention time 11.9 minutes; (C) Tandem MS product of m/z 660.3 at retention time 8.7 minutes; (D) Tandem MS product of m/z 660.3 at retention time 7.6 minutes.

Conclusions

A fully automated, on-line approach for the detection of covalent adducts to the cysteine³⁴ residue HSA has been developed. Human serum albumin adduct formation with the reactive metabolite of acetaminophen (NAPQI) could be detected by the analysis of the corresponding NAPQI-QCPF adduct by mass spectrometry. The applicability of the approach was confirmed by additional analysis of CDNB adducted HSA. This approach might therefore constitute a useful tool for the screening of covalent adducts to HSA in human samples without requiring time-consuming manual sample handling. This work also confirmed that the cysteine³⁴ residue of HSA serves as a highly reactive site for covalent binding of reactive electrophilic compounds. This can be attributed to the fact that cysteine³⁴ is the only freely available thiol-group present in intact albumin. An absolute amount of 15 pmol NAPQI-HSA could be analyzed when injecting 10 μl of a 1.5 $\mu\text{mol/l}$ NAPQI adducted human serum albumin solution onto the on-line system. Immunoaffinity chromatography has been applied as a selective sample purification step and it could be shown that the presence of native (non-adducted) albumin did not hinder the specific interaction with the immobilized antibodies. Also, continuous solution phase digestion has been presented as a new approach to perform on-line digestion, thereby excluding the need for immobilization of enzymes as usually done with IMERs. Data analysis was supported by ACD/SpecManager and although a rather high background signal was observed, the identity of several peptides could be confirmed by mass spectrometric experiments.

Acknowledgements

This research was supported by Roche Diagnostics GmbH in Penzberg (Germany). We acknowledge Agilent (Amstelveen, The Netherlands) for providing technical parts and equipment service. André Groenhof from our organic chemistry department is acknowledged for support and discussion.

References

- [1] S. Zhou, E. Chan, W. Duan, M. Huang, Y.Z. Chen, *Drug Metab. Rev.* 37 (2005) 41.
- [2] D.C. Evans, A.P. Watt, D.A. Nicoll-Griffith, T.A. Baillie, *Chem. Res. Toxicol.* 17 (2004) 3.
- [3] X.X. Yang, Z.P. Hu, S.Y. Chan, S.F. Zhou, *Clinica Chimica Acta* 365 (2006) 9.
- [4] M. Tornqvist, C. Fred, J. Haglund, H. Helleberg, B. Paulsson, P. Rydberg, *J. Chromatogr. B* 778 (2002) 279.
- [5] S. Zhou, *J. Chromatogr. B* 797 (2003) 63.
- [6] M. Damsten, J.N. Commandeur, A. Fidder, A.G. Hulst, D. Touw, D. Noort, N.P. Vermeulen, *Drug Metab. Dispos.* (2007).
- [7] K.J. Hoffmann, A.J. Streeter, D.B. Axworthy, T.A. Baillie, *Chem. Biol. Interact.* 53 (1985) 155.
- [8] S. Ito, T. Kato, K. Fujita, *Biochem. Pharmacol.* 37 (1988) 1707.
- [9] D. Noort, A.G. Hulst, L.P. de Jong, H.P. Benschop, *Chem. Res. Toxicol.* 12 (1999) 715.
- [10] D. Noort, A.G. Hulst, R. Jansen, *Arch. Toxicol.* 76 (2002) 83.
- [11] D. Noort, A. Fidder, A.G. Hulst, A.R. Woolfitt, D. Ash, J.R. Barr, *J. Anal. Toxicol.* 28 (2004) 333.
- [12] A.J. Streeter, D.C. Dahlin, S.D. Nelson, T.A. Baillie, *Chem. Biol. Interact.* 48 (1984) 349.
- [13] C.L. Cardoso, V.V. Lima, A. Zottis, G. Oliva, A.D. Andricopulo, I.W. Wainer, R. Moaddel, Q.B. Cass, *J. Chromatogr. A* 1120 (2006) 151.
- [14] L. Korecka, Z. Bilkova, M. Holeapek, J. Kralovsky, M. Benes, J. Lenfeld, N. Minc, R. Cecal, J.L. Viovy, M. Przybylski, *J. Chromatogr. B* 808 (2004) 15.
- [15] J. Krenkova, F. Foret, *Electrophoresis* 25 (2004) 3550.
- [16] N. Markoglou, R. Hsuesh, I.W. Wainer, *J. Chromatogr. B* 804 (2004) 295.
- [17] G. Massolini, E. Calleri, *J. Sep. Sci.* 28 (2005) 7.
- [18] C. Temporini, E. Perani, E. Calleri, L. Dolcini, D. Lubda, G. Caccialanza, G. Massolini, *Anal. Chem.* 79 (2007) 355.
- [19] B. Bruyneel, J.S. Hoos, M.T. Smoluch, H. Lingeman, W.M. Niessen, H. Irth, *Anal. Chem.* 79 (2007) 1591.
- [20] I.A. Blair, A.R. Boobis, D.S. Davies, T.M. Cresp, *Tetrahedron Letters* 21 (1980) 4947.
- [21] C.K. Riener, G. Kada, H.J. Gruber, *Anal. Bioanal. Chem.* 373 (2002) 266.
- [22] R. Hurst, Y. Bao, S. Ridley, G. Williamson, *Biochem. J.* 338 (1999) 723.
- [23] J.S. Hoos, H. Sudergat, J.P. Hoelck, M. Stahl, J.S.B. de Vlieger, W.M.A. Niessen, H. Lingeman, H. Irth, *J. Chromatogr. B* 830 (2006) 262.
- [24] G.A. Pico, *Int. J. Biol. Macromol.* 20 (1997) 63.
- [25] W. Chen, J.P. Shockcor, R. Tonge, A. Hunter, C. Gartner, S.D. Nelson, *Biochem.* 38 (1999) 8159.
- [26] D. Noort, A. Fidder, A.G. Hulst, *Arch. Toxicol.* 77 (2003) 543.

PART IV

CONCLUSIONS

Chapter 7

Summary, Conclusions and Perspectives

Summary

Although extensive research has been performed in the field, adverse drug reactions (ADRs) still constitute a major cause of failures in drug development programs and in drug therapy. In this regard, idiosyncratic adverse drug reactions are particularly challenging since they are usually unpredictable and occur only in a very minor part of the patients taking the specific drug. The precise underlying mechanisms are still unknown but it is believed that reactive drug metabolites and covalent binding to proteins (probably in combination with immune and/or inflammatory processes) play a role in the onset of idiosyncratic drug reactions (IDRs).

The work described in this thesis mainly focused on biotransformation-related bioactivation mechanisms potentially involved in ADRs and concentrated on two main aspects. First, novel strategies and *in vitro* methodologies were developed for the generation and screening of reactive metabolites of drugs. This part aimed at the development of tools that would facilitate the detection and characterization of reactive metabolites of drugs early in the drug discovery phase. The second part of the thesis focused on the development of strategies for the screening of reactive metabolites *in vivo* in humans. The main goal was the development of biomarkers reflecting bioactivation of drugs towards reactive intermediates (RIs) that covalently bind to proteins *in vivo*.

PART I of this thesis, i.e. **Chapter 1**, consists of a general introduction on ADRs with an emphasis on adverse drug reactions with an idiosyncratic nature. IDRs are rare but severe adverse events that can occur during drug therapy. Although the current mechanistic knowledge is limited, it is believed that bioactivation of drugs towards RIs that can subsequently react with proteins is required to trigger IDRs. One of the most important classes of enzymes involved in the bioactivation of drugs is the class of cytochromes P450 (P450s). P450s can generate several types of RIs (e.g. radicals and electrophiles) that can attack macromolecules in the body and lead to toxicity. The chemical reactivity of the intermediates, the efficiency of detoxification pathways (such as conjugation to glutathione) and individual susceptibility factors, amongst others, will ultimately define the toxic outcome. Examples of drugs causing IDRs and subject of study in this thesis are discussed in more detail in the second part of the introduction (e.g. acetaminophen, diclofenac, clozapine, carbamazepine, etc). Because RIs are playing an important role in IDRs, current strategies applied in drug discovery & development programs usually focus on the screening of reactive metabolites, the elucidation of novel bioactivation pathways and on the measurement

of covalent binding to proteins. Commonly used methodologies are discussed in the last part of **Chapter 1** and were divided in two main categories, notably (i) “early phase” *in vitro* screening tools aiming at the evaluation of the potential of novel chemical identities to form RIs and (ii) “late phase” *in vivo* biomonitoring tools concentrating on protein adduct analysis and on the identification of the target proteins of RIs. Finally, the aim and the scope of this thesis are formulated.

PART II of this thesis focuses on the development of novel *in vitro* methods for the generation, identification and characterization of reactive metabolites of drugs. The most commonly applied strategy for the *in vitro* screening of electrophilic RIs consists of trapping with small nucleophilic molecules such as glutathione (γ -Glu-Cys-Gly; GSH) and cyanide (CN). Drug-nucleophile adducts can subsequently be analyzed by analytical techniques such as liquid-chromatography (LC) and mass spectrometry (MS). A major difficulty in detecting and characterizing RIs, however, is their low abundance in often complex mixtures. This usually originates from low metabolic turnovers and the inherent chemical reactivity of the intermediates which react with multiple nucleophilic targets in the incubation mixtures. These factors result in low levels of trapped reactive metabolites and in sometimes problematic identification of novel RIs and bioactivation pathways.

In **Chapter 2**, we have evaluated the use of bacterial P450 mutants as biocatalysts for the generation of high levels of RIs. Increasing the production of reactive metabolites of drugs would facilitate their identification and structural elucidation. Previous work has yielded several mutants of cytochrome P450 BM3 (CYP102) with high activities towards drugs and drug-like molecules by a combination of site-directed and random mutagenesis of wild-type P450 BM3 [1]. In this thesis, we have investigated whether four of these P450 BM3 mutants (M01_{his}, M02_{his}, M05_{his} and M11_{his}) could produce high levels of RIs of acetaminophen, clozapine and diclofenac by analyzing their GSH adducts [2]. We generally found that the BM3 mutants were able to produce similar (reactive) metabolites as rat liver microsomes (RLM) and human liver microsomes (HLM), with activities up to 70-fold higher compared to the mammalian enzymes (**Table 5, page 79**). Additionally, three novel human-relevant GSH adducts of diclofenac were identified (**Figure 3, page 81**), indicating that the mutant P450 BM3's can assist in the elucidation of novel bioactivation pathways of drugs and in the structural characterization of reactive metabolites involved.

An important defense mechanism of organisms against reactive electrophilic metabolites of drugs is conjugation to the endogenous tripeptide GSH. The coupling

of reactive electrophiles to GSH can be spontaneous and/or mediated by glutathione S-transferases (GSTs). Previous clinical studies suggest that GSTs could play a role in the inter-individual susceptibility towards drugs. However, at present, still little is known about the role of GSTs in the detoxification of reactive metabolites of drugs involved in ADRs. In **Chapter 3**, we have investigated whether rat GSTs catalyze the conjugation of certain RIs of drugs with GSH, and consequently increase GSH adduct levels in incubations performed with RLM and/or with P450 BM3 mutant M11_{his}. Generally, we found that GSTs had limited effects on the GSH adduct levels of acetaminophen, 3-hydroxyacetanilide, clozapine and diclofenac. Interestingly, GSTs significantly increased the amounts of GSH adducts in carbamazepine incubations (**Figure 5, page 101**). More specifically, they catalyzed the conjugation of the most reactive side-ring arene oxide intermediates of the drug to GSH. Variations in GST activities could therefore influence exposure to RIs and thereby trigger individual susceptibilities towards carbamazepine, as previously reported in clinical studies [3]. So, although adding GSTs to *in vitro* incubation mixtures may not increase GSH-conjugate levels to the same extent as observed with the P450 BM3 mutants, it may give valuable insights in the role of RIs and GSTs in drug bio(in)activation pathways.

In **Chapter 4**, the trapping tools developed in the two previous chapters were applied to study the metabolism and bioactivation of trimethoprim (TMP), a drug that has been involved in rare but serious ADRs in humans [4]. TMP was incubated with HLM, RLM, recombinant human P450s and the bacterial P450 BM3 mutant M11_{his}. We found that TMP is metabolized to several stable, non GSH-dependent, metabolites and to five GSH adducts by HLM (**Table 1, page 115**). With TMP, M11_{his} was not significantly more active but produced similar metabolites as rat and human enzymes. Adding GSTs to the incubation mixtures did not change GSH adduct levels. Two major GSH adducts probably originate from an iminoquinone methide intermediate which has been described previously [5]. Interestingly, three novel GSH adducts, likely derived from other RIs (such as ortho-quinones and para-quinones), were formed upon O-demethylation of TMP (**Figure 2, page 114**). Human P450 1A2 and P450 3A4 produced the major GSH adducts of TMP, while the minor GSH adducts were generated by P450 1A2, 3A4 and 2D6, the latter enzyme being polymorphic in humans (**Table 3, page 120**). In summary, our results show for the first time that TMP is bioactivated to more reactive metabolites than previously described and also that genetically polymorphic P450s could play a role in the onset of TMP-related ADRs in humans.

Next to *in vitro* screening approaches that can identify the potential of drugs and novel chemical entities (NCE's) to generate electrophilic RIs, there is a great need for novel biomonitoring strategies that can detect reactive metabolites and covalent binding to proteins *in vivo* in humans. Many IDRs do not seem to be directly related to the concentration of the parent drug; however, it is more likely that they are related to levels of the reactive electrophilic metabolites. Additionally, IDRs are typically delayed reactions which may indicate that accumulation of RIs, or RI-related products such as protein adducts, could play a role in determining the onset of an adverse event. Since GSH adducts and their decomposition products (e.g. mercapturic acids) [6] only represent short-term exposure to electrophilic RIs, alternative biomarkers based on protein adduct analysis could be useful to monitor chronic exposure to reactive electrophiles *in vivo* in humans. The work described in **PART III** of this thesis is dealing with the latter aspects and aims at the development of novel biomonitoring tools and strategies to assess the potential of bioactivation of drugs towards electrophilic RIs and their covalent binding to proteins *in vivo*. These tools may improve risk assessments in the drug development phase.

In **Chapter 5**, a novel strategy is proposed in which adducts to the free cysteine³⁴ residue of human serum albumin serve as biomarkers for reactive metabolites of drugs [7]. Our methodology consists of the isolation of albumin from blood, its digestion to peptides by pronase E, and the detection by LC-MS of drug adducts to a characteristic cysteine³⁴-proline-phenylalanine (CPF) tripeptide. The overall strategy involves the *in vitro* generation of reference drug-CPF adducts allowing the optimization of the subsequent digestion and cleanup procedures as well as the “fine-tuning” of the detection by MS. The same adducts are then measured *in vivo*, e.g. in blood of patients exposed to the drug (**Figure 1, page 131**). This strategy was developed and validated using acetaminophen as model compound. NAPQI-CPF adducts were successfully detected in serum samples of patients exposed to high levels of acetaminophen (**Figure 5, page 141**). High levels of cysteine (NAPQI-Cys) and N-acetyl cysteine (NAPQI-NAc) adducts, as well as oxidation products such as mixed disulfide adducts of N-acetyl cysteine with albumin (QCPF-NAc) were also observed, thereby providing novel mechanistic information on *in vivo* bio(in)activation pathways of acetaminophen. More generally, and because of its generic nature, the strategy of measuring protein alkylation can be considered a new biomonitoring tool for exposure assessment to RIs and to evaluate protein adduct formation *in vivo*. This new approach may prove useful during the pre-clinical and clinical development phases of novel drug candidates.

Although the previously described methodology was successful in detecting drug adducts to human serum albumin, the whole procedure remains relatively long and labor-intensive. In order to increase the throughput of sample analysis, a fully automated system for the detection of albumin adducts was developed in **Chapter 6** [8]. The system relies on several sample pre-treatment and separation steps including albumin isolation by immunoaffinity chromatography, in-solution digestion of albumin by pronase and on-line MS detection of the characteristic glutamine-proline-cysteine-phenylalanine (QCPF) adducts (**Figure 2, page 161**). The system was validated by the detection of NAPQI-QCPF and CDNB-QCPF, two peptide adducts formed after pronase digestion of albumin previously incubated with the reactive metabolite of acetaminophen (NAPQI) and the direct alkylating agent 1-chloro-2,4-dinitrobenzene (CDNB). Using this fully-automated system, the entire process (from sample application to QCPF-adduct analysis by LC-MS) was decreased from several hours to 44 minutes.

Conclusions and Perspectives

The development of novel drugs is a challenging task. It has been estimated that on average from $\sim 10^4$ compounds tested, only 1 will eventually reach the market [9]. Considering the high costs related to bring a compound onto the market (\sim \$800 million to \$1 billion), the fact that only 1 out of 3 drugs reaching the market is profitable and the pressure of producing drugs that are nearly absolutely safe, there is a huge need of selecting the “right” drug-candidate molecule as early as possible in the drug discovery and development process [9]. Currently, the main reasons for drug attrition is lack of efficacy in humans and preclinical toxicology [10]. For the latter it is now well established that preclinical tools used in the safety evaluation of novel drug-candidates only poorly predict human ADRs. This is especially true for IDRs that are usually only detected in a very late stage, once the drug is launched on the market.

At current, predicting the potential of new chemical entities to generate IDRs is still not possible because of the lack of reliable pre-clinical models. However, the formation of reactive metabolites and protein covalent binding are both perceived as significant risk factors. Consequently, a pragmatic approach is usually taken, mainly relying on (i) the screening of reactive metabolites, (ii) the measurement of protein covalent binding levels *in vitro* and/or *in vivo*, (iii) the identification of relevant bioactivation pathways and (iv) rational structural modifications of hot-spots for

bioactivation thereby eliminating or minimizing the formation of reactive metabolites and/or protein covalent binding [11, 12]. The work described in this thesis focuses on the development of novel tools that could assist these processes. Briefly, the tools were divided in two categories: (i) “early-phase” *in vitro* screening tools for reactive metabolites and (ii) “late-phase” biomonitoring strategies to detect RIs *in vivo* in humans.

***In vitro* tools for the generation and detection of reactive metabolites**

Measuring the potential of novel drug candidates to be bioactivated to reactive metabolites early in the drug discovery phase is usually performed by *in vitro* trapping and identification experiments using small nucleophilic molecules such as GSH, CN and analogues (Tables 7-9, pages 39-41). Although there has been major progress both in the design of trapping agents and in the sensitivity of analytical techniques, it remains challenging to detect and characterize low levels of RIs. In this thesis, two new strategies were evaluated: (i) increasing the levels of RIs of drugs by using highly active metabolic enzymes and (ii) enzymatic catalysis of the conjugation of reactive drug metabolites with GSH (Figure 1).

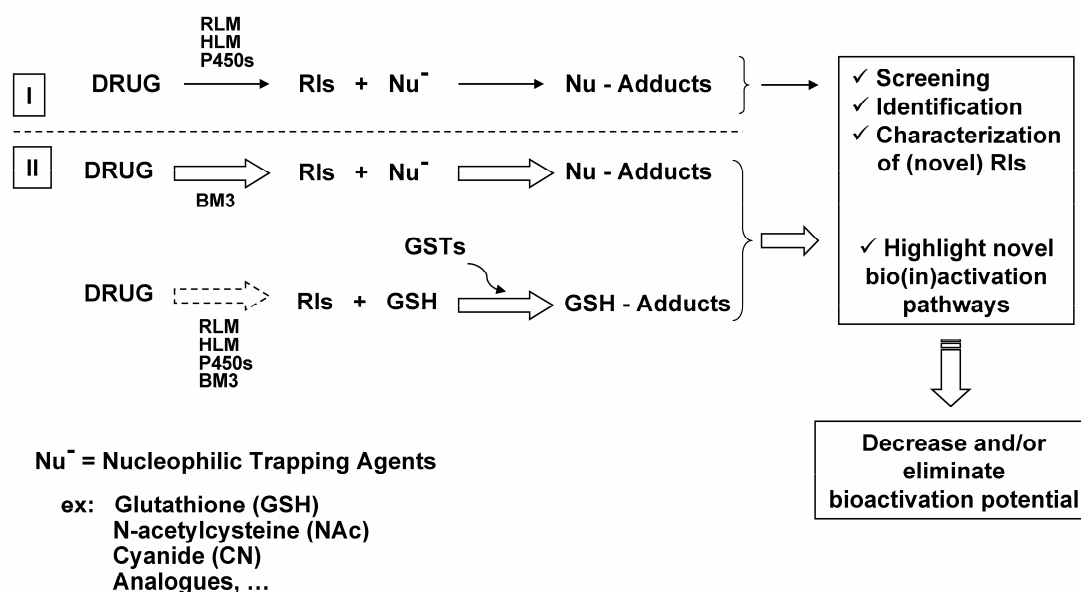


Figure 1. “Early-phase” *in vitro* screening tools for reactive metabolites: (I) Scheme of classical trapping experiments typically performed in drug discovery programs and (II) new concepts developed in this thesis. RLM: rat liver microsomes; HLM: human liver microsomes; P450s: cytochromes P450; RIs: reactive intermediates; BM3: P450 BM3 mutants; GSTs: glutathione S-transferases.

We have demonstrated in **Chapter 2** that the P450 BM3 mutants were successful in producing significantly higher amounts of rat- and human-like metabolites for several drugs. Overall, this work demonstrates that mutant bacterial enzymes with high catalytic activities can be used as biocatalysts to assist the identification of reactive metabolites of drugs and, importantly, the elucidation of novel bioactivation pathways (as demonstrated for diclofenac). It remains to be established whether the P450 BM3 mutants would be successful in generating sufficiently high amounts of drug metabolites (especially the minor ones) allowing the isolation of mg amounts of pure reactive metabolites for their full structural elucidation by Nuclear Magnetic Resonance (NMR). Improvements of analytical techniques (such as LC-NMR) and the use of bioreactors allowing the up-scaling of incubations will most likely help to overcome possible technical limitations. In parallel, the development of P450 BM3 mutants with even higher catalytic activities (e.g. random and/or site-directed mutagenesis) may be helpful.

Another approach is to increase the trapping efficiency of RIs by improving the GSH-conjugation by GSTs. In **Chapter 3**, we have evaluated whether rat GSTs could play this role in *in vitro* enzymatic incubations. Although the effect of GSTs on GSH adduct levels was generally limited, GSTs significantly increased the levels of minor GSH adducts of carbamazepine thereby providing a proof-of-concept. Further experiments with human GSTs and isolated GST isoforms should however be performed to assess the exact impact of GSTs on trapping RIs and to better characterize their role in detoxifying reactive metabolites of drugs involved in ADRs. The latter should also provide important additional information on the role that GST genetic polymorphisms could play in predisposing individuals to ADRs, as was suggested for carbamazepine [3].

Protein adducts as biomarkers for reactive intermediates

One major limitation of using *in vitro* tools to assess risks of ADRs, is that a bioactivation potential *in vitro* will not *per se* predict accurately types and amounts of reactive metabolites *in vivo*, when all biological processes are present (e.g. bioavailability, transport, bio(in)activation...) [11, 13]. Therefore, during the safety evaluation of new drug candidates, one has to predict or measure their occurrence and effects *in vivo* in humans. Currently, few methodologies exist for the biomonitoring of reactive metabolites. GSH adducts are typically reflecting short term exposure to RIs due to their rapid processing into mercapturic acids and their subsequent elimination from the body [6, 14]. In contrast, protein adducts have a

longer half-life and are more likely to reflect chronic exposure to RIs; a situation which is more relevant to assess risks of ADRs [15]. A major challenge, however, in measuring protein adducts *in vivo* is the low stoichiometry between modified versus non-modified proteins, which is mainly due to a “dilution effect” originating from the conversion of drugs to multiple metabolites that moreover may react at multiple nucleophilic sites on multiple macromolecular targets [16]. As a consequence, protein adduct levels *in vivo* are typically very low making their detection and protein target identification particularly challenging (especially when the use of radio-labeled tracers is not possible, as is the case in humans) [17].

Previous work has demonstrated that protein adducts can be used as biomarkers reflecting human occupational exposure to reactive potentially mutagenic chemicals [18-20]. In **Chapter 5**, we evaluated for the first time an analogous strategy in which albumin adducts were chosen as biomarkers reflecting *in vivo* bioactivation of drugs to reactive metabolites involved in ADRs. A generic strategy was developed, where acetaminophen-albumin adducts are first generated *in vitro* for method & development purposes, and where the same adducts are subsequently analyzed in the serum of patients exposed to the drug. Additional biomarkers, representative of short-term exposure to RIs and possibly of oxidative stress, were also identified (**Figure 2**).

Our rationale to choose albumin as model protein to detect RIs *in vivo* was firstly because it is the most abundant protein in human blood plasma (~ 30 mg/ml). Secondly, the half-life of albumin is 20 days which indicates that albumin adducts could accumulate in time and thereby represent chronic exposure of the organism to reactive metabolites. High adduct levels and alkylation efficiencies were also expected since prealbumin is synthesized in the liver, where the bioactivation of most drugs takes place. Although these factors would suggest that albumin constitutes a good model protein to trap and detect RIs *in vivo*, we found the albumin adduct levels to be surprisingly low considering the high doses of acetaminophen ingested by the patients in our study. This may, however, be partly explained by alternative reactions of NAPQI, such as protein- and non-protein thiol oxidations.

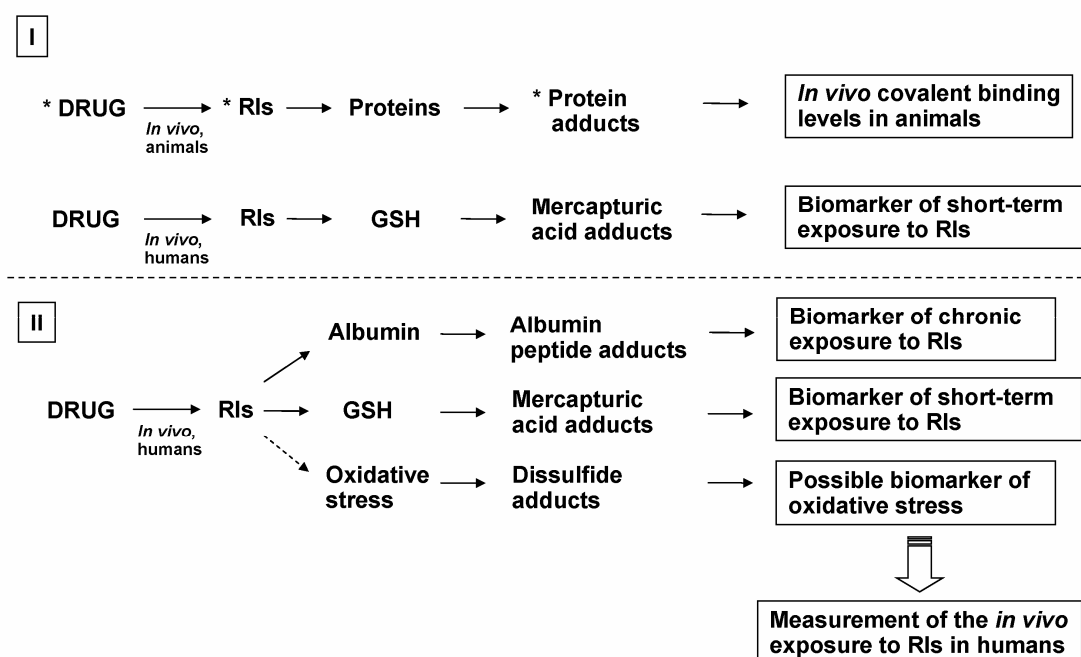


Figure 2. “Late-phase” *in vivo* biomonitoring tools for reactive metabolites: (I) scheme of classical *in vivo* experiments including the measurement of covalent binding levels in animals with radio-labeled drug analogues and the measurement of mercapturic acid adducts *in vivo* in humans and (II) scheme of the strategy described in this thesis. *: Radio-labeled; RIs: reactive intermediates; GSH: glutathione.

An alternative model protein for biomonitoring RIs might be GSTs. GSTs are present in high amounts in the cell (~ 10% of total cellular proteins), and straightforward methods exist for their isolation from complex mixtures and for the measurement of catalytic activities by functional assays. Moreover, GST adducts of several drugs have already been detected *in vivo* in animals [21, 22]. More recently, Jenkins *et al.* proposed GST Pi as model protein to characterize reactive metabolites of drugs [23]. Interestingly, this work combined the detection of GST adducts with functional assays determining the effect of covalent binding on GST activities. The need of highly sensitive analytical instruments to identify GST adducts was however stressed and it remains therefore to be established whether such tools would be sensitive enough to be applied to human *in vivo* samples. In addition, some studies have challenged the concept that covalent binding to GSTs, and subsequent inactivation of the enzyme, would be responsible for IDRs. For instance, considering the low levels of *in vivo* alkylation of GSTA1 and GSTA2 in rats, Koen *et al.* suggested that the main consequence of GST alkylation may not be inhibition of the enzyme but more likely the induction of down-stream pathways that may lead to cell death [16].

Protein alkylation sites and functional effects

Overall, several main questions related to the understanding of the biological consequences of protein adduction remain open. Obviously, without a better understanding on the impact of specific protein alkylation patterns and their role in the onset of ADRs or IDRs, little progress can be made in this field [17]. The case of acetaminophen and 3-hydroxyacetanilide is once again illustrative. While the hepatotoxic acetaminophen preferentially alkylates liver mitochondrial proteins, the nonhepatotoxic regioisomer mainly binds to cytosolic and endoplasmic reticulum protein targets [24]. Since total covalent binding levels of both compounds are similar, the selectivity in protein alkylation must determine the toxic outcome [25, 26]. As described in the “Hard-Soft” theory (**Figure 4, page 28**), the type, chemical characteristics and intrinsic properties of the RIs are likely to determine the macromolecular targets, and ultimately the toxicity. More work is therefore needed to rationalize the selectivity in protein alkylation and possibly to establish dose-response relationships. In this perspective, the development of novel tools (e.g. proteomics and genomics) has allowed a wider range of protein targets of reactive metabolites to be identified and drug-induced gene expression changes to be highlighted [26-30]. Databases gathering all current information on protein targets of drug metabolites are also starting to be established [31, 32]. It is therefore believed that “biomarkers” reflecting protein alkylation profiles and gene expression changes will be identified and related to specific toxic outcomes [26]. Of special current interest is the induction of sensory networks by electrophilic compounds (e.g. the Keap-1/Nrf2/ARE complex, GSTs, thioredoxin and the nuclear factor κ B) which are systems that respond to electrophiles and may trigger cell death, stress responses and/or stress adaptation [25, 26]. Selectivity of alkylation of those proteins may determine cell recovery versus cell death [33].

In summary, the occurrence of IDRs is still poorly understood. A pragmatic approach in drug R&D programs is to consider reactive metabolites as an undesirable feature of novel drug candidates, and consequently, major efforts will have to be made to eliminate or decrease this type of bioactivation of novel chemical entities [11]. Methods aiming at optimizing the identification and characterization processes of reactive metabolites, such as those described in this thesis, may help in better assessing the bioactivation potential of novel drug candidates. However, not all RIs are generating IDRs or ADRs and this constitutes a major bottleneck in performing adequate risk assessments. A better understanding of the links between specific

protein adduction and associated toxicity and/or biological function alterations is essential. Only then can predictions be done about the potential impact of drug alkylation on specific toxic outcomes. In this context, it is important to realize that not all protein alkylation is bad *per se*, some may even be protective [34]. In any case, the development of biomarkers, indicating qualitatively (and preferably also quantitatively) drug-related protein alkylation profiles and/or genetic expression changes in relation to specific types of toxicities, will prove valuable for safety assessment purposes. This thesis has contributed significantly to the development of novel and useful strategies and tools for these purposes.

References

- [1] Van Vugt-Lussenburg, B. M., Damsten, M. C., Maasdijk, D. M., Vermeulen, N. P. and Commandeur, J. N. (2006) Heterotropic and homotropic cooperativity by a drug-metabolising mutant of cytochrome P450 BM3. *Biochem Biophys Res Commun.* **346**, 810-818.
- [2] Damsten, M. C., Van Vugt-Lussenburg, B. M., Zeldenthuis, T., De Vlieger, J. S., Commandeur, J. N. and Vermeulen, N. P. (2008) Application of drug metabolising mutants of cytochrome P450 BM3 (CYP102A1) as biocatalysts for the generation of reactive metabolites. *Chem Biol Interact.* **171**, 96-107.
- [3] Ueda, K., Ishitsu, T., Seo, T., Ueda, N., Murata, T., Hori, M. and Nakagawa, K. (2007) Glutathione S-transferase M1 null genotype as a risk factor for carbamazepine-induced mild hepatotoxicity. *Pharmacogenomics.* **8**, 435-442.
- [4] Damsten, M. C., De Vlieger, J. S., Niessen, W. M., Irth, H., Vermeulen, N. P. and Commandeur, J. N. (2008) Trimethoprim: Novel Reactive Intermediates and Bioactivation Pathways by Cytochrome P450s. *Chem Res Toxicol.*
- [5] Lai, W. G., Zahid, N. and Utrecht, J. P. (1999) Metabolism of trimethoprim to a reactive iminoquinone methide by activated human neutrophils and hepatic microsomes. *J Pharmacol Exp Ther.* **291**, 292-299.
- [6] De Rooij, B. M., Boogaard, P. J., Commandeur, J. N., Van Sittert, N. J. and Vermeulen, N. P. (1997) Allylmercapturic acid as urinary biomarker of human exposure to allyl chloride. *Occup Environ Med.* **54**, 653-661.
- [7] Damsten, M. C., Commandeur, J. N., Fidler, A., Hulst, A. G., Touw, D., Noort, D. and Vermeulen, N. P. (2007) Liquid chromatography/tandem mass spectrometry detection of covalent binding of acetaminophen to human serum albumin. *Drug Metab Dispos.* **35**, 1408-1417.
- [8] Hoos, J. S., Damsten, M. C., De Vlieger, J. S., Commandeur, J. N., Vermeulen, N. P., Niessen, W. M., Lingeman, H. and Irth, H. (2007) Automated detection of covalent adducts to human serum albumin by immunoaffinity chromatography, on-line solution phase digestion and liquid chromatography-mass spectrometry. *J Chromatogr B Analyt Technol Biomed Life Sci.* **859**, 147-156.
- [9] Guengerich, F. P. (2006) Cytochrome P450s and other enzymes in drug metabolism and toxicity. *Aaps J.* **8**, E101-111.
- [10] Baillie, T. A. (2008) Metabolism and toxicity of drugs. Two decades of progress in industrial drug metabolism. *Chem Res Toxicol.* **21**, 129-137.
- [11] Kumar, S., Kassahun, K., Tschirret-Guth, R. A., Mitra, K. and Baillie, T. A. (2008) Minimizing metabolic activation during pharmaceutical lead optimization: progress, knowledge gaps and future directions. *Curr Opin Drug Discov Devel.* **11**, 43-52.
- [12] Evans, D. C., Watt, A. P., Nicoll-Griffith, D. A. and Baillie, T. A. (2004) Drug-protein adducts: an industry perspective on minimizing the potential for drug bioactivation in drug discovery and development. *Chem Res Toxicol.* **17**, 3-16.
- [13] Obach, R. S., Kalgutkar, A. S., Soglia, J. R. and Zhao, S. X. (2008) Can in vitro metabolism-dependent covalent binding data in liver microsomes distinguish hepatotoxic from nonhepatotoxic drugs? An analysis of 18 drugs with consideration of intrinsic clearance and daily dose. *Chem Res Toxicol.* **21**, 1814-1822.
- [14] Commandeur, J. N., Stijntjes, G. J. and Vermeulen, N. P. (1995) Enzymes and transport systems involved in the formation and disposition of glutathione S-conjugates. Role in bioactivation and detoxication mechanisms of xenobiotics. *Pharmacol Rev.* **47**, 271-330.
- [15] Van Welie, R. T., Van Dijck, R. G., Vermeulen, N. P. and Van Sittert, N. J. (1992) Mercapturic acids, protein adducts, and DNA adducts as biomarkers of electrophilic chemicals. *Crit Rev Toxicol.* **22**, 271-306.
- [16] Koen, Y. M., Yue, W., Galeva, N. A., Williams, T. D. and Hanzlik, R. P. (2006) Site-specific arylation of rat glutathione s-transferase A1 and A2 by bromobenzene metabolites in vivo. *Chem Res Toxicol.* **19**, 1426-1434.
- [17] Baillie, T. A. (2009) Approaches to the assessment of stable and chemically reactive drug metabolites in early clinical trials. *Chem Res Toxicol.* **22**, 263-266.
- [18] Osterman-Golkar, S., Peltonen, K., Anttinen-Klemetti, T., Landin, H. H., Zorcec, V. and Sorsa, M. (1996) Haemoglobin adducts as biomarkers of occupational exposure to 1,3-butadiene. *Mutagenesis.* **11**, 145-149.
- [19] Rappaport, S. M., Waidyanatha, S., Yeowell-O'Connell, K., Rothman, N., Smith, M. T., Zhang, L., Qu, Q., Shore, R., Li, G. and Yin, S. (2005) Protein adducts as biomarkers of human benzene metabolism. *Chem Biol Interact.* **153-154**, 103-109.
- [20] Omland, O., Sherson, D., Hansen, A. M., Sigsgaard, T., Autrup, H. and Overgaard, E. (1994) Exposure of iron foundry workers to polycyclic aromatic hydrocarbons: benzo(a)pyrene-

- albumin adducts and 1-hydroxypyrene as biomarkers for exposure. *Occup Environ Med.* 51, 513-518.
- [21] Qiu, Y., Benet, L. Z. and Burlingame, A. L. (1998) Identification of the hepatic protein targets of reactive metabolites of acetaminophen in vivo in mice using two-dimensional gel electrophoresis and mass spectrometry. *J Biol Chem.* 273, 17940-17953.
- [22] Koen, Y. M., Williams, T. D. and Hanzlik, R. P. (2000) Identification of three protein targets for reactive metabolites of bromobenzene in rat liver cytosol. *Chem Res Toxicol.* 13, 1326-1335.
- [23] Jenkins, R. E., Kitteringham, N. R., Goldring, C. E., Dowdall, S. M., Hamlett, J., Lane, C. S., Boerma, J. S., Vermeulen, N. P. and Park, B. K. (2008) Glutathione-S-transferase pi as a model protein for the characterisation of chemically reactive metabolites. *Proteomics.* 8, 301-315.
- [24] Streeter, A. J., Bjorge, S. M., Axworthy, D. B., Nelson, S. D. and Baillie, T. A. (1984) The microsomal metabolism and site of covalent binding to protein of 3'-hydroxyacetanilide, a nonhepatotoxic positional isomer of acetaminophen. *Drug Metab Dispos.* 12, 565-576.
- [25] Baillie, T. A. (2006) Future of toxicology-metabolic activation and drug design: challenges and opportunities in chemical toxicology. *Chem Res Toxicol.* 19, 889-893.
- [26] Guengerich, F. P. and Macdonald, J. S. (2007) Applying mechanisms of chemical toxicity to predict drug safety. *Chem Res Toxicol.* 20, 344-369.
- [27] Koen, Y. M., Gogichaeva, N. V., Alterman, M. A. and Hanzlik, R. P. (2007) A proteomic analysis of bromobenzene reactive metabolite targets in rat liver cytosol in vivo. *Chem Res Toxicol.* 20, 511-519.
- [28] Dennehy, M. K., Richards, K. A., Wernke, G. R., Shyr, Y. and Liebler, D. C. (2006) Cytosolic and nuclear protein targets of thiol-reactive electrophiles. *Chem Res Toxicol.* 19, 20-29.
- [29] Shin, N. Y., Liu, Q., Stamer, S. L. and Liebler, D. C. (2007) Protein targets of reactive electrophiles in human liver microsomes. *Chem Res Toxicol.* 20, 859-867.
- [30] Uetrecht, J. (2008) Idiosyncratic drug reactions: past, present, and future. *Chem Res Toxicol.* 21, 84-92.
- [31] [Http://Tpdb.Medchem.Ku.Edu:8080/Protein_Database/Serach.Jsp](http://Tpdb.Medchem.Ku.Edu:8080/Protein_Database/Serach.Jsp).
- [32] Hanzlik, R. P., Koen, Y. M., Theertham, B., Dong, Y. and Fang, J. (2007) The reactive metabolite target protein database (TPDB)—a web-accessible resource. *BMC Bioinformatics.* 8, 95.
- [33] Liebler, D. C. and Guengerich, F. P. (2005) Elucidating mechanisms of drug-induced toxicity. *Nat Rev Drug Discov.* 4, 410-420.
- [34] Osburn, W. O. and Kensler, T. W. (2008) Nrf2 signaling: an adaptive response pathway for protection against environmental toxic insults. *Mutat Res.* 659, 31-39.

APPENDICES

List of Abbreviations

ADR	adverse drug reaction
ALT	alanine aminotransferase
AMAP	3-hydroxyacetanilide
APAP	acetaminophen
ARE	antioxidant response element
ARE/ERE	antioxidant response element/electrophile response element
AST	aspartate aminotransferase
AU	arbitrary units
CDNB	1-chloro-2,4-dinitrobenzene
CE	carbamazepine 10,11-epoxide
Cloz	clozapine
CN	cyanide
CPF	cysteine-proline-phenylalanine
Cys	cysteine
Diclo	diclofenac
EA	ethacrynic acid
ECD	electrochemical detection
EH	epoxide hydrolase
FLD	fluorescence detection
GSH	glutathione (reduced)
GSSG	glutathione (oxidized)
GST	glutathione S-transferase
H/D exchange	hydrogen/deuterium exchange
HLM	human liver microsomes
HPLC	high performance liquid chromatography
HSA	human serum albumin
IDR	idiosyncratic drug reaction
KPi	potassium phosphate
LC-MS	liquid chromatography-mass spectrometry
M11 _{his}	cytochrome P450 BM3 mutant M11 _{his}
MPO	myeloperoxidase
MS	mass spectrometry
MS/MS	tandem mass spectrometry
NAc	N-acetyl cysteine
NAPQI	N-acetyl-p-benzoquinoneimine
NK (T)	natural killer (T) cells
NMR	nuclear magnetic resonance
Nrf2	transcription factor Nrf2
P450 BM3, CYP102A1	cytochrome P450 BM3
P450, CYP	cytochrome P450
QCPF	glutamine-cysteine-proline-phenylalanine
RI	reactive intermediate
RLM	rat liver microsomes
ST	sulfotransferase
TMP	trimethoprim
t _r	retention time
UGT	UDP-Glucuronosyltransferase

Nederlandse Samenvatting

De ontwikkeling van geneesmiddelen is een uitdagende taak. Geschat wordt dat van de 10.000 geteste stoffen uiteindelijk slechts gemiddeld 1 stof de markt bereikt als geneesmiddel. Het op de markt brengen van een geneesmiddel brengt hoge kosten met zich mee (800 miljoen tot 1 miljard USD) en slechts 1 op de 3 geneesmiddelen die uiteindelijk de markt bereiken is winstgevend. Bovenal is het zeer belangrijk dat de geneesmiddelen die ontwikkeld worden volledig veilig zijn. Deze omstandigheden maken dat het uitermate belangrijk is om zo vroeg mogelijk het “juiste” kandidaatgeneesmiddel molecuul te selecteren in het proces om een nieuw geneesmiddel verder te ontwikkelen. Momenteel zijn het feit dat de ontwikkelde stoffen niet werken in de mens en bijkomende toxicologische effecten vertonen, de belangrijkste oorzaken dat geneesmiddelen uiteindelijk de markt niet bereiken. Het is inmiddels duidelijk bewezen dat preklinische testen die gebruikt worden in het begin van het ontwikkelingsproces om nieuwe kandidaatgeneesmiddelen te vinden ongewenste reacties (adverse drug reactions; ADRs), welke veroorzaakt zijn door het geneesmiddel, slecht kunnen voorspellen. Dit geldt in the bijzonder voor het optreden van idiosyncratische geneesmiddelreacties (idiosyncratic drug reactions; IDRs). Deze zijn zeer zeldzaam en de onvoorspelbare ongewenste bijwerkingen worden normaliter pas waargenomen in een heel laat stadium van het geneesmiddel ontwikkelingsproces. Veel vaker worden deze ongewenste reacties pas waargenomen nadat het geneesmiddel al op de markt gebracht is. Behalve het feit dat dit zorgt voor gezondheidsrisico's voor de patiënten, zijn de economische gevolgen van het terug trekken van een geneesmiddel van de markt gigantisch.

Zoals beschreven is in **Hoofdstuk 1 (PART I)** van dit proefschrift, is er zeer veel onderzoek verricht op het gebied van ongewenste bijwerkingen, maar is het onderliggende mechanisme van optreden van deze ADRs uiteindelijk nog steeds onbekend. Het is echter wel duidelijk geworden dat geneesmiddel metabolisme, de vorming van reactieve metabolieten en covalente binding aan eiwitten, een rol speelt bij het optreden van deze vorm van toxiciteit. Normaliter wordt een geneesmiddel in het lichaam gemetaboliseerd tot een beter wateroplosbare metaboliet welke eenvoudiger kan worden uitgescheiden door het lichaam. Belangrijke enzymen die een rol spelen in dit proces zijn de cytochroom P450s (P450s). Hoewel metabolisme over het algemeen beschouwd wordt als een mechanisme van detoxificatie, kan het soms voorkomen dat door middel van metabolisme een reactieve metaboliet gevormd wordt die covalent kan binden aan macromoleculen (zoals bijvoorbeeld

eiwitten en DNA) in het lichaam, wat kan leiden tot toxiciteit. Het lichaam beschikt over beschermingsmechanismen tegen reactieve intermediairen, zoals bijvoorbeeld de spontane conjugatie met het endogene peptide glutathione (GSH), een reactie welke ook gekatalyseerd kan worden door glutathion S-transferase enzymen (GSTs). Het onderzoek dat beschreven wordt in dit proefschrift focust zich op deze bio(in)activatiemechanismen en probeert een beter inzicht te verschaffen hoe geneesmiddelen kunnen worden geactiveerd tot reactieve metabolieten en uiteindelijk voor ongewenste bijwerkingen kunnen veroorzaken bij mensen.

Twee hoofdaspecten zijn onderzocht in dit proefschrift. Het onderzoek dat is beschreven in het tweede gedeelte (**PART II**) van dit proefschrift, richt zich op het ontwikkelen van nieuwe methodes en strategieën die kunnen helpen bij het detecteren en karakteriseren van reactieve metabolieten van geneesmiddelen vroeg in het ontwikkelingsproces. De mogelijkheid dat een nieuw geneesmiddel kan worden gebioactiveerd tot een reactieve metaboliet wordt vaak gemeten met behulp van *in vitro* 'trapping' experimenten. In deze experimenten wordt GSH gebruikt om de reactie intermediairen te vangen (trappen) en de GSH adducten die daarbij gevormd worden, kunnen vervolgens worden gedetecteerd en gekarakteriseerd met behulp van diverse analytische technieken. Het blijft echter een uitdaging om lage concentraties van GSH adducten te kunnen meten. Gedurende dit onderzoek zijn twee nieuwe strategieën geëvalueerd om dit proces te vergemakkelijken. In **Hoofdstuk 2**, hebben we aangetoond dat bacteriële cytochroom P450 BM3 mutanten succesvol gebruikt kunnen worden om significant hogere hoeveelheden te maken van reactieve metabolieten van geneesmiddelen. Deze gevormde metabolieten zijn identiek aan de metabolieten welke gevormd worden in humane en rat *in vitro* systemen. Hiermee is aangetoond dat bacteriële enzymen met een hoge katalytische activiteit gebruikt worden als biokatalysatoren om te assisteren in de identificatie van reactieve metabolieten van geneesmiddelen en, nog belangrijker, het achterhalen van nieuwe bioactivatie routes (zoals is aangetoond voor diclofenac). Een andere strategie, welke is geëvalueerd in **Hoofdstuk 3**, is om GSH adduct concentraties te verhogen door GSTs te gebruiken om de conjugatie van reactieve metabolieten met GSH te katalyseren. Alhoewel het toevoegen van GSTs aan *in vitro* incubaties de gevormde GSH conjugaat concentraties niet verhoogde tot het zelfde level als eerder werd waargenomen met de BM3 mutanten, verhoogde het wel de hoeveelheden gevormde GSH adducten van het geneesmiddel carbamazepine wat leidde tot waardevolle inzichten in de rol van GSTs in bio(in)activatie routes van dit geneesmiddel. In **Hoofdstuk 4** zijn de twee methodes, welke beschreven zijn in de

voorgaande twee hoofdstukken, gebruikt om het metabolisme en de bioinactivatie van het geneesmiddel trimethoprim (TMP) te onderzoeken. Dit geneesmiddel zorgt voor zeldzame, maar ernstige ongewenste bijwerkingen (ADRs) in mensen. We hebben aangetoond dat TMP wordt gebioactiveerd tot meer reactieve metabolieten dan beschreven wordt in de literatuur en dat genetisch polymorphe P450s een rol kunnen spelen in het optreden van TMP-gerelateerd ADRs in mensen.

Een grote beperking van *in vitro* systemen om het risico van het optreden van ADRs in te schatten, is het feit dat de *in vitro* situatie niet altijd gebruikt kan worden om *in vivo*, wanneer alle biologische processen (zoals bijvoorbeeld de biologische beschikbaarheid, het transport, de bio(in)activatie...) een rol spelen, het type reactieve metabolieten en de gevormde hoeveelheden daarvan nauwkeurig te voorspellen. Daarom is het belangrijk om, tijdens het evalueren van de veiligheid van nieuwe kandidaatgeneesmiddelen, de vorming en effecten van reactieve metabolieten in mensen te voorspellen of te meten. Het werk beschreven in **PART III** van dit proefschrift, gaat over deze aspecten en betreft de ontwikkeling van nieuwe methodes en strategieën om in te schatten wat de kans is dat een geneesmiddel wordt gemetaboliseerd tot een reactieve metaboliet en de covalente binding van deze metabolieten *in vivo*. Eerder uitgevoerde wetenschappelijke studies hebben aangetoond dat eiwit adducten kunnen worden gebruikt als biomarkers om aan te tonen dat mensen zijn blootgesteld aan reactieve en mogelijk mutagene chemische stoffen tijdens arbeid. In **Hoofdstuk 5**, hebben we voor de eerste keer een soortgelijke strategie geëvalueerd waarbij we adducten van albumine hebben gekozen als biomarkers voor *in vivo* bioactivering van geneesmiddelen tot reactieve metabolieten welke een rol spelen in het optreden van ongewenste bijwerkingen (ADRs). Een algemene strategie was ontwikkeld, waarbij eerst acetaminofen-albumine adducten zijn gevormd met behulp van *in vitro* technieken voor methode ontwikkelingsdoeleinden, en waarbij vervolgens de analyse methode is gebruikt om dezelfde adducten te detecteren in het bloed van patiënten die zijn blootgesteld aan hetzelfde geneesmiddel. Extra biomarkers, die representatief zijn voor korte termijn blootstelling aan reactieve metabolieten en mogelijk oxidatieve stress, werden ook geïdentificeerd. De ontwikkeling van een volledig geautomatiseerd systeem om albumine adducten te meten om meer samples te kunnen meten, is beschreven in **Hoofdstuk 6**. Deze methodes kunnen zodoende gebruikt worden om de risicoschatting in het ontwikkelen van geneesmiddelen te verbeteren.

In conclusie, en zoals besproken in **PART IV**, het optreden van idiosyncratische ongewenste bijwerkingen van geneesmiddelen is nog steeds slecht verklaard. Een pragmatische strategie in ontwikkelingsprogramma's is om alle reactieve metabolieten te beschouwen als een ongewenste eigenschap van nieuwe kandidaatgeneesmiddelen. Dit betekent dat grote inspanningen moeten worden geleverd om de bioactivering van deze nieuwe chemische entiteiten te elimineren of te verminderen. Methodes die bedoeld zijn voor de identificatie en karakterisering van deze reactieve metabolieten, zoals beschreven in dit proefschrift, kunnen helpen om een betere risicoschatting te maken voor nieuwe kandidaatgeneesmiddelen. Echter, het is zeer belangrijk om op te merken dat het vormen van reactieve metabolieten of het covalent binden daarvan aan eiwitten niet altijd leidt tot IDRs of ADRs en dat dit zorgt voor een knelpunt in het uitvoeren van een adequate risicoschatting. Het verkrijgen van een beter inzicht in het verband tussen eiwit adduct vorming en de geassocieerde toxiciteit en/of verandering in biologische functie is daarom essentieel. Alleen dan kunnen voorspellingen worden gemaakt met betrekking tot de potentiële impact van geneesmiddelalkylering op specifieke toxische effecten. De ontwikkeling van biomarkers, die kwalitatief (en bij voorkeur ook kwantitatief) geneesmiddelgerelateerde eiwitalkyleringsprofielen en/of genetische expressie veranderingen kunnen relateren aan specifieke types van toxiciteit, zullen waardevol zijn bij het maken van risicoschattingen. Dit proefschrift heeft significant bijgedragen aan het ontwikkelen van nieuwe strategieën en methodes om deze doelstelling te bewerkstelligen.

Curriculum Vitae

Micaela Damsten is Finnish of nationality and was born in Neuilly-sur-Seine on the 31st August 1977. In 1995, she graduated from the College Saint-Michel in Brussels. In 2001, she obtained the title of “Licencié en Sciences Biomédicales, orientation Toxicologie” at Catholic University of Leuven (UCL) in Brussels. She conducted her Master’s thesis project in the Industrial Toxicology and Occupational Medicine unit of the Faculty of Medicine, under the supervision of prof. A. Bernard and dr. C. Hermans. The research consisted of the non-invasive assessment of the integrity of the lung epithelial barrier in populations chronically exposed to metropolitan air pollution.

She then started a Master in the division of Molecular Toxicology of the Leiden Amsterdam Center for Drug Research (LACDR), at the Department of Chemistry and Pharmaceutical Sciences of the Vrije Universiteit in Amsterdam. She obtained the degree of “Master of Science in Pharmaceutical Sciences” in 2003. Her Master’s thesis project consisted of investigating the metabolism and estrogenicity of di-halogenated biphenyls, under the supervision of prof.dr. N. P. E. Vermeulen and dr. J. N. M. Commandeur. In September 2003, she initiated her PhD project in the same department of the Vrije Universiteit.

She started working as toxicologist at Ashland B.V., a global chemical company, in February 2008. Her main tasks were to perform risk assessments on chemicals and prepare the company for the new EU regulation REACH (Registration, Evaluation, Authorisation & Restriction of Chemicals). Since February 2009, she is working as Scientific Policy Officer in the Directorate General for Health and Consumers (DG SANCO) at the European Commission in Brussels. Her main tasks include the assessment of issues related to consumer’s health and safety, develop and implement policy initiatives, monitor policy developments in the area of consumer health and safety and ensure that consumer health and safety concerns are taken into account in other policies. She also provides support and scientific advice to core Unit and broader Directorate activities related to chemicals, risk assessments and other scientific matters.

List of Publications

Damsten MC, de Vlieger JS, Niessen WM, Irth H, Vermeulen NP, Commandeur JN; Trimethoprim: novel reactive intermediates and bioactivation pathways by cytochrome P450s; *Chem Res Toxicol*. 2008 Nov; 21(11): 2181-7.

Damsten MC^{*}, van Vugt-Lussenburg BM^{*}, Zeldenthuis T, de Vlieger JS, Commandeur JN, Vermeulen NP; Application of drug metabolising mutants of cytochrome P450 BM3 (CYP102A1) as biocatalysts for the generation of reactive metabolites; *Chem Biol Interact*. 2008 Jan 10; 171(1): 96-107.

Hoos JS^{*}, **Damsten MC**^{*}, de Vlieger JS, Commandeur JN, Vermeulen NP, Niessen WM, Lingeman H, Irth H; Automated detection of covalent adducts to human serum albumin by immunoaffinity chromatography, on-line solution phase digestion and liquid chromatography-mass spectrometry; *J Chromatogr B Analyt Technol Biomed Life Sci*. 2007 Nov 15; 859(2):147-56.

Damsten MC, Commandeur JN, Fidder A, Hulst AG, Touw D, Noort D, Vermeulen NP; Liquid chromatography/tandem mass spectrometry detection of covalent binding of acetaminophen to human serum albumin; *Drug Metab Dispos*. 2007 Aug; 35(8): 1408-17.

van Vugt-Lussenburg BM, **Damsten MC**, Maasdijk DM, Vermeulen NP, Commandeur JN; Heterotropic and homotropic cooperativity by a drug-metabolising mutant of cytochrome P450 BM3; *Biochem Biophys Res Commun*. 2006 Aug 4;346(3):810-8.

van Lipzig MM, Commandeur JN, de Kanter FJ, **Damsten MC**, Vermeulen NP, Maat E, Groot EJ, Brouwer A, Kester MH, Visser TJ, Meerman JH; Bioactivation of dibrominated biphenyls by cytochrome P450 activity to metabolites with estrogenic activity and estrogen sulfotransferase inhibition capacity; *Chem Res Toxicol*. 2005 Nov; 18(11): 1691-700.

^{*} Both authors contributed equally to this work.

Acknowledgements

Ca y est! It's finally done. And therefore, I wish to thank all those who contributed to this work. In particular I wish to express my gratitude to Nico and Jan. Nico: thanks for being my promotor and for accepting me in your group since the very beginning, when first starting as a Master's student in MolTox. Jan: thank you for being my co-promotor; for your sharp comments and valuable input on the work. Furthermore, I wish to extend my gratitude to the members of the Reading Committee for the review of this thesis. I'd also like to thank all former colleagues at MolTox: Peter, Jeroen K., Chris D., Marola, Aldo, Anton, Robert, Barbara, Ed, Jeroen L., Jolanda, Eva, Bernardo, Jozef, Chris O., Chris V. and of course all the courageous students as well who took up the challenge to work alongside me! My special warm thanks go to Regina: my room-mate & plantain expert; Sebas: for the nice moments spent together; Jelle: thanks for the 4 pm cookie-breaks, for always being willing to help and for acting as my paranimf; and of course to Laura: for your assistance with the finalization of this PhD.

I probably spent as much time at the 3rd floor as at MolTox, so my gratitude goes of course to all the ACAS colleagues. My sincere thanks go out to Hubertus Irth for letting me measure on great mass spectrometers; Wilfried Niessen: thank you for your inspiring expertise in analyzing mass spectra's; Johannes & Jon: for the nice research we did together and the excellent coffee breaks; Ben & Marek: for all your help with the LCQ, IT-TOF, etc, etc... I must admit, I will truly never forget all the time spent in that room measuring (and fighting) with the machines!

The "albumin-work" would not have been possible without TNO and my deep gratitude goes also to all colleagues involved: Daan Noort: thanks for letting me work in your group; Alex: for showing me all the tricks in protein digestion; Debora and especially Albert: many, many thanks for your skills with the Q-TOF and for your enthusiasm in measuring the CPF adducts; Annemieke for your aid in the lab.

Daan Touw: thanks for providing us with the valuable human serum samples; Jan Bolscher & Kamran Nazmi: for learning me synthesizing peptides; Frans for your assistance with the NMR's and all FAR colleagues (so many to mention here) but in particular: Dennis, Obbe, Martijn and Janneke: thanks for always being present at the VU borrels!

Nalan, Harry, Halil, Hilmi, Hande, Anna, Pau, Anu, Erik, Paola, Remko, David, Atilla, Sylvia, Robert, Stephane, Max, Merel, Marije, Julie... who enriched my PhD life outside the lab: thanks for being that great company, for the dinners, drinks, parties, trips, movings (!), etc, etc...

Acknowledgements

Most of all, I would like to thank my family and all the friends that have been present since the very start of this “PhD experience”. In particular: les M&Ms: Maria, Mery et Maite, les filles, merci pour les meetings de crise; Annika, Tineke, Pati, Fabi, Vanessa, Nadia, Nerea, Joce, Mylene, Erik and Wendy: Thank you all for always being that motivated; Toffe: thanks for being my paranimf; and papa et maman: thank you so much for your never-ending support in all projects I undertake. Last but not least, Giovanni: thanks a million times for being there, for your patience, help and support during the finalization of this thesis.

*« La recherche n'avancerait-elle pas plus vite...
Si au lieu de recruter des chercheurs, on engageait des trouveurs? »*

Le Chat